ITRI-146
December 1995
CATEGORY: UC-408

INHALATION TOXICOLOGY RESEARCH INSTITUTE ANNUAL REPORT

1994 - 1995

by the Staff of the
Inhalation Toxicology Research Institute

ITRI

INHALATION TOXICOLOGY RESEARCH INSTITUTE
LOVELACE BIOMEDICAL & ENVIRONMENTAL RESEARCH INSTITUTE
P.O. Box 5890 Albuquerque, NM 87185-5890

Prepared for
THE OFFICE OF HEALTH & ENVIRONMENTAL RESEARCH
U.S. DEPARTMENT OF ENERGY
UNDER CONTRACT NUMBER DE-AC04-76EV01013

The research described in this report involved animals maintained in animal care facilities fully accredited by the American Association for Accreditation of Laboratory Animal Care. The research described in this report that involved humans was conducted in compliance with government regulations protecting human subjects.

Printed in the United States of America

Available to DOE and DOE contractors from the Office of Scientific and Technical Information, P. O. Box 62, Oak Ridge, TN 37831: prices available from (615) 576-8401.

Available to the public from the National Technical Information Service, U.S. Department of Commerce, 5285 Port Royal Rd., Springfield, VA 22161.

ITRI-146
December 1995
Category: UC-408

Annual Report of the Inhalation Toxicology Research Institute Operated for the United States Department of Energy by the Lovelace Biomedical and Environmental Research Institute

October 1, 1994 through September 30, 1995

by the Staff of the
Inhalation Toxicology Research Institute
Joe L. Mauderly, DVM, Director

Scientific Editors
David E. Bice, PhD
Fletcher F. Hahn, DVM, PhD
Mark D. Hoover, PhD
Robin E. Neft, PhD
Janice R. Thornton-Manning, PhD

Paula L. Bradley, MA, Technical Editor

December 1995

Prepared for the Office of Health and Environmental Research of the U.S. Department of Energy Under Contract Number DE-AC04-76EV01013

TABLE OF CONTENTS

IV. CARCINOGENIC RESPONSES TO TOXICANTS

V. MECHANISMS OF CARCINOGENIC RESPONSE TO TOXICANTS

INTRODUCTION

The Institute

The Inhalation Toxicology Research Institute (ITRI) is a Federally Funded Research and Development Center operated for the U. S. Department of Energy (DOE) by the Lovelace Biomedical and Environmental Research Institute, a nonprofit subsidiary of The Lovelace Institutes. ITRI is designated as a "Single Program Laboratory" within the DOE Office of Health and Environmental Research, Office of Energy Research. Approximately 80% of the Institute's research is funded by DOE; the remainder is funded by a variety of governmental, trade association, and industry sources.

The mission of ITRI is to conduct basic and applied research to improve our understanding of the nature and magnitude of the human health impacts of inhaling airborne materials in the home, workplace, and general environment. Institute research programs have a strong basic science orientation with emphasis on the nature and behavior of airborne materials, the fundamental biology of the respiratory tract, the fate of inhaled materials and the mechanisms by which they cause disease, and the means by which data produced in the laboratory can be used to estimate risks to human health. Disorders of the respiratory tract continue to be a major health concern, and inhaled toxicants are thought to contribute substantially to respiratory morbidity. As the largest laboratory dedicated to the study of basic inhalation toxicology, ITRI provides a national resource of specialized facilities, personnel, and educational activities serving the needs of government, academia, and industry.

The Institute's multidisciplinary staff works in specialized facilities and takes a collaborative research approach to resolving scientific issues. ITRI is located on Kirtland Air Force Base East, approximately 10 miles southeast of Albuquerque, New Mexico. The more than 280,000 square feet of laboratory and support facilities include unique facilities and equipment for basic biological research and exposures of animals to all types of airborne toxicants. The staff of approximately 170 includes doctoral-level scientists in physical, chemical, biological, medical, and mathematical disciplines. Working with the scientists are highly trained scientific technicians, laboratory animal technicians, and a full range of support staff. The entire range of biological systems is employed, including macromolecules, cells, tissues, laboratory animals, and humans. The research includes both field and laboratory studies. Strong emphasis is placed on the quality of research and resulting data; the Institute has a Quality Assurance Unit and is fully capable of research in adherence to Good Laboratory Practices guidelines.

The organization of the Institute is described in Appendix B. Research resources and activities are managed using a matrix approach. One element of the matrix is the research staff and laboratory resources, which are organized into scientific groups along disciplinary lines. The other element of the matrix is the collection of individual projects into thematic programs. Both groups and programs are supervised by scientist managers. Administrative and support functions are organized in a line management fashion into units and sections.

The Report

The papers in this report are organized along topical lines, rather than by research program, so that research within specific disciplines is more readily identified. The papers include summaries of research funded by both DOE and other sources, to represent the full scope of Institute activities. The source of funding is acknowledged for each paper. The appendices summarize the organization of the Institute's staff and research programs, publications and presentations by ITRI scientists, seminars by visiting scientists, collaborations with scientists in other institutions, and a description of ITRI's educational activities.

A separate series of reports summarizes the design and status of the long-term studies of the health effects of radionuclides in dogs, conducted at ITRI and the University of Utah. These separate reports also contain the status of each dog, the detailed tables which were previously included as appendices in the ITRI Annual Report. The reports of the long-term dose response studies can be obtained from NTIS or by request from the Institute.

Joe L. Mauderly, DVM
Director

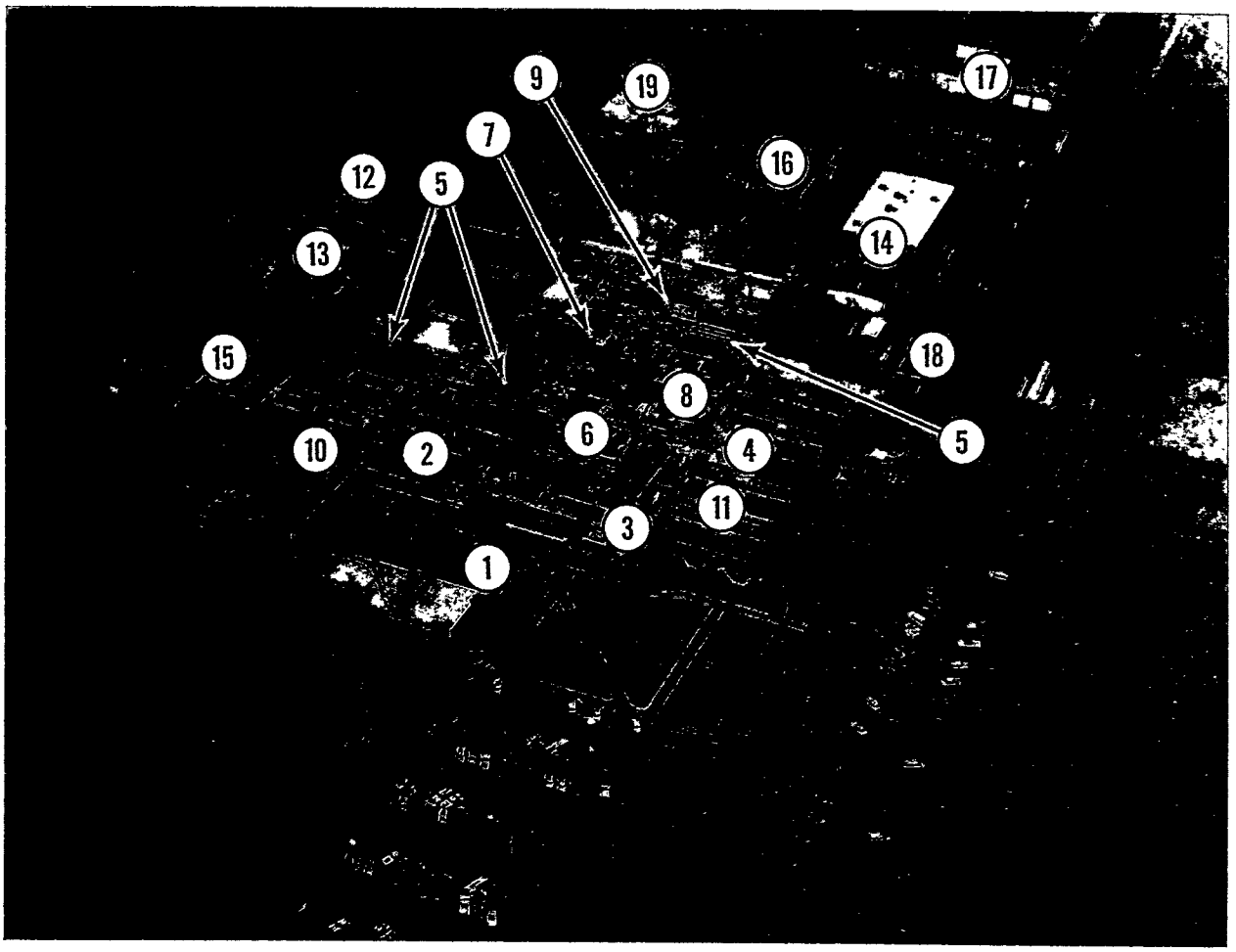

An aerial view of the Inhalation Toxicology Research Institute. The Institute's facilities, which were constructed in several increments starting in June 1962, consist of (1) administrative area, including the directorate, personnel, business, purchasing, and editorial offices, a cafeteria, conference rooms, and environment, safety and health operations; (2) central laboratory and office area, including aerosol science, radiobiology, pathology, chemistry, and toxicology laboratories; (3) cell toxicology laboratories; (4) pathophysiology laboratories; (5) chronic inhalation exposure complex with some laboratories suitable for use with carcinogenic materials; (6) exposure facility for acute inhalation exposures to chemical toxicants and beta- and gamma-radionuclides; (7) exposure facilities for acute inhalation exposures to alpha-emitting radionuclides; (8) veterinary hospital and facilities for detailed clinical observations; (9) small-animal barrier-type housing facilities; (10) library and quality assurance facilities; (11) kennel buildings; (12) analytical chemistry building; (13) engineering and maintenance support building; (14) property management, receiving, and storage building; (15) auxiliary office and classroom complex; (16) auxiliary laboratories; (17) waste storage and treatment facility; (18) standby power facility; and (19) animal quarantine facility.

LIST OF ANNUAL REPORTS

Selective Summary of Studies in the Fission Product Inhalation Program (July 1964 through June 1966):

LF-28, 1965
LF-33, 1966

Fission Product Inhalation Program Annual Report (1966–1972):

LF-38, 1967
LF-39, 1968
LF-41, 1969
LF-43, 1970
LF-44, 1971
LF-45, 1972

Inhalation Toxicology Research Institute Annual Report (1972–1995):

LF-46, 1973
LF-49, 1974
LF-52, 1975
LF-56, 1976
LF-58, 1977
LF-60, 1978
LF-69, 1979
LMF-84, 1980
LMF-91, 1981
LMF-102, 1982
LMF-107, 1983
LMF-113, 1984
LMF-114, 1985
LMF-115, 1986
LMF-120, 1987
LMF-121, 1988
LMF-126, 1989
LMF-129, 1990
LMF-134, 1991
LMF-138, 1992
ITRI-140, 1993
ITRI-144, 1994
ITRI-146, 1995

Long-Term Dose-Response Studies of Inhaled or Injected Radionuclides (1988–1993):

LMF-128, 1989
LMF-130, 1990
LMF-135, 1991
ITRI-139, 1992–1993

I. AEROSOL TECHNOLOGY AND CHARACTERIZATION OF AIRBORNE MATERIALS

GENERATION AND CHARACTERIZATION OF BIOLOGICAL AEROSOLS FOR LASER MEASUREMENTS

Yung-Sung Cheng and Edward B. Barr

Concerns for proliferation of biological weapons including bacteria, fungi, and viruses have prompted research and development on methods for the rapid detection of biological aerosols in the field. Real-time instruments that can distinguish biological aerosols from background dust would be especially useful. Sandia National Laboratories (SNL) is developing a laser-based, real-time instrument for rapid detection of biological aerosols, and ITRI is working with SNL scientists and engineers to evaluate this technology for a wide range of biological aerosols. This paper describes methods being used to generate and characterize the biological aerosols for these tests.

These experiments are being carried out in a Biosafety Level II Laboratory at ITRI (*Biosafety in Microbiological and Biomedical Laboratories*, 3rd Ed., HHS Publication No. [CDC] 93-8395, U.S. Department of Health and Human Services, 1993). Figure 1 shows the layout of the room including the laser system, aerosol chamber, autoclave, sink, biological safety cabinet, and HEPA-filtered recirculating exhaust units. The aerosol chamber, generation system, and aerosol sampling devices are placed inside an enclosure at the center of the room. Laser light enters the aerosol chamber through access ports in the enclosure. The enclosure is equipped with a pass box for transferring samplers and material into the enclosure, and glove ports for operating the aerosol generator and samplers inside the enclosure. The enclosure is ventilated by two double-HEPA-filtered recirculating units. The filtered exhaust air is returned to the room. Under normal operating conditions, only one recirculating unit is required to provide sufficient airflow. If the primary unit fails, the secondary unit will be turned on to ensure continued ventilation of the enclosure. A backup recirculating unit is available to replace the primary or secondary unit if necessary. The enclosure is maintained at a negative pressure with respect to the room, and the room pressure is negative with respect to the hallway. The air velocity flowing into the enclosure from the access ports is > 100 ft min^{-1}, which satisfies the criteria for a Level II Biosafety Cabinet.

The laser system employs two class-4 lasers which are operated by SNL personnel. A YAG ultraviolet laser is used to pump a dye laser, which has a tunable wavelength of between 200 and 400 nm. The output of the dye laser is channeled to illuminate the aerosol in the test chamber. Translucent orange-tinted polypropylene panels (absorbent at the wavelength of the laser) are oriented between the laser system and the entry to the room at all times that the laser is on. Panels are also located on the side of the test chamber enclosure opposite the laser system. The laser power unit is water-cooled. The transducer monitors the water pressure in the cooling unit and activates a warning light outside of the room whenever the laser is on. When the warning light is on, access is limited to authorized personnel, and all personnel entering the area must wear protective laser safety eyewear. The door to the room remains locked at all times.

The aerosol materials used in the study include pollens of cedar, oak, and ragweed; bacteria used in the experiment was *Bacillus subtilis*, which is a Biosafety Level I agent; and fungi was *Aspergillus fumigatus*, which was gamma irradiated by the manufacturer to kill the fungus. In addition, dust mite, insect, and plant debris are being evaluated to determine their fluorescent spectra and whether they will interfere with the spectra from the *Bacillus subtilis*. A commercial Level II Biosafety Cabinet is used for preparation of the biological samples.

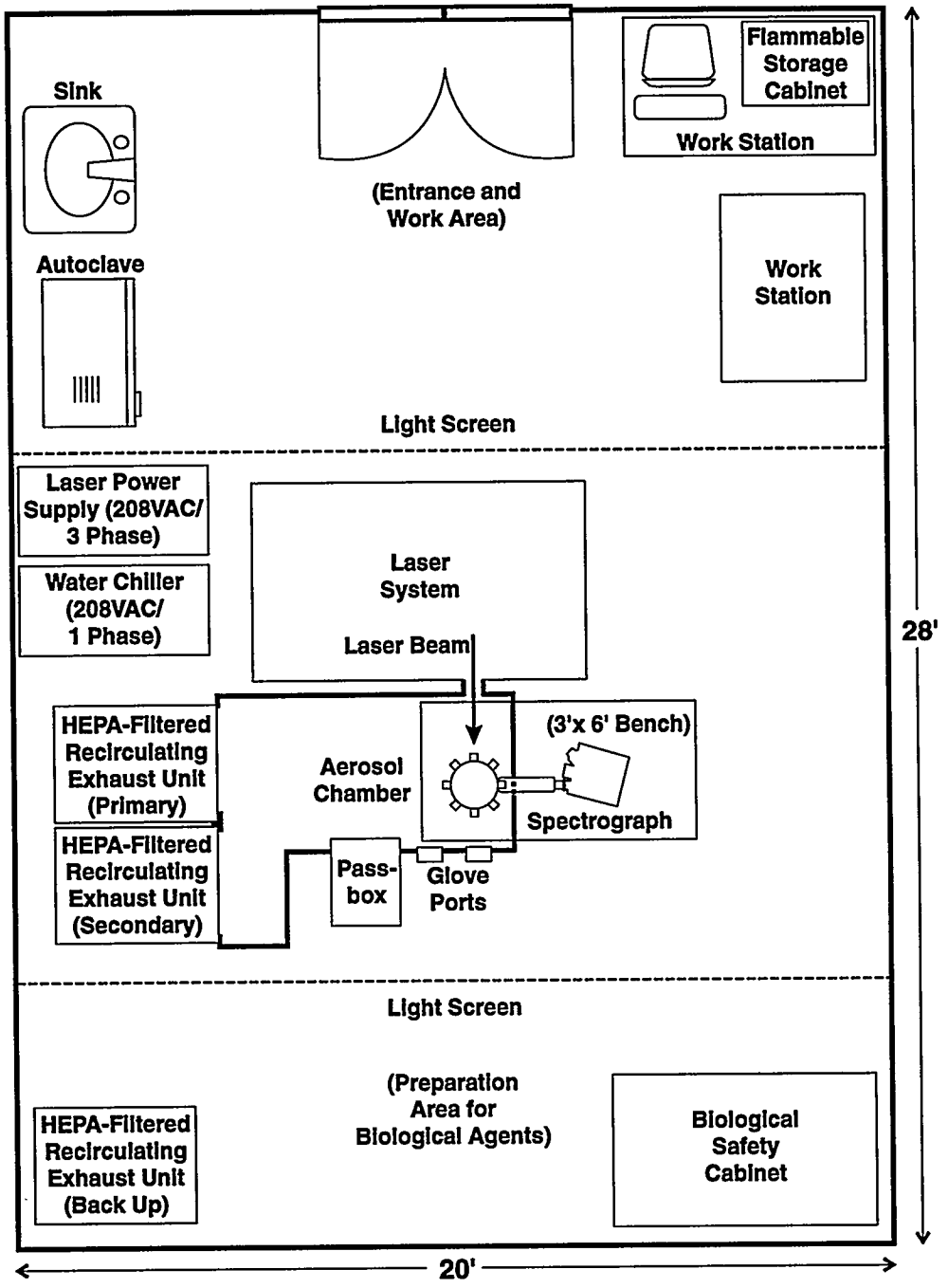

Figure 1. Floor plan of the ITRI Biosafety Level II Laboratory for testing of the SNL laser-based, real-time instrument for rapid detection of biological aerosols.

Figure 2 shows a schematic of the aerosol chamber used for generation and characterization of the pollens. The cylindrical section of the chamber is made of stainless steel with a 25-cm inner diameter and a 47-cm height. The chamber has eight windows with optical lens to allow laser light to enter the chamber and to permit remote detection of light scattered from particles in the chamber. Four sampling ports at the bottom plate of the chamber allow samples to be taken from the chamber. Airflow through the chamber is maintained between 10 and 20 L min^{-1} and is exhausted through a high-efficiency filter.

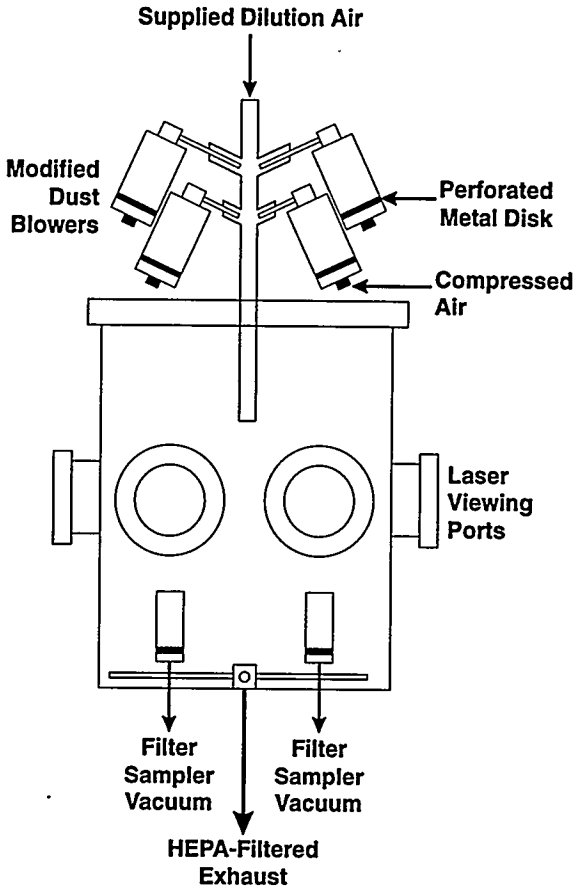

Figure 2. Schematic diagram of the modified dust blower system and the aerosol test chamber for laser-based detection of biological agents.

The pollen, insect, and plant debris are dry powders which are generated from an array of modified DeVilbiss dry powder dispersers (DeVilbiss Co., Somerset, PA). Modifications included replacing the glass reservoir with a larger, electronically grounded brass reservoir. This was done to provide a larger sample volume for longer generation times and to reduce electrostatic charge carried by the powder. Four generators were manifolded together to increase aerosol output. In addition, the compressed air tube for each disperser was removed, and a sintered metal screen was placed in the bottom of each reservoir. Each disperser is driven by a pulsed, compressed air jet to provide a more stable aerosol output. Compressed air is blown through the metal screen to provide a more uniform air jet, and the dispersers are pulsed alternatively in pairs to provide a stable output. The chamber and the aerosol delivery tube are designed to provide as short a distance as possible (about 3 cm) between the generators and the laser active volume. This minimizes wall losses of aerosol in the test system.

The bacteria and fungus spores were placed in aqueous suspension and aerosolized using a Retec nebulizer (InTox Products, Albuquerque, NM). The flow rate of the nebulizer was about 6 L min^{-1}. Filtered clean air was used to dilute the aerosol flow for a total of 10–20 L min^{-1} in the chamber. The desired aerosol concentration was between 100–10,000 particle cm^{-3}. For bacteria, an aerodynamic particle sizer was used to determine the concentration and size distribution in real time. In addition, an all-glass impinger was used to collect samples for determining the concentration of viable bacteria. The particle density was measured using a helium pycnometer (Multipycnometer, Quantachrome, Syosset, NY).

Preliminary tests have been completed on white oak pollen, *Bacillus subtilis*, and *Aspergillus fumigatus*. The measured aerosol sizes were 0.89 μm for *Bacillus subtilis*, 0.77 μm for *Aspergillus fumigatus*, and 19.7 μm for white oak pollen. The particle density was 1.27 g cm^{-3} for the pollen and 1.56 g cm^{-3} for the fungus. Pollen concentration ranged from 15–20 g m^{-3} (about 3000 particles cm^{-3}), while bacteria and fungus spore concentrations were 600 and 2500 particles cm^{-3}, respectively. Continuous generation of pollen and other test material for up to 2.5 h has been achieved. In the case of white oak pollen, the mass concentration is > 20 g m^{-3}, which is an extremely high concentration that challenges the characterizing and monitoring techniques.

In summary, a biosafe system has been developed for generating and characterizing biological aerosols and using those aerosols to test the SNL laser-based, real-time instrument. Such tests are essential in studying methods for rapid detection of airborne biological materials.

(Research performed under U.S. Department of Energy Contract No. DE-AC04-76EV01013 with funding from Sandia National Laboratories through Federal Agency Order AP-2829.)

EFFECT OF SOLVENT ON *IN VITRO* DISSOLUTION: SUMMARY OF RESULTS FOR URANIUM, AMERICIUM, AND COBALT AEROSOLS

Raymond A. Guilmette and Mark D. Hoover

The revised 10 CFR Part 20 has adopted the ICRP Publication 30 (*Annals of the ICRP, Limits of Intakes of Radionuclides by Workers*, Pergamon Press, Oxford, 1979) method for calculating the committed effective dose equivalent from intakes of radionuclides. This dosimetry scheme requires knowledge or assumptions about the chemical form of the radionuclide, its particle size, and its known or assumed solubility. The solubility is classified as being either D (relatively soluble), W, or Y (relatively insoluble), depending on whether the material dissolves over periods of days, weeks, or years. Although Nuclear Regulatory Commission licensees may wish to take advantage of material-specific knowledge in order to adjust annual limits on intake and derived air concentrations, relatively few radioactive materials to which workers and the general population may be exposed have been adequately characterized either in terms of physicochemical form or solubility. Experimental measurement of solubility using some type of *in vitro* dissolution measurement system is therefore needed. However, there is currently no clear consensus regarding the appropriate design of *in vitro* dissolution systems, particularly when considering the range of different radionuclides to be studied, and the complexity of the biological mechanisms involved in the retention and clearance of inhaled deposited radioactive particles. The purpose of this study was to evaluate the effect of several solvents on the dissolution of four test aerosols ($^{57}Co_3O_4$, $^{241}AmO_2$, ammonium diuranate [ADU], and U_3O_8) selected to encompass a variety of chemical and biochemical properties *in vivo*.

Aerosols of $^{57}Co_3O_4$ and $^{241}AmO_2$ (1.1–1.4 μm aerodynamic diameter, AD) were generated at ITRI using previously published methods (Kreyling, W. G. *et al. Am. J. Respir. Cell Mol. Biol. 2*: 413, 1990; Mewhinney, J. A. *et al. Health Phys. 42*: 611, 1982). Uranium mill products (designated in this report as ADU and U_3O_8) were obtained as bulk powders from two different mills in a previous research project (Eidson, A. F. and J. A. Mewhinney. *Health Phys. 39*: 893, 1980); these powders were size fractionated using a 5-stage cyclone train, with the particle size fraction corresponding to a range of 1.2–2.9 μm AD being used in this study. The design variables of the *in vitro* dissolution systems evaluated in this study included aqueous solvent composition, temperature, physical containment system, filter type, and pH. The effect of solvent is reported here. The solvents used were (1) synthetic ultrafiltrate, SUF (Kanapilly, G. M. *et al. Health Phys. 24*: 497, 1973), (2) synthetic lung fluid, SLF (Kalkwarf, D. *U.S. NRC Report No. NUREG/CR-0530*, 1978), (3) pH 5.0 HCl in H_2O, (4) SUF without the amino acids (but with diethylenetriaminepentaacetic acid, DTPA), and (5) carbonate and phosphate in equimolar amounts to those in SUF, buffered at pH 7.3 ± 0.1 with 0.1 M bis-tris propane (Sigma Chemical, St. Louis, MO). Except for the SLF and the pH 5.0 HCl, all solvents were maintained at pH 7.3 ± 0.1 for the duration of the 30-d studies. All samples were maintained at room temperature (≈ 20°C), and were contained in a static filter "sandwich" system. The filter medium was an aromatic copolymer membrane filter (Tuffryn-HT, 0.2 μm pore size; Gelman Sciences). Each experiment was done in duplicate. All ^{57}Co and ^{241}Am samples were assayed by gamma counting using a 5″ × 3″ NaI(Tl) scintillation detector. Samples containing uranium were assayed by laser phosphorimetry of acid-digested samples.

The dissolution data, expressed as percentage of undissolved radionuclide, were analyzed by sequentially fitting data sets to 1-, 2-, and 3-component negative exponential functions (SAS Proc NLIN, Cary, NC). The best mathematical fits were selected by comparing the respective residual sums of squares and the patterning of the residuals. The selected fit parameters were used to allocate the samples to classes D, W, and Y using the ICRP criteria on the half times: (1) class D for $T_{1/2}$ < 10 d; (2) class W for 10 d ≤ $T_{1/2}$ ≤ 100 d; and (3) class Y for $T_{1/2}$ > 100 d.

The dissolution behavior of the U_3O_8 particles in the various aqueous solvents is shown graphically in Figure 1. The best fits of their data are summarized in Table 1, along with the corresponding assignments to classes D, W, and Y. The range of assignable solubility classes varied significantly from mostly class D (pH 5.0), to mostly class W (SUF), to mostly class Y (carbonate/phosphate). In addition, the choice of solvent system greatly influenced the dissolution pattern. The pH 5.0 solvent manifested the most rapid dissolution, followed by the SUF + DTPA without amino acids, SUF, SLF, and carbonate/phosphate.

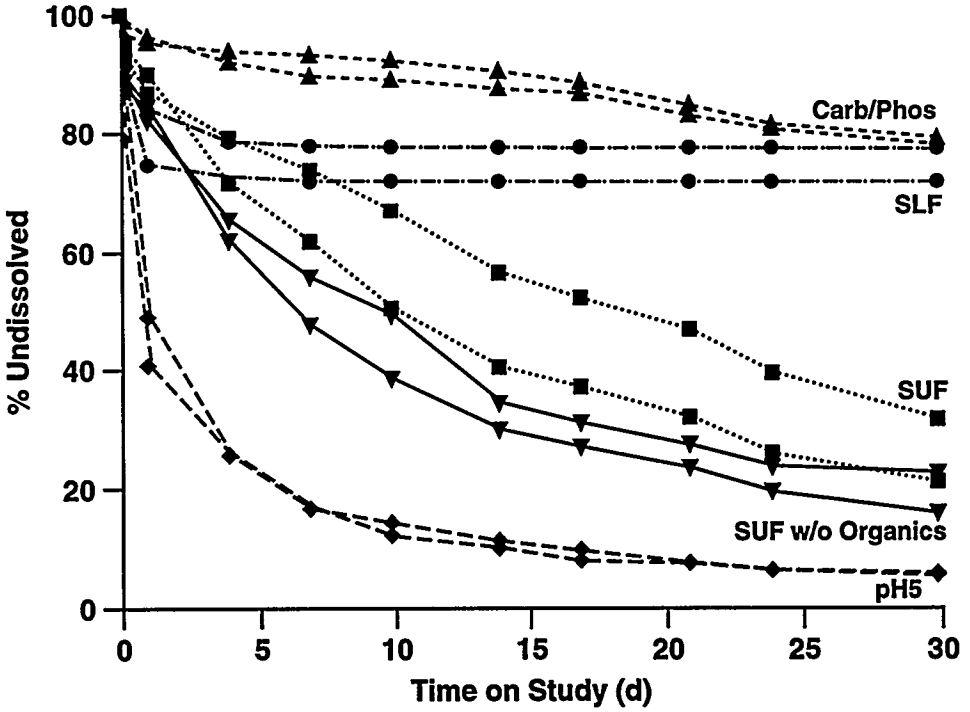

Figure 1. Dissolution of U_3O_8 uranium mill product in different solvent systems.

Table 1

Dissolution of U_3O_8 Mill Product in Different Solvents

	Fit Parameters[a]						Class Partition[b]		
Solvent	A_1	T_1	A_2	T_2	A_3	T_3	D	W	Y
Carbonate/Phosphate	4	0.16	96	100			4		96
SLF	17	0.10	8	1.2	75	4600	25		75
SUF	10	0.5	89	17			10	90	
SUF-Organics	62	5.0	32	35			66	34	
HCl (pH 5)	53	0.3	34	2.9	14	22	86	14	

[a]Dissolution coefficients, A_i, are given in percentages not normalized to 100%; the half-times, T_i, are in days.
[b]Based on solubility categories of ICRP 30.

The extreme range in solubility measurements observed with the U_3O_8 material was not found with the other test materials used in this study. Both ^{57}Co and ^{241}Am showed essentially complete class Y behavior regardless of solvent, whereas the soluble ADU material dissolved essentially as a class D material in all solvents, except for SLF, where > 80% dissolved as class Y, the remainder as class D.

Some of the divergent dissolution behaviors of the uranium oxides can be explained. The increased solubility of U_3O_8 noted with decreased pH is compatible with the known aqueous solubility characteristics of uranium oxides in mineral acid. This is of particular importance because particles deposited in the parenchymal region of the lung are phagocytized within about 24 h, whereupon their chemical environment changes from extracellular fluid at pH 7.3 to a phagolysosomal fluid medium with pH ranging from 4.5–5.5, depending on species. In the case of SLF, pH was not maintained at 7.3, consistent with the original method (Kalkwarf, 1978). Thus, the solvent pH increased over the first 2 d of the study to about 9.0. It can be seen in Figure 1 that U dissolution occurred during the first 2 d, and ended thereafter, consistent with the fact that U does not dissolve effectively at basic pH. The reason for the lack of dissolution using the simple carbonate/phosphate solvent is not known, although it is possible that the competitive balance between carbonate dissolution and phosphate precipitation may have been shifted to the precipitation reaction under the conditions of this study.

The results of this study provide some guidance on the usefulness of *in vitro* dissolution tests for estimating the solubility of unknown radionuclide particles within the context of a simple model such as the class D, W, and Y formulation of ICRP 30. It appears that consistent results can be obtained using different solvent systems if the material is either relatively soluble (class D) or relatively insoluble (class Y). However, for materials of intermediate solubility, such as the U_3O_8 used here, varying results can be obtained, leading to uncertain solubility estimates. It is clear that *in vitro* solubility results must be validated with *in vivo* studies if certain solvent systems are to be selected preferentially. Additionally, better understanding of the biochemistry of *in vivo* dissolution is needed to generalize results obtained with selected test materials to radionuclides in uncharacterized physicochemical forms.

(Research sponsored by the U.S. Nuclear Regulatory Commission under Fin No. L1264 NRC No. 60-93-952 with the U.S. Department of Energy, under Contract No. DE-AC04-76EV01013.)

DELIVERY OF AEROSOLIZED DRUGS ENCAPSULATED IN LIPOSOMES

Yung-Sung Cheng, Martin H. Schmid, and C. Richard Lyons***

Mycobacterium tuberculosis (Mtb) is an infectious disease that resides in the human lung. Due to the difficulty in completely killing off the disease in infected individuals, Mtb has developed drug-resistant forms and is on the rise in the human population. Therefore, ITRI and the University of New Mexico are collaborating to explore the treatment of Mtb by an aerosolized drug delivered directly to the lungs.

Aerosolized drugs are considered promising because they would deliver higher concentrations over prolonged periods of time directly to the infection, with fewer side effects than a drug consumed orally. However, the problem of aerosolizing the drug must be solved before the drug can be administered. One method to enhance the delivery of the drug is to encapsulate it within a liposome. Liposomes are small spherical vesicles made from phospholipids. Liposomes can create an artificial sac around the drug. Drugs encapsulated within liposomes have prolonged pulmonary retention times due to their low solubility in lung fluid. In addition, the size of the liposomes can be altered by sonification, which allows for the targeting of drug delivery to specific areas of the lungs. The purpose of this study was to test the size of the liposomes as a function of sonication and nebulization conditions and to determine whether a reasonable concentration of a drug can be contained within the liposomes for delivery to the lungs.

Liposomes were created by a simple, multistep procedure. First, L-a-Lecithin (egg phosphatidyl-choline) contained in hydrochloroform was dried over nitrogen gas (N_2) creating a layer of phospholipids. Next, that layer was resuspended in a desired solution (this could be water, a solution containing a drug, or a solution containing a fluorescent or radioactive tracer) and transferred into a clear, 6 mL polystyrene test tube. The concentration of the lipids for multilamellar liposomes must be between 1 and 5 mg mL^{-1}. Then the solution was placed under sonification in a Branson Sonifier 450 (Branson Ultrasonics Corp., Danburg, CT) until the solution looked clear when held up to the light (about 15 min for 1 mL of solution). The longer the liposomes are sonicated, the smaller they become, and as they are sonicated, they form spherical vesicles that encase the solution.

The liposomes were sized in two different ways. Several samples were sent off to a laboratory in Canada for sizing using a liquid-phase, laser-diffraction particle sizer. Other samples were sized in our laboratory using the electron microscope (EM). A published procedure was used to view the liposomes on the EM (New, R. R. C. In *Liposomes a Practical Approach*, IRL Press at Oxford University Press, p. 92, 1990).

Table 1 shows the physical size of the liposomes as determined by laser diffraction following three conditions of sonication (0, 7.5, and 15 min). The EM gave a maximum size of 60 nm, a minimum size of 23 nm, and an average size of 32 nm. These sizes were substantially smaller than those from the laser diffraction method (results in Table 1). The EM samples could not be used to get a reliable size distribution because only limited amounts of liposomes were viewed due to the difficulty of getting the liposomes on the grids. There were also aggregations of several liposome particles in the pictures.

---

*Lovelace-Anderson Endowment Fund Summer Student Research Participant
**Department of Pathology, University of New Mexico, Albuquerque, New Mexico

Table 1

Comparison of Liposome Size with Different Amounts of Sonification

	No Sonification	7.5 min of Sonification	15 min of Sonification (clear solution)
Liposomes created in water	2148 nm	1960 nm	630 nm
Liposomes created in fluorescence (10 mg/mL)	4950 nm	770 nm	270 nm
Liposomes created in fluorescence (1 mg/mL)	1670 nm	270 nm	350 nm

To estimate the amount of a drug which might be encapsulated within the liposomes, the phospholipid layer was resuspended in a solution of fluorescence mixed with ovalbumin diluted in phosphate buffered saline (PBS) at concentrations of 10, 1, and 0.1 mg/mL fluorescence. Next, the liposomes were purified by mixing 0.5 mL of clear, sonicated liposomes with 30% Ficoll solution by weight in PBS, and the mixture was placed in a 5 mL centrifuge tube. Then, 1 mL of 10% Ficoll and 1 mL of PBS were layered on top creating a separation gradient and centrifuged at 100,000 *g* for 30 min at room temperature. After being centrifuged, the pure liposomes were found between the PBS and 10% Ficoll layer and were drawn off using a pipette. Next, some of the liposomes were broken apart using a Triton X detergent to allow the fluorescence back into solution for determination of the concentration. A fluorescence spectrophotometer was used to measure the relative amount of fluorescence contained in the samples. Some of the liposomes were allowed to sit in solution for 6 d, then purified using the same method and broken up to determine the amount of fluorescence being lost over time.

The liposomes did retain a substantial amount of fluorescence inside the vesicles. At each of the three concentrations, the liposomes lost fluorescence after 6 d of storage, as can be seen in Figure 1. Cholesterol could be added to the phospholipid layer to strengthen the membrane of the liposomes which allows better retention of the fluorescence in the liposomes over time. Data for this have not yet been obtained.

The liposomes were nebulized using two different nebulizers, the RespirGard (Marquest, Englewood, CO) and the Hospitak (Hospitak, Lindenhurst, NY). Different solutions of liposomes were nebulized through a drying chamber and into a larger chamber with a flow laminator. Some flow was drawn onto an EM grid and treated with stain to view. The rest of the flow was drawn through a diffusion battery with five stages and an ultrafine condensation particle counter to determine the size of the aerosolized liposomes. All liposomes nebulized were prepared by sonicating 15 min (to clear solution) before nebulizing.

The results from the nebulizer sizing by using a serum diffusion battery/condensation nucleus counter (DB/CNC) are summarized in Table 2. The sizing from the EM gave an average size of 49 nm for both nebulizers. Although the results from the laser and EM methods were consistent in this case, again there were not enough liposomes to get a complete size distribution using the EM.

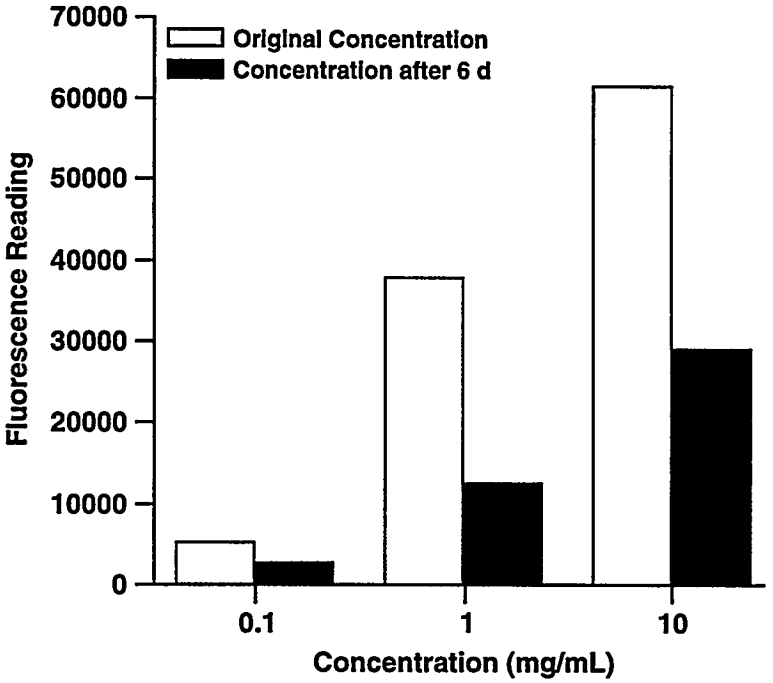

Figure 1. Influence of fluorescence concentration during liposome preparation on the concentration and retention of fluorescence in the liposomes.

Table 2

Size of Liposomes Using Different Nebulizers[a]

Nebulizer	Liposomes in Distilled Water (nm)	Liposomes in Fluorescence 1 mg/mL (nm)	Liposomes in Fluorescence 10 mg/mL (nm)	Average (nm)
RespirGard II	43	40	38	40
Hospitak	61	39	50	50

[a]Results obtained by DB/CNC.

In conclusion, it is feasible to obtain an appropriate size and concentration of the liposomes before and after aerosolization. Because the liposomes are submicrometer in size, they can reach the pulmonary region of the lung. In the next phase of the study, isoniazid will be placed in the liposomes and delivered to rats infected with Mtb to determine if the treatment will be effective.

(Research sponsored by the Office of Health and Environmental Research, U.S. Department of Energy, under Contract No. DE-AC04-76EV01013.)

COMPUTER SIMULATION OF AIRFLOW THROUGH A MULTI-GENERATION TRACHEOBRONCHIAL CONDUCTING AIRWAY

Bijian Fan, Yung-Sung Cheng, and Hsu-Chi Yeh*

Knowledge of airflow patterns in the human lung is important for an analysis of lung diseases and drug delivery of aerosolized medicine for medical treatment. However, very little systematic information is available on the pattern of airflow in the lung and on how this pattern affects the deposition of toxicants in the lung, and the efficacy of aerosol drug therapy. Most previous studies have only considered the airflow through a single bifurcating airway. However, the flow in a network of more than one bifurcation is more complicated due to the effect of interrelated lung generations. Because of the variation of airway geometry and flow condition from generation to generation, a single bifurcating airway cannot be taken as a representative for the others in different generations. The flow in the network varies significantly with airway generations because of a redistribution of axial momentum by the secondary flow motions. The influence of the redistribution of flow is expected in every generation. Therefore, a systematic information of the airflow through a multi-generation tracheobronchial conducting airway is needed, and it becomes the purpose of this study.

The lung model used in this study is a symmetric four-generation tracheobronchial tree with 16 branches of rigid bifurcating tubes. The tube dimensions and bifurcating angles are based on the Typical Lung Path Model (Yeh, H. C. and G. M. Schum. *Bull. Math. Biol. 42*: 461, 1980). The three-dimensional model was digitized, and its finite element mesh is shown in Figure 1. This model has the same topological structure as a lung and can be used to investigate the characteristics of the pulmonary flow. The airflow through the lung model was simulated on a computer. It was done by solving the flow governing equation using a computational fluid dynamics software, FIDAP (Fluid Dynamics International, *FIDAP User Manual*, v.7, 1995).

The resulting flow velocity vectors on the central bifurcation plane at the flow condition of Reynolds number Re = 700 is given in Figure 2. In the first bifurcation, air from the mother tube flows evenly into the daughter tubes; the flow peaks shift toward the inner side edge of the daughter tubes and separates in the outer side region. Because the daughter tubes are shorter than the mother tube, the flow of air cannot develop fully in the first generation. Underdeveloped flow in turn affects the flow in the following generation of daughter tubes. Therefore, the flow through each individual bifurcation varies, and knowledge of the flow through a single bifurcation is insufficient to understand the flow through a tracheobronchial tree.

Because each branch is oriented differently to the mother tube, the flow resistance varies, although each tube in the same generation has the same dimension and surface area. As a result, the flow resistance affects the flow rate through each branch of the tracheobronchial tree. More air flows into the branch with less flow resistance, and the binary distribution of flow rates no long applies beyond the first bifurcation. The flow rate was calculated at the end of each branch, and the distribution of flow rates through the tracheobronchial tree was shown in Figure 1 as well. This nonuniform distribution of flow agreed with our ongoing preliminary study (data not shown). It predicts that more oxygen can be carried to the lower lobes of lungs for the exchange of oxygen and carbon dioxide and may explain why the lower lobes are always attached to more alveoli and are thus larger than the upper lobes.

*Postdoctoral Fellow

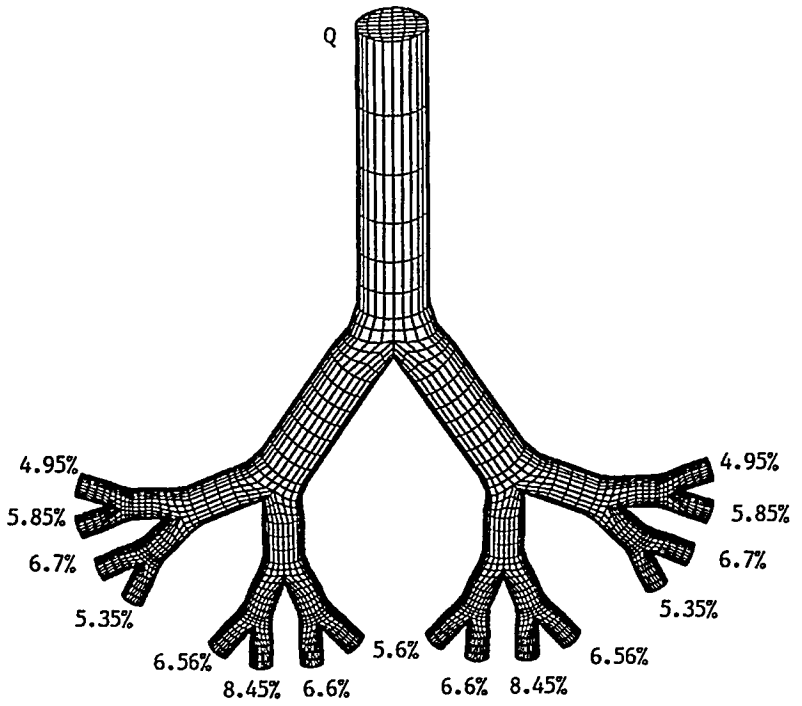

Figure 1. Illustration of the finite element mesh used in the three-dimensional fluid dynamics model of the human tracheobronchial tree. The calculated distribution of flow rates through the airways is also shown.

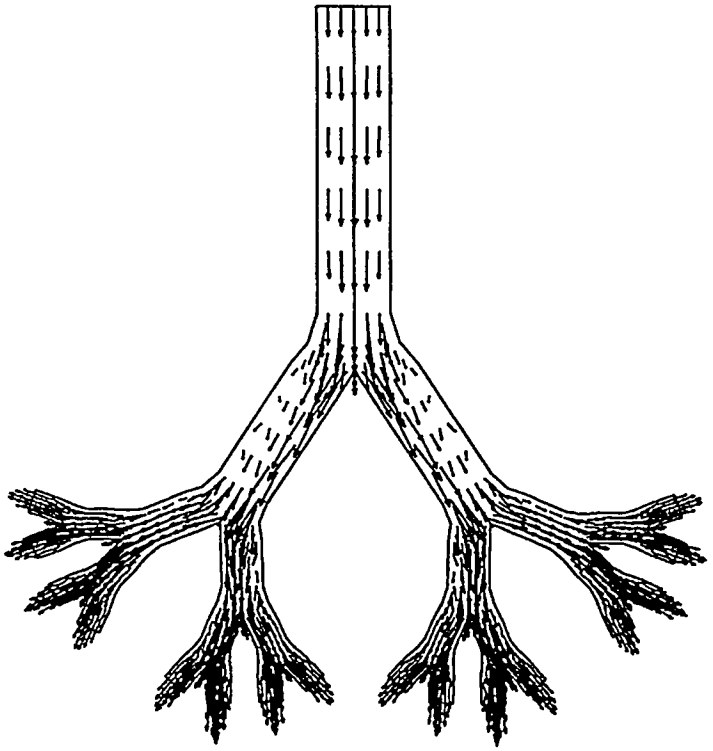

Figure 2. Illustration of the computed flow velocity vectors on the central bifurcation plane of the fluid dynamics model of the human lung (flow condition of Re = 700).

This study has provided information on airflow in a lung model which is necessary to the study of the deposition of toxicants and therapeutic aerosols. It provided evidence for the nonuniform distribution of air through lungs, which can be used to explain the anatomical structure of lungs from the point of view of fluid mechanics.

(Research sponsored by the Office of Health and Environmental Research, U.S. Department of Energy, under Contract No. DE-AC04-76EV01013.)

DEMOLITION AND REMOVAL OF RADIOACTIVELY CONTAMINATED CONCRETE AND SOIL: AEROSOL CONTROL AND MONITORING

George J. Newton, Mark D. Hoover, and Augustine C. Grace, III

From 1963 to 1985, two concrete-lined ponds were used to reduce the volume of radioactive liquids from the Institute's research programs. Following withdrawal of the "hot ponds" from active use, the residual sludges and plastic liners of the ponds were removed and shipped to a radioactive waste disposal site. From 1987 to 1994, the concrete structures remained undisturbed pending environmental restoration of the site. Restoration began in 1994 and was completed in 1995. Restoration involved mechanical breakup and removal of the concrete structures and removal of areas of contaminated soils from the site. This report describes the design and results of the aerosol control and monitoring program that was conducted to ensure protection of workers and the environment during the restoration process.

Radiation surveys of the hot pond site had revealed small quantities of both beta-gamma- and alpha-emitting radionuclides: ^{60}Co (0.004 mCi), ^{90}Sr-^{90}Y (13.7 mCi), ^{134}Cs (0.005 mCi), ^{137}Cs-^{137}Ba (5.5 mCi), ^{238}Pu (4.3 mCi), ^{239}Pu (1.1 mCi), ^{241}Am (0.4 mCi), and ^{244}Cm (0.1 mCi). Because this radioactivity was incorporated into the soil and concrete matrices, it did not pose an inhalation hazard during normal work activities at the site. However, it was anticipated that respirable aerosols of these radionuclides might be created during mechanical breakup of the concrete and removal of the contaminated concrete and soil. Although the airborne concentrations of these radionuclides were expected to be quite low, perhaps even within statutory limits without extensive dust suppression, remediation of the ITRI hot ponds was taken as an opportunity to demonstrate a comprehensive program of aerosol suppression and monitoring. This program involved the following steps: (1) a temporary, fabric-covered structure was erected over the hot ponds to limit dispersion of airborne materials during the restoration; (2) an adjoining temporary structure was erected to provide an enclosed area for remote control of the demolition tools, and for monitoring and packaging of contaminated materials; (3) a plastic spray was applied to concrete surfaces immediately prior to breakup of the concrete to suppress dust formation; (4) local vacuum filtration was used during breakup of the concrete to capture any dusts formed by sawing or jack-hammering; (5) jack-hammering was accomplished by remote control from the monitoring structure to minimize the need for workers to be inside the main structure during demolition; (6) an array of fixed and continuous air monitoring instruments was deployed within the temporary structures to monitor air quality in the workplace; and (7) five high-volume air samplers were deployed at the perimeter of the hot pond site to confirm that no offsite releases were occurring. Underground electrical lines were installed to provide 110 V power on ground-fault-protected circuits for the perimeter samplers. Figure 1 shows the layout of the temporary structures and the perimeter monitors on the 2-acre hot pond site.

Operation of the high-volume perimeter air samplers began 1 wk prior to initiation of work at the site. Sampling continued through the setup of the containment structures, removal of contaminated materials, and disassembly of the containment structures. Hi-volume samples (8 in × 10 in glass fiber filters) were analyzed by low-level radiochemistry at an outside, contract laboratory. Concentrations for the radionuclides of concern were below the limit of detection, indicating no offsite releases occurred.

Operation of the workplace samplers began after assembly of the containment structures and 1 wk prior to initiation of concrete removal. Workplace samples included 47-mm diameter filter samples for determination of total airborne dust and airborne radionuclide concentrations; Lovelace multi-jet cascade impactor samples for determination of airborne dust and radionuclide concentrations and for

determination of aerodynamic particle size distributions; 5-stage multi-cyclone train samples to obtain masses of size-selected dusts sufficient for potential use in other analyses such as determination of solubility in biological fluids; point-to-plain electrostatic precipitator samples for electron microscopy to determine particle size and morphology; Eberline Alpha 6 continuous air monitors (CAMs) (Eberline Instruments, Santa Fe, NM) for monitoring of airborne alpha-emitting radionuclides; and Eberline AMS-4 CAMs for monitoring of airborne beta-emitting radionuclides. Data from the alpha and beta CAMs were logged continuously to computers in the monitoring structure.

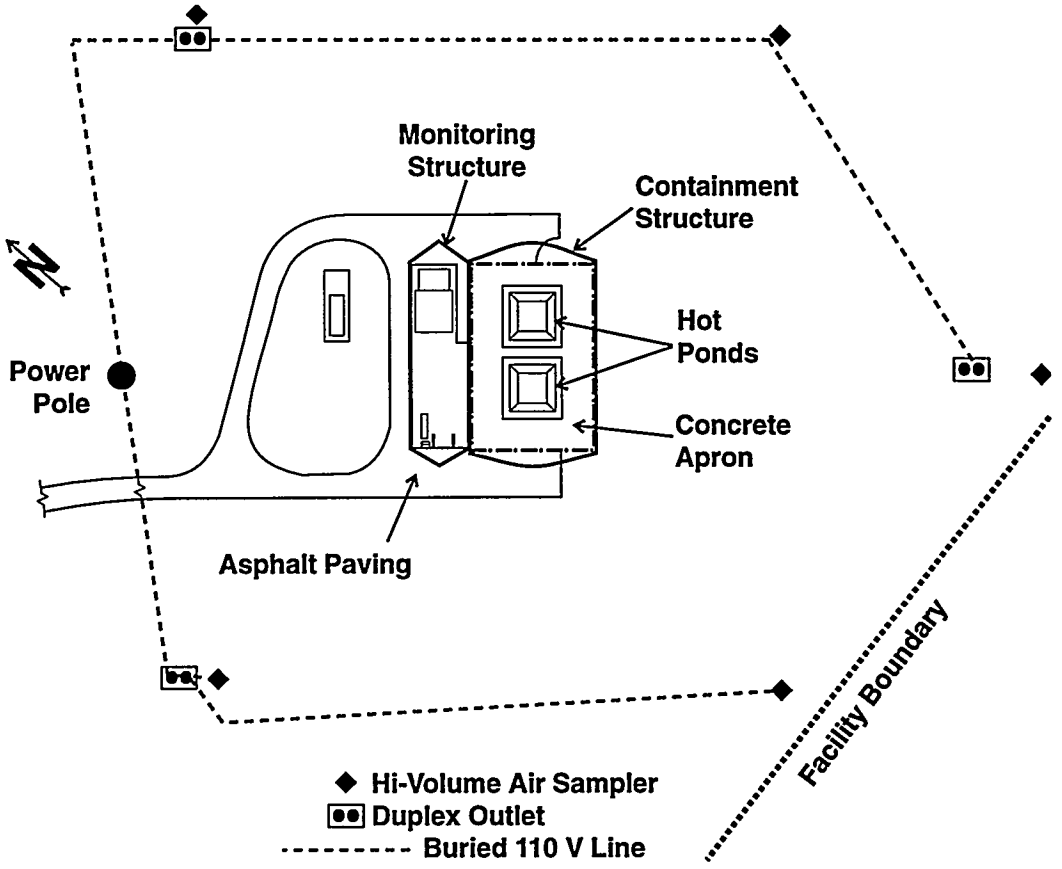

Figure 1. Layout of the ITRI hot pond site, showing the location of the concrete ponds, the containment and monitoring structures, and the perimeter air monitoring system.

Particle size distributions based on the gravimetric measurements of airborne dusts collected in the containment structure with cascade impactors were typically 8 μm mass median aerodynamic diameter with a geometric standard deviation of 1.8. The particle size distributions based on radioactivity in the airborne dusts were smaller, typically on the order of 2 μm activity median aerodynamic diameter with a geometric standard deviation of 1.8. Fortunately, no concentrations of airborne dust > 1 mg/m^3 were measured inside the containment structure during any of the restoration operations. This indicates the excellent performance of the dust suppression techniques.

In addition, radionuclide concentrations within the containment structure were also low to nondetectable. For example, even for ^{90}Sr-^{90}Y (the most prevalent radionuclides at the hot pond site, and the most restrictive of the beta-gamma-emitting radionuclides based on allowable air concentrations), no concentrations above 10% of the statutory derived air concentration (DAC) were observed. Figure 2 displays a typical 24-h concentration profile from one AMS-4 beta CAM during removal of contaminated concrete at the hot pond site. Results from the alpha CAMs were at or near

background for the existing conditions of ambient radon decay products. However, accumulation of high levels of dust on the collection filter of the alpha CAMs tended to cause some overreporting of counts in the plutonium region of interest (subsequent analyses by alpha spectroscopy after decay of radon progeny [4 h] indicated no Pu). Although overreporting of counts in the plutonium region is conservative for worker protection, false alarms are not desirable. These data indicate that we must either improve the correction algorithm for alpha CAMs operated in dusty environments or, alternatively, set alpha CAM alarm set points somewhat higher than 8 DAC-h (24 DAC-h would be adequate) to prevent false alarms during dusty operations.

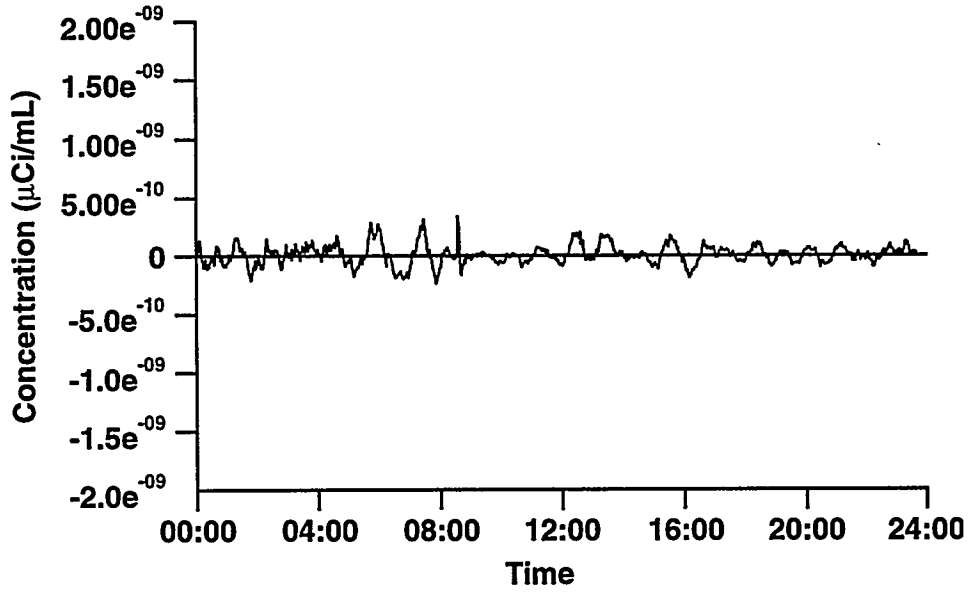

Figure 2. Graph of the workplace air concentration of beta-emitting radionuclides detected by the AMS-4 continuous air monitor during removal of contaminated concrete at the ITRI hot pond site. The alarm set point was 8.0×10^{-8} μCi/mL.

The aerosol control and monitoring strategy developed for remediation of the ITRI hot ponds was successful both in preventing dispersion of radioactive dusts and in demonstrating that exposures of workers and offsite releases were within statutory limits. The methods described here can be applied to remediation activities involving substantially higher levels of radioactivity.

(Research sponsored by the Office of Environmental Management, U.S. Department of Energy, under Contract No. DE-AC04-76EV01013.)

USE OF SULFUR HEXAFLUORIDE AIRFLOW STUDIES TO DETERMINE THE APPROPRIATE NUMBER AND PLACEMENT OF AIR MONITORS IN AN ALPHA INHALATION EXPOSURE LABORATORY

George J. Newton and Mark D. Hoover

Determination of the appropriate number and placement of air monitors in the workplace is quite subjective and is generally one of the more difficult tasks in radiation protection. General guidance for determining the number and placement of air sampling and monitoring instruments has been provided by technical reports such as Mishima, J. *et al.* (*Health Physics Manual of Good Practices for the Prompt Detection of Airborne Plutonium in the Workplace*, U.S. DOE, PNL-6612, 1988) and Hickey, E. E. *et al.* (*Air Sampling in the Workplace*, U.S. Nuclear Regulatory Commission, NUREG-1400, 1993). These two documents and other published guidelines suggest that some insight into sampler placement can be obtained by conducting airflow studies involving the dilution and clearance of the relatively inert tracer gas sulfur hexafluoride (SF_6). The work reported here reviews the important considerations for using SF_6 in sampler placement studies and describes the results of a study done within the ITRI alpha inhalation exposure laboratories. The objectives of the study were to document an appropriate method for conducting SF_6 dispersion studies, and to confirm the appropriate number and placement of air monitors and air samplers within a typical ITRI inhalation exposure laboratory.

Tracer gas characterization of ventilation systems has become widely accepted within the building engineering community, and ASTM Standard E-741 describes a standard method for using SF_6 to measure air-leakage (ventilation) rates within structures. However, SF_6 airflow studies for air sampler placement are restricted to the following conditions: (1) facilities with once-through ventilation, and (2) situations in which the particle sizes of toxicological concern are < 5 μm aerodynamic diameter. If air is recirculated, SF_6 cannot be used because of the reintroduction of exhaust air into the room. In those cases, a method employing labeled particles and filtration of recirculated air must be used. If the sizes of potential releases would be > 5 μm aerodynamic diameter, labeled particles of the appropriate sizes should be used.

Development and application of an SF_6 dispersion methodology for use at ITRI involved the following steps: (1) selection and calibration of a commercial SF_6 analyzer; (2) determination of an appropriate volume and concentration for the SF_6 releases; (3) selection of appropriate syringes for collection and retention of room air samples; (4) identification of potential aerosol release points (appropriate SF_6 release points) within the workplace; (5) selection of potential locations for worker exposures (potential locations for air samplers and monitors, and, therefore, suitable locations for collection of room air samples during the dispersion tests); and (6) determination of an appropriate schedule (based on the dynamics of air dilution and dispersion in the workplace) for collection of room air samples following an SF_6 release.

We selected the Model 101 AccuTrack gas chromatograph (Lagus Applied Technology, Inc., San Diego, CA) for use at ITRI because it is the only commercial gas analyzer package with an electron-capture, gas chromatograph which is specifically designed for detection of SF_6. We calibrated the analyzer with NIST-traceable SF_6 samples and conducted the dispersion studies with reagent-grade SF_6 from a specialty gas supplier.

Figure 1 shows the typical ITRI inhalation exposure laboratory that was chosen for characterization in this study. Based on a detection limit of < 1 part per trillion (ppt) for the AccuTrack, a room volume of 60 m^3 (4.83 m long × 4.06 m wide × 3.05 m high), and a room ventilation rate of 10 air

changes per hour, each release of SF_6 involved a volume of 2 mL at a concentration of 1% by volume. At such a low concentration, the known asphyxiation hazard (oxygen displacement) associated with use of SF_6 is not a practical concern.

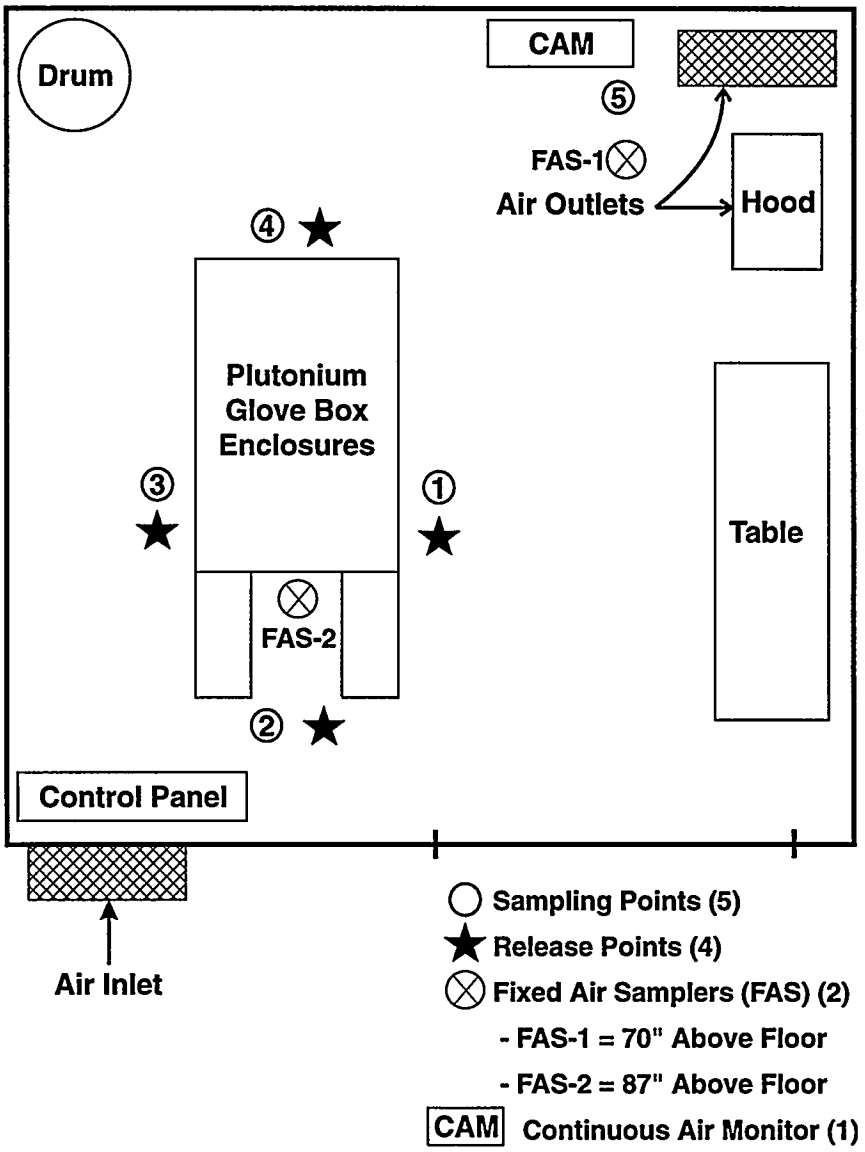

Figure 1. Sketch of the inhalation exposure test room showing the five sampling points and the four points for release of SF_6. Inlet air passed through a 20″ x 24″ filter, 12″ above the floor. Exhaust exited through a 20″ × 24″ filter, 85″ above the floor.

The primary, compressed SF_6 storage tank (1% concentration) was stored in a laboratory remote from the test location. Prior to each test series, a small (200 mL) transfer flask was evacuated and filled with SF_6. The transfer flask was held outside the test location (typically outdoors) so that the 2-mL injection sample syringe could be filled without contaminating the test room.

The selection of appropriate syringes for injection of the SF_6 release and collection of the SF_6-containing room air samples was an important aspect of the study. Initial tests were done with syringes that were equipped with standard rubber caps. These traditional caps did not adequately contain the SF_6 and typically resulted in losses of up to 15% of the SF_6 concentration from the

syringes within 2 h. We, therefore, obtained less-permeable syringe caps made of polyethylene (B-D Cat #9604, Becton Dickinson, Franklin Lakes, NJ). Use of these caps provided substantial improvement in sample retention with no detectable loss of sample after times as long as 48 h.

We released SF_6 from four different simulated release locations within the test room (see Fig. 1) at glove-port height (4 ft above the floor). These locations correspond to those where workers typically manipulate the apparatus within the glovebox enclosure. Syringe samples (10 mL) of the assumed breathing air from these four locations were simultaneously obtained manually at a height of 2 m above the floor at elapsed times of 0.5, 1.0, 2.0, 4.0, 10, 20, 30, and 40 min after release. A polyethylene sampling line was also connected directly to the AccuTrack so that repetitive samples (every 2.5 min minimum recovery time for the analyzer) could be taken near the exhaust outlet of the room (sample location 5, also shown in Fig. 1). That location corresponds to the current location of the alpha continuous air monitor in the room. Because there is a 2.5 min recovery time for the AccuTrack analyzer, manual samples at location 5 were also taken at 0.5, 1.0, and 2.0 min time intervals to characterize the early dynamics of the release.

Following collection of all samples, the concentration of SF_6 at each sampling position was determined by injection of the syringe contents into the sample port of the AccuTrack gas chromatograph. Data for concentrations of SF_6 from each sampling point were downloaded from the computer memory in the Model 101 Accutrack and plotted on a personal computer using PlanPerfect, (WordPerfect Corp., Orem, UT). The integrated concentration $\times$ time after release was determined for each sampling point, Σ(ppt $\times$ minutes).

Figure 2 illustrates data obtained from SF_6 released at point 2. These data are representative of SF_6 concentration data obtained at the other three release points. Note the initial rapid increase of SF_6 concentration at each sampling point. This indicates the importance of frequent sampling at the early time points. The integrated concentration $\times$ time data approached a plateau within only 3 min and indicated relatively little change in integrated exposure after 5 min. This confirms that any brief release of aerosol is essentially cleared from the room within 5 min, which is consistent with the known ventilation rate of 10 air changes per hour in the room. In addition, it is encouraging to note that the integrated exposure concentrations at all sampling locations were within a factor of two, indicating that any sampling location would have been adequate to provide a representative sample during a release from point 2. Similar results were obtained at other release points. Note that the actual locations of release were not always the location of highest integrated concentrations because the bolus of the release gets carried away from the release point. The dynamics of airflow often caused a release at one point to result in a higher concentration at another location. In nearly all cases, however, the sampling location near the exhaust duct provided one of the higher integrated concentrations.

The results of this study have become part of the technical bases for air sampling and monitoring in the test room. They indicate that the air monitoring requirements for this room can be met with a single continuous air monitor placed near the room exhaust register. In addition, nonuniform dispersion of aerosol releases may explain why some historical exposure cases have resulted in higher exposures to workers away from the source than to workers at the source. This emphasizes the importance of using actual airflow patterns to assist in dose reconstructions. Finally, valuable lessons have been learned about use of improved syringe caps for maintaining sample integrity and the importance of early-time sampling to adequately assess the dynamics of SF_6 dispersion in the workplace.

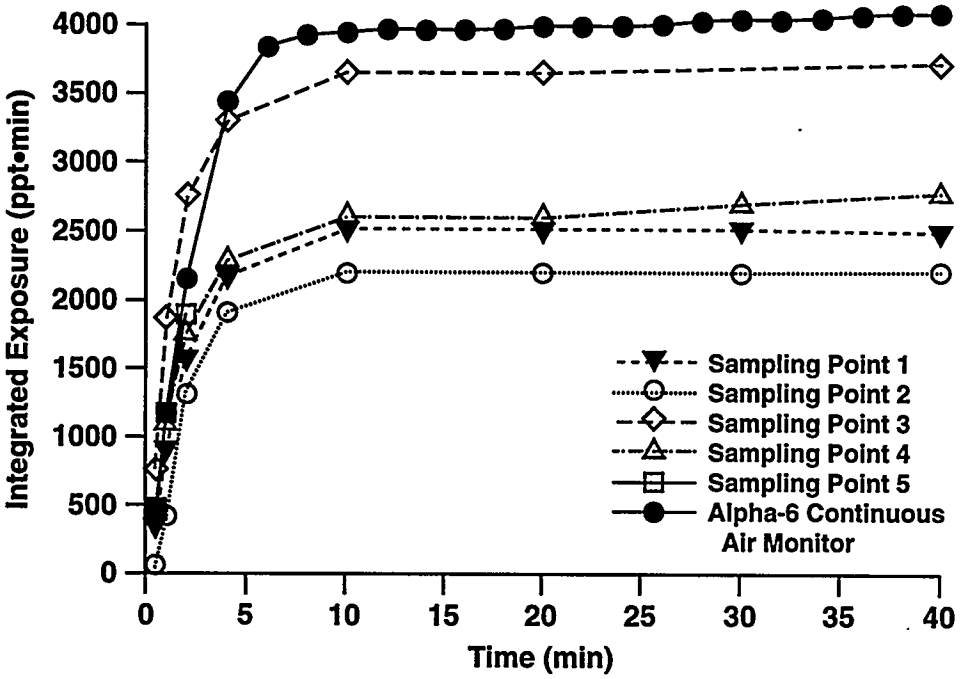

Figure 2. Graph of the integrated exposure, Σ(ppt × min), concentration of SF_6 measured at the various sampling points in the test room after release of SF_6 at position 2.

(Research sponsored by the Albuquerque Operations Office, U.S. Department of Energy, under Contract No. DE-AC04-76EV01013.)

LESSONS LEARNED FROM CASE STUDIES OF INHALATION EXPOSURES OF WORKERS TO RADIOACTIVE AEROSOLS

Mark D. Hoover, Alice F. Fencl, George J. Newton,
Raymond A. Guilmette, Bobby R. Scott, and Bruce B. Boecker

Various Department of Energy requirements, rules, and orders mandate that lessons learned be identified, evaluated, shared, and incorporated into current practices. The recently issued, nonmandatory DOE standard for *Development of DOE Lessons Learned Programs* (DOE-STD-7501-95) states that a DOE-wide lessons learned program will "help to prevent recurrences of negative experiences, highlight best practices, and spotlight innovative ways to solve problems or perform work more safely, efficiently, and cost effectively." Additional information about the lessons learned program is contained in the recently issued DOE handbook on *Implementing U.S. Department of Energy Lessons Learned Programs* (DOE-HDBK-7502-95) and in the October 1995 DOE Safety Notice on *Lessons Learned Programs* (Safety Notice Issue No. 95-03). This report summarizes work in progress at ITRI to identify lessons learned for worker exposures to radioactive aerosols, and describes how this work will be incorporated into the DOE lessons learned program, including a new technical guide for measuring, modeling, and mitigating airborne radioactive particles.

During the past 2 y, we have been evaluating strategies for minimizing occupational exposures to airborne radionuclides (see, for example, Boecker, B. B. *et al. Radiat. Prot. Dosim. 53*: 69, 1994). This has included assembling and reviewing case studies from the U.S. Department of Energy's Operating Experience Weekly Summary (OEWS) Reports, the U.S. Nuclear Regulatory Commission License Event Report Data Base for Power Reactors, the U.S. NRC Material Events Data Base, open literature publications, and personal communications. We have incorporated this information into an inhalation-exposure data base. We are using past experiences from inhalation exposures of workers to radioactive aerosols to identify (1) root causes of exposures, (2) typical physical characteristics of exposure aerosols, (3) typical severity of exposures, (4) relative importance of worker training, administrative controls, engineered controls, respiratory protection, and alarming air monitors, and (5) requirements for improved occupational health treatment and follow-up of exposed workers.

We have identified several root causes for inhalation exposures of workers. They include (1) poor labeling of equipment or ambiguous instructions to workers about the location and status of equipment to be serviced, (2) failure to follow procedures, (3) confusion regarding responsibilities, especially during facility startup or changeover, (4) failure to understand or anticipate potential interactions of systems and equipment during facility startup or changeover, (5) improperly installed or modified equipment, (6) inadvertent shutoff of safety systems during maintenance, and (7) aging or deteriorating equipment.

Some general observations are that (1) inhalation exposures of workers above the statutory limits are rare, (2) improved air monitoring would not have prevented these exposures, (3) multiple indicators of problems were generally present, and that (4) even when available, correlations of measurements from area sampling, personal air sampling, and bioassay were poor. In conjunction with these poor correlations, we have identified some special concerns for high-specific-activity radionuclides such as ^{238}Pu. High-specific-activity aerosols can have extremely low number concentrations at the statutory limits for derived air concentration in the workplace, i.e. << than 1 particle per breath (1992–93 Annual Report, p. 136). Assuming a uniform distribution of airborne radioactivity for radionuclides such as ^{238}Pu can lead to overestimation of inhalation uptake and poor correlation of area samples, personal samples, and bioassay results. We need improved models and approaches for assessing worker exposures to high-specific-activity aerosols.

Some additional general observations about inhalation exposures of workers are that (1) they usually result from relatively brief and intermittent "puff-type" releases of radionuclides, rather than from continuous releases of radioactivity in workplace air, (2) hand, foot, and surface contaminations are frequently the first indicators of a problem, (3) depending on placement and sensitivity, air monitors sometimes provide an early warning, and (4) excessive false alarms in the air monitoring systems often cause workers to ignore "real" alarms, thus allowing exposures to continue.

Areas for needed improvements include development of (1) defensible methods for determining appropriate numbers and placement of air samplers and monitors, (2) procedures to collect aerosol samples for use in biodosimetry modeling (note that collecting samples runs counter to the normal health physics accident response, which is to prevent further exposures), (3) better models for evaluating inhalation and deposition of high-specific-activity aerosols in the respiratory tract, and (4) improved *in vitro* characterization methods for moderately soluble particles to improve the estimation of doses to workers from inhalation of moderately soluble materials.

Follow-on work is focusing on preparation of "lessons learned" training materials for facility designers, managers, health protection professionals, line supervisors, and workers. We intend to disseminate this material by direct dialog with users through the DOE Operating Contractors Air Monitoring User Group, by electronic communication through the DOE Lessons Learned Information System, and through development of a technical guide for measuring, modeling, and mitigating airborne radioactive particles. This should improve the effectiveness and efficiency of worker protection programs in DOE facilities.

(Research sponsored by the Assistant Secretary for Defense Programs, U.S. Department of Energy, under Contract No. DE-AC04-76EV01013.)

ASSESSMENT OF POTENTIAL DOSES TO WORKERS DURING POSTULATED ACCIDENT CONDITIONS AT THE WASTE ISOLATION PILOT PLANT

*Mark D. Hoover, George J. Newton, and Richard F. Farrell**

The recent *1995 WIPP Safety Analysis Report (SAR) Update* (DOE/WIPP-2065) provided detailed analyses of potential radiation doses to members of the public at the site boundary during postulated accident scenarios at the U.S. Department of Energy's Waste Isolation Pilot Plant (WIPP). The SAR Update addressed the complete spectrum of potential accidents associated with handling and emplacing transuranic waste at WIPP, including damage to waste drums from fires, punctures, drops, and other disruptions. The report focused on the adequacy of the multiple layers of safety practice ("defense-in-depth") at WIPP, which are designed to (1) reduce the likelihood of accidents and (2) limit the consequences of those accidents. The safeguards which contribute to defense-in-depth at WIPP include a substantial array of inherent design features, engineered controls, and administrative procedures. The SAR Update confirmed that the defense-in-depth at WIPP is adequate to assure the protection of the public and environment. As a supplement to the 1995 SAR Update, we have conducted additional analyses to confirm that these controls will also provide adequate protection to workers at the WIPP. The approaches and results of the worker dose assessment are summarized here.

As recommended in the DOE order *Nuclear Safety Analysis Reports* (DOE 5480.23) and in the DOE Standard *Preparation Guide for U.S. Department of Energy Nonreactor Nuclear Facility Safety Analysis Reports* (DOE-STD-3009-94), the worker dose assessment used the approach of a qualitative hazard evaluation. Four typical accident scenarios were taken from the SAR Update: spontaneous ignition of a waste drum, puncture of a waste drum by a forklift, dropping of a waste drum from a forklift, and simultaneous dropping of seven drums during a crane failure. The descriptions and estimated frequencies of occurrence for these accidents were taken from the SAR Update, and had been developed by the *Hazard and Operability Study for CH TRU Waste Handling System* (WCAP 14312, Westinghouse Electric Corporation, Pittsburgh, PA, 1995).

DOE Standard 3009-94, draft Appendix A, and the DOE Handbook *Airborne Release Fractions/Rates and Respirable Fractions for Nonreactor Nuclear Facilities* (DOE-HDBK-3010-94) present release and dispersion equations that can be used to estimate doses to members of the public at the site boundary. However, the DOE Order and Standard for safety analysis reports do not require a mathematical calculation of estimated doses to workers, and therefore do not specify a method to be used for estimating such doses. We adopted the following eight-component linear equation for use in calculation of doses to workers:

$$\text{CEDE (rem)} = \text{MAR} * \text{DR} * \text{ARF} * \text{RF} * \text{BR} * \text{T} * \text{DCF} / \text{V}$$

where CEDE is the 50-y committed effective dose equivalent to the exposed individuals (rem), MAR is the Material-at-Risk (curies or grams), DR is the Damage Ratio, ARF is the Airborne Release Fraction (or rate for a continuous release), RF is the Respirable Fraction, BR is the Breathing Rate (0.02 m^3/min for ICRP Standard Reference Man involved in light work activity), T is the Time duration of exposure (minutes), DCF is the Dose Conversion Factor (5.1×10^8 rem/Ci for Class W

*Carlsbad Area Office, U.S. Department of Energy, Carlsbad, New Mexico

Pu-239) to convert curies of inhalation intake to a CEDE (in rems), and V is the effective volume in which the radionuclides are dispersed (m^3). This is a traditional equation which is similar in form to the method used in a recent DOE Safety Notice on *Decision Analysis Techniques* (Safety Notice Issue No. 95-1) to estimate potential inhalation doses to workers from a fire involving Pu-contaminated rags in a glovebox.

The estimated MARs, DRs, ARFs, and RFs for the fire, puncture, drop, and crane failure accidents were taken from the 1995 SAR Update and from the DOE airborne release handbook. We assumed that all of the activity released would be instantaneously dispersed within a 20 ft (6.1 m) radius of the source. This corresponds to a hemisphere of approximately 500 m^3 volume. As in the SAR Update, MARs were expressed as Pu-equivalent curies (PE-Ci) to normalize the activity of all transuranium elements in the waste to an equivalent activity of ^{239}Pu, based on CEDE. Simulations were done for both weapons-grade Pu waste, which comprises > 80% of the waste scheduled for WIPP, and for heat-source-grade Pu waste, which comprises < 20% of the scheduled waste. For weapons-grade waste, maximum drum content would be 16 PE-Ci, with an average of 4 PE-Ci, and a minimum of 0.1 PE-Ci. For heat-source-grade waste, a drum could contain as much as 80 PE-Ci, with an average of 7.4 PE-Ci, and a minimum of 0.1 PE-Ci.

As a general point of reference for evaluating the predicted consequences and, thereby evaluating the adequacy of defense-in-depth for worker protection at WIPP, this report adopted a set of evaluation guidelines based on a scheme presented by the International Commission on Radiological Protection in its publication on *Protection from Potential Exposure: A Conceptual Framework* (ICRP Publication 64). These modified guidelines are that normal operations (events with a likelihood > 10^{-1}) should result in worker doses < an administrative limit of 2 rem, anticipated events (likelihood between 10^{-1} and 10^{-2}) should result in doses < the statutory annual limit of 5 rem, unlikely events (likelihood between 10^{-2} and 10^{-4}) should result in doses < 50 rem (a dose associated with stochastic effects only), extremely unlikely events (likelihood between 10^{-4} and 10^{-6}) should result in doses < 300 rem (a dose associated with some deterministic radiation effects, but unlikely to cause death), and events leading to radiation doses where death is likely to occur (doses > 300 rem) should have a likelihood that is beyond extremely unlikely (< 10^{-6}).

Whereas the SAR Update focused on the upper bounding ("worst case") conditions for accidental exposures of the public, this report used a Monte Carlo forecasting and risk analysis program named *Crystal Ball* (Decisioneering, Inc., Denver, CO) to estimate the range of worker exposures that could result from each accident. Although the bounding calculations are interesting as worst cases, the estimated distributions of potential consequences provide much more information about the adequacy of worker protection strategies.

The total probability for a consequence was taken as the conditional probability of the consequence (e.g., the probability that a sustained fire will result in a dose > a given guideline) times the probability of the initiating event (e.g., the probability that a sustained fire will occur in the first place). Tables 1 and 2 illustrate the accident assumptions and the consequences predicted by the simulation model for the most disruptive accident considered (a sustained fire in a waste drum). As shown in Table 2 for weapons-grade Pu waste, if such an accident occurs, 77% of the time the dose to a worker will be > 2 rem, 53% of the time it will be > 5 rem, 26% of the time it will be > 50 rem, and < 0.01% of the time it will be > 300 rem. This compares to a bounding calculation of 385 rem if the drum is loaded to a maximum of 16 PE-Ci. For a drum loaded at 80 PE-Ci of heat-source-grade material, the bounding calculation is 1925 rem, and the distribution from the simulation is 94% > 2 rem, 85% > 5 rem, 25% > 50 rem, and 1% > 300 rem.

Note that for the fire accident described in Tables 1 and 2, as well as for the drum puncture, drum drop, and crane failure accidents, the predicted likelihoods and consequences were within the informal evaluation guidelines, indicating the adequacy of the WIPP defense-in-depth. In conformance with the guidance of DOE Standard 3009-94, draft Appendix A, we emphasize that use of these evaluation guidelines is not intended to imply that these numbers constitute acceptable limits for worker exposures under accident conditions. However, in conjunction with the extensive safety assessment in the 1995 SAR Update, these results indicate that the Carlsbad Area Office strategy for the assessment of hazards and accidents assures the protection of workers, members of the public, and the environment.

Table 1

Comparison of the Bounding Values of Accident Parameters Used in the 1995 SAR Update for Estimation of Potential Offsite Doses to the Public with the Distributions of Parameter Values Used in the Assessment of Potential Doses to Workers at WIPP from an Accident Involving Spontaneous Ignition of a Waste Drum Containing Weapons-Grade Plutonium Waste

Parameter	Bounding Value Used in the SAR Update	Distribution of Values Used in the Monte Carlo Simulation
Estimated Likelihood	10^{-4} to 10^{-6}	10^{-4} to 10^{-6}
Material-at-Risk (MAR)	80 PE-Ci	0.1 to 16 PE-Ci with 4 PE-Ci most likely
Damage Ratio (DR)	1.0	0.05 to 1.0 with 0.1 most likely
Combustible Fraction	40% combustible material and 60% noncombustible material	Combustible fraction of 0.05 to 1.0 with 0.4 most likely
Airborne Release Fraction (ARF)	Combustible: 5×10^{-4} Noncombustible: 6×10^{-3}	Combustible: 3×10^{-5} to 5×10^{-4} with 8×10^{-5} most likely Noncombustible: 6×10^{-6} to 6×10^{-3} with 6×10^{-5} most likely
Respirable Fraction (RF)	Combustible: 1.0 Noncombustible: 0.01	Combustible: 1.0 Noncombustible: 0.01

Table 2

Summary of Probability and Consequences for Potential Exposures to Workers for an Accident Involving Spontaneous Ignition of a Waste Drum at WIPP Containing Weapons-Grade Plutonium Waste

Event Category	Dose Evaluation Guideline	Guideline for Acceptable Probability	Annual Probability of Drum Fire for all Pu Waste	Conditional Probability of Exposure > Category Dose Guideline	Total Probability of Exposure > Category Guideline	Within the Evaluation Guidelines?
Normal Operations	< Administrative Limit (2 rem)	$> 10^{-1}$	Extremely Unlikely 10^{-4} to 10^{-6}			yes
Anticipated Events	> Administrative Limit (2 rem)	$< 10^{-1}$	Extremely Unlikely 10^{-4} to 10^{-6}	0.77	8×10^{-5} to 8×10^{-7}	yes
Unlikely Events	> 5 rem	$< 10^{-2}$	Extremely Unlikely 10^{-4} to 10^{-6}	0.53	5×10^{-5} to 5×10^{-7}	yes
Extremely Unlikely Events	> 50 rem	$< 10^{-4}$	Extremely Unlikely 10^{-4} to 10^{-6}	0.26	3×10^{-5} to 3×10^{-7}	yes
Beyond Extremely Unlikely	> 300 rem	$< 10^{-6}$	Extremely Unlikely 10^{-4} to 10^{-6}	< 0.0001	$< 1 \times 10^{-8}$ to $< 1 \times 10^{-10}$	yes

(Research sponsored by the Albuquerque Operations and Carlsbad Area Offices, U.S. Department of Energy, under Contract No. DE-AC04-76EV01013.)

II. DEPOSITION, TRANSPORT, AND CLEARANCE OF INHALED TOXICANTS

COMPARISONS OF CALCULATED RESPIRATORY TRACT DEPOSITION OF PARTICLES BASED ON THE NCRP/ITRI MODEL AND THE NEW ICRP66 MODEL

Hsu-Chi Yeh, Richard G. Cuddihy, Robert F. Phalen, and I-Yiin Chang***

The National Council on Radiation Protection and Measurements (NCRP) in the United States and the International Commission on Radiological Protection (ICRP) have been independently reviewing and revising respiratory tract dosimetry models for inhaled radioactive aerosols. The newly proposed NCRP respiratory tract dosimetry model represents a significant change in philosophy from the old ICRP Task Group model (Task Group on Lung Dynamics. *Health Phys. 12*: 173, 1966; ICRP. *Limits for Intakes of Radionuclides by Workers*, Publication 30, Pergamon Press, New York, 1979). The proposed NCRP model describes respiratory tract deposition, clearance, and dosimetry for radioactive substances inhaled by workers and the general public and is expected to be published soon. In support of the NCRP proposed model, ITRI staff members have been developing computer software (NCRP/ITRI model) (Chang, I. Y. *et al. Radiat. Prot. Dosim. 38(1/3)*: 193, 1991; 1992–93 Annual Report, p. 127). Although this software is still incomplete, the deposition portion has been completed and can be used to calculate inhaled particle deposition within the respiratory tract for particle sizes as small as radon and radon progeny (≈ 1 nm) to particles larger than 100 μm. Recently, ICRP published their new dosimetric model for the respiratory tract, ICRP66 (ICRP. *Human Respiratory Tract Model for Radiological Protection*, Publication 66, Pergamon Press, New York, 1994). Based on ICRP66, the National Radiological Protection Board of the UK developed PC-based software, LUDEP, for calculating particle deposition and internal doses (Jarvis, N. S. *et al. NRPB-SR264, 1994*, NRPB, Chilton, Didcot, Oxon OX11 0RQ, UK). The purpose of this report is to compare the calculated respiratory tract deposition of particles using the NCRP/ITRI model and the ICRP66 model (LUDEP, version 1.1), under the same particle size distribution and breathing conditions.

In the NCRP/ITRI model, the respiratory tract is divided into three main regions: the naso-oro-pharyngo-laryngeal (NOPL), tracheobronchial (TB), and pulmonary (P) regions. For the ICRP66 model (and thus the LUDEP), the respiratory tract is divided into five regions: extrathoracic 1 (ET_1), extrathoracic 2 (ET_2), bronchial (BB), bronchiolar (bb), and alveolar-interstitial (AI) regions. The corresponding regions between the NCRP/ITRI and ICRP66 are: NOPL vs. (ET_1 + ET_2), TB vs. (BB + bb), and P vs. AI. Therefore, for comparison, the depositions within ET_1 and ET_2 were summed to compare with the NOPL, and the BB and bb were summed to compare with the TB. The calculations were based on the following conditions for both models: tidal volume = 770 mL, breathing frequency = 13 breaths/min, functional residual capacity = 3000 mL, particle density = 1.0 g/cm^3, and particle size range 0.001–10 μm with two particle size distributions (monodisperse with the geometric standard deviation, σ_g, = 1.0 and polydisperse with σ_g = 2.5). The most recent versions of the NCRP/ITRI software (1992–93 Annual Report, p. 127) and LUDEP version 1.1 were used for the calculations.

Results are shown in Figures 1 and 2. Figure 1 compares the two models for monodisperse aerosols. For particles > 3.0 μm, the ICRP66 model predicted higher NOPL deposition than the NCRP/ITRI model. Because particles deposited in the NOPL will not be available for deposition in the TB, the ICRP66 model had a slightly lower TB and P deposition. This can be explained by the fact that the two models used different inhalability equations. The NCRP/ITRI model used the inhalability equation recommended by the American Conference of Governmental Industrial Hygienists (ACGIH. *Particle Size-Selective Sampling in the Workplace*, Cincinnati, OH, 1985), whereas the

*Department of Community and Environmental Medicine, University of California, Irvine, California
**Institute for Health and Population Research, The Lovelace Institutes, Albuquerque, New Mexico

ICRP66 model used an alternative equation that included wind speeds (ICRP, 1994). For particles ≤ 0.2 μm, the ICRP model predicted a slightly higher NOPL deposition; however, the NCRP/ITRI model predicted a higher TB deposition, resulting in a lower P deposition for particles < 0.05 μm. The discrepancy between the two models on the NOPL deposition of ultrafine particles is unclear because the same data sets (Cheng, Y. S. *et al. Aerosol Sci. Technol. 18*: 359, 1993; Swift, D. L. *et al. J. Aerosol Sci. 23*: 65, 1992) were used by both models. The discrepancy may have occurred because different equations were used to fit the data. The NCRP/ITRI model predicted higher TB deposition for ultrafine particles where deposition is dominated by diffusion mechanism. This is because the NCRP/ITRI model considers the effects of branching (or entrance configuration) on diffusional deposition at a bifurcation (Yeh, H. C. *Bull. Math. Biol. 36*: 105, 1974; Cohen, B. S. *et al. Aerosol Sci. Technol. 12*: 1082, 1990). Consequently, the ICRP66 model predicted a higher P deposition for ultrafine particles; this difference was substantial for particles < 0.03 μm.

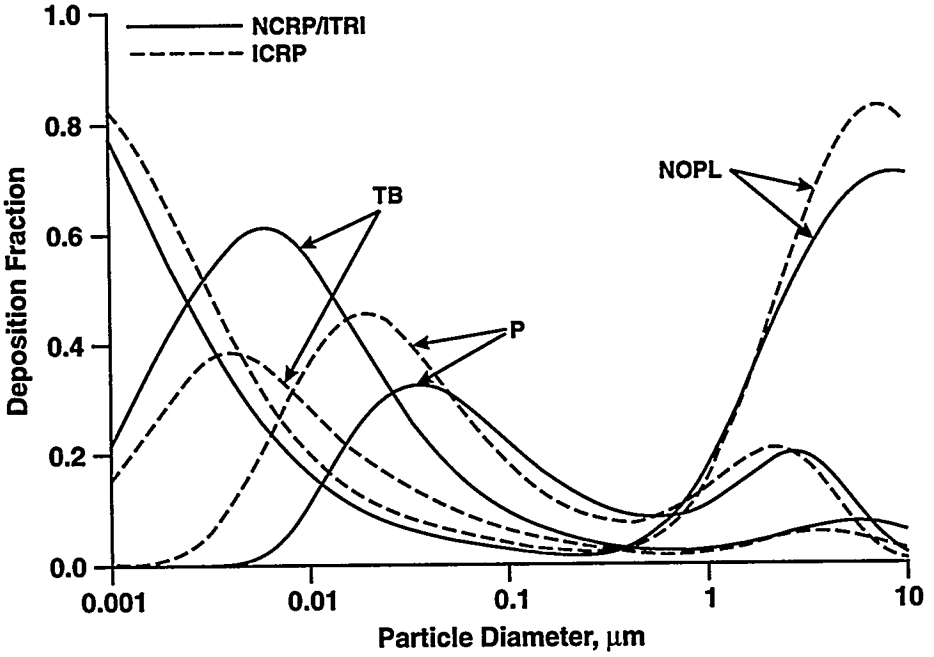

Figure 1. Comparison between the NCRP/ITRI and ICRP66 models for deposition of inhaled monodisperse aerosols (σ_g = 1.0, particle density = 1.0 g/cm^3, tidal volume = 770 mL, breathing frequency = 13/min, functional residual capacity = 3000 mL). TB = tracheobronchial; P = pulmonary; NOPL = naso-oro-pharyngo-laryngeal.

Polydisperse aerosols are most commonly encountered in the environment. Figure 2 shows the comparison between the two models for polydisperse aerosols with σ_g = 2.5. The relative trends were similar to results for the monodisperse aerosols, showing two peaks in the deposition curves for both TB and P: around 0.003–0.008 μm and 3–6 μm for TB and 0.02–0.05 μm and 2–4 μm for P. However, these two peaks were somewhat flattened and lower for the polydisperse aerosols than for the monodisperse aerosols.

In summary, the general trends of the deposition curves for the two models were similar. For particles > 0.2 μm, the difference between the two models is small; the ICRP66 model predicts a slightly higher NOPL (or ET) deposition when particles are > about 1–2 μm. However, because the ICRP66 model did not consider the enhanced diffusion deposition due to branching bifurcations, the ICRP66 model predicted a much lower TB deposition and, thus, a much higher P deposition than the NCRP/ITRI model for particles < 0.2 μm. This difference will have significant implications on the

dosimetry of radon and radon progeny because their particle sizes are in the ultrafine regime (< 0.2 μm).

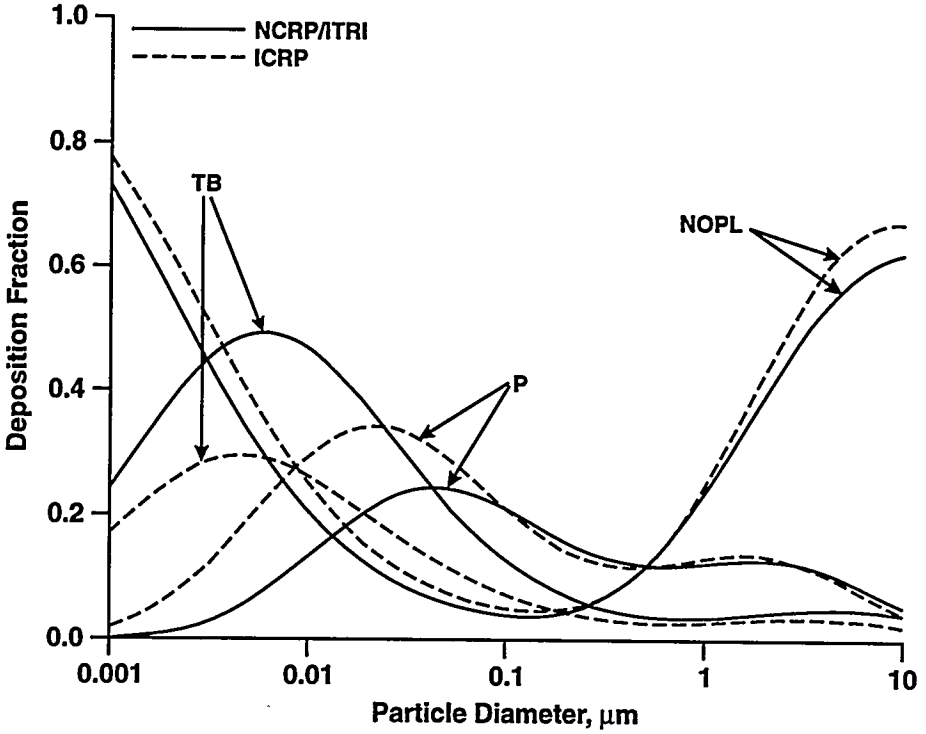

Figure 2. Comparison between the NCRP/ITRI and ICRP66 models for deposition of inhaled polydisperse aerosols (σ_g = 2.5, particle density = 1.0 g/cm^3, tidal volume = 770 mL, breathing frequency = 13/min, functional residual capacity = 3000 mL). TB = tracheobronchial; P = pulmonary; NOPL = naso-oro-pharyngo-laryngeal.

(Research sponsored by the Office of Health and Environmental Research, U.S. Department of Energy, under Contract No. DE-AC04-76EV01013.)

IN VIVO DEPOSITION OF ULTRAFINE AEROSOLS IN HUMAN NASAL AND ORAL AIRWAYS

Hsu-Chi Yeh, Kuo-Hsi Cheng, Yung-Sung Cheng,*
*Raymond A. Guilmette, Steven Q. Simpson**, and David L. Swift**

The extrathoracic airways, including the nasal passage, oral passage, pharynx, and larynx, are the first targets for inhaled particles and provide an important defense for the lung. Understanding the deposition efficiency of the nasal and oral passages is therefore crucial for assessing doses of inhaled particles to the extrathoracic airways and the lung. Significant inter-subject variability in nasal deposition has been shown in recent studies by Rasmussen, T. R. *et al.* (*J. Aerosol Med. 3*: 15, 1990) using 2.6 μm particles in 10 human subjects and in our preliminary studies using 0.004–0.15 μm particles in four adult volunteers (1992–93 Annual Report, p. 29). No oral deposition was reported in either of these studies. Reasons for the intersubject variations have been frequently attributed to the geometry of the nasal passages. The aims of the present study were to measure *in vivo* the nasal airway dimensions and the deposition of ultrafine aerosols in both the nasal and oral passages, and to determine the relationship between nasal airway dimensions and aerosol deposition. A statistical procedure incorporated with the diffusion theory was used to model the dimensional features of the nasal airways which may be responsible for the biological variability in particle deposition.

Ten healthy, nonsmoking, adult male volunteers (ages 24–58 y) participated in this study. Magnetic resonance imaging (MRI) (Guilmette, R. A. *et al. J. Aerosol Med. 2*: 365, 1989) was used to determine the physical perimeters of the left and right nasal airways of each subject at contiguous 3-mm intervals prior to the experiments. Acoustic rhinometry (AR) (Hilbert, O. *et al. J. Appl. Physiol. 66*: 295, 1989) was used to measure the cross-sectional areas of the left and right nasal airways immediately before and after each set of deposition measurements.

Deposition measurements were made in all 10 subjects with aerosols of four different particle diameters (0.004, 0.008, 0.02, and 0.15 μm) at two constant flow rates (166.7 and 333.4 cm^3/sec) (ITRI Protocol No. FY93-029). The aerosols smaller than 0.02 μm in diameter were produced from silver wools (99.9+%, Aldrich Chemical Company Inc., Milwaukee, WI), using a vaporization-condensation method. The 0.15 μm particles were generated by nebulizing polystyrene latex particles in an aqueous suspension (Duke Scientific Corp., Palo Alto, CA) using a Retec X-70 nebulizer. The aerosol exposure procedures consisted of four breathing patterns: (1) the aerosol was drawn into the nose and out through the mouth (nose-in/mouth-out), (2) the aerosol was drawn into the mouth and out through the nose (mouth-in/nose-out), (3) nose-in/mouth-out (pattern 1) with an oral extension tube to bypass the oral cavity, and (4) mouth-in/nose-out (pattern 2) with an oral extension tube. Deposition efficiencies were obtained by measuring aerosol concentrations in the inspired and expired air using a TSI condensation particle counter (Model 3025, St. Paul, MN). Corrections were made for particles losses in the transport lines and masks (1992–93 Annual Report, p. 29).

A general equation for the nasal and oral deposition of ultrafine particles was proposed, based on (1) a turbulent diffusion theory (Cheng, Y. S. *et al. Aerosol Sci. Technol. 18*: 359, 1993) and (2) flow dynamics in the nasal cast (Swift, D. L. and D. F. Proctor. In *Respiratory Defense Mechanisms* [J. Brain, D. Proctor, and L. Reid, eds.], Marcel Dekker, New York, p. 63, 1977), which can be written as:

*School of Hygiene and Public Health, Johns Hopkins University, Baltimore, Maryland
**Department of Medicine, University of New Mexico, Albuquerque, New Mexico

$$E = 1 - \exp[-K(\frac{A_s}{A_{min}})^a(\bar{S}_f)^b(D)^c(Q)^d] \quad (1)$$

where E is the deposition efficiency, K is a constant, A_s is the total surface area of the nasal passage in cm^2, A_{min} is the nasal minimum cross-sectional area in cm^2, $\bar{S}_f$ is the average airway shape factor (defined as the ratio of the airway perimeter to a reference perimeter calculated from the periphery of the rectangle drawn on the maximum horizontal and vertical boundaries of each 3 mm airway section) of the nasal turbinate region, D is the diffusion coefficient of the particles in cm^2/sec, and Q is the flow rate in cm^3/sec. To account for the effects of repeated measurements on each subject (32 combinations of experimental conditions), the MIXed-effects NonLINear Regression Procedure (MIXNLIN) (Vonesh, E. F. *MIXNLIN: A SAS Procedure for Nonlinear Mixed-effects Models*, Technical Report Number TR92M-0300, Applied Statistics Center, Baxter Healthcare Corporation, Round Lake, IL, 1992) was used to estimate parameters a, b, c, and d in Equation (1).

Deposition efficiencies varied widely among individuals, with up to a two-fold difference for 4-nm particles. The nasal dimensions measured by MRI and AR also showed wide variability. The mean A_s calculated from MRI was 217 ± 23 cm^2. The mean values of A_{min} and $\bar{S}_f$ were 2.08 ± 0.53 cm^2 and 2.51 ± 0.23, respectively. No correlations were found among these dimensional measurements and the body height and weight of the subjects.

The MIXNLIN was used to fit Equation (1) to the experimental data by assuming the same effects of airway geometry, particle size, and flow rate on aerosol deposition for the four breathing patterns. The best estimates of the parameters are: $a = 0.27 \pm 0.08$, $b = 1.24 \pm 0.71$, $c = 0.39 \pm 0.01$, and $d = -0.28 \pm 0.02$. With these parameter estimates, values from the fitting procedure of 1.73 ± 0.15, 1.57 ± 0.14, 1.42 ± 0.14, and 1.26 ± 0.13 were obtained for the constant K for each breathing pattern by repeating the MIXNLIN procedure performed on each data set. These four equations were used to obtain equations for regional deposition in the nasal and oral airways (Cheng, K. H. *Ph.D. Thesis*, The Johns Hopkins University, May 1995).

Our previous study with nasal/oral casts (1993–94 Annual Report, p. 39) indicated that depositions with nose-in/mouth-out and mouth-in/nose-out are equivalent to nasal-pharyngeal-tracheal deposition during inspiration and expiration, respectively. Therefore, the nasal-pharyngeal-tracheal deposition (equivalent to conventional nasal deposition) during inspiration (INPL) and expiration (ENPL) can be estimated as:

$$\begin{aligned} \text{INPL Deposition} &= 1 - \exp[-1.73(\frac{A_s}{A_{min}})^{0.27}(\bar{S})^{1.24}(D)^{0.39}(Q)^{-0.28}] \\ &= 1 - \exp[-19.08(D)^{0.39}(Q)^{-0.28}] \end{aligned} \quad (2)$$

$$\begin{aligned} \text{ENPL Deposition} &= 1 - \exp[-1.57(\frac{A_s}{A_{min}})^{0.27}(\bar{S}_f)^{1.24}(D)^{0.39}(Q)^{-0.28}] \\ &= 1 - \exp[-17.50(D)^{0.39}(Q)^{-0.28}] \end{aligned} \quad (3)$$

when the values of $A_s = 217$ cm^2, $A_{min} = 2.08$ cm^2, and $\bar{S}_f = 2.51$ were used. The predictions of Equations (2) and (3) are shown in Figures 1 and 2 along with data obtained from the 10 subjects. The nasal/oral deposition data show significant variability among subjects.

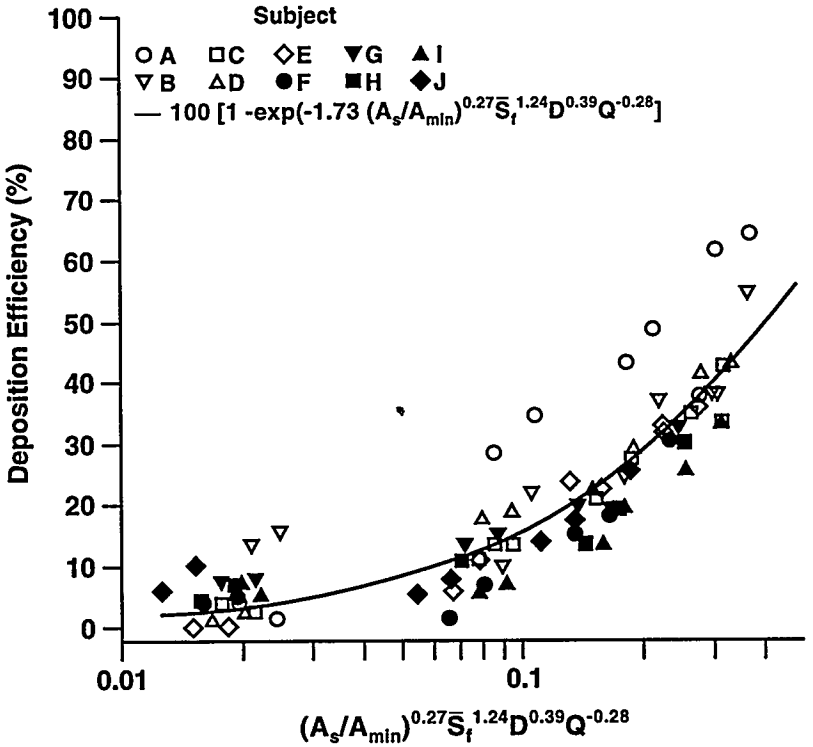

Figure 1. Nasal (nasal-pharyngeal-tracheal) deposition during inspiration as a function of a geometry-related diffusion parameter. The solid line is the best-fitting equation from the MIXNLIN procedure.

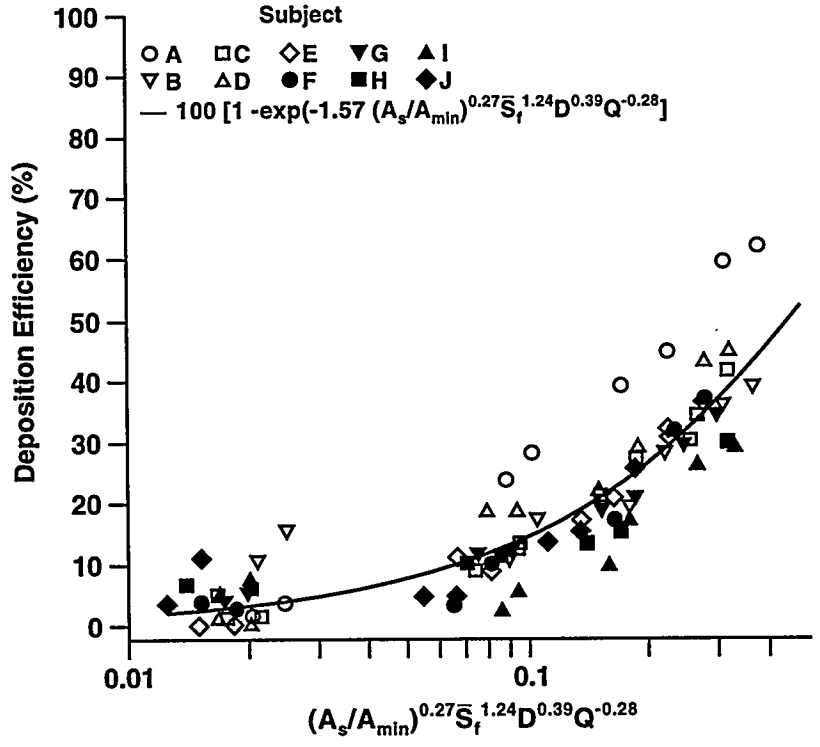

Figure 2. Nasal (nasal-pharyngeal-tracheal) deposition during expiration as a function of a geometry-related diffusion parameter. The solid line is the best-fitting equation from the MIXNLIN procedure.

In summary, we have correlated deposition of particles in the size range of 0.004 to 0.15 μm with the nasal dimensions of each subject. A greater surface area, smaller cross-sectional area, and increasing complexity of airway shape were found to be associated with higher deposition of ultrafine aerosols in the extrathoracic airways. The significance of the present study is not only in the development of *in vivo* dosimetric models for the average population, but in the recognition, based on the experimental data, that assessing the health effects on a population basis would not be complete without considering the wide range of biological variability. It is necessary to include the information of biological variability in the extrathoracic filtration to define the population-wide lung dosimetry resulting from aerosol intakes.

(Research sponsored by the Office of Health and Environmental Research, U.S. Department of Energy, under Contract No. DE-FG02-88ER60655 at Johns Hopkins University and Contract No. DE-AC04-76EV01013 at ITRI.)

REGIONAL DEPOSITION OF THORON PROGENY IN MODELS OF THE HUMAN TRACHEOBRONCHIAL TREE

Shawna M. Smith, Yung-Sung Cheng, and Hsu-Chi Yeh*

Models of the human tracheobronchial tree have been used to determine total and regional aerosol deposition of inhaled particles (Cohen, B. In *Radon and Its Decay Products* [P. K. Hopke, ed.], American Chemical Society, Washington, DC, p. 475, 1987). Particle sizes measured in these studies have all been > 40 nm in diameter. The deposition of aerosols < 40 nm in diameter has not been measured. Particles in the ultrafine aerosol size range include some combustion aerosols and indoor radon progeny. Also, the influence of reduced lung size and airflow rates on particle deposition in young children has not been determined. With their smaller lung size and smaller minute volumes, children may be at increased risk from ultrafine pollutants. In order to accurately determine dose of inhaled aerosols, the effects of particle size, minute volume, and age at exposure must be quantified. The purpose of this study was to determine the deposition efficiency of ultrafine aerosols smaller than 40 nm in diameter in models of the human tracheobronchial tree.

Aerosols of thoron progeny (^{212}Pb) and silver (Ag) were generated as previously described (Cheng, Y. S. *et. al. J. Aerosol Sci. 23*: 364, 1992). The gamma-emission (239 keV) and half-life (10.6 h) of ^{212}Pb make it an excellent radiotracer for determining deposition in each branching segment of the tracheobronchial tree. Unattached ^{212}Pb served as a small ultrafine aerosol with a 1.7 nm particle size. Radiolabeling of Ag with ^{212}Pb allowed us to create particles of 10 nm which, in turn, created a range of sizes not previously covered in deposition studies. Aerosols of the two particle sizes were deposited at 10 and 20 L·min^{-1} in models derived from the lungs of a 3-y-old child, and in 16- and 23-y-old adults at 20 and 40 L·min^{-1}. These flow rates represent minute volumes at rest and during moderate exercise for each age group. The tracheobronchial tree models were made from an electroconductive silicone rubber to prevent electrostatic charge buildup during particle deposition. Each model included a larynx and was 100% complete to the fifth branching generation. After exposure, the casts were cut into separate branch segments. By counting the radioactivity in each segment and on a collection filter, we determined the deposition efficiency in the total cast and in each segment.

The deposition of spherical particles in circular pipes was predicted for fully developed and plug flow (Ingham, D. B. *J. Aerosol Sci. 6*: 125, 1975). In this model, the deposition of ultrafine particles is dependent upon the diffusional parameter $\mu = \pi DL/Q$, where μ is proportional to the particle diffusion coefficient (D) and segment length (L), and inversely proportional to the flow rate (Q) through each segment.

Figure 1 shows the deposition efficiency of aerosols in individual branches plotted versus the diffusion parameter, μ, of that branch. This was the deposition efficiency of aerosols that actually entered that branch. Theoretical predictions for deposition during plug flow and fully developed flow are also included (Ingham, D. B. *J. Aerosol Sci. 6*: 125, 1975). Fully developed laminar flow generally occurs in a pipe or branch segment when the length is 10 times the diameter. This does not occur until the 15th or 16th generation of the tracheobronchial tree. For models where only the first few generations are present, such as ours, fully developed flow does not occur. Therefore, any theory based upon fully developed flow is likely to underestimate aerosol deposition at all values of μ in the upper airways of the tracheobronchial tree. For smaller μ, Figure 1 shows that the theory for plug flow overestimates the deposition in a given segment. Predictions based upon fully developed

*UNM/ITRI Graduate Student

flow in the tracheobronchial tree underestimated aerosol deposition. However, as the diffusion parameter increased, predictions based upon plug flow also underestimated particle deposition. At large μ, the theory based upon plug flow begins to converge with that of fully developed flow. This demonstrates that the influence of developing flow should be taken into account when trying to apply these models to aerosol deposition in the tracheobronchial tree. The effects of particle size may also be seen in this figure. The deposition efficiency decreased as the particle size increased.

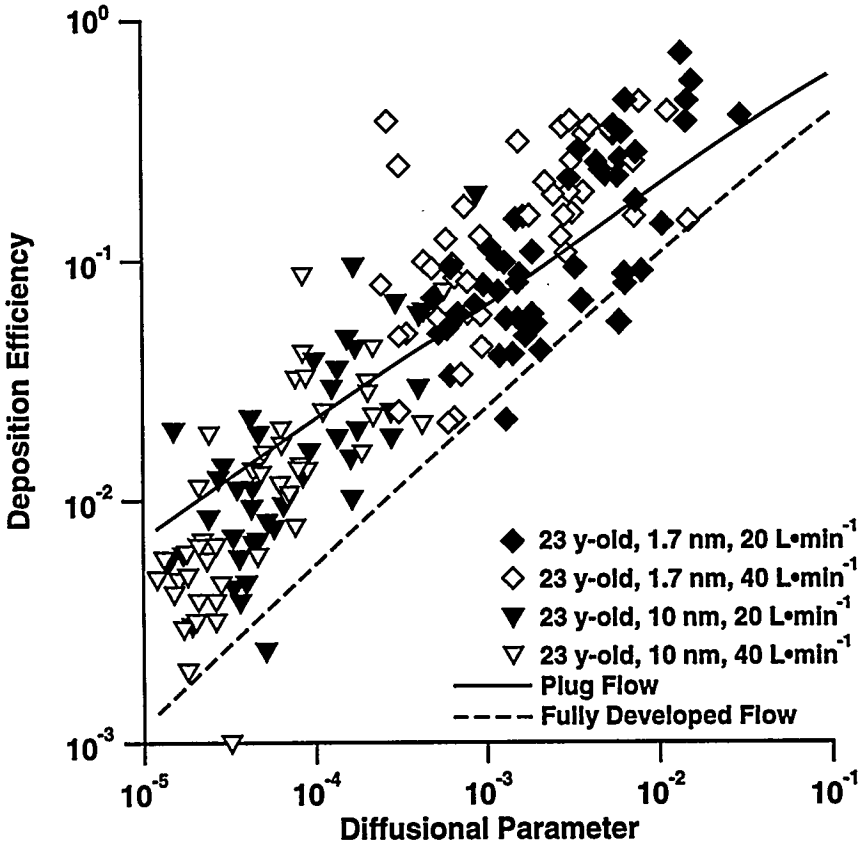

Figure 1. The deposition efficiency of 1.7 nm and 10 nm particles as a function of the diffusional parameter, μ, in the morphological model of an adult at rest (20 L·min^{-1}) and during moderate exercise (40 L·min^{-1}).

Figure 2 shows the average deposition by airway generation for 1.7 nm particles in the three morphological models used in this study. When comparing minute volumes at rest, deposition for most generations was higher for the model of the 3-y-old than for the other two models. The same effect was also seen at flow rates corresponding to moderate exercise (data not shown). There seemed to be no differences between deposition in the 16-y-old and 23-y-old models at any flow rate. For all ages, there was a slight decrease in deposition efficiency from the main bronchi to lobar bronchi (generation 2 and 3), after which deposition efficiency in succeeding generations increased incrementally.

The depositional theories based upon laminar flow predict a decrease in diffusional deposition at higher flow rates. This is based upon the concept that a decrease in the amount of time a particle spends in a branch segment provides less time for diffusion to the walls. However, for the 1.7 nm particles, there was no clear dependence of aerosol deposition on flow rate for the two flow rates measured in each cast (data not shown). Due to the laryngeal jet, caused by the presence of the

epiglottic restriction in the larynx, airflow may be turbulent in the upper tracheobronchial tree even at subcritical Reynold's numbers (Re < 2000). The lack of flow rate dependence for the smaller particles may be due to turbulent diffusion in the upper generations increasing the deposition of particles over what is predicted for laminar flow.

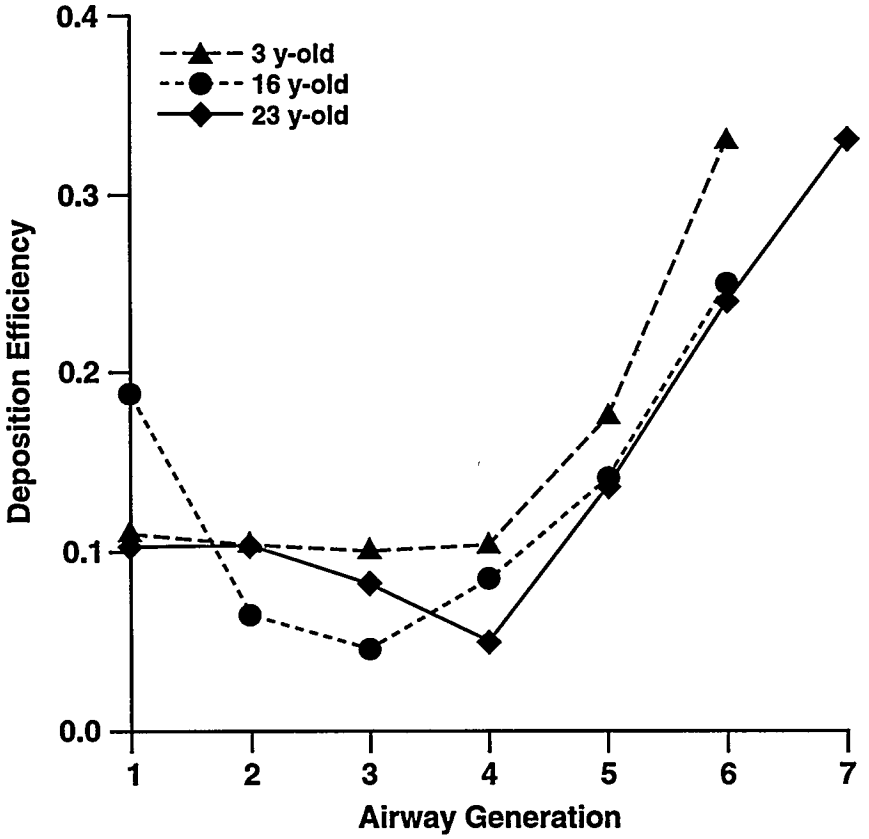

Figure 2. Average deposition by airway generation during inhalation at rest for 1.7 nm particles in the morphological models of humans. (Trachea is generation 1, main bronchi are generation 2, and so on.)

This study demonstrates that the deposition efficiency of aerosols in the model of the child's tracheobronchial tree may be slightly higher than in the adult models. This may have implications in modifying indoor air pollution standards in buildings where children are often present, such as in homes or schools. In the same ambient environment, a child may receive a higher dose of an inhaled toxic substance than an adult. Statistical analysis will be performed to confirm the finding. In addition, the use of equations to model the deposition of aerosols in circular pipes appears to be inadequate for modeling deposition in the tracheobronchial tree. The deposition of aerosols in the ultrafine size range was substantially higher than predicted in the tracheobronchial tree. This is especially true for aerosols corresponding to the diameter of ^{222}Rn progeny. Airflow in the upper bronchial airways appears to be neither fully laminar nor fully turbulent. Correction factors must be added to the laminar flow equation, or entirely new models must be developed if they are to be of use in predicting aerosol deposition in the tracheobronchial tree.

(Research sponsored by the Office of Health and Environmental Research, U.S. Department of Energy, under Contract No. DE-AC04-76EV01013.)

EXPERIMENTAL VALIDATION OF A MODEL FOR DIFFUSION-CONTROLLED ABSORPTION OF ORGANIC COMPOUNDS IN THE TRACHEA

Per Gerde, Bruce A. Muggenburg, Janice R. Thornton-Manning, and Alan R. Dahl*

Most chemically induced lung cancer originates in the epithelial cells in the airways. Common conceptions are that chemicals deposited on the airway surface are rapidly absorbed through mucous membranes, limited primarily by the rate of blood perfusion in the mucosa. It is also commonly thought that for chemicals to induce toxicity at the site of entry, they must be either rapidly reactive, readily metabolizable, or especially toxic to the tissues at the site of entry. For highly lipophilic toxicants, there is a third option. Our mathematical model predicts that as lipophilicity increases, chemicals partition more readily into the cellular lipid membranes and diffuse more slowly through the tissues. Therefore, absorption of very lipophilic compounds will be almost entirely limited by the rate of diffusion through the epithelium rather than by perfusion of the capillary bed in the subepithelium (Gerde, P. *et al. Toxicol. Appl. Pharmacol. 107*: 239, 1991). We have reported on a preliminary model for absorption through mucous membranes of any substance with a lipid/aqueous partition coefficient larger than one (1993–94 Annual Report, p. 49). The purpose of this work was to experimentally validate the model in Beagle dogs.

Three dogs were exposed to each of three toxicants of different lipophilicity, namely, 4-(methyl-nitrosamino)-1-(3-pyridyl)-1-butanone (NNK), pyrene (Pyr), and benzo(a)pyrene (BaP). The respective octanol/water partition coefficients for these toxicants are: 180, 150,000, and 1,000,000. Each compound was evaluated separately in each dog. Using the Lovelace microspray nozzle, ng amounts of each toxicant dissolved in a saline/phospholipid suspension were instilled as a single bolus in the trachea about 30 mm from the carinal ridge of the main bifurcation. Bloodborne clearance was monitored by repeatedly sampling blood from the catheterized azygous vein, and from the aorta and posterior vena cava. The azygous vein drains the local area around the point of instillation in the trachea (Fig. 1). Tissue retention was measured after the bloodborne clearance had been monitored: at 30 min for NNK, and at 3 h for Pyr and BaP. Each compound was radiolabeled with tritium. Complete combustion followed by liquid scintillation counting was used to determine total tritium in tissues and blood. Metabolite patterns were determined by solvent extraction and fractionation using HPLC.

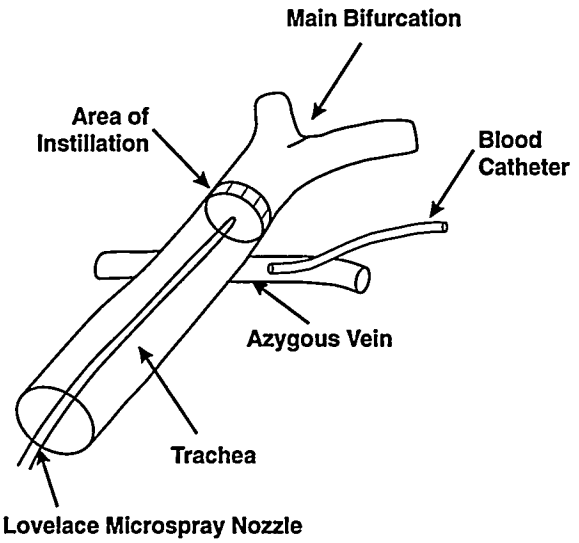

Figure 1. Schematic of the area of instillation in the distal trachea, including the location of the blood catheter in the azygous vein.

*National Institute for Working Life, Solna, Sweden

In agreement with the model, the rate of absorption of organic toxicants in the tracheobronchial mucosa was found to be inversely related to lipophilicity (Fig. 2). The most active phase of clearance, during which the concentration in the azygous vein was substantially higher than the concentration in the systemic circulation, lasted for ~ 10 min for NNK, ~ 50 min for Pyr, and > 3 h for BaP. None of the substances cleared in an ideal monophasic process, as predicted by the model, but the general rate of absorption of the three toxicants studied was sufficiently close to the *á priori* predictions of the model to strongly support the assumed mechanism of absorption in the airway mucosa.

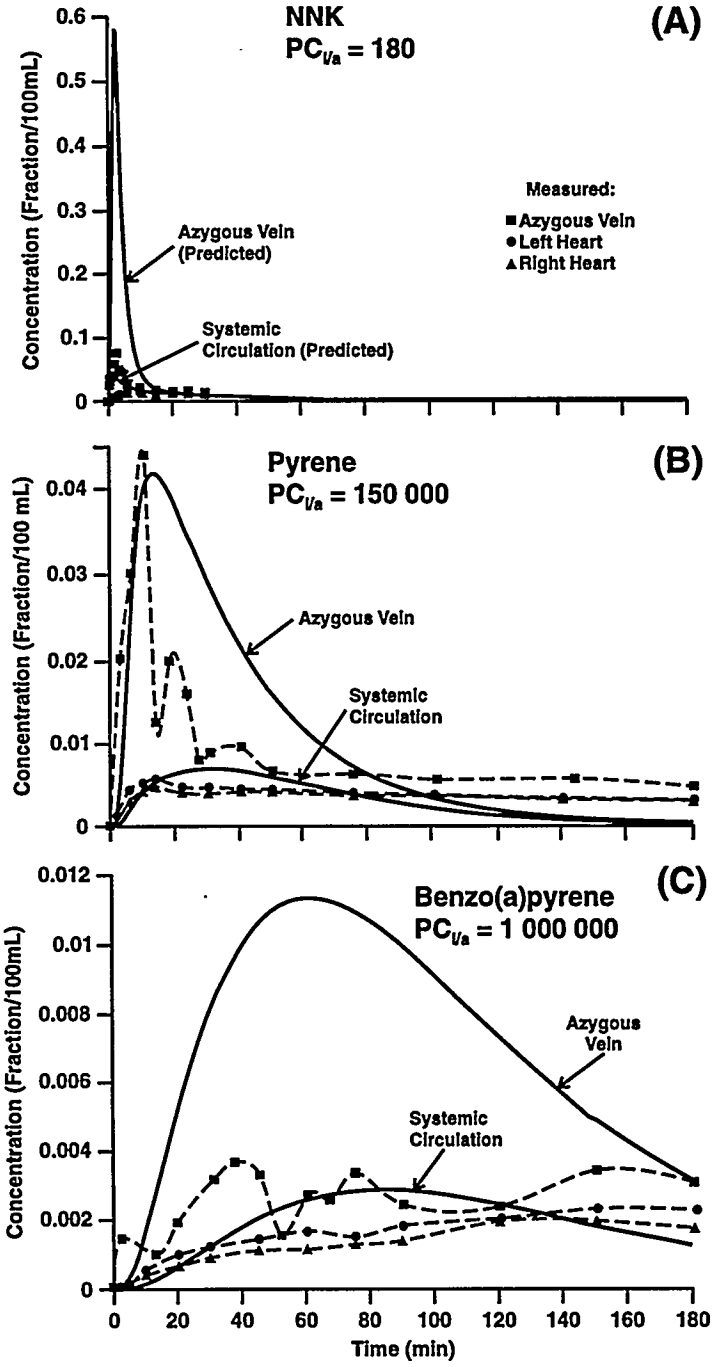

Figure 2. Concentration of (A) NNK, (B) Pyr, and (C) BaP in the azygous vein, and in the left and right sides of the systemic circulation following instillation of the three toxicants in the distal trachea. Solid lines show model predictions using a "best-guess" setting of the parameters.

Conclusions to be drawn from these findings are: (1) diffusion-limited absorption affords more time for highly lipophilic toxicants to induce tissue damage in the epithelium before entering the systemic circulation; (2) highly lipophilic substances may, therefore, be relatively unreactive and slowly metabolized, and still behave as site-of-entry toxicants; (3) the target dose of highly lipophilic toxicants at the site of entry is likely to be much higher than that of less lipophilic toxicants, even if the substances are deposited on the airway epithelium at identical densities; and (4) thicker epithelia, such as those in the conducting airways, receive a higher dose of highly lipophilic toxicants than thinner epithelia such as in the alveoli.

This validated model on toxicant absorption in the airway mucosa will improve risk assessment of inhaled carcinogens by permitting extrapolation of exposure-target-dose relationships over wider ranges of concentrations than before, and between different species of animals and humans. The experimental results support the prediction that bronchial cancer is more likely to be induced by highly lipophilic carcinogens, such as BaP, than by less lipophilic ones, such as NNK (Gerde *et al.*, 1991). Understanding the mechanism of absorption of organic toxicants in the airway mucosa opens ways to determine the target dose in the tracheobronchial epithelium of inhaled carcinogens with such different physicochemical and metabolic properties as NNK and BaP.

(Research sponsored by the PHS/NIH under Grant R01-ES05910 from the National Institute of Environmental Health Science with the U.S. Department of Energy, under Contract No. DE-AC04-76EV01013, and by the Swedish Environment Fund.)

AN EXPOSURE SYSTEM FOR MEASURING NASAL AND LUNG UPTAKE OF VAPORS IN RATS

*Alan R. Dahl, Lori K. Brookins, and Per Gerde**

Inhaled gases and vapors often produce biological damage in the nasal cavity and lower respiratory tract. The specific site within the respiratory tract at which a gas or vapor is absorbed strongly influences the tissues at risk to potential toxic effects; to predict or to explain tissue or cell specific toxicity of inhaled gases or vapors, the sites at which they are absorbed must be known. The purpose of the work reported here was to develop a system for determining nose and lung absorption of vapors in rats, an animal commonly used in inhalation toxicity studies.

The system (Fig. 1) was based on one reported for dogs (Snipes, M. B. *et al. Fundam. Appl. Toxicol. 16*: 81, 1991). Six major system modifications that facilitate accurate determinations of vapor uptake in a rat's nose and lungs during varied breathing regimes are outlined here. (1) Because of the small sample volumes obtainable from a rat, pumps were installed to push air sampled from the rat's nose or trachea to a gas chromatograph (GC). If the sampled air were pulled by a vacuum, as was the case for dogs, even minute leaks in the sampling line could result in significant dilution of the sampled vapor. (2) The apparatus was mounted on a plexiglass board to facilitate operation of the more complicated system. (3) In the previous work using dogs, a correction was made for the fact that airflow during breathing was approximately sinusoidal, whereas the sampling airflow was in the form of a square wave (Dahl, A. R. *et al. Toxicol. Appl. Pharmacol. 109*: 263, 1991; Gerde, P. and A. R. Dahl. *Toxicol. Appl. Pharmacol. 109*: 276, 1991). For the low flow rates encountered in experiments using rats, a satisfactory correction would be difficult to achieve; therefore, a reciprocating syringe system was developed that samples proportionally from a rat's trachea in a sinusoidal airflow pattern synchronized with breathing. (4) Components were miniaturized to lessen dead space, thereby decreasing time to equilibrium. (5) A solenoid was inserted to protect against back-mixing of exhaled air with air in the pneumotach "dead space". (6) Diffusion of vapor through the sampling lines was minimized by using metal tubing wherever practical.

The exposure system can sustain an apneic rat for > 30 min at tidal volumes ranging from 0.6–3.6 mL and at frequencies ranging from 33–63 breaths/min; however, the larger tidal volumes cannot be achieved at the higher frequencies, limiting the minute volume range to 36–140 mL/min.

The system was operated in two modes, one with tracheostomized rats (a tracheostomy is necessary to place the t-tube for sampling inhaled nasal and exhaled lung vapor) and the other with normal rats (Table 1). The results from operation in either mode were similar for total uptake, assuring that the tracheostomy was not introducing artifacts. The relative humidity of the inhaled air was approximately 0%, and the temperature was ~ 25°C. Tracheal sampling was kept at ≤ 5% of the inhaled volume so that volume losses from sampling were approximately compensated for by increased volume due to the warming of inhaled air and the addition of water vapor from the rat (Dahl *et al.*, 1991).

This exposure system is the first reported that can measure vapor uptake in rats in both the upper airways and lung during cyclic breathing. Both are important measurements in determining nasal uptake because the lung depletes the air that has passed through the trachea during inhalation. During exhalation this air—now unsaturated relative to the vapor still absorbed in the outermost layer of the nasal airway mucosa—passes over and absorbs vapor from the nasal mucosa. This phenomenon was first quantitated in dogs (Dahl *et al.*, 1991); by extending the technique to include rats, we can

*National Institute for Working Life, Solna, Sweden

measure uptake of vapors in the nasal cavity of a species commonly used in inhalation toxicology studies.

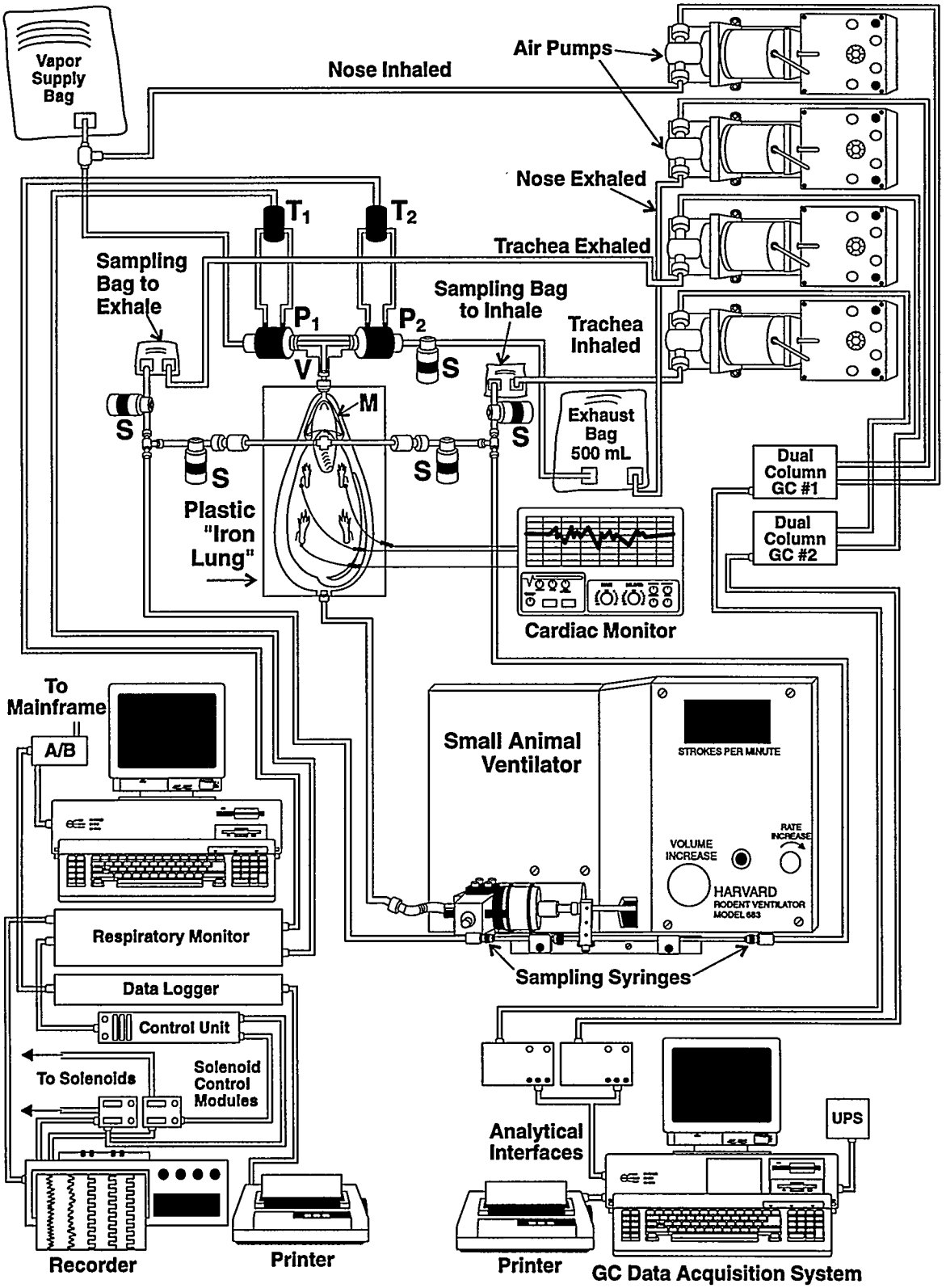

Figure 1. Schematic of the exposure system.

Table 1

Representative Uptake Data for 1,3-Dioxolane Inhaled at 500 ppm by Rats[a]

Experiment Number	Tidal Volume (mL)	Respiratory Frequency (min^{-1})	Minute Volume (mL/min)	Nasal Uptake (inhaled) (%)[b]	Lung Uptake (%)	Lung Uptake (% of available)[c]	Nasal Uptake (exhaled) (%)	Net Nasal Uptake (%)	Total Uptake (%)
1[d]	0.7 ± 0.1	60 ± 0	44 ± 6	–	–	–	–	–	14 ± 1
2	0.6 ± 0	60 ± 0	36 ± 0	72 ± 1	9 ± 1	31 ± 3	–65 ± 1	7	15 ± 1
3[d]	0.9 ± 0	60 ± 0	55 ± 2	–	–	–	–	–	25 ± 1
4	0.9 ± 0	61 ± 1	57 ± 2	66 ± 1	8 ± 1	25 ± 1	–52 ± 2	14	22 ± 2

[a]Concentrations in air samples attained steady-state values in approximately 3 min. Data were collected for approximately 20 min, and only those data collected after steady state was achieved were used for calculations. Error is standard deviation for n = 8 determinations in a single rat.

[b]% of inhaled unless indicated.

[c]The "available" vapor for lung uptake is that which passed through the nose during inhalation.

[d]Data from rats that did not have a tracheostomy. Only total uptake can be calculated for these animals.

We will use the system described to produce data necessary to validate a mathematical model for calculating uptake of vapors in rats similar to the one developed for dogs (Gerde and Dahl, 1991). Although the model will be capable of calculating the nasal and lung uptake of gases when the concentration at the air/mucosa interface is larger than zero, only an average dose over the main airway nasal mucosal surfaces will be calculable. Calculation of local doses within the nasal cavity of vapors having > 0 concentrations in the mucosa at the air interface will require coupling of an airflow-dependent uptake model (e.g., Kimbell, J. S. *et al. Toxicol. Appl. Pharmacol. 121*: 253, 1993) with the model to be validated using the exposure system reported here.

In summary, the exposure system described allows us to measure in the rat: (1) nasal absorption and desorption of vapors; (2) net lung uptake of vapors; and (3) the effects of changed breathing parameters on vapor uptake.

(Research sponsored by the PHS/NIH under Grant R01-ES04422 from the National Institute for Environmental Health Sciences with the U.S. Department of Energy, under Contract No. DE-AC04-76EV01013.)

DISSOLUTION AND CLEARANCE OF TITANIUM TRITIDE PARTICLES IN THE LUNGS OF F344/Crl RATS

*Yung-Sung Cheng, M. Burton Snipes, and Yansheng Wang**

Metal tritides are compounds in which the radioactive isotope tritium, following adsorption onto a metal, forms a stable chemical compound with the metal. When particles of tritiated metals become airborne, they can be inhaled by workers (Barta, K. and K. Turek. *Jaderna Energie 18*: 347, 1972). Because the particles may be retained in the lung for extended periods, the resulting dose will be greater than doses following exposure to tritium gas or tritium oxide (HTO). Particles of tritiated metals may be dispersed into the air during routine handling, disruption of contaminated metals, or as a result of spontaneous radioactive decay processes. Unlike metal hydrides and deuterides, tritides are radioactive, and the decay of the tritium atoms affects the metal. Because helium is a product of the decay, helium bubbles form within the metal tritide matrix. The pressure from these bubbles leads to respirable particles breaking off from the tritide surface (Beavis, L. C. and C. J. Miglionico. *J. Less-Common Metals 27*: 201, 1972).

The dissolution rate of tritiated metal particles deposited in the respiratory tract is a major factor governing retention and translocation of their constituents to other organs in the body. Dissolution of titanium tritide particles in a simulated lung fluid has been reported (1993–94 Annual Report, p. 33). The results showed that the dissolution rate of particles with a count median diameter of about 1 μm had a half-time of about 33 d. The purpose of this study was to investigate the dissolution and clearance of titanium tritide particles intratracheally instilled into rat lungs. Experimental data were also compared to a mathematical model to help evaluate the mechanism of tritium dissolution from tritide particles. Data from these studies are providing information to estimate the dosimetry of inhaled metal tritides. The dosimetric model can be used as the technical basis for setting health protection limits.

This study used fine titanium tritide powder (count median diameter = 1 μm) obtained from the Martin Marietta Pinellas Plant (Largo, FL). Thirty-six male F344/Crl rats about 11–12 wk old were intratracheally instilled with titanium tritide in 0.5 mL saline solution containing 0.45 mg of titanium tritide. The mean amount of tritium instilled into each rat lung was 27 μCi. Six rats were placed in separate glass metabolic cages, where urine and feces were collected daily for 10 d, then consecutively for 5 d at 1, 2, and 4 mo. Exhaled air from two of the metabolic cages was also sampled and analyzed for tritium gas and HTO. The remaining 30 rats in groups of six rats were sacrificed at 3 d, 2 wk, 1, 2, and 4 mo after instillation of the tritide, and lungs and bronchial lymph nodes (BLNs) were collected for analysis of their tritium content. Samples to be analyzed for ^{3}H content were processed for liquid scintillation counting using a 40% aqueous solution of tetraethyl ammonium hydroxide to dissolve biological samples. Samples were neutralized and decolorized; liquid scintillation cocktail was added. Samples were then counted for ^{3}H using a Packard 2500 TR Liquid Scintillation Analyzer (Packard Instrument Co., Downers Grove, IL). Quench correction standards were prepared using the same procedures as for the biological samples and counted along with the biological samples.

About 30% of the instilled tritide particles were physically cleared from the lung to the gastrointestinal (GI) tract within about 10 d. Thereafter, physical clearance via this pathway decreased to about 0.005 d^{-1} after 120 d. Translocation to BLNs occurred at a variable rate that is typical for rats (Snipes, M. B. *et al. Toxicol. Appl. Pharmacol. 69*: 345, 1983) (data not shown). The dissolution-

*UNM/ITRI Graduate Student

absorption rate was variable, with an initial rapid rate that decreased to a constant rate of 0.006 d^{-1} after 4 d. During the first 10 d after instillation, about 30% of the initial instilled burden of ^{3}H was dissolved from the tritide particles and absorbed into the circulatory system. Thus, the physical clearance and dissolution of tritium from the lung were about equal. After 120 d, about 44% of the tritium had been cleared physically cleared from the lung, and 44% had been cleared by dissolution-absorption. The cumulative excretion in urine after 120 d was 40% of the initial body burden. Tritium was excreted in the feces due mainly to physical clearance of tritide particles from the lung into the GI tract. After 120 d, about 47% of the initial tritium burden was excreted in feces from the rat.

Based on data from this study, a simulation model including compartments of the lung, BLNs, GI tract, body, urine, and feces was developed as shown in Figure 1. The particulate and dissolved phases of ^{3}H in the lung, BLNs, and GI tract were placed in separate compartments. Experimental data were used to determine the best-fitted rate constants, including the dissolution rate of the metal tritide, S(t), using the SAAM II^{TM} simulation software (University of Washington, Seattle, WA). The model was simulated using (1) the best-fitted rate constant parameters and (2) the same parameters, except for substitution of dissolution rate of metal tritide, S(t), which had been obtained in the previous *in vitro* study (1993–94 Annual Report, p. 33). Figure 2 shows that both simulations gave good agreement with experimental values, indicating the usefulness of the *in vitro* dissolution study.

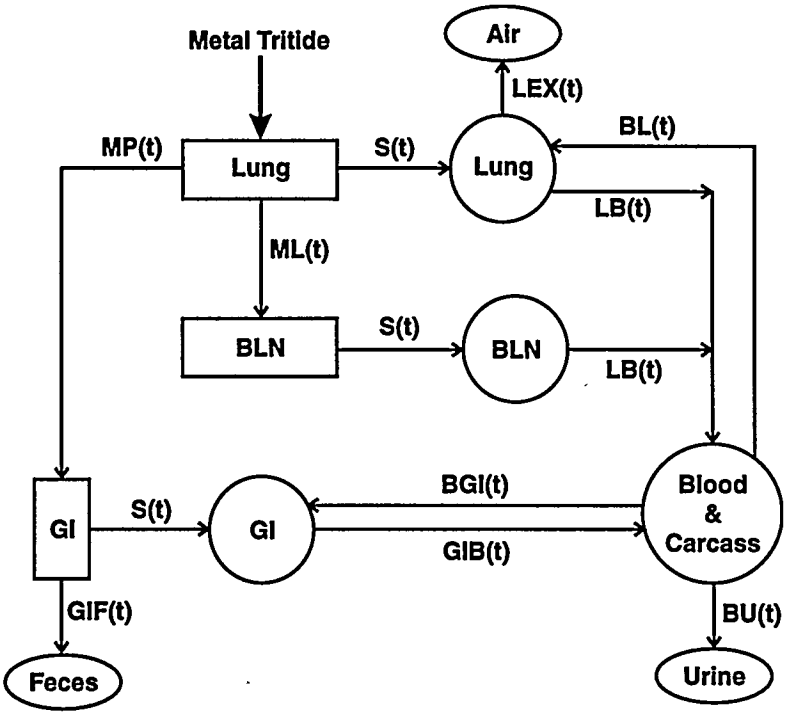

Figure 1. Schematic diagram of a metabolic simulation model of distribution and clearance of metal tritides in rats.

Our results show that a substantial amount of titanium tritide remains in the rat lung 10 d after intratracheal instillation, confirming results previously obtained in an in vitro dissolution study (1993–94 Annual Report, p. 33). This indicates that titanium tritide should not be considered a class-D compound like tritiated water, but should be considered a class-W compound. This should have implications in the radiation dosimetry of tritium-containing metal hydrides. Based on the model proposed in this report, work on the radiation dosimetry of titanium tritides is underway.

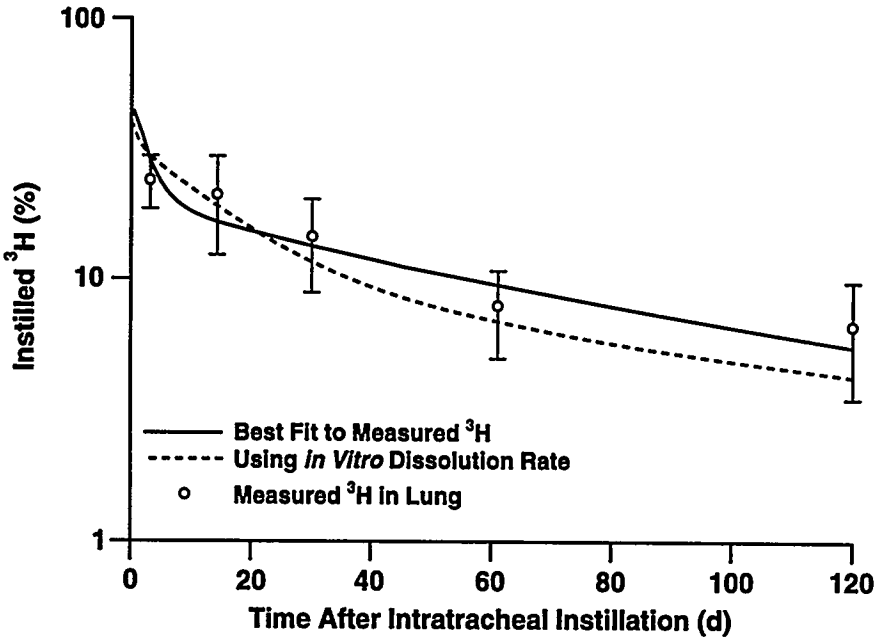

Figure 2. Retention of tritium in the rat lung after intratracheal instillation of titanium tritide particles. Experimental data (mean and standard deviation) are compared to results of a simulation model using (1) best-fit parameters for the measured ^{3}H retention and (2) the dissolution rate parameter from a previous *in vitro* study.

(Research performed under the U.S. Department of Energy Contract No. DE-AC04-76EV01013 with funding from Sandia National Laboratory Purchase Order No. AB-3148.)

MICROSCOPIC DISTRIBUTION PATTERNS OF MICROSPHERES DEPOSITED BY INHALATION IN LUNGS OF RATS, GUINEA PIGS, AND DOGS

M. Burton Snipes, Raymond A. Guilmette, and Kristen J. Nikula

Acute inhalation exposures of mammalian species to small amounts of poorly soluble particles result in deposition of the particles in the head airways, tracheobronchial region, and pulmonary region of the respiratory tract. Most of the particles that deposit in the head airways and tracheobronchial region are believed to clear rapidly, but some as yet undefined fraction of the particles is retained in the airway epithelium or subepithelial interstitium for extended times. This long-term retention has important implications for the new respiratory tract dosimetry model of the International Commission on Radiological Protection (*Annals of the ICRP*, Vol. 24, Pergamon Press, 1994) because particles retained within the region can result in long-term exposure of airway epithelial cells.

Particles that deposit in the pulmonary region become sequestered in tissue constituents of the region and are cleared by the competing processes of physical clearance and dissolution-absorption. Physical clearance of particles is believed to be mediated by macrophages and results in movement of the particles from retention sites in lung tissue to the ciliated airways of the tracheobronchial region, or to thoracic lymph nodes.

Physical clearance of particles from the lungs of most rodent species (e.g., rats and mice) is relatively fast compared to clearance from lungs of larger mammalian species (e.g., dogs and monkeys), including humans (Snipes, M. B. *Crit. Rev. Toxicol. 20*: 175, 1989). An exception to this generalization is the guinea pig, which is a rodent species with pulmonary region physical clearance rates similar to those in the larger mammalian species (Lee, P. S. *et al. J. Toxicol. Environ. Health 12*: 801, 1983; Snipes, 1989). The reasons for these species differences in pulmonary clearance rates are not known, but may be related to particle retention sites in the lung that influence availability of particles for physical clearance.

We hypothesize that anatomical retention sites for poorly soluble particles deposited in the lung have a major impact on clearance pathways and clearance rates. Further, we hypothesize that most inhaled particles that deposit in the pulmonary region of fast-clearing mammalian species are retained preferentially in respiratory air spaces distal to conducting airways and therefore have an increased potential for macrophage-mediated clearance via the mucociliary escalator. In contrast, we hypothesize that most particles that deposit in the lungs of slow-clearing mammalian species are preferentially retained in the pulmonary interstitium where the particles are not readily available for clearance via the mucociliary pathway (Mueller, H.-L. *et al. J. Toxicol. Environ. Health 30*: 141, 1990).

The purpose of this study was to determine temporal patterns for retention of small amounts of relatively inert, poorly soluble particles inhaled by rats, dogs, and guinea pigs. An important aspect of the study is the direct, visual determination of particle retention patterns in the tracheobronchial region of the respiratory tract.

Thirty CDF®(F344)/CrlBR rats (15F:15M), 30 Crl:(HA)BR guinea pigs (15F:15M), 10–12 wk old, and 10 Beagle dogs (6F:4M) from the Institute's colony were used. All of the animals were exposed per nasal to a mixture of aerosolized fluorescent yellow-green polystyrene latex (PSL) microspheres and ^{85}Sr-labeled fused aluminosilicate particles (^{85}Sr-FAPs). The PSL microspheres were monodisperse, 1.5 μm; the ^{85}SrFAPs were polydisperse, about 1.6–1.8 μm activity median aerodynamic diameter (~ 1.0–1.1 μm geometric diameter), with a geometric standard deviation of about 1.8. Rats and guinea pigs were exposed simultaneously for 4 h; dogs were exposed individually for 2 h. Initial

lung burdens of PSL microspheres were calculated from PSL/^{85}Sr ratios in exposure aerosols, and averaged about 10^6 PSL microspheres/g lung for all three species.

Three female/three male rats, three female/three male guinea pigs, and two dogs were sacrificed 1, 14, 42, 91, and 182 d after exposure. Lungs were removed, tracheas were intubated, and the lungs were suspended in a microwave oven. Air was used to inflate the lungs and maintain inflation at 25 cm hydrostatic pressure. The lungs were dried for 3 h using intermittent microwave heating to maintain lung temperature in the range 40–44°C. Warming with microwaves was discontinued after 3 h, but air flow through the inflated lungs continued for an additional 21 h. Dried lungs were systematically sampled, and the samples were rehydrated and embedded in glycol methacrylate. Embedded lung was sectioned at 2.5 μm; the sections were mounted on glass slides, stained with toluidine blue, and examined using epifluorescent and light microscopy. The slides were individually scanned in a raster pattern using an overall magnification of 200X. Locations of fluorescent PSL microspheres were recorded with respect to associated cells or tissue constituents that were identifiable in the 2.5 μm thick tissue sections.

Preliminary results from all three species for days 1 and 14 are presented in Table 1. On days 1 and 14, a small percentage of the PSL microspheres in the lung was noted as free or associated with macrophages on the surface of tracheobronchial airways. Additional microspheres were within or wedged between bronchial epithelial cells, and other microspheres were incorporated into the tracheobronchial subepithelial interstitium. The sample size is relatively small at this time, but suggests that as much as 5–10% of the PSL microspheres deposited by inhalation in all three species may have been incorporated into the tracheobronchial tissues; the final results of the study will allow more definitive conclusions about relative amounts and temporal patterns for retention of the PSL microspheres at these locations in the respiratory tract. Interstitialized microspheres in all three species appeared to be preferentially located near either alveolar ducts in the rats or guinea pigs, or near respiratory bronchioles in the dogs. Some particles were scored as free in the alveolar ducts and alveoli, because there were no obvious indications of cell membranes associated with the microspheres. A significant difference between the rats and guinea pigs versus the dogs was the presence of respiratory bronchioles in the dogs. About 23 and 28% of the microspheres were found associated with the epithelium or subepithelium of the respiratory bronchioles on days 1 and 14, respectively. The general patterns for particle retention were similar among these three species if the analogy is made that the alveolar ducts and respiratory bronchioles serve anatomically similar roles among the species in terms of particle deposition sites.

A surprising result was the finding that most PSL microspheres found to date for animals evaluated after 1 or 14 d were located in the pulmonary interstitium in all three species. Our hypothesis was that most of the microspheres in the rats would be found associated with alveolar macrophages at these times. Our preliminary results indicate that the retention patterns for the inhaled microspheres are quite similar for all three species. Some of the microspheres were evident in interstitial macrophages, some appeared to be wedged between structural cells, some were clearly associated with type I and type II cells, and others were found in lymphatic channels. The microspheres in lymphatic channels rarely appeared to be associated with a macrophage.

Preliminary results from this study demonstrate that a substantial fraction of the PSL microspheres inhaled by these rats, guinea pigs, and dogs was incorporated into the epithelium and interstitium of the tracheobronchial region. Importantly, no substantial differences have been noted in the fractions of PSL microspheres retained in alveolar macrophages versus the pulmonary interstitium of these species. More definitive descriptions of the microsphere retention sites and temporal retention patterns will be possible when the study is completed.

Table 1

Retention Locations for Inhaled 1.5-μm Fluorescent Polystyrene Latex Microspheres in Lungs of Rats, Guinea Pigs, and Dogs.
Values are percentage of total microspheres scored to date.

	Rat		Guinea Pig		Dog	
Microsphere location	1	14	1	14	1	14
Free on tracheobronchial surface	0.3	0.3	0	0	0.1	1.2
With macrophage on tracheobronchial surface	0.3	0	0	0	0.1	0.6
With tracheobronchial epithelial cells	4.6	1.9	6.2	0.2	4.9	5.4
With tracheobronchial interstitium	0.7	0.5	3.6	0.2	0.8	3.2
With respiratory bronchioles	NA[a]	NA[a]	NA[a]	NA[a]	23.4	28.0
Free in alveolar duct	1.6	1.9	1.6	0.2	0	0
Free in alveolus	2.1	1.5	3.1	0.5	1.7	1.4
With macrophage in alveolar duct	3.2	1.8	6.3	0.5	0.2	0.8
With macrophage in alveolus	4.5	6.3	3.7	2.9	3.3	3.8
In pulmonary interstitium	82.7	85.8	75.5	95.5	65.5	55.6
Total microspheres scored	2445	784	192	1068	2872	1572

[a]NA = not applicable.

(Research sponsored by the Office of Health and Environmental Research, U.S. Department of Energy, under Contract No. DE–AC04–76EV01013.)

EVIDENCE FOR PARTICLE TRANSPORT BETWEEN ALVEOLAR MACROPHAGES *IN VIVO*

Janet M. Benson, Kristen J. Nikula, and Raymond A. Guilmette

Recent studies at this Institute have focused on determining the role of alveolar macrophages (AMs) in the transport of particles within and from the lung (1993–94 Annual Report, p. 45). For those studies, AMs previously labeled using the nuclear stain Hoechst 33342 and polychromatic Fluoresbrite microspheres (1 μm diameter, Polysciences, Inc., Warrington, PA) were instilled into lungs of recipient F344 rats. The fate of the donor particles and the doubly labeled AMs within recipient lungs was followed for 32 d. Within 2–4 d after instillation, the polychromatic microspheres were found in both donor and resident AMs, suggesting that particle transfer occurred between the donor and resident AMs. However, this may also have been an artifact resulting from phagocytosis of the microspheres from dead donor cells or from the fading or degradation of Hoechst 33342 within the donor cells leading to their misidentification as resident AMs.

The purpose of the present study was to verify that particle transfer occurs between rat AMs *in vivo*. Resident AMs were labeled with green-fluorescing microspheres. Donor AMs were labeled with Hoechst 33342 and red-fluorescing microspheres. By this method, the presence of red microspheres in AMs containing chiefly green microspheres (and vice versa) was interpreted as indicating that particle transfer occurred, especially at early times after instillation of donor AMs when minimal cell death may be expected.

Male F344/NHsd rats were purchased from Harlan Sprague Dawley, Inc. (Indianapolis, IN). Six male F344/NHsd rats (10 wk old) were administered approximately 10 million green-fluorescing microspheres in 0.5 mL sterile saline by intratracheal instillation 2 d before the donor AMs were prepared and instilled.

The donor AMs were obtained from F344/NHsd rats by bronchoalveolar lavage (Benson, J. M. *J. Toxicol. Environ. Health 19*: 105, 1986). The cells were washed once in RPMI culture medium, and the concentration of cells in suspension was adjusted to 1 million cells/mL medium. The donor AMs were sedimented by centrifugation, resuspended in saline containing 2.5 μg Hoechst dye/mL medium, and incubated for 30 min at 37°C. After incubation, the cells were sedimented, resuspended in RPMI, and transferred to 100-mm plastic petri dishes where the AMs were incubated (37°C, 5% CO_2) with polychromatic red-fluorescing Fluoresbrite microspheres for 2 h. The microsphere to cell ratio was 15:1. At the end of the incubation period, the cells were recovered from the plates, sedimented by centrifugation, and resuspended in RPMI (2–3 million cells/mL) for instillation into donor rats. Examination of cytospin preparations of the donor cells indicated that more than 95% of the cells were labeled with Hoechst and that the majority of cells contained at least five or more red-fluorescing microspheres.

Approximately 1.5–2 million donor AMs were immediately instilled into the six recipient rats. Subgroups of two recipient rats were sacrificed 2, 4, and 8 d later. The lungs were excised and instilled with Tissue Tek:saline (60:40); individual lobes were frozen in liquid N_2. The samples were stored at –80°C until processed. The lobes were cryosectioned at 5 μm and neither fixed nor counterstained prior to evaluation by epifluorescent microscopy. Donor AMs within the lung sections were identified as having blue-fluorescing nuclei and containing only or a majority of red microspheres in the cytoplasm. In some cases, it was difficult to see the nuclei because of the large numbers of red microspheres contained within the AMs. Resident AMs contained only green microspheres. AMs containing chiefly red microspheres, but also containing one or a few green microspheres were

considered as donor cells that had ingested green microspheres from resident AMs. AMs containing chiefly green microspheres but also containing one or a few red microspheres were identified as resident AMs that had phagocytized red microspheres from donor cells. AMs containing 2–3 red and green microspheres were classified as originally unlabeled AMs that had ingested microspheres from both donor and resident AMs. Results are discussed in terms of the location of donor particles.

Most AMs observed in sections of left lungs from recipient rats sacrificed 2 d after instillation of donor AMs were labeled with 5 to 10 or more green-fluorescing microspheres. Few totally unlabeled AMs or free red or green particles were observed. The distribution of red-fluorescing microspheres among AMs in recipient rats as a function of time after instillation of donor AMs is summarized in Table 1. By day 2 after donor AMs were instilled, > 50% of cells containing red microspheres were donors that had ingested small numbers of green microspheres and resident AMs that had ingested small numbers of red microspheres. These results suggest that the mixing of particle types in the AMs was a result of particle transfer between donor and resident AMs rather than a result of phagocytosis of dead or dying AMs. We conclude this because of the relatively few numbers of red or green microspheres in the recipient and donor AMs, respectively, compared to the numbers of microspheres originally contained by the donor and resident AMs. Only 6% of the AMs containing red microspheres at day 2 contained two or three red and two or three green microspheres, further suggesting that previously unlabeled AMs acquired microspheres by particle transfer. On day 2 post instillation, almost all of the AMs containing red microspheres were alveolar. Only one aggregate of free red microspheres and four clusters of red and green microspheres were noted in alveolar septa. No free red particles were noted in bronchovascular interstitial tissue. The distribution of red microspheres within AMs shifted somewhat by day 4 and day 8 post instillation. The numbers of donor cells with green microspheres and, more notably, the numbers of resident AMs with red microspheres decreased, while the numbers of AMs containing relatively equal numbers of red and green particles increased (Table 1). In AMs containing large numbers of both red and green microspheres, it was not possible to identify the origin of the AMs by Hoechst fluorescence or by the preponderance of one color microsphere over the other in the AMs. The large decrease in numbers of resident AMs with red microspheres by day 8, coupled with the large increase in numbers of AMs with large numbers of both red and green microspheres suggest that microsphere transfer continued to occur among donor and resident AMs.

Table 1

Distribution of Alveolar Macrophages Based on Their Content of Donor (Red-Fluorescing) and Resident (Green-Fluorescing) Microspheres as a Function of Time after Instillation of Donor Alveolar Macrophages

	Percentage of AMs Days after Instillation of Donor AMs		
AM Type	2	4	8
Donor AMs with Only Red Microspheres	41	28	38
Donor AMs with Some Green Microspheres	34	26	22
Resident AMs with Some Red Microspheres	20	24	1
AMs with a Few Red and Green Microspheres	6	18	16
AMs with Many Red and Green Microspheres	0	4	22

The location of red microsphere-containing AMs shifted between day 2 and day 8 post instillation. While the majority of AMs were alveolar 2 d after instillation, AMs became associated with alveolar septa and interstitial tissue by day 8. Twenty-five clusters of "free" red and/or red and green microspheres were associated with alveolar septa at 4 d post instillation, while 22 clusters of such microspheres were noted in bronchovascular interstitial tissue at this time. These particles were not obviously associated with AMs. At 8 d post instillation, the numbers of microsphere clusters associated with alveolar septa decreased to 17, while the numbers of microspheres or microsphere aggregates in bronchovascular interstitial increased to 61.

These results support the earlier findings that microspheres in donor AMs can be transferred to resident AMs within 2 d after instillation. Particle transfer from resident to donor AMs also appears to occur. The results also confirm earlier findings that intratracheally instilled particles redistribute to the alveolar septa and bronchovascular interstitium with time after instillation.

(Research sponsored by the Office of Health and Environmental Research, U.S. Department of Energy, under Contract No. DE-AC04-76EV01013.)

III. METABOLISM AND MARKERS OF INHALED TOXICANTS

AN ISOTOPE DILUTION GAS CHROMATOGRAPHY/MASS SPECTROMETRY METHOD FOR TRACE ANALYSIS OF XYLENE AND ITS METABOLITES IN TISSUES FOLLOWING THRESHOLD LIMIT VALUE EXPOSURES

Kee H. Pyon, Dean A. Kracko, Michael R. Strunk, William E. Bechtold, Alan R. Dahl, and Johnnye L. Lewis*

The existence of a nose-brain barrier that functions to protect the central nervous system (CNS) from inhaled toxicants has been postulated (Lewis, J. L. *et al.* In *The Vulnerable Brain and Environmental Risks, Vol. 3: Toxins in Air and Water* [R. L. Isaacson and K. F. Jenson, eds.], Plenum Press, New York, p. 77, 1994). Just as a blood-brain barrier protects the CNS from systemic toxicants, the nose-brain barrier may have similar characteristic functions. One component of interest is nasal xenobiotic metabolism and its effect on the transport of pollutants into the CNS at environmentally plausible levels of exposure. Previous results have shown that inhaled xylene is metabolized within the olfactory epithelium of rats. The primary volatile metabolites of xylene are dimethyl phenol (DMP) and methyl benzyl alcohol (MBA), and the nonvolatile metabolites are toluic acid (TA) and methyl hippuric acid (MHA). The nonvolatile metabolites of xylene, along with a small quantity of volatiles, representing either parent xylene or volatile metabolites, are transported via the olfactory epithelium to the glomeruli within the olfactory bulbs of the brain (1993–94 Annual Report, p. 47).

There are many methods for the determination of these metabolites, such as thin-layer chromatography, high-performance liquid chromatography, and gas chromatography. However, these methods were applicable only for detection at concentrations greater than those expected from our studies at threshold limit value (TLV; 123 ppm of xylene). In order to detect low concentration levels of xylene and its metabolites in frozen tissues of specific brain regions, a more selective and sensitive method was needed.

The purpose of this paper is to report a highly sensitive gas chromatograph/mass spectrometer (GC/MS) isotope dilution method to detect and quantitate xylene and its metabolites at low concentrations in the range of pg to ng of analyte/mg of tissue.

The MS was operated in the selected ion mode. The characteristic ion pairs for xylene, its metabolites, and their corresponding deuterated internal standard analogs are as follows: xylene (91/106 and 98/116), DMP (179/194 and 182/197), MBA (179/194 and 182/197), TA (193/208 and 200/215), and MHA (119/220 and 126/226). Deuterated TA (TA-d_7) and deuterated MHA (MHA-d_7) were produced in-house by collecting the urine from rats induced with phenobarbital and then injected with deuterated xylene (xylene-d_7). However, deuterated volatile metabolites were not produced in a large enough quantity; hence, deuterated DMP (DMP-d_3) was purchased as internal standard for both DMP and MBA.

Peaks were integrated, and ion ratios were calculated to both internal standards and to the other ion from the same analyte. The ion ratio of analyte to internal standard was used for quantitation, while the ion ratio of one analyte ion to the other ion of the same analyte was used to confirm the identity of the analyte. Standard curves for all analytes were created by serially diluting analyte standards in acetonitrile and adding a constant amount of internal standard consisting of a mixture of xylene-d_7, DMP-d_3, TA-d_7, and MHA-d_7. Figures 1 and 2 show the standard curves of all the analytes. Based on the reproducibility and linearity of the responses, the GC/MS detection sensitivity

---

*Postdoctoral Fellow

limits were 530, 120, 85, 80, and 80 pg for xylene, MHA, TA, MBA, and DMP, respectively. The upper limits ranged from 1.2 to 2.7 ng (highest concentration of standards tested to date).

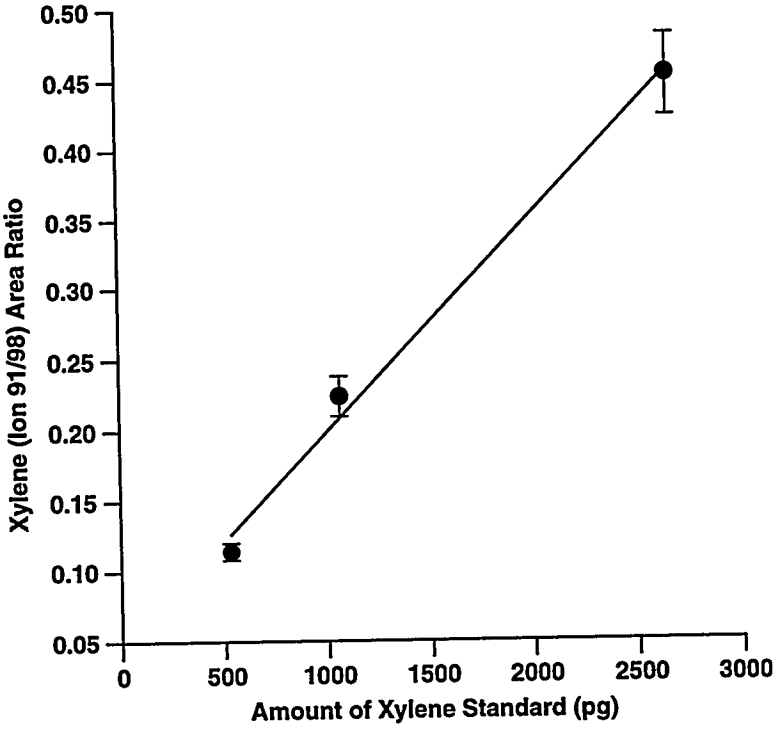

Figure 1. Standard curve of xylene (mean ± SD; n = 3).

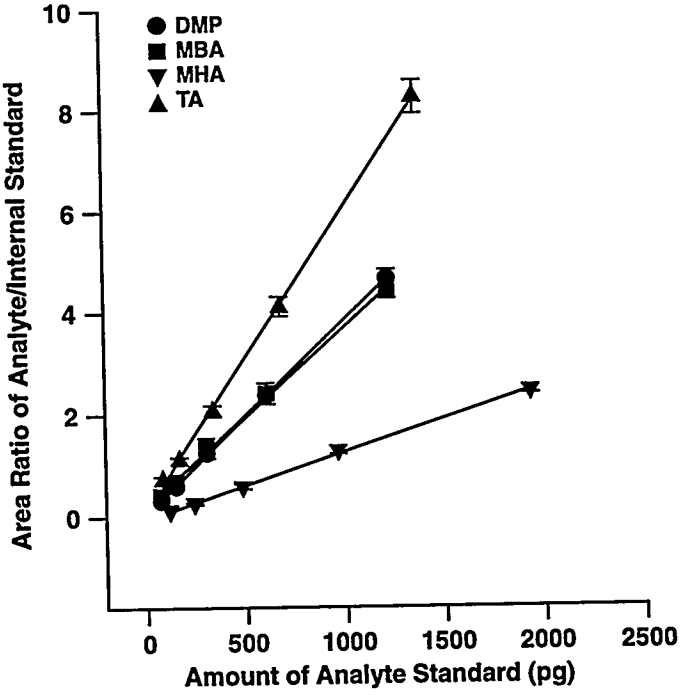

Figure 2. Standard curves of metabolites (mean ± SD; n = 5).

Once the method was tested with analyte standards, another method was developed for preparing tissue samples for GC/MS analysis of xylene and its metabolites. The brain tissue samples were prepared by first homogenizing the tissue in a mixture of 100 μL of internal standard and buffer solution. The homogenized sample was then extracted with ethyl acetate, and the organic phase was reduced to 50 μL volume under a stream of nitrogen gas. One μL of the sample was injected into the GC for xylene analysis. The remaining sample was then dried under nitrogen gas and derivatized with 50 μL of N,O-bis(trimethylsilyl)trifluoroacetamide with 1% trimethylchlorosilane. One μL of the derivatized sample was then injected into the GC for the analysis of the metabolites.

Preliminary tests have been conducted on control rat brain tissues. No metabolites were detected in the cerebellum and basal ganglia of these rats, and < 1 ng of xylene/mg of tissue was detected. Further analyses of both control and TLV-exposed tissues are in progress to determine whether xylene was present in control tissues or whether interference occurred due to the presence of endogenous compounds with fragmentation patterns similar to xylene, and whether sensitivity was sufficient for xylene determinations in brain tissues of exposed animals.

This highly sensitive method for analysis of xylene and its metabolites has several advantages. Extraction and volume concentration of the brain tissues result in a sample with its analytes concentrated enough to be detected and quantitated by the GC/MS. This assay is sensitive enough that a sample injection volume of 1 μL is adequate for the detection of the analytes. This technique may also be a more sensitive method for biologically monitoring the magnitude of pollutant exposure to industrial workers from blood and urine samples.

Further work will be done to establish the linearity for each analyte at the actual highest detection limit of the GC/MS. Future work will focus on analyzing the brain tissues of rats that have undergone the TLV xylene exposures. These results should give us more insight into the transport of xylene and its metabolites into the brain and allow us to test the hypothesis of the existence of a nose-brain barrier.

(Research sponsored by the PHS/NIH under Grant R01-DC01714 from the National Institute on Deafness and Other Communication Disorders with the U.S. Department of Energy, under Contract No. DE-AC04-76EV01013.)

DEMONSTRATION OF CARBOXYLESTERASE IN CYTOLOGY SAMPLES OF HUMAN NASAL RESPIRATORY EPITHELIUM

Darrell A. Rodgers, Kristen J. Nikula, Kelly Avila, and Johnnye L. Lewis*

The epithelial lining of the nasal airways is a target for responses induced by a variety of toxicant exposures. The high metabolic capacity of this tissue has been suggested to play a role in both protection of the airways through detoxication of certain toxicants, as well as in activation of other compounds to more toxic metabolites (Dahl, A. R. and J. L. Lewis. *Annu. Rev. Pharmacol. Toxicol. 32*: 383, 1993). Specifically, nasal carboxylesterase (CE) has been shown to mediate the toxicity of inhaled esters and acrylates by converting them to more toxic acid and alcohol metabolites which can be cytotoxic and/or carcinogenic to the nasal mucosa (Bogdanffy, M. S. and M. L. Taylor. *Drug Metab. Dispos. 19(1)*: 124, 1991).

Species-specific differences in nasal architecture and percentages of the various types of nasal epithelium (squamous, transitional, respiratory, and olfactory) cause difficulties in extrapolation from studies using animals to humans (Harkema, J. R. *Toxicol. Pathol. 19(4)*: 321, 1991). Nasal CE is similarly distributed among the tissues of rats, dogs, and humans. The enzyme concentration decreases progressively with humans having the least concentration. Among all species, nasal CE concentrations may decrease or even disappear in the presence of inflammation and other histopathologic lesions of the mucosa that can result from common environmental exposures (Lewis, J. L. *et al. Anat. Rec. 239(1)*: 55, 1994a). In addition, nasal CE can be induced following exposure to toxicants, even if those toxicants are not substrates for the enzyme (Nikula, K. J. *et al. Drug Metab. Dispos. 23(5)*: 529, 1995; Lewis, J. L. *et al. Inhal. Toxicol. 6(Suppl.)*: 422, 1994b). Prediction of toxic responses in humans could be improved by determining the metabolic status of the nasal epithelium in both unexposed individuals and those exposed to common environmental toxicants such as ozone and cigarette smoke (Lewis *et al.*, 1994a). The present work was designed to develop a noninvasive technique for obtaining cells from human nasal respiratory epithelium and to demonstrate the presence of CE in these cells.

Human nasal respiratory epithelium is pseudostratified, ciliated epithelium, composed primarily of ciliated cells, goblet cells, and basal cells. Cytology samples of this epithelium were obtained using a narrow, sterilized, nylon histobrush® (Fisher Scientific, Pittsburgh, PA). The brush was inserted into either nostril up to the middle turbinate to obtain respiratory epithelial cells by a gentle turning of the brush against the nasal septum. The cells obtained upon the bristles were then transferred to ProbeOn® Plus microscope slides by gently rolling the bristled end onto the slides. Cells were then preserved in Saccomano's fixative for 10 min, removed, air dried, and maintained at 4°C until time of staining.

A total of 50 slides from six individuals was used to maximize the technique. Twenty-five of the slides were stained positively for CE, and 25 were used as controls. Briefly, the staining procedure consisted of rehydrating the cells through a series of graded ethanols (90% to 30%), followed by washing with automation buffer (AB) (Biomeda Corp., Foster City, CA) at a 1:5 dilution in di-ionized water (DIW). Endogenous peroxidase activity was quenched by using 10% hydrogen peroxide in methanol followed by AB washing. To eliminate nonspecific background staining, samples were exposed to a 1:50 dilution of Power Block® (Biogenex, San Ramon, CA) in DIW for 15 min. After blocking, the slides were rinsed twice with Dulbecco's phosphate buffered saline (DPBS), followed by an AB rinse. Polyclonal CE primary antibody (ICT, Wayne State University, Detroit, MI) from goat

*UNM/ITRI Pulmonary Epidemiology and Toxicology Training Program Participant

was applied to cells in a serum solution diluted to 1:6000 with 1:10 AB and 1% BSA. Negative controls were incubated under the same conditions using normal goat serum in place of CE antisera. Slides were then incubated at 37°C for 2 h, followed by three washings with AB. Next, samples were incubated in a secondary antibody at 1:200 in DPBS for 30 min at 37°C, followed by three washings with AB.

A pre-diluted (30 min prior) solution of Avidin-Biotin Complex (Vector Laboratories, Inc., Burlingame, CA) was applied to the slides for 45 min at 37°C, and rinsed three times with AB. To stain for CE, a solution of chromogen 3,3'-diaminobenzidine was applied for 2 min, followed by washings with cold AB, DIW, and ambient temperature AB solutions, respectively. Cells were then counterstained using Harris Alum hematoxylin in DIW at a 1:3 dilution for 1 min, washed with AB and DIW. Rehydration was done in a graded ethanol series of 50%–100%, followed by xylene. Slides were then air dried and mounted.

CE immunoreactivity in the cells was determined by comparison of reaction product in cells incubated with normal goat serum and those incubated with CE primary antibody. Evaluation at the light microscope level was qualitative and based on intensity, granularity, background, and absence of staining in squamous epithelial cells. Ciliated, goblet, and squamous cells could be visually identified on all slides.

CE in respiratory cells was distinctly prominent with minimum nonspecific staining. Rat turbinate sections were used as positive controls to ensure staining. In the human cells, ciliated respiratory epithelial cells were intensely stained, with no or very little staining of the background squamous cells and residual mucus. Negative control slides using goat serum did not show evidence of significant staining of the respiratory cells. A slight, diffuse brown could be seen in ciliated cells of some individuals, but lacked the granularity and intensity seen in the cells incubated with CE antibody.

To better evaluate the staining process, alternative measurement techniques are being investigated. Currently, work is in progress to develop a quantitative method to determine the density of CE staining in cells and tissue, using a video microscopic imaging system with Nomarski optics.

Due to difficulties in extrapolating rodent models to humans, new paradigms using human cells and tissues are essential to understanding and evaluating the metabolic processes in human nasal epithelium. Nasal CE concentration has been used as an indicator of nasal toxicity. This technique for obtaining and evaluating the presence of CE in humans may prove a useful biomarker of exposure and benchmark of metabolic status in the nose, as well as aiding in prediction of toxic responses. The procedure is cost-effective for screening purposes and results in a minimum of discomfort for subjects due to its noninvasiveness.

(Research sponsored by the National Institutes of Health by subcontract with Wayne State University under Funds-In-Agreement No. DE-FI04-89AL58635 with the U.S. Department of Energy, under Contract No. DE-AC04-76EV01013.)

NASAL CYTOCHROME P4502A: IDENTIFICATION IN RATS AND HUMANS

Janice R. Thornton-Manning, Jon A. Hotchkiss, Kevin D. Rohrbacher**, Xinxin Ding***, and Alan R. Dahl*

The nasal mucosa, the first tissue of contact for inhaled xenobiotics, possesses substantial xenobiotic-metabolizing capacity. Enzymes of the nasal cavity may metabolize xenobiotics to innocuous, more water-soluble compounds that are eliminated from the body, or they may bioactivate them to toxic metabolites. These toxic metabolites may bind to cellular macromolecules in the nasal cavity or be transported to other parts of the body where they may react. Nasal carcinogenesis in rodents often results from bioactivation of xenobiotics (reviewed by Dahl, A. R. and W. M. Hadley. *CRC Crit. Rev. Toxicol. 21*: 345, 1991). The increased incidences of nasal tumors associated with certain occupations suggest that xenobiotic bioactivation may be important in human nasal cancer etiology, as well. The increasing popularity of the nose as a route of drug administration makes information concerning nasal drug metabolism and disposition vital to accomplish therapeutic goals. For these reasons, the study of the xenobiotic-metabolizing capacity of the nasal cavity is an important area of health-related research.

Several xenobiotic-metabolizing enzymes, including cytochrome P450s, are present in nasal tissues of various species (Dahl and Hadley, 1991). The rabbit nasal mucosa contains an abundance of two cytochrome P450 enzymes; CYP2G1 is present only in olfactory mucosa, and members of the CYP2A subfamily are present in both olfactory and respiratory tissues (Ding, X. and M. J. Coon. *Mol. Pharmacol. 37*: 489, 1990). Proteins immunochemically related to CYP2A are present in both rat and human olfactory and respiratory mucosa (Chen, Y. *et al. Neuro. Report 3*: 749, 1993; Getchell, M. L. *et al. Ann. Otol. Rhinol. Laryngol. 102*: 368, 1993); however, positive confirmation of these proteins as members of the CYP2A subfamily has not been reported. A human isoform of the CYP2A subfamily, CYP2A6, is present in human liver, but in most samples examined, it accounted for > 1% of the total P450s (Yun, C. H. *et al. Mol. Pharmacol. 40*: 679, 1991). This P450 is thought to be toxicologically important because of its ability to metabolize several toxicants including aflatoxin B_1, dimethylnitrosamine, and diethylnitrosamine to cytotoxic and mutagenic species (Crespi, C. L. *et al. Carcinogenesis 11*: 1293, 1990). Nasal expression of this P450 isoform could greatly affect the toxicity of inhaled toxicants.

The purpose of the present study was to confirm the presence of CYP2A in rat nasal tissue and to evaluate the expression of CYP2A6 mRNA in human nasal respiratory samples. Furthermore, the metabolism of the rat nasal carcinogen HMPA by human CYP2A6 and rat olfactory and nasal respiratory microsomes was evaluated.

Male Fischer 344/N rats (13–15 wk) obtained from Harlan-Sprague Dawley, Inc. (Indianapolis, IN) were sacrificed, and the livers and lungs were removed and placed in cold saline. The nasal cavities were opened, and olfactory and respiratory mucosa were removed and rinsed with cold saline. Microsomes were prepared from these tissues using standard procedures and resuspended in sodium phosphate buffer, pH 7.4.

*Department of Pathology, Michigan State University, East Lansing, Michigan
**UNM/ITRI Graduate Student
***Wadsworth Center for Laboratories and Research, New York State Department of Health, Albany, New York

Western blot analysis was carried out using olfactory mucosa microsomes (three samples from pools of four rats) and respiratory mucosa microsomes (one sample pooled from 12 rats). The samples (5 μg protein) were subjected to sodium dodecyl sulfate-polyacrylamide gel electrophoresis on a 10% gel, and the protein was transferred to a nitrocellulose membrane. Western blot analyses were performed according to previously published procedures (Hotchkiss, J. A. *et al. Toxicol. Appl. Pharmacol. 118*: 98, 1993). The primary antibody was rabbit anti-rabbit CYP2A10/11 which has been extensively characterized (Ding and Coon, 1990). The secondary antibody was biotinylated goat anti-rabbit IgG. Color was developed using avidin-horseradish peroxidase as described in the Vectastain ABC immunoperoxidase kit (goat anti-rabbit IgG, Vector Laboratories, Burlingame, CA) instructions. Western blot analysis of microsomes from olfactory and respiratory tissues of rats indicated that a protein immunochemically related to CYP2A was present in these tissues (Fig. 1). The CYP2A10/11 antibody reacted with a protein of approximately 50 kD in all four samples, but the levels were consistently greater in the olfactory microsomes than in the respiratory microsomes.

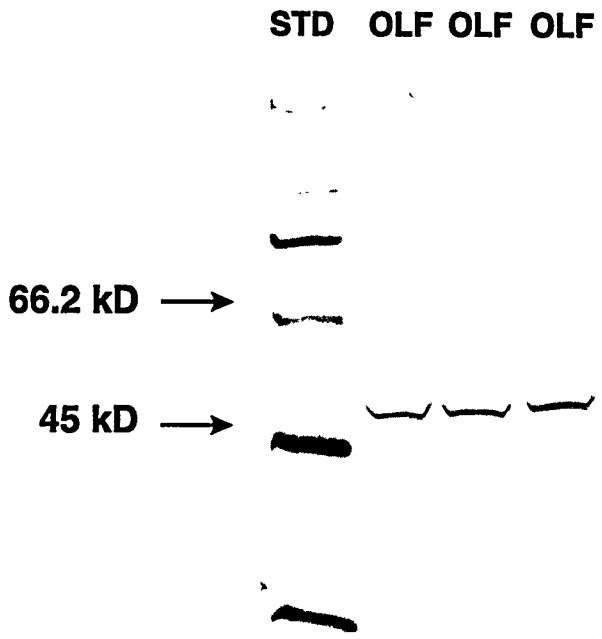

Figure 1. Immunoblot analysis of olfactory (OLF) and respiratory (RESP) microsomes prepared from rats. Immunochemical detection of three olfactory mucosa (pools of four rats) and one respiratory mucosa (pooled from 12 rats) microsome samples was conducted using an antibody to rabbit CYP2A10/11.

The presence of CYP2A mRNA in human nasal respiratory mucosa was evaluated using reverse transcription-polymerase chain reaction (RT-PCR). Samples of human respiratory mucosa were obtained from 11 patients undergoing middle turbinectomies within 30 min following the surgical procedure and immediately frozen in liquid nitrogen. RNA was purified from the human nasal respiratory mucosa samples using the method of Chomczynski, P. and N. Sacchi (*Anal. Biochem. 162*: 156, 1987). RT-PCR was performed with a GeneAmp RNA PCR kit (Perkin Elmer Cetus, Foster City, CA). First strand cDNAs were synthesized at 42°C with the use of 0.5 μg of total RNA and 2.5 μM of an oligo $d(T)_{16}$ primer. PCR reactions were performed for 35 cycles, with the following conditions: denaturation at 94°C, annealing at 58°C, and elongation at 72°C, all for 45 sec. The 5′ primer (5′GCCCTTCATTGGAAACTACC3′) and the 3′ primer (5′GTGACAGGAACTCTTTGTCC3′)

were complimentary to nucleotides 120–139 and 582–601, respectively, in the coding region of 2A6 cDNA (Yamano, S. *et al. Biochemistry 29*: 1322, 1990). PCR products were analyzed by electrophoresis on a 1.5% agarose gel and visualized by staining with ethidium bromide. A 0.5 Kb fragment of CYP2A6 was identified in the respiratory mucosa of each patient (data not shown). The identity of these amplified fragments was confirmed by sequencing.

Formaldehyde production from cytochrome P450-mediated metabolism of HMPA was measured as previously described (Dahl, A. R. and W. M. Hadley. *Toxicol. Appl. Pharmacol. 67*: 200, 1983) using 0.5–1 mg microsomal protein prepared from rat liver, lung, and nasal respiratory mucosa and 0.2 mg microsomal protein prepared from rat olfactory S9. The initial concentration of HMPA was 2 mM in each case, and the incubation was carried out for 20 min. The formaldehyde produced was converted to 3,5-diacetyl-1,4-dihydrolutidine using Nash reagent and then quantified by measuring absorbance at 410 nm on a UV/VIS Spectrophotometer.

Olfactory microsomes from rats were 6-fold more active toward HMPA metabolism than microsomes from rat liver and nasal respiratory epithelia and 19-fold more active than microsomes from rat lungs (Table 1). Levels of HMPA metabolism in rat lung were about 3-fold lower than those in rat liver microsomes.

Table 1

Metabolism of Hexamethylphosphoramide in Microsomal Fractions

Microsomal Fraction	nmol Formaldehyde/min/mg/Protein (mean ± SE)[a]
Rat olfactory epithelia	3.8 ± 0.80
Rat nasal respiratory epithelia	0.5 ± 0.03
Rat liver	0.6 ± 0.02
Rat lung	0.2 ± 0.02
Human β-lymphoblastoid cells transfected with CYP2A6	0.2 ± 0.1

[a]n = 3 for each determination, except for lung where n = 4.

To evaluate the ability of human CYP2A to metabolize HMPA, microsomes from human β-lymphoblastoid cells expressing human CYP2A6 were purchased from the Gentest Corporation (Woburn, MA). Microsomes from the parental cell line that contained no transfected P450 were also purchased to serve as controls. For the experiments with the human β-lymphoblastoid cell microsomes, 2 mg protein was used, and HMPA metabolism was evaluated as described above. No detectable level of formaldehyde was produced in the control cells, while in the cells transfected with CYP2A6, the production was 0.2 nmol/min/mg protein (Table 1). Human CYP2A6, while active toward HMPA, exhibited less activity than that previously shown by the rabbit CYP2A isoforms CYP2A10 and CYP2A11 (Peng, H. M. *et al. J. Biol. Chem. 268*: 17253, 1993).

The olfactory epithelium of every species studied has greater xenobiotic-metabolizing ability for most P450 substrates than does the nasal respiratory epithelium (reviewed by Reed, C. J. *Drug Metab.*

Rev. 25: 173, 1993). In the present study, HMPA metabolism to formaldehyde also exhibited this pattern in rat microsomes, and, correspondingly, levels of CYP2A protein were greater in olfactory than in respiratory mucosa by Western analysis in rat nasal tissue. CYP2A10/11 is present in the olfactory mucosa of rabbits at a concentration about 5-fold greater than that in respiratory mucosa or liver (Ding and Coon, 1990). The greater expression in olfactory mucosa suggests a role for this P450 in olfaction. In prenatal and newborn rabbits, CYP2A is present in the olfactory tissue before being expressed in the liver (Ding, X. *et al. Mol. Pharmacol. 42*: 1027, 1992). Because olfactory ability is vital for the survival of the newborn further indicates that this isoform may be important in olfaction. Moreover, rabbit CYP2A is active in the metabolism of odorants.

HMPA is a potent carcinogen in rats causing tumors during and after chronic inhalation exposures at concentrations as low as 50 ppb (Lee, K. P. and H. J. Trochimovicz. *J. Natl. Cancer Inst. 68*: 157, 1982). While this solvent has been widely used in industry, no epidemiological study indicating that this chemical is a nasal carcinogen in humans has been reported. The mechanism of carcinogenicity of HMPA may be due to its cytochrome P450-mediated conversion to formaldehyde (Dahl, A. R. *et al. Science 216*: 57, 1982). In the present study, a human nasal P450, CYP2A6, metabolized HMPA to formaldehyde, albeit at a rate lower than that for CYP2A proteins in rabbit nasal tissue. These data suggest that the apparent lack of carcinogenicity of HMPA in humans is not due to the complete inability to convert this compound to formaldehyde. However, the low levels of CYP2A6 mRNA in human respiratory mucosa and the quantitatively lower levels of HMPA-demethylase activity of the human CYP2A isoform may contribute to the lower susceptibility of humans to HMPA nasal carcinogenicity.

In the present study, we have confirmed the presence of CYP2A6 mRNA in human respiratory mucosa. Human CYP2A6 metabolizes the olfactory-toxic, highly odorous compound 3-methylindole to both reactive and nontoxic metabolites (Thornton-Manning, J. R. *et al. Biochem. Biophys. Res. Commun. 181*: 100, 1991; Thornton-Manning, J. R. *et al. J. Pharmacol. Exp. Therap.*, in press). The ability of CYP2A6 to accept a number of procarcinogens and toxicants as substrates suggests that this enzyme may play a protective role in nasal mucosa. However, metabolism often results in the formation of reactive metabolites, and CYP2A6 activates a number of compounds, including 6-aminochrysene, N-nitrosodiethylamine, N-nitrosodimethylamine, and aflatoxin B_1 to toxic or genotoxic metabolites (Davies, R. L. *et al. Carcinogenesis 10*: 885, 1989; Crespi *et al.*, 1990; Yun, C. H. *et al. Mol. Pharmacol. 40*: 679, 1991). Aflatoxin B_1 bioactivation by human CYP2A6 may be of particular relevance in nasal toxicology because airborne particulate matter contaminated with aflatoxin B_1 is sometimes encountered in the agricultural industry (Sorenson, W. G. *et al. J. Toxicol. Environ. Health 14*: 525, 1984). 1,3-Butadiene, a gaseous compound used extensively in the rubber industry, is also metabolized by CYP2A6 to a reactive epoxide (Duescher, R. J. and A. A. Elfarra. *Arch. Biochem. Biophys. 311*: 343, 1994). Whether nasal metabolism of either of these compounds in concentrations encountered by humans results in pathological consequences in the human nose is unknown. Further studies are needed to determine if CYP2A6 has a specific physiological function in nasal mucosa and to understand its potential role in olfaction.

(Research sponsored by the Office of Health and Environmental Research, U.S. Department of Energy, under Contract No. DE-AC04-76EV01013.)

GENDER DIFFERENCES IN THE METABOLISM OF 1,3-BUTADIENE TO BUTADIENE DIEPOXIDE IN SPRAGUE-DAWLEY RATS

Janice R. Thornton-Manning, Alan R. Dahl, William E. Bechtold, William C. Griffith, and Rogene F. Henderson

1,3-Butadiene (BD), a gaseous compound used in the production of rubber, is a potent carcinogen in mice and a weak carcinogen in rats (Huff, J. E. *et al. Science 277*: 548, 1985; Owen, P. E. *et al. Am. Ind. Hyg. Assoc. J. 48*: 407, 1987; Melnick, R. L. *et al. Cancer Res. 50*: 6592, 1990). The mechanism of BD-induced carcinogenicity is thought to involve genotoxic effects of its reactive epoxide metabolites butadiene monoepoxide (BDO) and butadiene diepoxide (BDO_2) (reviewed by Bond, J. A. *et al. Carcinogenesis 16*: 165, 1995). Studies in our laboratory (Bechtold, W. E. *et al. Chem. Res. Toxicol 8*: 182, 1994; Thornton-Manning, J. R. *et al. Carcinogenesis 16*: 1723, 1995) have shown that levels of the epoxides, particularly BDO_2, are greater in mice—the more sensitive species—than rats. While both epoxides are genotoxic in a number of assays (reviewed by de Meester, C. *Mutat. Res. 195*: 273, 1988), BDO_2 is mutagenic in TK6 human lymphoblastoid cells at concentrations approximately 100-fold lower than BDO (Cochrane, J. E. and T. R. Skopek. *Carcinogenesis 15*: 713, 1994).

Subtle gender differences were evident in chronic BD carcinogenicity studies with rats and mice (Huff *et al.*, 1985; Owen *et al.*, 1987; Melnick *et al.*, 1990). In rats, females exposed to 1000 and 8000 ppm BD had a greater incidence of tumors than males, primarily as a result of tumors in mammary tissue. The purpose of this study was to explore gender differences in BD metabolism in rats that might explain gender differences in BD carcinogenicity. The effect of gender on the metabolism of BD was examined by comparing levels of BDO and BDO_2 in blood, femurs, lungs, and fat from male and female rats immediately following a 6-h exposure to a target concentration of 62.5 ppm BD. Levels of the epoxides were also quantified in mammary tissue of female rats.

Inhalation exposures, metabolite analyses, and quantification were carried out as previously described (Thornton-Manning *et al.*, 1995). Male and female Sprague-Dawley rats, approximately 11 wk old, were exposed nose-only to 59.00 ± 0.11 ppm BD diluted with house air using a multiport, nose-only system. The animals were exposed to either BD or house air for 5 h, 55 min and anesthetized with sodium pentobarbital (250 mg/kg body weight) by intraperitoneal injection. While the animals were breathing the exposure atmosphere, blood was collected via cardiac puncture and immediately placed into a round bottom flask maintained in liquid nitrogen. Internal standards (BDO-d_6 and BDO_2-d_6) were added to the blood at the time of collection. Other tissues, including lungs, abdominal fat, mammary tissue, and femurs, were then removed from the rats and placed in liquid nitrogen. Tissues from three rats were pooled at the time of sacrifice and stored in liquid nitrogen until preparation for gas chromatography/mass spectroscopy (GC/MS) analysis.

The tissues were removed from liquid nitrogen, pulverized, and placed in round bottom flasks containing internal standards. Volatile BD epoxides were removed from the tissues using vacuum line-cryogenic distillation as previously described (Dahl, A. R. *et al. Am. Ind. Hyg. Assoc. J. 45*: 193, 1984). This technique isolated the BD epoxides and internal standards into a septaport U-trap maintained in liquid nitrogen. Following the distillation, the septaport U-traps were closed, removed from the vacuum line, and the contents analyzed by isotope dilution multidimensional GC/MS as previously described (Bechtold *et al.*, 1994). Instrument detection limits, defined as the concentration of BDO_2 which gave a signal-to-noise ratio of 3:1, were 1.2 pmol. Based on tissue weights, detections limits for BDO_2 ranged from 0.2–0.4 pmol/g tissue. For statistical analysis, data were log transformed after adding a value of 10 and analyzed by a one-way analysis of variance.

Levels of the epoxides in male and female rats are shown in Table 1. The levels of BDO did not differ significantly between males and females in any tissue examined. The greatest amounts of BDO were observed in fat of both males and females. Tissue BDO_2 levels were consistently greater in females as compared with males. Blood BDO_2 levels of female rats were 4.75-fold greater than those of male rats. The greatest gender disparity was in the levels of BDO_2 in fat tissue; fat tissue of females had 7-fold more BDO_2 present per gram fat than did males. Also, mammary tissue of females contained a relatively high level of BDO_2.

Table 1

BD Epoxide Levels in Tissues of Male and Female Rats
Following a 6-h Exposure to 62.5 ppm BD
(mean ± SE)

	pmol BDO/g Tissue[a,b]		pmol BDO_2/g Tissue[b]	
Tissue	Male	Female	Male	Female
Blood	25.9 ± 2.9	29.4 ± 2.0	2.4 ± 0.4	11.4 ± 1.7[c]
Femurs	9.7, 9.3[d]	10.4 ± 1.0	1.1, 1.8[d]	7.1 ± 1.3[c]
Lung	12.7 ± 5.0	2.7 ± 4.3	1.4 ± 0.8[e]	4.8 ± 0.7[c]
Fat	175 ± 21	203 ± 13	1.1 ± 0.1	7.7 ± 1.3[c]
Mammary	ND[f]	57.4 ± 4	ND	10.5 ± 2.4

[a]A low background level of substances with electron impact fragmentation properties similar to BDO was present in controls; values for these were quantified and subtracted from values from exposed animals.
[b]n = 3 for each determination, except for male femur where n = 2.
[c]Statistically greater than male tissue value, $p \leq 0.05$.
[d]Two individual determinations.
[e]One value was not detectable; instrument detection limit/2 was substituted to calculate the mean.
[f]ND = not determined.

This study shows that after a single inhalation exposure to a low level of 59 ppm BD, tissues from female rats contained higher concentrations of the highly mutagenic BDO_2 than tissues from male rats. Further, our study shows that levels of the initial product of BD metabolism, BDO, were similar in male and female rats. This suggests that gender differences in xenobiotic-metabolizing enzymes exist in rats which affect the metabolism of BDO or BDO_2, but not the parent compound. These gender differences may result from differences in the production of BDO_2 or in the hydrolysis or conjugation of BDO or BDO_2. Gender-specific cytochrome P450 isoforms have been purified from rats (reviewed by Gonzales, F. J. *Pharmacol. Rev. 40*: 243, 1989). It is possible that one of these isoforms contributes to the production of BDO_2 in females.

Species differences in carcinogenicity of BD have posed a dilemma to investigators deciding which animal model is most appropriate for BD risk assessment. Some investigators feel that the mouse is a more appropriate model because the mouse develops lymphomas after chronic exposures to BD, and epidemiological studies have suggested an association between BD exposure and lymphatic and hematopoietic cancers in humans (Melnick, R. L. and M. C. Kohn. *Carcinogenesis 16*: 157, 1995). Other investigators have suggested that the rat is more appropriate than the mouse for use in BD cancer risk assessment because of the probable role of BDO_2 in BD carcinogenesis and the quantitative differences in the production of this metabolite in rats and mice (Bond *et al.*, 1995). Also, human urinary metabolite and *in vitro* data suggest that humans will metabolize BD more similarly to rats than mice. If the rat is deemed the most appropriate model for BD risk assessment, the gender differences in BD metabolism reported in the present study should be considered.

(Research supported by the Chemical Manufacturers Association under Funds-In-Agreements No. DE-FI04-91AL66351 and DE-FI04-93AL94550 with the U.S. Department of Energy, under Contract No. DE-AC04-76EV01013.)

ANALYSIS OF BRONCHOALVEOLAR LAVAGE FLUID (BALF) FROM PATIENTS WITH ADULT RESPIRATORY DISTRESS SYNDROME (ARDS)

*Rogene F. Henderson, James J. Waide, and Robert P. Baughman**

The pathogenesis of ARDS is largely unknown, but many factors are known to predispose one to ARDS: sepsis, aspiration of gastric contents, pneumonia, fracture, multiple transfusions, cardiopulmonary bypass, burn, disseminated intravascular coagulation, pulmonary contusion, near drowning, and pancreatitis (Kindt, G. C. and J. E. Gadek. In *Bronchoalveolar Lavage* [R. P. Baughman, ed.], Mosby Year Book, St. Louis, p. 212, 1992). ARDS is characterized by severe hypoxemia, diffuse pulmonary infiltrates, and decreased pulmonary compliance. Current treatment methods still result in 50% mortality. Studies are underway at the University of Cincinnati to determine if treatment with a synthetic pulmonary surfactant, Exosurf® (contains dipalmitoyl phosphatidyl choline, Burroughs-Wellcome), improves the prognosis of these patients. BALF from these patients, before and after treatment, was analyzed to determine if the treatment resulted in an increase in disaturated phospholipids (surfactant phospholipids) in the epithelial lining fluid and if the treatments reduced the concentration of markers of inflammation and toxicity in the BALF.

Patients participating in the study had been diagnosed with sepsis-based ARDS. All patients had a diagnosis of sepsis within 96 h prior to onset of ARDS. Sepsis syndrome was based on a high clinical suspicion for infection, hyperthermia (> 38.3°C) or hypothermia (< 35.6°C), tachycardia (> 90 beats/min), tachypnea (respiratory rate > 20), or need for mechanical ventilation. Patients were considered to have ARDS if they developed diffuse pulmonary infiltrates, hypoxemia with a PaO_2/PiO_2 ratio between 50 and 299, required mechanical ventilation, and had no evidence of fluid overload. In order to undergo bronchoscopy, patients had to have a $PO_2 \geq 60$ Torr on room air at 1 atm with ventilatory support. Patients underwent bronchoscopy with bronchoalveolar lavage (BAL) while on mechanical ventilation prior to receiving either saline or Exosurf®; no cause of their respiratory failure other than ARDS was found.

Lavage was performed in either the right middle lobe or lingula. In all cases, two aliquots of 60 mL of normal saline were instilled and immediately aspirated using a hand-held syringe. The aspirated fluid was pooled, and an aliquot of fluid was used to analyze the cell and differential counts using a cytocentrifuge-prepared slide of the unconcentrated BAL sample. Slides were stained using a modified Wright-Giemsa stain (Diff-Quick, American Scientific). An aliquot was then spun at 400 *g* for 5 min and the cell-free supernatant was frozen at –80°C until further analysis.

A control group consisted of nonintubated healthy volunteers who underwent bronchoscopy with lavage using topical anesthesia supplemented by intravenous sedation. The controls and the patient or his representative gave written, informed consent of a protocol approved by the University of Cincinnati Institutional Review Board.

After the initial bronchoscopy, patients received either Exosurf® or saline via a nebulizer unit (VISAN-9, Vortran Medical Technology, Inc., Sacramento, CA). Patients were treated for a total of 4 d. After therapy, those patients still on mechanical ventilation underwent repeat bronchoscopy and lavage. Lavage was done in the same area as the first bronchoscopy. Patients were followed for 6 mo after initiating treatment to determine 30 and 180 d mortality.

*University of Cincinnati College of Medicine, Cincinnati, Ohio

Comparisons were made between and within patient groups using analysis of variance, with Bonferroni pairwise comparison between means; a p value of < 0.05 was considered significant. Because most data were not normally distributed, results are reported with median values and ranges. Paired samples before and after therapy were analyzed using Wilcoxan's rank sum test, and different groups were compared using the Krukal-Wallis ANOVA test.

BALF samples from ARDS patients treated with saline or with Exosurf® were analyzed for indicators of surfactant protein (SP-A) and surfactant lipids (disaturated phospholipids) to determine if the treatment actually increased the amount of surfactant in the alveolar region. The BALF was also analyzed for indicators of inflammation (% polymorphonuclear cells, protein, albumin), surfactant lipid (disaturated phospholipid), surfactant secretion (alkaline phosphatase activity), and macrophage phagocytic activity (β-glucuronidase activity). Comparisons were made between the level of these factors before and after treatment and in those patients that survived ARDS versus those who died.

The results of the analyses for surfactant protein and lipid in BALF from patients before and after treatment with either saline or Exosurf® are shown in Table 1. There was no significant difference between the amount of surfactant lipid or protein in the BALF from the saline-treated versus the Exosurf®-treated patients. There was some decrease in phospholipid (both saturated and unsaturated) associated with 4 d of saline treatment, but no change in the percent disaturated phospholipid.

Table 1

Surfactant Initially and After 4 Days of Therapy[a]

	Exosurf®		Saline	
BALF:	Initial	Follow-up	Initial	Follow-up
Number:	18	18	9	9
SP-A (ng/mL)	2.3 (0.39–7.09)	5.05 (0.02–21.1)	3.9 (0.30–20.7)	2.86 (0.29–14.0)
Disaturated Phospholipid[b] (μg Pi/mL)	1.22 (0.36–3.44)	1.26 (0.24–3.47)	1.28 (0.30–2.19)	0.48 (0.10–0.94)[c]
Unsaturated Phospholipid[b] (μg Pi/mL)	1.05 (0–2.19)	0.97 (0.30–2.14)	0.95 (0.20–1.87)	0.44 (0.08–0.91)[c]
% Disaturated Phospholipid	49.0 (27.5–79)	53 (31.5–76.7)	55.8 (37.0–68)	55 (37–77)

[a]Mean (range).
[b]Differences between groups, $p < 0.05$ (Krukal-Wallis ANOVA test).
[c]Differs from saline initial, $p < 0.05$ (Wilcoxan rank sum test).

Comparisons of various factors in the BALF before and after treatment to determine if any factor was associated with predictability of a good outcome indicated only a decrease in the percent polymorphonuclear leukocytes as an indicator of a good prognosis (Table 2). A reduction in the percent polymorphonuclear cells following treatment was associated with those patients who lived, but not with those patients who died.

Table 2

Comparison of BALF Characteristics: Alive Versus Dead[a]

	Alive	N = 19	Dead	N = 8
BALF Timing:	Initial	Follow-up	Initial	Follow-up
Percent Polys	58 (0–98)	30 (4–88)[b]	50 (1–92)	68 (28–91)[c]
Albumin (μg/mL)	1345 (262–3744)	475 (119–2436)	1104 (240–3432)	341 (178–525)
Protein (mg/mL)	1.26 (0.25–2.92)	0.29 (0.005–0.86)	1.01 (0.06–3.20)	0.51 (0.07–1.15)
β-Glucuronidase (mIU/mL)	1.04 (0.013–13.9)	0.05 (0–0.27)	0.17 (0.02–0.64)	0.098 (0.02–0.18)
Alkaline Phosphatase (mIU/mL)	31.8 (5.8–95.6)	29.0 (5.2–109.9)	25.4 (5.1–79.7)	20.0 (4.8–35.0)
Disaturated Phospholipid (μg Pi/mL)	1.3 (0.36–2.19)	0.93 (0.10–2.52)	0.77 (0.31–1.46)	1.2 (0.22–3.47)

[a]Mean (range).
[b]Differs from initial, $p < 0.05$ (Wilcoxan rank sum test).
[c]Differs from alive, $p < 0.05$ (Krukal-Wallis ANOVA test).

This study indicates that the method of administering Exosurf® did not lead to an increase in surfactant lipid or protein in the bronchoalveolar region of the respiratory tract. Also, treatments resulting in decreases in the percent of polymorphonuclear leukocytes in BALF appear to be the most promising.

(The portion of this research related to analysis of the BALF was sponsored by the Office of Health and Environmental Research, U.S. Department of Energy, under Contract No. DE-AC04-76EV01013.)

BENZENE METABOLITE LEVELS IN BLOOD AND BONE MARROW OF B6C3F$_1$ MICE AFTER LOW-LEVEL EXPOSURE

William E. Bechtold, Michael R. Strunk, Janice R. Thornton-Manning, and Rogene F. Henderson

Studies at the Inhalation Toxicology Research Institute (ITRI) have explored the species-specific uptake and metabolism of benzene. Results have shown that metabolism is dependent on both dose and route of administration (Henderson, R. F. *et al. Environ. Health Perspect. 82*: 9, 1989). Of particular interest were shifts in the major metabolic pathways as a function of exposure concentration. In these studies, B6C3F$_1$ mice were exposed to increasing levels of benzene by either gavage or inhalation. As benzene internal dose increased, the relative amounts of muconic acid and hydroquinone decreased. In contrast, the relative amount of catechol increased with increasing exposure. These results show that the relative levels of toxic metabolites are a function of exposure level.

Extrapolation of results determined in animal models to humans requires the measurement of the exposure-dose relationship after exposures to concentrations ranging from ≤ 1 ppm to ~ 60 ppm. Of particular interest are levels of toxic metabolites in the target tissue, bone marrow. The objective of the present study was to measure phenol, catechol, hydroquinone, and muconic acid in the bone marrow of mice after inhalation exposures to graded concentrations of benzene.

Initially, B6C3F$_1$ mice were exposed nose only to 61 ± 1.3 ppm benzene by inhalation for 6 h (mean ± SE). Groups of three animals were sacrificed at 2, 4, 6, 7, 8, and 10 h after the initiation of the exposure. Blood and bone marrow were collected post sacrifice, and the tissues were analyzed for benzene metabolites. Control animals (n = 6) were placed on a plenum and exposed for 6 h to air, then sacrificed.

Blood was drawn in syringes and added to vials containing isotopically labeled internal standard solution ($^{13}C_6$-labeled analogues of the metabolites) and methanol. The vials were weighed again for the weight of blood. After mixing and centrifugation, the methanol was decanted, 100 µL of 0.1 M KOH in methanol was added, and the solution was dried under nitrogen. Bone marrow metabolites were measured in the entire femur which was quickly isolated at the end of the exposure, frozen in liquid nitrogen, and ground under liquid nitrogen in a mortar and pestle. An aliquot was measured as described above for blood.

Analytes were treated with pentafluorobenzyl bromide, a good derivatization reagent for negative ion chemical ionization (NICI) mass spectroscopy. Acetonitrile was added to the dried sample along with 10 µL of pentafluorobenzyl bromide and approximately 2 mg of K_2CO_3. The sample was heated for 12 h at 60°C. The resulting mixture was concentrated under N_2 gas to approximately 50 µL and analyzed by two-dimensional gas chromatography/NICI mass spectroscopy. Initially, work was done by electron impact mass spectroscopy. A Restek 30 meters × 0.53 mm RTx-1 GC column (clean-up/primary separation) was used in the first dimension, and a Restek RT 30 meters × 0.25 mm RTx-200 capillary column was used as the second dimension (analytical separation).

All four metabolites could be measured in both tissues at all time points examined, including low background levels in unexposed mice (Fig. 1). The highest concentrations measured for all metabolites were at the end of the 6 h time period in both blood and bone marrow. By the end of the 6 h exposure, catechol, hydroquinone, muconic acid, and phenol were increased over background concentrations by factors of 3.7, 1.8, 1.8, and 3.0 in blood, respectively. Bone marrow levels of the

same metabolites were increased over background concentrations by factors of 2.2, 4.8, 24, and 1.4, respectively.

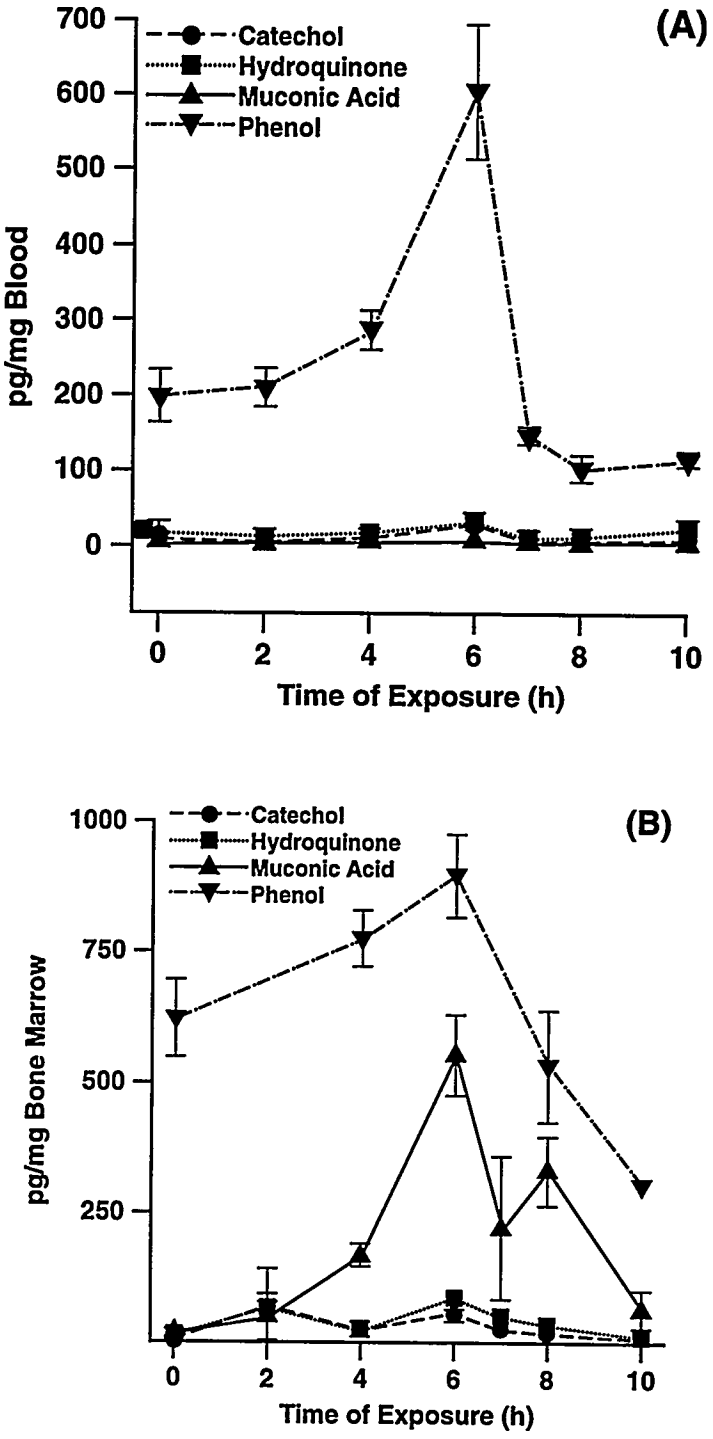

Figure 1. Levels of phenol, catechol, hydroquinone, and muconic acid in the blood (A) and bone marrow (B) of $B6C3F_1$ mice exposed by inhalation to 61 ppm benzene for 6 h (± standard error; n = 3).

Based on these results and assuming a linear relationship between exposure concentration and levels of bone marrow metabolites, it would be difficult to detect an elevation of any phenolic metabolites above background after occupational exposures to the OSHA Permissible Exposure Limit of 1 ppm benzene. In contrast, levels of the ring-breakage metabolite muconic acid, and presumably its hematotoxic precursor muconaldehyde, should be significantly elevated relative to unexposed individuals following low-level benzene exposures. These observations are consistent with the patterns of metabolites found in the urine of benzene-exposed and unexposed humans and suggest that diet and endogenous metabolism of proteins contribute to a body burden of phenolic compounds unrelated to benzene exposure (Inoue, D. *et al. Br. J. Ind. Med. 46*: 122, 1989). Future studies will examine the levels of these metabolites in bone marrow of mice exposed to lower benzene levels (10 ppm). In addition, the metabolic pathways leading to the highly elevated levels of muconic acid in bone marrow (24-fold) after the 6 h exposure will be explored.

(Research sponsored by the American Petroleum Institute under Funds-In-Agreement No. DE-FI04-94AL97353 with the U.S. Department of Energy, under Contract No. DE-AC04-76EV01013.)

BIOLOGICAL MONITORING TO DETERMINE WORKER DOSE IN A BUTADIENE PROCESSING PLANT

*William E. Bechtold and Richard B. Hayes**

Butadiene (BD) is a reactive gas used extensively in the rubber industry and is also found in combustion products. Although BD is genotoxic and acts as an animal carcinogen, the evidence for carcinogenicity in humans is limited. Extrapolation from animal studies on BD carcinogenicity to risk in humans has been controversial because of uncertainties regarding relative biologic exposure and related effects in humans vs. experimental animals. To reduce this uncertainty, a study was designed to characterize exposure to BD at a polymer production facility and to relate this exposure to mutational and cytogenetic effects. Biological monitoring was used to better assess the internal dose of BD received by the workers. Measurement of 1,2-dihydroxy-4-(N-acetylcysteinyl)butane (M1) in urine served as the biomarker in this study. M1 has been shown to correlate with area monitoring in previous studies (Bechtold, W. E. *et al. Toxicol. Appl. Pharmacol. 127*: 44-40, 1994).

Workers were studied at a polybutadiene rubber production facility at Yan Shan, China. The purification of BD from an initial hydrocarbon stream occurred at two sites: the dimethylformamide (DMF) facility, where initial distillation and extraction occurred using a proprietary DMF process, and the recovery facility, where final distillation occurred. Polymerization and packing of the final product took place in the polymerization facility, with remaining unpolymerized material returning to the recovery unit for further processing. Because the production process was enclosed, high BD levels in the vicinity of the process plant were not consistently expected.

Three groups of workers with high potential exposure were identified. The DMF-process analysts sampled process lines in the DMF facility and analyzed the product for BD content, while polymer-process analysts carried out these tasks at the recovery and polymerization units. The third group of exposed workers were process operators at the recovery unit who carried out routine minor maintenance and, as needed, major repair operations at this unit. Within the third group, a subset of workers was identified who received much higher exposures during a specific repair operation. After obtaining informed consent, 41 exposed workers and 40 unexposed controls were included for study.

Personal samplers were used for collecting air at the breathing zone during the entire 6-h work shift. Atmospheres were drawn through charcoal tubes, and the tubes were analyzed for BD by gas chromatography using an adaptation of the NIOSH method 1020. Results were calculated as parts per million (ppm) over a 6-h time weighted average. In addition, numerous grab samples were collected during the study period and analyzed on site using a portable gas chromatograph.

Urine samples were collected pre-shift, 0–3 h, 3–6 h, and post-shift from exposed workers, while only a post-shift sample was collected from unexposed workers. A subset of exposed workers also provided urine for the subsequent 18 h, completing a full 24-h collection. Urine samples were analyzed for the BD metabolite M1 as previously described (Kelsey, K. *et al. Mutat. Res.*, in press). Final values represent the average concentration, as normalized to creatinine, over the full day.

Personal air samples were available for 40 exposed subjects, among whom 20 had measurements taken on two separate days. For polymer and DMF analysts, the median air levels were 1.0 and 3.5 ppm, respectively (Fig. 1). Among recovery operators, median air levels of 1.1 ppm were found during routine activities, while the median air level during pump repair was 45 ppm. Grab samples

*National Cancer Institute, Bethesda, Maryland

and visual observation of workers involved in acquiring process stream materials revealed a consistent exposure pattern. Operators were exposed to very low levels of BD when not acquiring process material (< 3 ppm BD). However, levels of BD as high as 3,000 ppm were measured at the breathing zone of workers when valves were opened to sample the BD process stream. The median air level of BD for the grab samples was 54 ppm for the DMF unit (n = 50), 6.5 ppm for the polymerization unit (n = 41), and 5 ppm for the recovery area (n = 15). Exposures were no longer than 30 to 60 sec. Levels of BD measured from three grab samples in the breathing zones of workers in the repair operations were 110, 1,430, and 15,000 ppm, respectively. In contrast to workers involved in routine operations, the exposure durations for these workers were as long as 15 to 20 min.

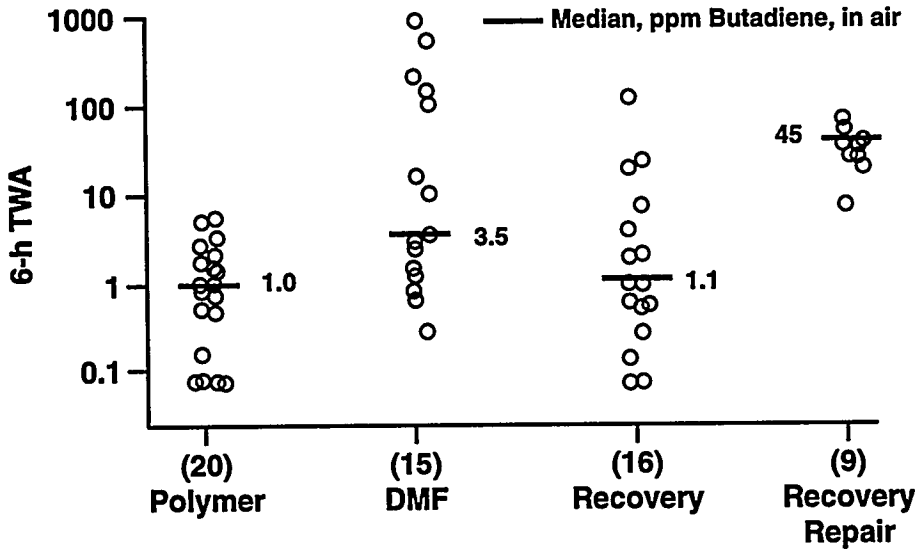

Figure 1. Time weighted average (TWA) exposures of Chinese workers to butadiene. The bar represents the median concentration; circles represent individual concentration measurements. DMF = dimethylformamide.

Urinalysis for the BD metabolite M1 showed distinctly different patterns according to work description (Fig. 2; recovery workers are combined). For the workers performing routine tasks that involved short, high-level exposures, little correlation was found between exposure and M1 excretion (r^2 = 0.1 for both DMF and polymerization). However, for the recovery area, where exposures extended for up to 20 min, a high correlation was observed between exposure and M1 (r^2 = 0.7). In addition, the slope of the exposure-dose curve is steeper.

Most studies that relate exposure to a toxic chemical with its biological effects rely on exposure concentration as the dose metric; however, exposure concentration may or may not reflect the actual internal dose of the chemical. The results presented here suggest that exposure concentration poorly relates to internal dose, as measured by excretion of M1, for many of these workers who experienced intense but very brief exposures. Apparently, this exposure paradigm resulted in very little uptake of BD. Potentially, the workers held their breaths during the periods when the valves were opened to sample process stream materials. Alternatively, the very high concentrations were poorly absorbed or metabolized. Regardless, development of relationships between chemical exposure and biological response could lead to erroneous conclusions if based only on personal dosimeters. These studies demonstrate the necessity for measuring a biomarker of internal dose when determining dose-response relationships.

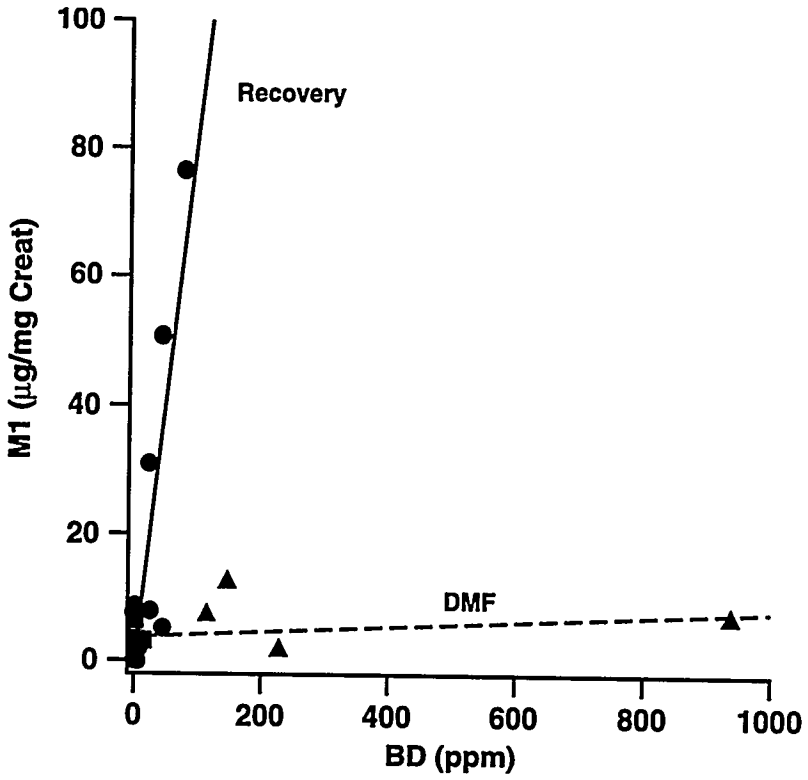

Figure 2. Exposure vs. M1 in urine for Chinese workers. Polymerization workers excreted < 5 µg/mg creatine; data are not shown. DMF = dimethylformamide.

(Research sponsored by the Office of Health and Environmental Research, U.S. Department of Energy, under Contract No. DE-AC04-76EV01013.)

IN VIVO MEASUREMENTS OF LEAD-210 FOR ASSESSING CUMULATIVE RADON EXPOSURE IN URANIUM MINERS

Raymond A. Guilmette, Gerard R. Laurer, M. Burton Snipes, William E. Lambert**, and Frank D. Gilliland**,****

It has long been recognized that a major contributor to the uncertainty in risk analysis of lung cancer in uranium and other hard rock miners is the estimation of total radon progeny exposure of individual miners under study. These uncertainties arise from the fact that only a limited number of measurements of airborne ^{222}Rn progeny concentrations were made in the mines during the times that the miners were being exposed, and that dosimeters capable of integrating the Rn progeny exposures of the miners did not exist. Historically, the cumulative exposures for individual uranium and other hard rock miners have been calculated by combining the employee's work history, which may or may not have included time spent at different jobs within the mines and at different locations within the mines, with whatever periodic measurements of Rn and Rn progeny were available. The amount and quality of the measurement data varied enormously from mine to mine and from population to population. Because the quality of the exposure data collected during the period of active mining in the United States cannot now be altered substantially, significant improvement in individual miner exposure estimates is only likely to be achieved if a new cumulative exposure metric is developed and implemented. The decay chain of Rn includes the production of ^{210}Pb, which can accumulate in the skeleton in amounts proportional to the intake of Rn progeny. We hypothesize that the *in vivo* measurement of ^{210}Pb in the skulls of miners will provide such a metric.

The time that has elapsed between the period of maximal Rn progeny exposure and the present is significant, amounting to two effective half lives for retention of ^{210}Pb in bone. Additionally, measurement of low-energy gamma rays such as the 47-keV photons emitted by ^{210}Pb is complex. Therefore, the purpose of this pilot study was to demonstrate the feasibility of making ^{210}Pb measurements in subjects exposed to Rn and Rn progeny during their uranium mining careers.

Modifications to the ITRI whole-body counting (WBC) facility were required to improve the counting efficiency for low-energy gamma rays. The interior walls of the original room (9′w × 16′l × 8′h), which are fabricated of 6″ laminated steel plate, were covered with 0.25″ lead (Pb), 0.125″ tin (Sn), and 0.06″ stainless steel. This "graded-Z" shield reduces the low-energy photon background, which is due to gamma-ray interactions within the original steel walls.

^{210}Pb gamma rays are measured *in vivo* using four 5″-diameter, dual-crystal scintillation detectors or "phoswiches" operated in anticoincidence mode. These detectors and associated electronics are optimized for counting low-energy photons. For the *in vivo* measurement, each miner is placed in a reclining chair, and the four detectors are positioned around the head (Fig. 1). The *in vivo* measurement consists of nine sequential 10-min counts, which are summed to yield a 90-min measurement. The spectrum collected from each miner is then compared with spectra taken from a ^{210}Pb-free plastic phantom skull, which contains quantities of potassium and calcium physiologically equivalent to those contained in the head of Standard Man (*Reference Man, ICRP 23*, 1974). These latter counts provide a means for accounting for background radiation sources, which are due to both internal (^{40}K) and external radiation (cosmic rays, Rn, and progeny). Efficiency calibration was done using a set of human cadaver skulls that were uniformly labeled with known amounts of ^{210}Pb painted

*New York University Institute of Environmental Medicine, Tuxedo, New York
**New Mexico Tumor Registry, University of New Mexico, Albuquerque, New Mexico
***Department of Medicine, University of New Mexico, Albuquerque, New Mexico

on either the exterior or interior bone surfaces; the net counting efficiency was taken to be the geometric mean of efficiencies from both skulls.

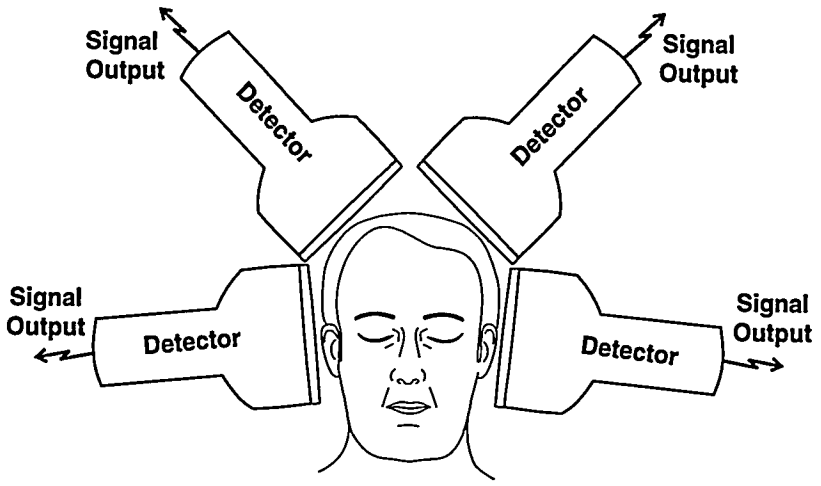

Figure 1. Detector positioning geometry for measuring ^{210}Pb *in vivo*.

A group of 20 former uranium miners was selected from the New Mexico Tumor Registry miner data base, which contains employment and demographic data for approximately 4000 miners who worked for a significant time in the Grants, New Mexico, mining district. Prior to selection, the data base was sorted according to estimated cumulative Rn exposure (in working level months, WLM), and the 100 miners with the highest WLMs were identified and recruited for this study. Each participant answered a questionnaire, which focused on individual work history and personal lifestyle factors, such as diet and smoking habits, which could affect the magnitude of ^{210}Pb contributions from nonmining sources; then the miners were measured for ^{210}Pb in the ITRI WBC facility.

The results of the ^{210}Pb measurements performed on 20 former uranium miners are plotted in Figure 2 against the cumulative exposures of each miner in WLM, as listed in the miner's work history records. Nineteen miners had statistically significant levels of ^{210}Pb, ranging from 6.7 to 36.3 Bq. The correlation coefficient (r) obtained by regressing the ^{210}Pb measurements on the cumulative WLM was 0.84, a correlation significantly higher than that found by Laurer, G. R. *et al.* in Chinese tin miners (R = 0.01; *Health Phys. 64*: 253, 1993). It is clear that the number of data points provided in this study are insufficient to establish a firm relationship between WLM and ^{210}Pb levels. Nevertheless, these preliminary results are encouraging.

During the 1-mo period over which the miner measurements were done, it was discovered that the head-phantom background count rates were unusually variable. This variability complicated the analysis of the miner data, as it was not possible to simply subtract the average background counts obtained with the cumulative measurements of the head phantom. This procedure would have provided an optimum method for accounting for non-^{210}Pb counts. Short-term measurements of the Rn progeny, ^{218}Po and ^{216}Po, taken over a period of several weeks indicated that the background variability was primarily due to the presence of varying levels of Rn progeny within the WBC room itself. It is clear that real-time removal of Rn progeny within the room must be accomplished before further miner measurements are performed.

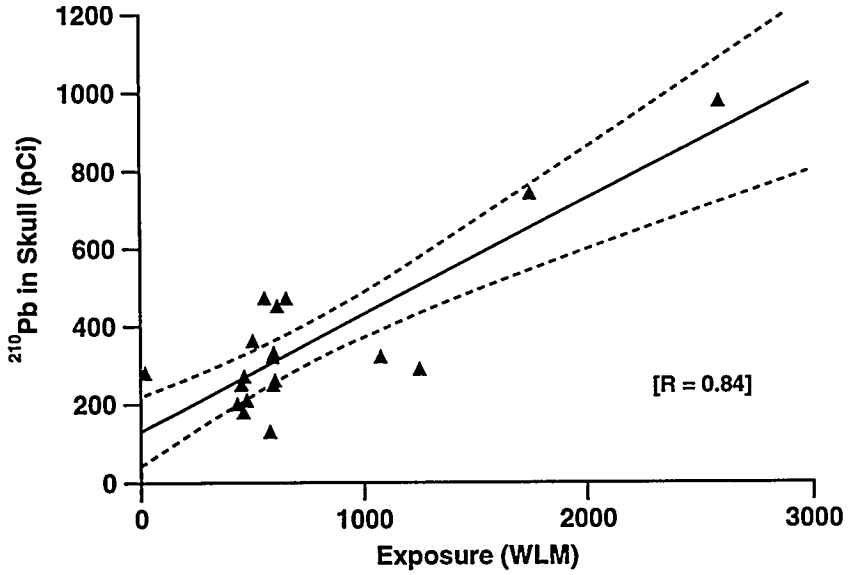

Figure 2. Relationship between *in vivo* ^{210}Pb measurements and working level months (WLM) exposure estimates derived from individual miner work histories. Solid line is linear regression of the data set; dashed lines represent the 95% confidence intervals. R is the correlation coefficient.

In summary, the primary purpose of this pilot study to demonstrate the feasibility of measuring ^{210}Pb in the heads of former uranium miners has been accomplished. Adequate sensitivity was found to measure ^{210}Pb burdens in miners with WLM $\geq$ 400. Our intent is to expand the current study to encompass more miners with a broader range of exposures, and to link these measurements to biological endpoints being measured in ongoing or planned epidemiological studies. The result will be improved estimates of exposures of miners to Rn and progeny that will provide improved risk estimates for the biological effects of Rn exposures for both miners and the general population.

(Research sponsored by the Office of Health and Environmental Research, U.S. Department of Energy, under Contract No. DE-AC04-76EV01013.)

IV. CARCINOGENIC RESPONSES TO TOXICANTS

EFFECTS OF COMBINED EXPOSURE OF F344 RATS TO RADIATION AND CHRONICALLY INHALED CIGARETTE SMOKE

Gregory L. Finch, Kristen J. Nikula, Edward B. Barr, William E. Bechtold, Bean T. Chen, William C. Griffith, Fletcher F. Hahn, Charles H. Hobbs, Mark D. Hoover, David. L. Lundgren, and Joe L. Mauderly*

Nuclear workers may be exposed to radiation in various forms, such as low-LET γ-irradiation or α-irradiation from inhaled $^{239}PuO_2$ particles. These workers may then have increased risk for lung cancer compared to the general population. Of additional concern is the possibility that interactions between radiation and other carcinogens may increase the risk of cancer induction, compared to the risks from either type of agent alone. An important and common lung carcinogen is cigarette smoke. The purpose of this project is to better determine the combined effects of chronically inhaled cigarette smoke and either inhaled $^{239}PuO_2$ or external, thoracic X-irradiation on the induction of lung cancer in rats.

For our study of combined cigarette smoke and $^{239}PuO_2$, male and female CDF®(F-344)/CrlBR rats (4 ± 1 wk old, a total of 2165; Charles River Laboratories, Raleigh, NC) were placed on study from September 1991 to May 1992. Beginning at 6 wk of age, groups of rats were exposed by the whole-body mode for 6 h/d, 5 d/wk, to either filtered air (FA) or to mainstream cigarette smoke (CS) diluted to concentrations of either 100 or 250 mg total particulate matter (TPM)/m^3 (LCS or HCS groups, respectively). At 12 wk of age, rats were removed from the chambers, exposed nose-only to either FA or to a $^{239}PuO_2$ aerosol (initial lung burdens ~ 440 Bq), then returned to the chambers 1 wk later for continued exposure to FA or CS for a total of 30 mo. This study included six exposure groups: FA alone, $^{239}PuO_2$ alone, LCS alone, LCS + $^{239}PuO_2$, HCS alone, and HCS + $^{239}PuO_2$. Exposures were completed in November 1994. Additional details of the exposures are given in previous reports (1991–92 Annual Report, p. 110; 1992–93 Annual Report, p. 53; 1993–94 Annual Report, p. 71).

CS exposure caused a exposure-related decrease in body weight gain compared to controls. For both genders, survival ranged between 89% and 103% of controls; a significant decrease from control survival was observed only in female rats exposed to CS + $^{239}PuO_2$. Lung clearance of ^{239}Pu was reduced by CS in an exposure concentration-dependent manner, and conversely, α-radiation dose to lungs was increased. Initial estimates of radiation doses to lungs for rats on study for at least 350 d after $^{239}PuO_2$ exposure are 4.0, 4.7, and 9.1 Gy for female rats, and 3.7, 3.5, and 6.2 Gy for male rats, in the FA, LCS, and HCS groups, respectively.

Histological evaluation of lungs continues. As of July 1, 1995, animals on study for at least 1 y have been examined. A significant influence of CS exposure on the induction of lung tumors was found in female, but not male rats. The incidence of benign and/or malignant lung tumors in female rats was 0/113 (number of animals with tumors over the number of rats examined), 4/145, and 6/83, for the FA alone, LCS, and HCS groups, respectively; this incidence for the HCS group is significantly different from controls (using a one-sided Yates test). Corresponding incidences for males were 3/119, 3/173, and 7/87 for FA, LCS, and HCS groups, respectively. In both genders, we have observed a pronounced interaction between smoke and $^{239}PuO_2$ exposure in producing lung tumors. Figure 1 illustrates the prevalence (number of rats with lung tumors divided by the total number of rats examined at necropsy) of lung tumors observed in male and female rats exposed to smoke for at least 12 mo, the approximate time at which the first tumor was observed. Tumor prevalence reached over 70% in HCS + $^{239}PuO_2$-exposed rats, whereas prevalence was 20–33% and 7.2–8.0%

*Currently at Gram, Inc., Albuquerque, New Mexico

in rats exposed to $^{239}PuO_2$ or HCS alone, respectively. The most prevalent malignant neoplasms were adenocarcinomas, followed by squamous cell carcinomas and adenosquamous carcinomas. Interestingly, in groups exposed to both agents, there were increased tumor multiplicity, an increased proportion of neoplasms of the squamous phenotype, and several animals with airway-associated lung neoplasms.

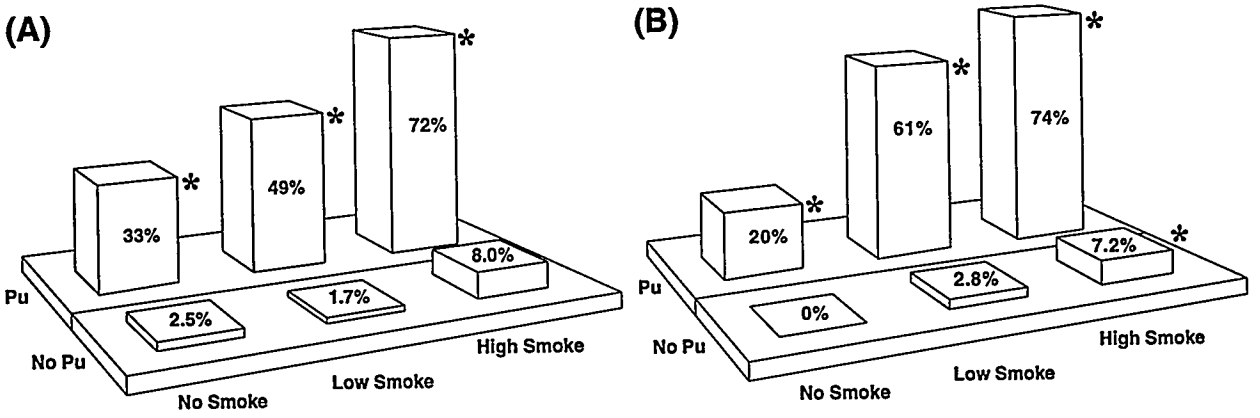

Figure 1. Prevalence of (A) male or (B) female rats with benign or malignant lung tumors as a function of exposure group for animals on study for at least 12 mo. Asterisk (*) denotes a statistically significant difference (one-sided Yates test, $p \leq 0.05$) compared to unexposed controls.

Results indicated that cigarette smoke and ^{239}Pu interacted synergistically in producing lung cancer in rats. Our current efforts in this study are oriented toward determining if the increased risk is due to the increased radiation dose from the CS-induced reduction of $^{239}PuO_2$ particle clearance, or if some other interaction between these agents is causing cancer.

As analysis of results from our CS + $^{239}PuO_2$ study continues, we have begun a new study involving combined exposures to CS + X rays. This area of research is important because of (1) the prevalence of cigarette smoking, (2) concerns for workers exposed to low-LET radiation in ongoing DOE nuclear operations and in decontaminating, decommissioning, and environmental restoration activities, and (3) conflicting epidemiologic data regarding possible CS/X-ray interactions. In addition, the issue of CS-induced decreased lung clearance of radioactive particles and associated dose increase will be avoided using X-ray exposures.

The experimental design for the new study of interactions between CS and X-irradiation is shown in Table 1. Significant design features include the following: (1) only one level of CS exposure will be used (HCS; 250 mg TPM/m^3), because this level showed the greatest carcinogenic and interactive effects in our first study, yet did not have a major impact on life span; (2) fractionated, thoracic X-irradiation will be used to partially mitigate the significant effect of whole-body X-irradiation on life span (see 1992–93 Annual Report, p. 61); (3) levels of X-ray exposure will be based on our previous work with rats and literature reports on effects in mice; and (4) both F344/Crl rats and $B6C3F_1$ mice will be studied, because the use of more than one animal species may provide information defining pathways of lung neoplasia and help to extrapolate results to humans. Additional limited exposures will be done with $^{239}PuO_2$ with or without CS exposure in $B6C3F_1$ mice, because of the same reasons noted above for CS + X-irradiation. We will also expose a hybrid strain of rat ($FBNF_1$) to $^{239}PuO_2$ alone or CS + $^{239}PuO_2$ and perform a microsatellite assay on lung tumors. This technique may reveal mutations characteristic of specific agents and mutations in as yet unidentified tumor suppressor genes in rats (L. M. Davis *et al. Carcinogenesis 15*: 1637, 1994).

Table 1

Experimental Design for Study of Combined Effects of Cigarette Smoke with Either X rays or $^{239}PuO_2$[a] on Rats and Mice

Radiation:		None		X rays		$^{239}PuO_2$	
Animal:		Rats	Mice	Rats	Mice	$FBNF_1$ hybrid rat	Mice
Cigarette	0	300 (270/30)	372 (342/30)	252 (222/30)	192 (162/30)	54 (48/6)	198 (156/42)
Smoke (mg TPM/m^3)	250	300 (270/30)	372 (342/30)	252 (222/30)	192 (162/30)	54 (48/6)	198 (156/42)

Totals: CDF®(F344)/CrlBR rats: 1104 (984/120)
$B6C3F_1$ mice 1524 (1320/204)
$FBNF_1$ rats 108 (96/12)

[a]Total number of animals with the number of life-span/number of serial sacrifice animals given in parentheses.

The experimental approach will be similar to that used in the first CS + $^{239}PuO_2$ study. Exposures to CS will begin at 6 wk of age, and radiation exposure will occur at either 12 wk of age (for $^{239}PuO_2$) or during the 12th and 13th wk of age (for the X-irradiation). Exposures to CS or FA will then continue through 30 mo. Approximately 10% of the animals will be serially sacrificed for dosimetric and histological evaluations, and the remainder will be held and exposed for their life spans. Animals will be added into the study in five exposure blocks, the first of which will begin in October 1995; the last will be placed on study during the third quarter of FY-1996.

Histologic and dosimetric evaluations of rats in the CS + $^{239}PuO_2$ study continue, and the study of CS + X rays is beginning. This research will generate significant new information regarding the induction of cigarette smoke-induced lung cancer in rats, and the potential for interaction between cigarette smoke and lung irradiation in the induction of lung cancer.

(Research sponsored by the Assistant Secretary for Defense Programs, U.S. Department of Energy, under Contract No. DE-AC04-76EV01013.)

EFFECTS OF COMBINED EXPOSURE OF F344 RATS TO INHALED PLUTONIUM-239 DIOXIDE AND A CHEMICAL CARCINOGEN (NNK)

David L. Lundgren, William W. Carlton,*
William C. Griffith, Kristen J. Nikula, and Steven A. Belinsky

Workers in nuclear weapons facilities have a significant potential for exposure to chemical carcinogens and to radiation from external sources or from internally deposited radionuclides such as ^{239}Pu. Although the carcinogenic effects of inhaled ^{239}Pu and many chemicals have been studied individually, very little information is available on their combined effects (Fry, R. J. M. and R. L. Ullrich. In *Radiation Carcinogenesis* [A. C. Upton, R. E. Albert, F. J. Burns and R. E. Shore, eds.], Elsevier, New York, p. 437, 1986). One chemical carcinogen that workers could be exposed to via tobacco smoke is the tobacco-specific nitrosamine 4-(N-methyl-n-nitrosamino)-1-(3-pyridyl)-1-butanone (NNK), a product of tobacco curing and the pyrolysis of nicotine in tobacco (Hoffman, D. and S. S. Hecht. *Cancer Res. 45:* 935, 1985). NNK causes lung tumors in rats, regardless of the route of administration (Rivenson, D. *et al. Cancer Res. 48:* 6912, 1988) and to a lesser extent liver, nasal, and pancreatic tumors.

The purpose of this study was to characterize the effects of combined exposure of rats to NNK and plutonium deposited in the lung by inhalation, as well as the effects resulting from exposure to these agents alone. We hypothesized that the combined exposures would interact synergistically, thus resulting in a higher incidence of lung tumors in the rats exposed to both agents compared with the sum of the incidence in rats exposed to either agent alone. Data have been collected on age-specific cancer incidence rates for cancers that occur spontaneously and as a result of exposure to α-radiation of the lung with or without exposure to NNK. This information will aid in determining the appropriateness of different mathematical cancer risk models based upon observations of large populations of laboratory animals. A model for the development of lung tumors, illustrating the various rates to be taken into account in predicting the occurrence of lung tumors, has been presented (1986–87 Annual Report, p. 318). Our primary interest in this model is the rate at which the rats develop lung tumors and whether the combined exposure to radiation and a chemical carcinogen alters this rate.

The experimental design for this study has been previously summarized (1991–92 Annual Report, p. 118). Briefly, 740 male 4 ± 1-wk-old CDF®(F344)/CrlBR rats purchased from Charles River Laboratories (Kingston, NY) were used in two blocks of 370 rats each. The blocks of rats were entered into this study in FY-92 and FY-93. Rats were randomized by weight for assignment to dose groups within each block. Low and medium doses of NNK, dissolved in physiological saline, were given by subcutaneous injection three times per week for 20 wk. These doses were expected to result in about a 15% and 50% incidence of lung tumors, respectively. Doses were based on previous work with male F344 rats that were more responsive to NNK than female F344 rats (Belinsky, S. A. *et al. Cancer Res. 50*: 3772, 1990).

The NNK injections began when the rats were 6 wk of age, and $^{239}PuO_2$ exposures occurred when the rats were 12 wk of age. For this study, the α-particle dose to lungs was expected to induce about a 15% incidence of lung tumors (1987–88 Annual Report, p. 245; Lundgren, D. L. *et al. Human Exp. Toxicol. 9:* 295, 1990: Lundgren, D. L. *et al. Health Phys. 60:* 353, 1991). The methods used for the inhalation exposures of rats to $^{239}PuO_2$ have been described (Lundgren *et al.*, 1991).

*Department of Veterinary Pathobiology, Purdue University, Lafayette, Indiana

Because exposure to the combination of $^{239}PuO_2$ and NNK may alter the lung tumor incidences and/or death rates, it was necessary to include interim sacrifices to determine the rate at which animals were developing lung tumors (1986–87 Annual Report, p. 318; McKnight, B. and J. Crowely. *J. Am. Stat. Assoc. 79*: 639, 1984). Four rats per group exposed to ^{239}Pu were sacrificed at each of eight time intervals from 8 through 450 d after exposure to obtain more detailed information on the clearance of ^{239}Pu for dosimetry purposes. Some rats from each group were sacrificed late in life to obtain data on the prevalence of lung tumors at different times after exposure. Additional data on ^{239}Pu retention are being obtained from these rats and from those that died spontaneously. At death, all rats were necropsied, and major organs and all lesions were fixed in 4% buffered paraformaldehyde for histologic examination.

The last of the rats in this study died during 1995. Of the 740 rats exposed, 104 died spontaneously, 472 were euthanized when moribund, 161 were sacrificed for dosimetry or to obtain data on the late-in-life prevalence of lung tumors, and three were removed from study for other reasons. The median survival times (Brookmeyer and Crowley 50% confidence intervals) of all rats were decreased relative to those of the rats sham treated with NNK and sham exposed to $^{239}PuO_2$ (Table 1). However, there were no significant differences in the median survival times among the groups of rats exposed to $^{239}PuO_2$ with or without treatment with 0.3 or 1.0 mg NNK kg^{-1}. The median survival time of the NNK- treated rats with or without exposure to $^{239}PuO_2$ was decreased by 8 to 15% relative to the sham-NNK- and sham-$^{239}PuO_2$-exposed control group.

The incidences of benign (adenoma and papilloma) and malignant (adenocarcinoma, squamous cell carcinoma, adenosquamous carcinoma, and mesothelioma) lung tumors in rats that died a year or more after sham exposure or exposure to $^{239}PuO_2$ are also summarized in Table 1. There was a lower incidence of lung tumors than expected in the rats treated with NNK alone and a greater than expected incidence of lung tumors in the rats exposed only to $^{239}PuO_2$. From our preliminary analysis of these data, it can be concluded that the incidence of lung tumors in the rats exposed to both NNK and $^{239}PuO_2$ was, at best, additive compared with rats exposed to either agent alone.

The retention of inhaled ^{239}Pu in the lungs of all exposed rats in this study and the α-particle doses to the lungs of the rats that died at times > 1 y after exposure are summarized in Table 2. The initial lung burdens of ^{239}Pu kg^{-1} body weight, retention of ^{239}Pu, and α-particle doses to the lungs were similar among all three groups of rats that had been exposed to $^{239}PuO_2$.

From the results presented, it can be concluded that exposure to a chemical carcinogen (NNK) in combination with α-particle radiation from inhaled $^{239}PuO_2$ acts in, at best, an additive manner in inducing lung cancer in rats. Additional analyses, including the time to occurrence of lung tumors, will further clarify the extent of the interactions.

Table 1

Survival and Incidence of Lung Tumors in Male F344 Rats Exposed to Inhaled $^{239}PuO_2$ and Given Repeated Subcutaneous Injection of a Chemical Carcinogen (NNK)[a]

Experimental Groups	Exposures		Number Exposed	MST (days) with 95% CI[d]	MST as a Percentage of Group I	Crude Incidence (%) of Lung Tumors[e]		
	^{239}Pu ILB[b]	NNK[c]				Benign	Malignant	Combined
I	Sham	Sham	100	722 (682, 737)	–	0/99 (0%)[f]	0/99 (0%)	0/99 (0%)
II	480 ± 70 Bq	Sham	140[g]	650 (624, 680)	90	17/107 (16%)	39/107 (36%)	49/107 (45%)
III	Sham	0.3 mg kg^{-1}	110	667 (624, 700)	92	2/107 (1.9%)	2/107 (1.9%)	3/107 (2.8%)
IV	470 ± 68 Bq	0.3 mg kg^{-1}	150[g]	658 (625, 678)	91	21/121 (17%)	31/121 (26%)	47/121 (39%)
V	Sham	1.0 mg kg^{-1}	80	624 (595, 652)	86	2/80 (2.5%)	7/80 (8.8%)	8/80 (10%)
VI	460 ± 76 Bq	1.0 mg kg^{-1}	120[g]	615 (582, 646)	85	21/90 (23%)	28/90 (31%)	41/90 (46%)

[a]NNK = 4-(N-methyl-N-nitrosamino)-1-(3-pyridyl)-1-butanone.
[b]ILB = mean initial lung burden ± SD.
[c]Dose of NNK in saline given by subcutaneous injection three times per week for 20 wk.
[d]Median survival time (MST) with its corresponding Brookmeyer-Crowley 95% confidence interval.
[e]Only rats that died or were sacrificed at times > 1 y after sham exposure or exposure to $^{239}Pu0_2$ included in this tabulation. Benign tumors were adenomas and a papilloma. Malignant tumors were adenocarcinomas, squamous cell carcinomas, adenosquamous carcinomas, and mesotheliomas.
[f]Number of rats with lung tumors per number included in this tabulation.
[g]Four rats from each group exposed to ^{239}Pu were serially sacrificed at eight time points between 8 and 450 d after exposure for dosimetry.

Table 2

Parameters Describing the Retention of ^{239}Pu Inhaled as $^{239}PuO_2$ Aerosols by Male F344 Rats with and Without Treatment with NNK and α-Particle Doses to the Lungs from the Inhaled ^{239}Pu

NNK Treatment[a]	ILB (kBq kg^{-1} body weight ± SD)	Retention Parameters (± SE)[b]				Mean Dose (Gy ± SD) to Lungs to Death[c,d]
		A_1 (%)	T_1 (days)	A_2 (%)	T_2 (days)	
Sham	1.9 ± 0.3	89 ± 1.1	14 ± 1.3	11 ± 1.1	360 ± 32	1.2 ± 0.2
0.3 mg/kg^{-1}	1.9 ± 0.3	83 ± 1.8	9.6 ± 1.4	17 ± 1.8	290 ± 24	1.3 ± 0.2
1.0 mg/kg^{-1}	2.0 ± 0.3	85 ± 1.6	14 ± 1.7	15 ± 1.6	350 ± 36	1.4 ± 0.2

[a]Dose of NNK injected subcutaneously kg^{-1} body weight three times a week for 20 wk.

[b]Retention described by $Y(t) = A_1e^{-0.693t/T_1} + A_2e^{-0.693t/T_2}$, where $Y(t)$ is the retention of ^{239}Pu in % of the initial lung burden, t the time after exposure, and $A_1 = 100 - (A_2)$.

[c]Rats that died or were sacrificed 1 y or more after exposure to ^{239}Pu.

[d]The retention patterns were significantly different among the three treatment groups (generalized F test; $p < 0.05$). Therefore, doses to the lungs of each groups were calculated using the retention parameters from each respective group.

(Research sponsored by the Assistant Secretary for Defense Programs, U.S. Department of Energy, under Contract No. DE-AC04-76EV01013.)

COMBINED EXPOSURE OF F344 RATS TO BERYLLIUM METAL AND PLUTONIUM-239 DIOXIDE

Gregory L. Finch, Fletcher F. Hahn, William W. Carlton, Alan H. Rebar*, Mark D. Hoover, William C. Griffith, James A. Mewhinney**, and Richard G. Cuddihy*

Nuclear weapons industry workers have the potential for inhalation exposures to plutonium (Pu) and other agents, such as beryllium (Be) metal. The purpose of this ongoing study is to investigate potential interactions between Pu and Be in the production of lung tumors in rats exposed by inhalation to particles of $^{239}PuO_2$, Be metal, or these agents in combination. Inhaled Pu deposited in the lung delivers high-linear-energy transfer, alpha-particle radiation and is known to induce pulmonary cancer in laboratory animals (*Biological Effects of Ionizing Radiation-IV*, National Academy of Sciences, 1988). Although the epidemiological evidence implicating Be in the induction of human lung cancer is weak and controversial, various studies in laboratory animals have demonstrated the pulmonary carcinogenicity of Be. As a result, Be is classified as a suspect human carcinogen in the United States (*Health Assessment Document for Beryllium*, U.S. EPA/600/8-84/026F, 1987) and as a demonstrated human carcinogen by the International Agency for Research on Cancer (IARC, *Beryllium, Cadmium, Mercury, and Exposures in the Glass Manufacturing Industry*, Vol. 58, Lyon, France, 1993).

This study is being conducted in two phases; Table 1 shows the experimental design. In Phase I, F344/N rats (ITRI bred; both male and female; 12 ± 1 wk old at exposure) were exposed once nose-only to respirable aerosols of $^{239}PuO_2$ and/or Be metal from October 1987–January 1989. Groups of rats received $^{239}PuO_2$ followed immediately by exposure to Be metal, or the appropriate air control. Rats received one of two target initial lung burdens (ILBs) of $^{239}PuO_2$ (56 or 170 Bq), and/or one of three target ILBs of Be metal (50, 150, or 450 μg).

Rats were either serially sacrificed or held for life-span observation; moribund rats were euthanized. Approximately 20% of the life-span rats were sacrificed late in their lives. At death, a complete necropsy was performed, and lungs, other selected tissues, and all lesions were fixed in formalin for histological analysis. Lungs of exposed rats were analyzed for Be and/or ^{239}Pu as appropriate. All Phase I rats were dead as of March 1991.

Exposure to Be significantly retarded the clearance of ^{239}Pu (1989–90 Annual Report, p. 125). The 450 μg ILB of Be caused significant mortality from acute pneumonitis within 3 wk of exposure, and longer term survival was affected by Be metal in a dose-dependent manner (1990–91 Annual Report, p. 99). It was further observed that inhaled Be metal induced significant tumorigenicity in the lungs of rats (1993–94 Annual Report, p. 77). For example, in the group receiving a mean ILB of 450 μg Be metal, a crude benign and/or malignant lung tumor incidence of 93% (117 of 125 rats) was observed in male and female rats. In addition, substantial lung tumor multiplicity was observed (data not shown).

Incidences of Be metal-induced lung tumors observed were significantly higher than expected based on extrapolations from a limited data base in the literature (Sanders, C. L. *et al. Health Phys. 35*: 193, 1978; Groth, D. H. *Environ. Res. 21*: 84, 1980; Nolibe, D. *et al. Commissariat A L'Energie Atomique 1984 Annual Report*, CEA, France, 1984). Because interactions between two carcinogens are best analyzed when lung tumor incidences from the individual agents are relatively low, Phase II of this study was initiated using lower ILBs of Be.

---

*Department of Veterinary Pathobiology, Purdue University, Lafayette, Indiana
**Currently at U.S. D.O.E. Carlsbad Area Office, Carlsbad, New Mexico

Table 1

Experimental Design to Study the Combined Effects of $^{239}PuO_2$ and Beryllium Metal in Rats

Be Metal ILB	Numbers of Rats by Experimental Group					
	$^{239}PuO_2$ ILB[a]					
	0 Bq	60 Bq	170 Bq	230 Bq	460 Bq	Total
0 µg	478[b] (208^{I}; 270^{II})	240^{I}	240^{I}	288^{II}	156^{II}	1402
0.3 µg	288^{II}	–[c]	–	–	–	288
1.0 µg	288^{II}	–	–	288^{II}	–	576
3.0 µg	288^{II}	–	–	–	–	288
10 µg	288^{II}	–	–	288^{II}	–	576
50 µg	396 (240^{I}; 156^{II})	240^{I}	240^{I}	–	–	876
150 µg	240^{I}	240^{I}	240^{I}	–	–	720
450 µg	240^{I}	240^{I}	240^{I}	–	–	720
TOTAL	2506	960	960	864	156	5446

[a]ILB = initial lung burden.
[b]Number of rats per group. Equal numbers of males and females. Superscripts (I) and (II) refer to phase of the study. The total numbers of rats used by phase of the study were 2848 rats in Phase I and 2598 in Phase II. For each group, approximately 80% of the rats are designated for life-span observation, and about 20% for serial sacrifice.
[c]Dash (–) indicates no animals included within this matrix cell.

CDF®(F-344)/CrlBR rats (Charles River Laboratories, Raleigh, NC) are being used in Phase II. Significant design features (see Table 1) include (1) the use of a sufficient number of rats inhaling Be metal alone to define dose-response relationships for Be metal-induced carcinogenicity, (2) the combined exposure of two Be metal dose groups with $^{239}PuO_2$, and (3) the addition of a group of rats exposed only to $^{239}PuO_2$ at a relatively higher initial dose rate to mimic the increased radiation dose caused by Be-induced reductions in lung ^{239}Pu clearance.

All Phase-II exposures were conducted between April 1993–November 1994. As of September 30, 1995, 39% of the rats remain alive, 23% have been sacrificed for Be and/or ^{239}Pu dosimetry and histologic lung changes, and 38% have died or been euthanized as moribund. Preliminary results from whole-body counting the $^{239}PuO_2$-exposed rats for a ^{169}Yb radiolabel incorporated within the PuO_2 indicate that Be metal exposure decreased $^{239}PuO_2$ clearance compared to controls over a 42-d period.

Clearance half-times were 39 ± 7 (S.D.), 76 ± 10, or 137 ± 17 d for groups of rats receiving ILBs of 0, 1, or 10 μg Be, respectively.

Although many of the rats are still alive, and those that are dead have not yet been histologically analyzed, a crude tumor incidence can be estimated by examining lungs at necropsy for evidence of masses and/or nodules (Table 2). Preliminary indications from these data indicate that (1) the presence of a dose-response relationship for the individual agents alone, (2) an apparent no-effect level for lung carcinogenesis from Be metal at the 0.3 μg target ILB, (3) the incidence of masses and/or nodules in the 50 μg ILB group is similar between the two phases of the study, and (4) no conclusions can yet be drawn regarding possible carcinogenic interactions between inhaled $^{239}PuO_2$ and Be metal in the rat.

Table 2

Incidences of Lung Masses and/or Nodules Observed During Necropsy for Male and Female Rats Exposed to $^{239}PuO_2$ and/or Beryllium (Be) Metal in Phase II of the Study

Be Metal ILB	$^{239}PuO_2$ ILB[a]		
	0 Bq	230 Bq	460 Bq
0 μg	Males: 0% (0/76)[b] Females: 3% (2/59)	Males: 11% (11/96) Females: 3% (2/75)	Males: 18% (11/62) Females: 11% (5/47)
0.3 μg	Males: 1% (1/85) Females: 0% (0/71)	–[c]	–
1.0 μg	Males: 7% (6/86) Females: 3% (2/63)	Males: 15% (15/98) Females: 19% (12/64)	–
3.0 μg	Males: 4% (3/85) Females: 26% (19/72)	–	–
10 μg	Males: 4% (4/93) Females: 17% (12/71)	Males: 31% (33/107) Females: 50% (49/98)	–
50 μg	Males: 32% (19/60) Females: 37% (19/52)	–	–

[a]ILB = initial lung burden.
[b]Crude incidence with number of rats having masses and/or nodules at necropsy over the number examined shown in parentheses. Data are for rats that died, or were euthanized or sacrificed after having been on study for at least 1 y after exposure. Rats having lung masses and/or nodules, but suspected of having leukemia, as indicated by an enlarged spleen at necropsy, were not included in the lung mass/nodule category.
[c]Dash (–) indicates no animals included within this matrix cell.

This study is in progress. As data are obtained and analyzed, this work will define dose-response relationships for Be-induced lung cancer in the rat and will provide information regarding the potential interaction between Be and ^{239}Pu in causing lung cancer.

(Research sponsored by the Assistant Secretary for Defense Programs, U.S. Department of Energy, under Contract No. DE-AC04-76EV01013.)

BIOLOGICAL EFFECTS OF CESIUM-137 INJECTED IN BEAGLE DOGS OF DIFFERENT AGES

Kristen J. Nikula, Bruce A. Muggenburg, William C. Griffith, Thomas E. Fritz, and Bruce B. Boecker*

The toxicity of cesium-137 (^{137}Cs) in the Beagle dog was investigated at the Argonne National Laboratory (ANL) as part of a program to evaluate the biological effects of internally deposited radionuclides. The toxicity and health effects of ^{137}Cs are important to understand because ^{137}Cs is produced in large amounts in light-water nuclear reactors. Large quantities of cesium radioisotopes have entered the human food chain as a result of atmospheric nuclear weapons tests, and additional cesium radioisotopes were released during the Chernobyl accident.

The ^{137}Cs exposures, husbandry of the dogs throughout their life spans, and necropsies were conducted at ANL. The clinical records, necropsy reports, and histopathology slides were transferred to ITRI for final review and analysis. The $^{137}CsCl$ was administered intravenously because it was known that after intravenous injection, inhalation, or ingestion, internally deposited $^{137}CsCl$ is rapidly absorbed and distributed throughout the body, exposing the whole body to beta and gamma radiation (Boecker, B. B. *Health Phys. 16:* 785, 1969).

Sixty-three purebred Beagle dogs (35 males and 28 females) from the ANL dog colony were given ^{137}Cs intravenously in doses near those expected to be lethal within 30 d after injection. The dogs were in three age groups at the time of injection: 15 dogs were 142–151 d old (immature dogs), 38 were 388–427 d old (young adult dogs), and 10 were 1387–1509 d old or 2060 d old (five in each age group, referred to as older dogs). The amounts of ^{137}Cs injected in dogs of different ages were as follows: immature dogs, 120–142 MBq/kg; 25 "high-dose" young adults, 98–159 MBq/kg; 13 "low-dose" young adults, 61–90 MBq/kg; and the older dogs, 121–138 MBq/kg. At the time the study was initiated, every tenth dog weaned was assigned to the control colony. There were 17 dogs (11 males and six females) entered into the control colony whose birthdates spanned the same years as the dogs injected with ^{137}Cs. The control dogs were not sham exposed.

The biological half-life of ^{137}Cs in the immature dogs ranged from 12–23 d and averaged 16 d. For the young adult dogs, the values ranged from 15–26 d and averaged 20 d. In the older dogs, the range was 26–50 d with an average of 37 d.

Three of the immature dogs, 10 of the high-dose young adult dogs, and all 10 of the older dogs died within 52 d after injection from hematopoietic cell damage resulting in severe pancytopenia which led to fatal hemorrhage and/or septicemia. The radiation dose to death was calculated for each of these dogs. In all three age groups the doses ranged from 7–11 Gy, the average being 9 Gy.

Other nonneoplastic effects were (1) permanent sterility of male ^{137}Cs-injected dogs due to testicular atrophy and (2) a greater frequency of hepatic lesions (nodular hyperplasia, degeneration, and biliary cysts) in long-term surviving ^{137}Cs-injected dogs than in controls.

The occurrence of carcinomas and sarcomas in ^{137}Cs-injected dogs and controls is summarized in Table 1. The incidence of sarcomas was greater in ^{137}Cs-injected dogs than in controls. When the sarcomas were categorized by general type (Table 2), the most striking differences between ^{137}Cs-injected dogs and controls were the increased numbers of sarcomas with a "spindle cell" morphology in young adult ^{137}Cs-injected dogs, the occurrence of leukemias and myeloproliferative diseases in

*Argonne National Laboratory, Argonne, Illinois

^{137}Cs-injected dogs, and the numbers of sarcomas with a "round cell" morphology in immature ^{137}Cs-injected dogs.

Table 1

^{137}Cs-Injected and Control Dogs with Carcinomas and Sarcomas

Group (no. long-term survivors)	Dogs with Only Carcinomas	Dogs with Only Sarcomas	Dogs with Both Sarcomas and Carcinomas	Total No. Dogs (%) with Sarcomas	Total No. Dogs (%) with Carcinomas
Immature (12)	3	4	1	5 (42%)	4 (33%)
Young Adult, High Dose (15)	5	2	5	7 (47%)	10 (67%)
Young Adult, Low Dose (13)	5	4	3	7 (54%)	8 (62%)
Control (17)	7	1	2	3 (18%)	9 (53%)

Table 2

Numbers of Sarcomas of Different Types in ^{137}Cs-Injected Dogs and Controls

	Spindle Cell Sarcomas[a]			Round Cell Sarcomas[b]		
Group (no. long-term survivors)	Splenic	Non-splenic	Total	Leukemia and Myeloproliferative Disease	Other	Total
Immature (12)	1	0	1	1	3	4
Young Adult, High Dose (15)	3	4	7	1	1	2
Young Adult, Low Dose (13)	3	2	5	1	1	2
Control (17)	1	1	2	0	1	1

[a]Leiomyosarcomas, fibrosarcomas, malignant Schwanomas, undifferentiated spindle cell sarcomas, and one malignant hemangiopericytoma in the subcutis of a control dog.
[b]Granulocytic or lymphocytic leukemia, myeloproliferative disease, lymphosarcoma, malignant plasmacytoma, mast cell sarcoma.

There were 13 sarcomas with a spindle cell morphology in 12 affected ^{137}Cs-injected dogs and two sarcomas with a spindle cell morphology in two affected control dogs. All of these sarcomas occurred in the spleen or alimentary system, except for one malignant Schwanoma in the skin of a ^{137}Cs-injected dog that also had a splenic sarcoma, and one malignant hemangiopericytoma in a control dog. The splenic sarcomas were undifferentiated, pleomorphic, spindle-cell sarcomas that sometimes had morphologic features resembling malignant Schwanomas or leiomyosarcomas. Because none

exhibited features pathognomonic for these neoplasms, yet they all shared similar morphologic features, they were grouped together as undifferentiated sarcomas. Seven ^{137}Cs-injected dogs had undifferentiated sarcomas of the spleen. One undifferentiated sarcoma occurred in an immature dog, three in high-dose young adult dogs, and three in low-dose young adult dogs. One control dog had a small undifferentiated sarcoma of similar morphology in the spleen.

Five ^{137}Cs-injected dogs had spindle cell sarcomas of the alimentary tract. Two high-dose young adults had malignant Schwanomas of the small intestine, one high-dose and one low-dose young adult had leiomyosarcomas of the small intestine, and one low-dose young adult had a palatine fibrosarcoma. No control dogs had sarcomas of the alimentary tract.

Three ^{137}Cs-injected dogs had primary neoplasms of bone marrow origin. One immature ^{137}Cs-injected dog had granulocytic leukemia, one high-dose young adult had lymphocytic leukemia, and one low-dose young adult had myeloproliferative disease. None of the control dogs had primary neoplasms arising from bone marrow. The other round cell sarcomas in the ^{137}Cs-injected dogs included: a splenic malignant plasmacytoma and two cases of lymphosarcoma in immature dogs, a small intestinal malignant plasmacytoma in a high-dose young adult dog, and a mast cell sarcoma in the subcutis of a low-dose young adult dog. One control dog had generalized lymphosarcoma.

Review is in progress of the dosimetry, survival analysis, and statistical analyses of neoplastic diseases in the different age-at-injection and dose groups by general categories of neoplasms and by specific organ affected. When these analyses are completed, the results will be compared with those from the recently published ITRI research (Nikula, K. J. *et al. Radiat. Res. 142*: 347, 1995) that examined effects over a lower dose range of injected ^{137}Cs.

Although the final analyses are not complete, three findings are significant. First, analysis of the mortality rates for dogs dying from the early effects of radiation shows that the older dogs died significantly earlier than the juvenile and young adult dogs. Second, there is a greater occurrence of sarcomas in the ^{137}Cs-injected dogs compared to the controls, which raises the concern for soft tissue sarcomas as a late effect in people exposed to high doses of internally deposited ^{137}Cs. Third, the major nonneoplastic effect in the dogs that survived beyond 52 d appears to be testicular atrophy resulting in sterility, which suggests that testicular degeneration and atrophy might also be late effects in men exposed to internally deposited ^{137}Cs.

(Research sponsored by the Office of Health and Environmental Research, U.S. Department of Energy, under Contract No. DE-AC04-76EV01013.)

CERIUM-144-INDUCED LUNG TUMORS IN TWO STRAINS OF MICE

Fletcher F. Hahn and William C. Griffith

A major problem in the extrapolation of radiation cancer risk factors from one species or population to another is the choice of the risk model to use, either absolute or relative. The purpose of this study was to compare absolute and relative risk models in predicting the lung-tumor risks between a low lung-tumor incidence strain of mice and a high-incidence strain of mice.

To make this comparison, BALB/c mice, a strain with a relatively high (~ 30%) spontaneous incidence of lung tumors, were exposed to aerosols containing cerium-144. The lung tumor incidence was determined, and results were compared with those from similarly exposed C57/Bl/6J mice, a low (~ 1.5%) lung tumor incidence strain. A total of 312 BALB/c mice were exposed briefly (< 30 min), nose only, to aerosols of ^{144}Ce-fused aluminosilicate particles to achieve initial lung burdens of ^{144}Ce between 1.1 and 59 kBq and were observed for their life spans. The lifetime doses to the lung of exposed groups ranged from a mean of 0.69–20 Gy. In a similar manner, 177 C57/Bl/6J mice were exposed by inhalation to aerosols of $^{144}CeO_2$ resulting in two groups of mice with lifetime doses to the lung of 4.5 and 24 Gy. The effective retention of ^{144}Ce in the lung and the survival of the mice relative to controls were similar between the two strains of mice. Both types of particles are primarily retained in the respiratory tract, and very little of the ^{144}Ce is translocated to other organs (Hahn, F. F. *et al. Radiat. Res. 82*: 123, 1980). Thus, competing risks from radiation-induced diseases in nonrespiratory tract organs are not significant factors.

The dose and lung tumor response are noted in Table 1. The lung tumor incidence (adenomas and adenocarcinomas combined) did not increase in the group with the mean dose of 0.69 Gy. At 1.4 and 4.6 Gy, the excess incidence was 9–10%, but not significantly different from controls; at 12 and 20 Gy, it was 14–16%, a rather flat dose response which was significantly elevated above controls, $p = < 0.05$. In the C57 mice, there was a significant increase in lung tumor incidence above controls of 17%, $p = < 0.05$, at 24 Gy.

Table 1
Lung Tumor Incidence and Risk

Initial Lung Burden (kBq)	Dose to Lung (Gy)	Number of Mice	% Incidence Lung Tumors	Excess % Incidence	Absolute Risk: Tumors 10^4 Gy	Relative Risk: Excess RR Gy
BALB/c						
Sham/FAP	0	83	29	–	–	–
0.70	0.69	54	29	–0.8	0	0
2.1	1.4	56	39	10	770	0.24
6.3	4.6	55	38	9	200	0.068
19	12	51	45	16	130[a]	0.044
37	20	60	43	14	66[a]	0.024
C57/Bl/6J						
Sham	0	597	1.5	–	–	–
6.3	4.5	74	4.1	2.6	55	3.9
37	24	103	17	16	66[b]	0.44

[a]Significantly increased from zero.
[b]From Hahn *et al.*, 1980.

A progression of proliferative epithelial lesions in the lung has been described for spontaneous lung tumors; from alveolar epithelial hyperplasia to adenoma to adenocarcinoma (Dixon, D. *et al. Exp. Lung Res. 17*: 131, 1991). A similar progression was noted in the mice of both strains exposed to ^{144}Ce. In addition, with increased dose and increased incidence of tumors, there was a shift in the progression toward malignancy (Fig. 1). In the BALB/c strain, the increased incidence was due primarily to an increase in adenocarcinomas. In the C57 strain, the increased incidence was due primarily to an increase in adenomas.

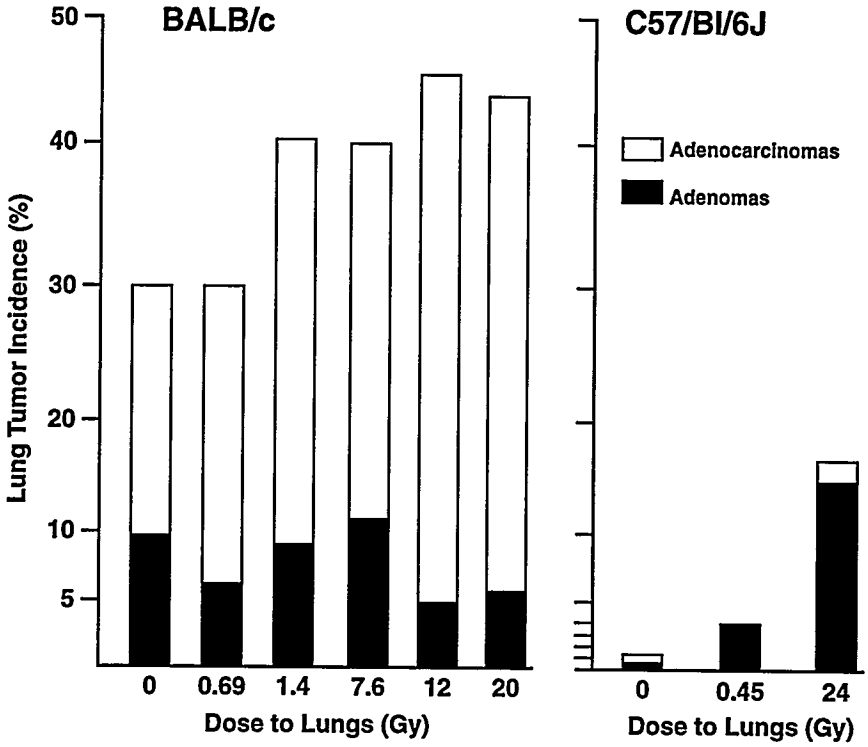

Figure 1. Increased lung tumor incidence associated with shift toward malignancy.

The absolute risk for lung tumors in the BALB/c strain was 130 and 66 tumors per 10^4 Gy in the 12 and 20 Gy groups, respectively (Table 1). The risk is similar to the absolute risk of 66 lung tumors per 10^4 Gy in the C57 strain exposed to a similar dose of 24 Gy in previous studies at the Institute. On the other hand, the relative risk factors differed between the two strains by a factor of 10 (Table 1).

The conclusion from this study is that absolute risk is more accurate than relative risk for predicting lung tumor risk from high to low lung-tumor incidence strains of mice. This conclusion strengthens the idea that absolute risk is an appropriate model for interspecies extrapolation of lung-tumor risk.

(Research sponsored by the Office of Health and Environmental Research, U.S. Department of Energy, under Contract No. DE-AC04-76EV01013.)

HOT BETA PARTICLES IN THE LUNG: RESULTS FROM DOGS EXPOSED TO FISSION PRODUCT RADIONUCLIDES

Fletcher F. Hahn, William C. Griffith, Charles H. Hobbs,
Bruce A. Muggenburg, George J. Newton, and Bruce B. Boecker

The Chernobyl nuclear reactor accident resulted in the release of uranium dioxide fuel and fission product radionuclides into the environment with the fallout of respirable, highly radioactive particles that have been termed "hot beta particles." There is concern that these hot beta particles (containing an average of 150–20,000 Bq/particle), when inhaled and deposited in the lung, may present an extraordinary hazard for the induction of lung cancer (Osuch, S. *et al. Health Phys. 57*: 707, 1989). We reviewed data from a group of studies in dogs exposed to different quantities of beta-emitting radionuclides with varied physical half-lives to determine if those that inhaled hot beta particles were at unusual risk for lung cancer.

The experimental approach and design for the longevity studies of dogs exposed to fission product radionuclides have been described in detail (McClellan, R. O. *et al.* In *Life-span Radiation Effects Studies in Animals: What Can They Tell Us?* [R. C. Thompson and J. A. Mahaffey, eds.], CONF-830951, Office of Scientific and Technical Information, U.S. DOE, Springfield, VA, p. 74, 1986). Each exposed dog received a single brief (< 76 min) nose-only inhalation exposure to a polydisperse aerosol of ^{90}Y, ^{91}Y, ^{144}Ce-^{144}Pr, or ^{90}Sr-^{90}Y in fused aluminosilicate particles. Pure ^{90}Y was obtained by separation from its parent ^{90}Sr. The aerosols were prepared by cation exchange of the radionuclide into montmorillonite clay, aerosolization with a Lovelace nebulizer, and high-temperature fusion (1100°C) of the airborne particles to form relatively insoluble, fused aluminosilicate containing one of the four radionuclides (Newton, G. J. *et al.* In *Generation of Aerosols* [K. Willeke, ed.], Ann Arbor Science Publishers, Ann Arbor, MI, p. 399, 1980). Aerosol characteristics are listed in Table 1. For all radionuclides, the activity median aerodynamic diameter (AMAD) ranged from 0.8–2.8 μm with σ_g from 1.4–2.7. The real diameter, D_r, for particles > 0.3 μm, is related to the AMAD by (Raabe, O. G. *JAPCA 9*: 26, 856, 1976).

$$D = \sqrt{\frac{AMAD_r^2 + 0.01}{\rho}} - 0.1 \qquad (1)$$

where ρ = particle density in g/cm^3.

The specific activities of the particles were calculated from the formulation:

$$\text{activity/particle} = \frac{\pi D_r^3}{6} \rho \times \text{S. A.} \qquad (2)$$

where D_r = particle diameter in cm
ρ = density of fused clay = 2.3 g/cm^3
S. A. = Specific activity of radionuclide in generator solution (Ci/g)

The half-lives of the radionuclides in the lung, when incorporated in fused aluminosilicate particles, are noted in Table 1. The longer the half-life in the lung, the more protracted the delivery of dose.

The corresponding control dogs inhaled a nonradioactive aerosol of fused aluminosilicate particles.

Table 1

Characteristics of Aerosols Used in Exposure of Dogs
to Fission Product Radionuclides in Fused Aluminosilicate Particles

	^{90}Y	^{91}Y	^{144}Ce-^{144}Pr	^{90}Sr-^{90}Y
Average AMAD[a] (μm ± SD)	1.1 ± 0.13	2.0 ± 0.26	1.8 ± 0.28	2.0 ± 0.35
Average Size Distribution (σ_g ± SD)	1.6 ± 0.1	1.7 ± 0.1	1.8 ± 0.1	1.7 ± 0.2
Real size, median diameter, D_r, (μm)	0.71	1.3	1.2	1.3
Specific activity/particle for median diameter particle (Bq/particle)	28	0.59	0.46	0.12
Half-time in lung after deposition in the lung (days)	2.5	50	180	500

[a]AMAD = activity median aerodynamic diameter.

Lung carcinomas were the primary biologic endpoint of interest. The tumor incidence rates for lung carcinomas were expressed as relative risk functions that relate tumor incidence rate to both total dose and dose pattern. A proportional hazard rate model was applied to describe how the tumor incidence rates change with radiation dose (Griffith, W. C. *et al. IRPA 8*: 896, 1992).

The relative risk that best described these studies was a linear function of dose added to a power function of dose. The excess relative risk (relative risk – 1) is shown in Figure 1. By the likelihood ratio test, this model was a statistically significant improvement ($p = <0.01$) over models with just a linear or a power function of dose. There was not statistically significant improvement to estimate separate linear coefficients for each radionuclide.

Results of this analysis show no effect of dose protraction on the incidence of lung carcinomas at the lower range of doses used in the study. It was not possible to discern a difference between the four radionuclides below about 50 Gy. At higher doses, however, it is much more hazardous to deliver the dose over a short period of time.

Table 1 shows a wide range of specific activities of particles deposited in the lung, from about 0.1–100 Bq/particle, three orders of magnitude, with ^{90}Y having the highest specific activity and ^{90}Sr the lowest. If specific activity of the particles was an important factor, one would expect the ^{90}Y to result in more risk for lung cancer than ^{91}Y and so on. Lung cancer risk predicted from specific activity of particles:

$$^{90}Y >> ^{91}Y = ^{144}Ce\text{-}^{144}Pr \geq ^{90}Sr\text{-}^{90}Y \quad (3)$$

In fact, the lung cancer risks are essentially equal, at doses < 50 Gy to the lung. From this analysis, we conclude that hot beta particles in the range of 0.10–30 Bq/particle do not present an extraordinary risk for lung cancer, at least in the 0.5–50 Gy range of doses to the lung.

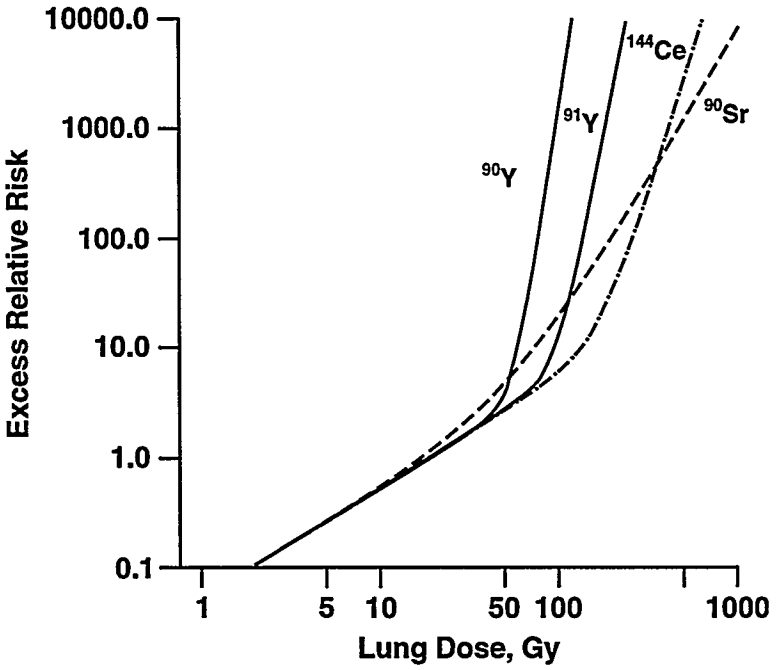

Figure 1. Excess relative risk of lung cancer from inhaled beta emitters in fused aluminosilicate particles.

This analysis indicates that the average dose to the lung is adequate to predict biologic effects of lung cancer for inhaled beta-emitting radionuclides in the range of 5–50 Gy to the lung and with particle activities in the range of 0.10–50 Bq/particle.

(Research sponsored by the Office of Health and Environmental Research, U.S. Department of Energy, under Contract No. DE-AC04-76EV01013.)

TOXICITY OF INJECTED RADIUM-226 IN IMMATURE DOGS

Bruce A. Muggenburg, Fletcher F. Hahn, William C. Griffith, Ray D. Lloyd, and Bruce B. Boecker*

This study was conducted to determine the toxicity of injected ^{226}Ra in immature dogs and to compare the results with those from studies of injected ^{226}Ra in young adult dogs. An historic objective of these studies, initiated at the University of Utah and continued at ITRI, was to compare the results in dogs to the population of dial painters who ingested ^{226}Ra as young adults. Age at the time of exposure is considered to be an important factor in dosimetry and risk of developing radiation-induced disease, particularly bone cancer.

The study was conducted in 54 Beagle dogs from the University of Utah colony; 27 males and 24 females were injected with one of five levels of ^{226}Ra citrate, and a small control group was injected with only the citrate solution. The dogs were 3 mo old at the time of injection. The injection amounts, survival times, and doses to skeleton are given in Table 1. The average amount injected in the various levels ranged from 38.5 kBq/kg body mass in the highest level, level 3, to 0.69 kBq/kg in the lowest group, level 0.5. (The numbering of the injection levels was developed at the University of Utah, 1987–88 Annual Report, p. 587). The amounts injected resulted in a median average dose to the total skeleton at death of 26 Gy for the dogs in level 3 to 0.88 Gy in level 0.5.

Table 1

Experimental Design and Survival Data for Immature Dogs Injected with ^{226}Ra

Level	Number of Dogs		Age at Injection d ($\bar{X} \pm SD$)	Amount Injected kBq/kg ($\bar{X} \pm SD$)	Survival after Exposure Median (d) (range)	Dose to Skeleton (Gy) Median (range)
	Males	Females				
3	5	5	91 ± 2	38.5 ± 1.1	2558 (1659–3788)	26.0 (16.7–32.9)
2	5	5	90 ± 1	12.0 ± 0.4	3822 (3022–5930)	10.4 (8.73–14.1)
1.7	6[a]	5	91 ± 2	6.1 ± 0.3	4451 (2369–5583)	6.58 (3.97–8.74)
1	6	4	90 ± 2	2.0 ± 0.1	4223 (2010–5787)	2.13 (1.23–2.59)
0.5	5	5	90 ± 2	0.69 ± 0.02	5019 (3001–5604)	0.88 (0.49–1.02)
Controls	1	2	92 ± 3	0	5256 (4301–5733)	0

[a]One dog was not included in the calculations because he died due to an anesthetic accident only 8 d after the ^{226}Ra injection.

Thirty dogs in this study died at the University of Utah. The remaining 24 living dogs were transferred to ITRI on September 15, 1987; the last dog died in 1995. At both the University of Utah and at ITRI, the dogs were housed in kennel buildings, usually two dogs to a run. The dogs were observed twice daily and received annual medical evaluations consisting of a physical examination,

*Radiobiology Division, University of Utah School of Medicine, Salt Lake City, Utah

hematology and clinical chemistry samples, and a series of radiographs. The dogs were euthanized if they had significant discomfort that could not be treated effectively. All dogs that died or were euthanized were given a detailed necropsy, with histologic examination of all major organ systems. When all of the dogs had died, the pathology and clinical records were reviewed, and a consistent criteria for diagnosis and standard terminology were used in evaluation of the study.

Life shortening occurred in the dogs injected with 38.5 or 12 kBq of ^{226}Ra/kg body mass (levels 3 and 2) primarily due to the occurrence of bone tumors in those two groups. Thirteen dogs developed bone tumors which were considered the cause of death. These dogs died from 2102–4245 d after injection with ^{226}Ra. One dog had three bone tumors, two dogs had two tumors, and the remaining 10 dogs each had one tumor. All bone tumors were osteosarcomas. Fourteen of the tumors were osteoblastic, one was fibroblastic, and one a combined type. The distribution of bone tumors relative to average skeletal dose is shown in Figure 1. The alpha-particle doses for the dogs developing bone tumors ranged from 9.5–33 Gy. The tumor sites were mostly in the appendicular skeleton and head. None of the dogs in levels 1.7, 1, or 0.5 developed bone tumors. Most of the dogs with bone tumors also had radiation osteodystrophy either associated with the site of the bone tumor or in other bone samples. Pool, R. R. *et al.* (*Am. J. Roentgenol., Radium Ther. Nucl. Med. 14*: 900, 1973) and Gillett, N. A. *et al.* (*J. Natl. Cancer Inst. 79*: 359, 1987) have reported the association of radiation osteodystrophy and bone tumors in dogs injected with ^{226}Ra or exposed by inhalation to $^{90}SrCl_2$. Radiation osteodystrophy may be a pre-cancerous lesion.

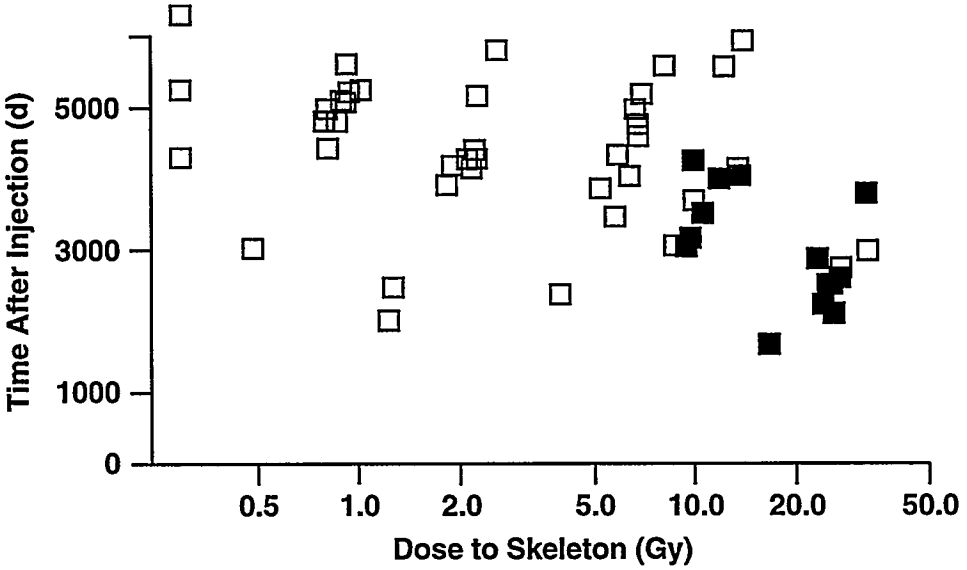

Figure 1. Survival of dogs after injection of ^{226}Ra and the relationship to skeletal dose. The occurrences of bone tumors are shown as closed symbols, and the open symbols denote no bone tumors. Each symbol represents an individual dog plotted against time after radium injection and dose to death averaged over the skeletal mass. The three control dogs are shown on the far left.

Two of the immature dogs developed malignant melanomas of the eye. The tumors were found 2993 and 5788 d after the radium injection. These two dogs were injected with approximately 10 kBq of ^{226}Ra/kg body mass (level 2). Radium is known to accumulate in the iris and surrounding structures. In a previous study, melanomas were found in young adult dogs injected with ^{226}Ra at levels ranging from 0.81–39 kBq/kg body mass (Taylor G. N. *et al. Risks from Radium and Thorotrast* [D. M. Taylor *et al.*, eds.] British Institute of Radiology Report 21, London, 1989).

Mammary tumors were found in female dogs in exposure levels 0.5–2. Of the 19 female dogs in those groups, 15 had mammary tumors. In only one dog was the tumor the cause of death. In all other dogs, these tumors were considered incidental findings. The dogs died from 3001–5604 d after injection with ^{226}Ra. Fourteen of the dogs had two or more tumors, and one dog had one tumor. There were 29 malignant tumors found in 12 dogs. Three dogs had only benign tumors. Both female control dogs had mammary tumors. One dog had a malignant mammary tumor which was the cause of death, and the other control had benign tumors. Bruenger, F. W. *et al.* (*Radiat. Res. 138*: 423, 1994) reported an increase in malignant mammary tumors in young adult dogs injected with ^{226}Ra, but no increase was found in dogs injected with ^{239}Pu (Lloyd, R. D. *et al. Health Phys. 69*: 385, 1995).

Tumors in only two other sites appeared to be increased in incidence. An hepatocellular carcinoma and a hemangiosarcoma were observed in the liver, and two tumors were found in the nasal cavity. Both are rare sites for tumors in control dogs. No tumors were found in the bone marrow.

The major findings in the study conducted in young adult dogs injected with ^{226}Ra at the University of Utah were increases in the occurrence of bone tumors, malignant melanomas of the eye, two malignant liver tumors, two tumors of the nasal cavity, and a small increase in mammary tumors. In general, the findings in the immature and young adult studies agree, and no unexpected findings occurred in the immature dogs.

In summary, dogs injected with ^{226}Ra when immature had increased occurrences of bone tumors in a dose-related fashion. They also had a higher than expected incidence of melanomas of the eye. Tumors of the liver and nasal mucosa and a number of malignant mammary tumors were also observed, but statistical analysis will be needed to determine if the incidences are higher than expected.

(Research sponsored by the Office of Health and Environmental Research, U.S. Department of Energy, under Contract No. DE-AC04-76EV01013.)

V. MECHANISMS OF CARCINOGENIC RESPONSE TO TOXICANTS

DETECTION OF TRISOMY 7 IN BRONCHIAL CELLS FROM URANIUM MINERS

John F. Lechner, Robin E. Neft, Steven A. Belinsky, Richard E. Crowell, and Frank D. Gilliland***

New Mexico was the largest producer of uranium in the western world during the 1960s and 1970s. Investigators at the University of New Mexico School of Medicine's Epidemiology and Cancer Control Program have been conducting epidemiological studies on uranium miners over the past 2 decades. Currently, this cohort includes more than 3600 men who had completed at least 1 y of underground work experience in New Mexico by December 31, 1976. These miners, who are now in their 5th through 7th decades, the age when lung cancer incidence is highest, are at high risk for developing this disease because they were exposed to high levels of radon progeny in the mines, and they also smoked tobacco. However, not all people comparably exposed develop lung cancer; in fact, the lifetime risk of lung cancer for the smoking uranium miners has been projected by epidemiological analyses to be no higher than 50%. Therefore, the identification of gene alterations in bronchial epithelium would be a valuable tool to ascertain which miners are at greatest risk for lung cancer.

The foundation on which this project rests is the pathological condition referred to as "field cancerization." This phenomenon develops in precancerous individuals because tobacco carcinogens and radon daughters induce genetic abnormalities in many cells within the bronchial epithelium. Thus, it is presumed that cancer-free people who exhibit field cancerization have the greatest risk of ultimately developing clinical disease. The purpose of this work was to evaluate the use of fluorescence *in situ* hybridization (FISH) to identify cells with genetic alterations within the epithelium of highly exposed, but currently cancer-free individuals. Specifically, we are examining respiratory tract epithelial cells collected by bronchoscopy from the ex-uranium miners for evidence of aneuploidy and for particular chromosomal losses. The relative frequency of individuals with epithelial cells harboring these molecular alterations is being compared against specimens collected from an age-matched control population. The first FISH marker being evaluated is trisomy of chromosome 7. This abnormality is relatively easy to detect; it is observed in 50% of non-small cell lung cancer and has been frequently detected in the far margins from resected lung tumors (Lee, J. S. *et al. Cancer Res. 54*: 1634, 1987). The molecular mechanism by which the extra copy of chromosome 7 provides a growth advantage is unknown. However, this chromosome harbors the protooncogenes *EGFR* and *Met*, and the gene products of both of these loci are frequently overexpressed in human lung tumor cells (Liu, C. *et al. Am. J. Pathol. 142*: 1155, 1993).

The prospect of using cells obtained by bronchial brushing to detect chromosome alterations has been assessed using cells recovered from nine ex-uranium miners without evidence of clinical disease. Bronchoscopy was conducted by brushing four standard sites with an ordinary cytology brush; particle deposition is high and tumors commonly arise (Auerbach, O. *et al. N. Engl. J. Med. 265*: 253, 1961) at these sites. Each area was pre-washed with saline to remove any nonadhered cells before it was sampled by two brushes. The population of cells recovered by the first brush was expanded using routine methods (Lechner, J. F. and M. A. LaVeck. *J. Tissue Culture Methods 9*: 43, 1985). Briefly, after the cells were removed from brushes by brisk shaking, they were inoculated into 60 mm fibronectin-coated culture dishes and incubated in BEGM medium (Clonetics®) at 37°C in a 3% carbon dioxide/97% air atmosphere. The efficiency of culturing these samples has been 100% to date. The individual cultures were grown until they were 80% confluent, and then they were passaged. These

*Pulmonary Department, University of New Mexico, and Veterans Administration Medical Center, Albuquerque, New Mexico

**New Mexico Tumor Registry and Department of Medicine, University of New Mexico, Albuquerque, New Mexico

cultures could be maintained for up to nine passages (a minimum of 16 population doublings), and many underwent 30 divisions before senescence. Prior to subculturing, aliquots of cells were cryopreserved (Lechner and LaVeck, 1985). In addition, samples of cells were fixed in methanol-acetic acid (3:1) for interphase FISH. The bronchial epithelial cells obtained through bronchoscopy were evaluated for trisomy 7 by hybridization with a biotinylated chromosome 7 centromere probe (Oncor). The hybridized probe was detected with fluorescein-labeled avidin, and the cell nucleus was visualized by staining with propidium iodide. Optimized hybridization conditions were established using cell lines which exhibit trisomy 7. To maintain quality control, 20% of all slides were scored by two trained technologists; their results differed by > 0.4%.

Before analyzing the cells from the uranium miners, it was necessary to empirically determine the experimental background rate of chromosome abnormalities in cultured normal human epithelial cells. This was accomplished using the cells established into culture at autopsy from four people who were never-smokers, and the bronchial epithelial cells obtained by bronchoscopy from the never-smokers. The age of donors for this study ranged from 6–45 y. The results were that only 1.4 ± 0.4% (SD) of 400 cells/sample contained three hybridization signals for chromosome 7. The effect of cell culture on chromosome aberration frequency was also pre-evaluated by examining the frequency of trisomy 7 at passages 1, 4, and 7; the value did not differ as a function of passage. Based on these results, the percentage of cells possessing trisomy 7 were > 2 standard deviations above the mean of the controls, i.e., > 2.2% are considered as significantly different (positive) from the controls.

The analyses to date for trisomy 7 of cells from multiple sites from the first seven clinically cancer-free ex-uranium miner volunteers are presented in Table 1. Four of these individuals had significant numbers of cells in their bronchial cell cultures that contained three copies of chromosome 7, although cytopathology did not detect any atypia in three of these people. The frequency for positive trisomy 7 has ranged from 2.5–3.3%. While these values are low, they are clearly statistically different from controls. Moreover, trisomy 7 was frequently observed at multiple sites throughout the bronchial tree, suggesting the presence of an extensive ongoing field cancerization. Ultimately, a total of 75 participants having habitual cigarette usage of at least 10 pack years and extensive radon exposure will be recruited into this project. The data obtained on these volunteers will be compared with 25 control participants who were never employed in the mining industry and never smoked. Informed consent documentation has and will precede all clinical procedures. These volunteers will also complete a questionnaire published by the American Thoracic Society (Ferris, B. G. *Am. Rev. Respir. Dis. 118*: 118, 1978) that will provide information reflecting smoking habits and levels of radon daughter exposures. The questionnaire is administered by personnel specifically trained in interviewing skills.

The underlying significance of the current effort confirms the hypothesis that chronic exposure to high concentrations of α-particles and tobacco smoke produces genetically altered lung epithelial cells throughout the respiratory tract of some susceptible individuals before they develop clinical disease. Further significance is the demonstration that these aberrant cells occur in sufficient frequency to permit the identification of this subgroup of people. Ultimately, these studies will identify which individuals should be at greatest risk for developing cancer. The results of these investigations will also provide the foundation for initiating a prospective study to monitor these ex-uranium miners (as well as heavy smokers and other high-risk groups) throughout their life spans to affirm, by prospective study criteria, the efficacy of screening for presence of cells with genetic alterations to accurately identify high-risk people. Furthermore, the results will facilitate the future use of defined markers to assess the efficiency of lung cancer risk reduction through interventions such as smoking cessation or chemopreventation.

Table 1

Analysis of Bronchial Epithelial Cells Recovered from Uranium Miners for Evidence of Trisomy 7

Case No.	Age	Smoking (pack y)	Exposure (WLM)	Brush Location[a]	Trisomy 7 (%)	Cytological Diagnosis
1	59	7.5	27.1	LLL	3.0[b]	Negative
				LUL	3.0[b]	Negative
2	65	9	515.5	LUL	1.3	Negative
				RUL	3.3[b]	Negative
3	64	30	235.1	LUL	1.5	Negative
				RLL	1.0	Negative
4	56	0	186.1	LUL	2.0	Negative
				RLL	2.3[b]	Negative
5	64	0	214.2	RLL	1.8	Hyperplasia
6	64	9	577.2	LUL	1.8	Negative
				RLL	0.8	Hyperplasia
7	67	30.75	123.7	LLL	1.3	Hyperplasia
				LUL	2.8[b]	Hyperplasia
				RLL	2.5[b]	Hyperplasia
				RUL	3.3[b]	Hyperplasia

[a]RLL = Right Lower Lobe; RUL = Right Upper Lobe; LLL = Left Lower Lobe; LUL = Left Upper Lobe.

[b]$p < 0.05$ as compared to cells from never-smokers.

(Research at ITRI sponsored in part by NIH SPORE Contract No. 1-P50-CA58184, through Johns Hopkins University, and by the U.S. Department of Energy, under Contract No. DE-AC04-76EV01013.)

INCREASED POLYSOMY OF CHROMOSOME 7 IN BRONCHIAL EPITHELIUM FROM PATIENTS AT HIGH RISK FOR LUNG CANCER

*Steven A. Belinsky, Robin E. Neft, John F. Lechner, and Richard E. Crowell**

Current models of carcinogenesis (i.e., colon cancer, Fearon, E. R. and B. Vogelstein. *Cell 61*: 759, 1990) suggest that tissues progress through multiple genetic and epigenetic changes which ultimately lead to development of invasive cancer. Epidemiologic studies of Peto, R. R. and J. A. Doll (*The Causes of Cancer: Quantitative Estimates of Avoidable Risks of Cancer in the United States Today.* Oxford University Press, NY, 1961) indicate that the accumulation of these genetic changes over time, rather than any single unique genetic change, is probably responsible for development of the malignant phenotype. The bronchial epithelium of cigarette smokers is diffusely exposed to a broad spectrum of carcinogens, toxicants, and tumor promoters contained in tobacco smoke. This exposure increases the risk of developing multiple, independent premalignant foci throughout the lower respiratory tract that may contain independent gene aberrations. This "field cancerization" theory is supported by studies that have demonstrated progressive histologic changes distributed throughout the lower respiratory tract of smokers. A series of autopsy studies (Auerbach, O. *N. Engl. J. Med. 265*: 253, 1961) demonstrated that cigarette smokers exhibit premalignant histologic changes ranging from hyperplasia and metaplasia to severe dysplasia and carcinoma *in situ* diffusely throughout the bronchial mucosa. The proximal bronchi appear to exhibit the greatest number of changes, particularly at bifurcations (Auerbach, 1961).

Recent pathologic studies suggest that genetic abnormalities also occur throughout the bronchial epithelium of lung cancer patients. Mutations in the p*53* gene have been observed in dysplastic bronchial epithelial cells microdissected from areas adjacent to lung tumors (Sundaresan, V. *et al. Oncogene 7*: 1989, 1992; Nyorva, K. *et al. Am. J. Pathol. 142*: 725, 1993; Sozzi, G. *et al. Cancer Res. 52*: 6079, 1992; Bennett, W. P. *et al. Cancer Res. 53*: 4817, 1993). Loss of heterozygosity on chromosome 3p has also been reported in bronchial epithelium exhibiting mild and severe dysplasia recovered from areas in close proximity to the tumor mass (Sundaresan *et al.*, 1992). A recent study suggests that genetic abnormalities can be found in histologically normal airway cells (Pastorino, U. *et al. J. Cell Biochem. [Suppl.] 17F*: 237, 1993). Examination of normal bronchial epithelium in the proximal airways of lungs resected from patients with lung cancer showed that 46% of the samples contained genetic changes, mostly involving simple rearrangements of chromosomes 3p, 7, 9, 11, and 17 (Pastorino *et al.*, 1993). Together, these studies have identified specific chromosome alterations that occur frequently in lung cancer and have also suggested that some alterations may be candidates for markers of premalignancy.

Trisomy 7 has been observed in 50% of non-small-cell lung cancers (NSCLCs) (Testa, J. *et al. Cancer Res. [Suppl.] 52*: 2702, 1992). Moreover, trisomy 7 has been detected in premalignant lesions such as villous adenoma of the colon (Reichmann, A. *et al. Cancer Genet. Cytogenet. 7*: 51, 1982), colonic mucosa from individuals with familial polyposis, and in the far margins from some resected lung tumors (Lee, J. S. *et al. Cancer Res. 47*: 6349, 1987), suggesting that an extra copy of chromosome 7 may play a role in the early stages of neoplastic development in some tumors. Although the molecular mechanism whereby this extra chromosome provides a growth advantage is unknown, the minimal region of overlap on chromosome 7 harbors the protooncogenes EGFR and Met, and the gene products of both of these loci are frequently over-expressed in human lung tumor cells

*Pulmonary Department, University of New Mexico, and Veterans Administration Medical Center, Albuquerque, New Mexico

(Testa *et al.*, 1992). The purpose of this investigation was to determine the frequency of trisomy 7 in bronchial epithelium from people at risk for lung cancer.

Ten current smokers were recruited; all were enrolled while undergoing evaluation for possible lung cancer. Samples were collected during diagnostic bronchoscopies in 8 of 10 patients with tumors, and during thoracic procedures in the other two subjects. Samples were also collected from five subjects having no evidence of lung cancer. Bronchial cells were obtained from two people during diagnostic bronchoscopy and from the other three people during thoracic procedures. Two of the five people without evidence of lung cancer were never-smokers. Two of the five people were ex-smokers, stopping 2 and 30 y prior to enrollment, with 51 and 15 pack y of prior smoking history, respectively. The other nontumor patient enrolled was a current smoker (24 pack y). Bronchial epithelial cells derived at autopsy by Clonetics, Inc. (San Diego, CA) from four never-smokers were also obtained to serve as additional controls.

The protocol developed for harvesting viable bronchial epithelium from the lower respiratory tract entails brushing the bronchial mucosa with a standard cytology brush during bronchoscopy. Informed consent was obtained before bronchoscopy was begun. When the bronchoscope was introduced into the lower respiratory tract, it was directed into each upper and lower lobe, and the carinal margin of a segmental orifice was identified for brushing. These sites were chosen because: (1) they are high deposition areas for particles, (2) they are frequently associated with histologic changes in smokers, and (3) they represent sites where tumors commonly occur (Auerbach, 1961; Ishikawa, Y. *et al. Cancer Res. 54*: 2342, 1994). The area was washed with saline to remove any nonadhered cells, a brush was introduced through the bronchoscope, and the area was brushed. The brush was withdrawn, immediately placed in serum-free medium, and kept on ice during transportation to the tissue culture laboratory. The process was repeated with another brush for a total of two brushes at each site.

Replicative cultures of the bronchial epithelial cells obtained by the bronchial brushing procedure described above were established in our laboratory using a serum-free medium (Bronchial Epithelium Growth Medium, BEGM; Clonetics, Inc.). Cells were removed from brushes by brisk shaking, washed, resuspended in BEGM, then added to 60 mm fibronectin-coated culture dishes, and cultured at 37°C in an atmosphere of 21% oxygen, 3% carbon dioxide. The efficiency of obtaining cultures from these samples was 100%. The serum-free medium used for these cultures was optimal for growth of bronchial epithelial cells and did not support growth of fibroblasts. Cells at passage 1 were fixed in methanol-acetic acid for interphase fluorescence *in situ* hybridization used to detect trisomy of chromosome 7. Trisomy 7 was determined by hybridization of cells with a biotinylated chromosome 7 centromere probe (Oncor, Gaithersburg, MD) and detected with fluorescein-labeled avidin. The cell nucleus was visualized by staining with propidium iodide.

In current smokers with lung cancer, 37% of the samples exhibited cytologic abnormalities, mostly squamous metaplasia (Table 1). These cytologic changes were present in < 10% of the cells recovered from the diagnostic brush. Two subjects had three sites that exhibited cytologic abnormalities, and three subjects had no cytologic abnormalities at any site. No samples contained tumor cells by cytology, even though one of the four sites in four subjects was collected from the same lobe where a tumor was later diagnosed. In subjects without lung cancer, two of eight sites in ex-smokers were cytologically abnormal (both in the same person, Table 2) while no atypical cells were present in the eight sites from the two never-smokers. Bronchial cells obtained from the only current smoker (24 pack y) had no abnormal cytology. These results indicate that cytologically abnormal cells can be harvested from sites throughout the lower respiratory tract, and that these samples are not contaminated with malignant cells from lung tumors in other locations.

Table 1
Frequency of Trisomy 7 in Bronchial Epithelial Cells from Lung Cancer Patients

Case	Age	Smoking (pack y)	Tumor Diagnosis	Brush Location	Brush Diagnosis	Trisomy 7 (frequency, %)
1	64	104	ND	RLL	N	2.8[c]
				RUL	AGC	4.0[c]
				RLL[a]	N	3.0[c]
				RUL[a]	N	4.0[c]
				LLL[a]	N	6.0[c]
				LUL[a,b]	SM	4.3[c]
2	69	26	SCC	RUL	SM	2.8[c]
				LLL	SM	3.3[c]
				LUL	N	3.8[c]
3	65	120	SCC	RLL	AGC	2.0
				RUL	AGC	2.3[c]
				LLL	AGC	2.0
4	52	90	AC	RLL	SM	1.5
				RUL	N	1.8
				LLL	SM	1.5
				LUL	SM	1.8
5	70	50	SCC	RLL	N	1.5
				RUL	N	1.5
				LLL	N	1.5
				LUL	SM	1.3
6	61	93	AC	RLL	N	1.5
				RUL[b]	N	1.3
				LLL	N	2.0
				LUL	N	1.5
7	58	40	NSCLC	RLL	N	1.8
				RUL	N	2.3[c]
				LLL[b]	N	2.5[c]
				LUL	N	2.8[c]
8	59	120	AC	RLL	N	1.5
				RUL[b]	N	2.0
				LLL	N	2.5[c]
				LUL	AGC	2.0
9	65	71	NSCLC	RLL	SM	2.0
				RUL	SM	2.5[c]
10	63	45	AC	RLL	N	1.0
				RUL	N	1.8
				LLL	N	1.8
				LUL	N	1.3

ND, not determined; AGC, atypical glandular cells; SM, squamous metaplasia; N, normal cells; NSCLC, non-small-cell lung cancer; SCC, squamous cell carcinoma; AC, adenocarcinoma; RLL, right lower lobe; RUL, right upper lobe; LLL, left lower lobe; LUL, left upper lobe.
[a]Resampled 4 mo later.
[b]Tumor location.
[c]$p < 0.05$ as compared to never-smoker controls.

Table 2

Frequency of Trisomy 7 in Bronchial Epithelial Cells from Never-Smokers and Smokers

Case	Age	Smoking (pack y)	Brush Location	Brush Diagnosis	Trisomy 7 (frequency, %)
11	45	0	RLL	N	1.8
			RUL	N	1.0
			LLL	N	1.0
			LUL	N	1.3
12	35	0	RLL	N	1.0
			RUL	N	1.8
			LLL	N	1.5
			LUL	N	1.8
13	81	15	RLL	N	1.8
			RUL	AGC	1.5
			LLL	N	1.8
			LUL	SM	2.0
14	34	24	RLL	N	1.3
			RUL	N	1.3
			LLL	N	1.0
			LUL	N	1.3
15	68	51	RLL	N	4.0
			RUL	N	3.0
			LLL	N	4.3
			LUL	N	3.5

AGC, atypical glandular cells; SM, squamous metaplasia; N, normal cells; RLL, right lower lobe; RUL, right upper lobe; LLL, left lower lobe; LUL, left upper lobe

Background rates of trisomy 7 were determined by examining normal human bronchial epithelial cell lines (Clonetics, data not shown) obtained from autopsy cases of never-smokers and bronchial epithelium collected from never-smokers. In bronchial cell lines (passage 2) from four donors (Table 2) and bronchial epithelial cell samples obtained by bronchial brushing from the recruited never-smokers (Table 2), only 1.4 ± 0.4% (SD) of the cells (400 cells counted per sample) contained three hybridization signals for chromosome 7 with values ranging from 1–1.8%. This value has been used to establish the background levels for assessment of trisomy 7 positivity in smokers. This low background frequency of trisomy 7 in bronchial cells is comparable to values reported from the manufacturer (Oncor) and most likely stems from nonspecific hybridization of the probe.

Trisomy 7 frequencies of > 2.2% (> 2 SD above the mean for controls) were considered as significantly different from controls. Of the two ex-smokers, four of eight samples were positive for trisomy 7; all four of the samples were collected from different bronchial sites in the subject with 51 pack y of smoking who quit 2 y prior to bronchoscopy. All of these samples were cytologically normal. In the current smoker without a tumor (24 pack-y history), no samples were positive for trisomy 7.

In studies to date, 12 of 35 (34%) samples cultured from 35 different bronchial sites contain trisomy 7 at frequencies > 2 SD above the mean for controls (Table 1). Six of the 10 smokers with lung cancer had one or more positive sites for trisomy 7. Two subjects (Cases 1 and 2) exhibited trisomy 7 in all samples collected during bronchoscopy. Five of the 12 positive trisomy 7 sites were associated with abnormal cytology. One patient with all sites positive for trisomy 7 (Case 1) required repeated bronchoscopy for clinical reasons. In the two sites in which cells were collected during both bronchoscopies, trisomy 7 was similarly increased in both samples, even though cytology in the first sample showed atypical cells and in the second was normal (Table 1). The other two sites collected during the second bronchoscopy also showed elevated frequencies of trisomy.

These results indicate that chromosome aberrations can be detected in bronchial epithelial cells collected from smokers with lung cancer distant from the tumor site and that bronchial epithelial cells expanded through tissue culture are a useful resource for identifying these genetic alterations. These data also indicate that evidence of premalignancy through detection of genetic changes may be more sensitive than identifying cytologic abnormalities. The percentage of people with bronchial cells containing trisomy 7 was similar to prevalences reported in NSCLCs (Testa *et al.*, 1992). Moreover, trisomy 7 was often observed at multiple sites throughout the bronchial tree of an individual, suggesting that individual inherent susceptibility may influence the type of chromosome alterations induced within the lower respiratory tract. The detection of trisomy 7 in an ex-smoker with a high number of pack-years indicates that gene alterations are both present and detectable in bronchial epithelial cells from persons without lung cancer.

The results described are the first to quantitate the frequency for a chromosome aberration in "normal" bronchial epithelial cells. Previous studies (Pastorino *et al.*, 1993) have looked at chromosome rearrangements in normal bronchial epithelial cells but did not indicate the frequency for the changes observed. The frequency for trisomy 7 at sites positive ranged from 2.3–6%. While these values are low, they are clearly statistically different from controls. The fact that the cells harvested from the bronchial epithelium have abnormal cytology in < 10% of the cells or appear normal is consistent with our detecting chromosome abnormalities at frequencies < 10%. The detection of trisomy 7 in normal bronchial epithelium suggests that this chromosome alteration may be useful as a biomarker for identifying those individuals at highest risk for lung cancer.

(Research sponsored by the Office of Health and Environmental Research, U.S. Department of Energy, under Contract No. DE-AC04-76V01013.)

FEASIBILITY OF USING FLUORESCENCE *IN SITU* HYBRIDIZATION (FISH) TO DETECT EARLY GENE CHANGES IN SPUTUM CELLS FROM URANIUM MINERS

Robin E. Neft, Janice L. Rogers, Steven A. Belinsky,*
*Frank D. Gilliland**, Richard E. Crowell***, and John F. Lechner*

Epidemiological studies have shown that combined exposure to radon progeny and tobacco smoke produce a greater than additive or synergistic increase in lung cancer risk (Doll, R. *Epidemiology of Lung Cancer*, Vol. 74, Marcel Dekker, Inc., NY, 1994). Lung cancer results from multiple genetic changes over a long period of time. An early change that occurs in lung cancer is trisomy 7 which is found in 50% of non-small cell lung cancer and in the far margins of resected lung tumors. The 80% mortality associated with lung cancer is in part related to the high proportion of patients who present with an advanced, unresectable tumor. Therefore, early detection of patients at risk for tumor development is critical to improve treatment of this disease. Currently, it is difficult to detect lung cancer early while it is still amendable by surgery. Saccomanno, G. (*Diagnostic Pulmonary Cytology*, 2nd Ed., American Society of Clinical Pathologists Press, Chicago, 1986) has shown that premalignant cytologic changes in sputum cells collected from uranium miners can be detected by a skilled, highly trained cytopathologist. A more objective alternative for identifying premalignant cells in sputum may be to determine whether an early genetic change such as trisomy 7 is present in these cells. Fluorescence *in situ* hybridization (FISH) can be used to identify cells with trisomy 7.

FISH is a technique that labels chromosomes with specific fluorescent DNA probes. Probes are made by nick translating a cloned DNA sequence with a fluorescently labeled nucleotide. The double-stranded probe is then denatured and incubated with denatured DNA in sputum cells, allowing the probe to hybridize with the cellular DNA. The labeled chromosomes are visible with a fluorescence microscope using a fluorescein filter. The purpose of this study was to perform FISH on sputum samples collected in 1993 and 1995 from ex-uranium miners to determine the feasibility of using FISH to detect early gene changes in the sputum cells of individuals at risk of developing lung cancer.

Sputum samples were fixed in PreservCyt fixative (CYTYC Corporation, Marlborough, MA) and stored at 4°C. A cytospin was made using 75 µL of a sputum sample. The slide was observed under the fluorescence microscope to determine the cellularity, cell morphology, and amount of autofluorescence. Two slides were made from each sputum sample. One was untreated and one was pretreated with 0.1% $NaBH_4$ for 30 min or 2X Dulbecco's phosphate buffered saline (DPBS)/2% bovine serum albumin (BSA)/0.5% BRIJ detergent overnight. $NaBH_4$, a strong reducing agent, was used to attempt to decrease autofluorescence in the cells by reducing double bonds. The DPBS/BSA/BRIJ was used to facilitate mixing of the solutions, reduce surface tension, and increase the permeability of the membranes to the DNA probe.

Microscope slides were placed in denaturing solution (70% formamide) at 75°C for 3 min, then dehydrated in a series of 1 min ethanol washes, at concentrations of 70%, 85%, and 100%. Hybridization buffer, DNA probe for the centromere of chromosome 7 (VYSIS, Inc., Framingham, MA), and sterile water were mixed in a microcentrifuge tube, placed in a 75°C water bath for 5 min

*Department of Energy/Associated Western Universities Teacher Research Associate Program (TRAC) Participant
**New Mexico Tumor Registry and Department of Medicine, University of New Mexico, Albuquerque, New Mexico
***Pulmonary Department, University of New Mexico, and Veterans Administration Medical Center, Albuquerque, New Mexico

to denature the probe, and kept on a warming tray at 45–50°C until the slide was ready. Then 10 μL of probe mixture was applied to the slide. The slide was coverslipped, sealed with rubber cement to prevent drying, placed in a humidifying chamber, and incubated at 42°C overnight. The coverslip was then removed, and the slide was immersed in three washes of 50% formamide/2X saline sodium citrate (SSC) for 10 min each, then in 2X SSC for 10 min, and finally in 2X SSC/0.1%NP-40 for 5 min. All washes were done at 45–47°C. The slide was allowed to dry slightly in the dark, and the chromosomes were counterstained with 10 μL propidium iodide (PI).

Results are shown in Table 1. The general condition of the sputum samples collected in 1993 varied greatly. The sputum samples were heterogeneous with respect to cellularity and types of cells present. Some of the samples contained a high percentage of oral squamous epithelial cells, and other samples contained a variety of cells including macrophages. Sample quality was assessed by examining nuclear staining with PI and the effect of autofluorescence on signal intensity. In several samples, nuclei stained bright red with PI while others remained unstained. Intensity of the FISH signal did not correlate with other characteristics of the sputum samples such as autofluoresence. Pretreatment of the cells with $NaBH_4$ or DPBS/BSA/BRIJ had no effect on autofluorescence. In 11 of 14 cases that were pretreated and assayed for trisomy 7, the signal intensity decreased compared to the untreated sample. Of 14 untreated samples, signal was seen in 12 samples. Trisomy 7 was observed in two of five samples scored so far.

Additional samples were collected during May 1995. Three of these were from the patients who produced samples collected in 1993. FISH was performed on these samples in order to determine if it was easier to assay for trisomy 7 on fresh samples. In two of these cases, the signal intensity was good. There was no correlation between sputum quality or suitability for FISH in the 1993 and 1995 samples collected from the same patients.

The results of this investigation indicate that FISH may prove to be an accurate, efficient method to test at-risk individuals for genetic alterations in bronchial epithelial cells from sputum. Future studies will focus on obtaining data on the frequency of trisomy 7 in sputum samples from uranium miners with intensely fluorescing FISH signal.

Table 1
Fluorescence *In Situ* Hybridization (FISH) for Chromosome 7 on Sputum Cells

Sample	Date Collected	Cellularity, Morphology	Autofluo-rescence	Treatment	FISH Untreated	FISH Treated
919 IR147	93	oral low, mac low, cell low	low	0.1% $NaBH_4$ overnight	ns high, sig low	ns none, sig none
909 IR106	8/31/93	oral high, mac none, cell low	low	0.1% $NaBH_4$ 30 min	ns med, sig none	ns none, sig low
910 IR125	8/26/93	oral med, mac med, cell high	low-med	0.1% $NaBH_4$ 30 min	ns low, sig low	ns high, sig none
911 IR107	8/27/93	oral high, mac none, cell high	low-med	0.1% $NaBH_4$ 30 min	ns low, sig low	ns low, sig none
912 IR119	8/30/93	oral high, mac low, cell med	low	0.1% $NaBH_4$ 30 min	ns none, sig low	ns med, sig none
1271 IR119	5/95	oral high, mac low, cell high	high	none	ns none, sig none	not done
921 IR142	93	oral low, mac high, cell high	low-med	none	ns high, sig high	ns high, sig low
639 IR143	93	oral high, mac none, cell high	low	none	ns high, sig high	ns high, sig high
914 IR131	8/26/93	oral low, mac high, cell high	low	2X DPBS + 2% BSA + 0.5% BRIJ overnight	ns high, sig high	ns low, sig none
1267 IR131	5/95	oral low, mac low, cell high	high	none	ns med, sig med	not done
915 IR138	8/26/93	oral high, mac none, cell high	very low	none	ns high, sig low	ns none, sig none
917 IR141	93	oral low, mac high, cell high	high	none	ns high, sig low	ns none, sig low
1276 IR141	5/95	oral high, mac med, cell high	high	none	ns none, sig none	not done
918 IR146	9/14/93	oral low, mac none, cell med	med	none	ns low, sig low	ns none, sig none
920 IR108	8/27/93	oral high, mac none, cell high	low-med	none	ns none, sig none	ns low, sig none
641 IR85	8/16/93	oral low, mac none, cell low	low	none	ns high, sig high	ns high, sig high
225 IR133	93	oral med, mac none, cell med	low	none	ns high, sig high	ns med, sig med
1275 IR77	5/95	oral high, mac low, cell high	high	none	ns none, sig none	not done
1279 IR414	5/95	oral high, mac low, cell high	med	none	ns low, sig med	not done

oral = oral cells; mac = macrophage cells; cell = cellularity; ns = nuclear stain; sig = signal; med = medium

(Research sponsored by the Office of Health and Environmental Research, U.S. Department of Energy, under Contract No. DE-AC04-76EV01013.)

RADIATION-INDUCED p53 PROTEIN RESPONSE IN THE A549 CELL LINE IS CULTURE GROWTH-PHASE DEPENDENT

Neil F. Johnson, Debbie M. Gurulé, and Thomas R. Carpenter***

One role of the p53 tumor suppressor protein has been recently revealed. Kastan, M. B. *et al.* (*Cancer Res. 51*: 6304, 1991) reported that p53 protein accumulates in cells exposed to ionizing radiation. The accumulation of p53 protein is in response to DNA damage, most importantly double-strand breaks, that results from exposure to ionizing radiation (Lu, X. and D. P. Lane. *Cell 75*: 765, 1993). The rise in cellular p53 levels is necessary for an arrest in the G_1 phase of the cell cycle to provide additional time for DNA repair (Kastan *et al.*, 1991). The p53 response has also been demonstrated to enhance PCNA-dependent repair (Smith, M. L. *et al. Science 266*: 1376, 1994). p53 is thus an important regulator of the cellular response to DNA-damaging radiation.

The cell-cycle phase of cells in culture varies as cell numbers increase. The change in the cell-cycle profile of the logarithmic, early-plateau, and late-plateau phases of culture growth suggests that cell-cycle-related responses may also change with culture growth phase. This project sought to determine if the growth phase of cultured cells exposed to ionizing radiation alters the p53 response to DNA damage.

The A549 cell line, known to possess wild-type copies of the p53 gene (Lehman, T. A. *Cancer Res. 51*: 4090, 1991), was incubated at 36.5°C with 5% CO_2 in RPMI 1640 media supplemented with 10% fetal bovine serum, 2 mM L-glutamine, and 50 mg/mL gentamicin. Cells used were limited to passages 76–80. Culture media were exchanged with fresh media 24 h prior to X-ray exposure. Cells in tissue culture flasks were exposed to X rays produced by a Phillips RT 250 Radiotherapy Unit (Philips Medical Systems, Shelton, CT) at 250 kV at ~ 0.8 Gy/min with a 0.5 mm Cu filter. All exposures were performed at room temperature (≈ 21°C). After exposure, cells were harvested by trypsinization at predetermined intervals, rinsed in Dulbecco's phosphate buffered saline (DPBS), fixed, and stored in 70% methanol at –20°C. Cells were immunostained for p53 using clone DO-1 antibody (Oncogene Sciences, Uniondale, NY) and were analyzed by flow cytometry as described previously (Hickman, A. W. *et al. Cancer Res. 54*: 5797, 1994). The percentages of positively stained cells were determined by the channel subtraction method using the CellQuest program (Becton Dickinson, San Jose, CA). Cell-cycle status was determined by staining with 25 µg/mL propidium iodide in DPBS containing 100 µg/mL RNAase A (Hickman *et al.*, 1994) and analyzed by using the MacCycle program (Phoenix Flow Systems, San Diego, CA).

The number of cells that contained elevated p53 protein after 4 Gy X-irradiation increased in all three phases of growth (Fig. 1). The magnitude of the p53 protein response was similar in all three phases of growth as well, with around 20% positive cells at the peak of the initial response. However, the duration of the initial p53 protein response diminished in the later phases of cell growth. The p53 response in logarithmic phase cells lasted through 36 h post irradiation. The response in the early-plateau phase appeared to last through 12 h post irradiation, while the late-plateau phase lasted only 6 h. Additional peaks of p53-positive cells followed the initial peak, though lesser in magnitude.

---

*Minority Student Research Participant
**UNM/ITRI Graduate Student

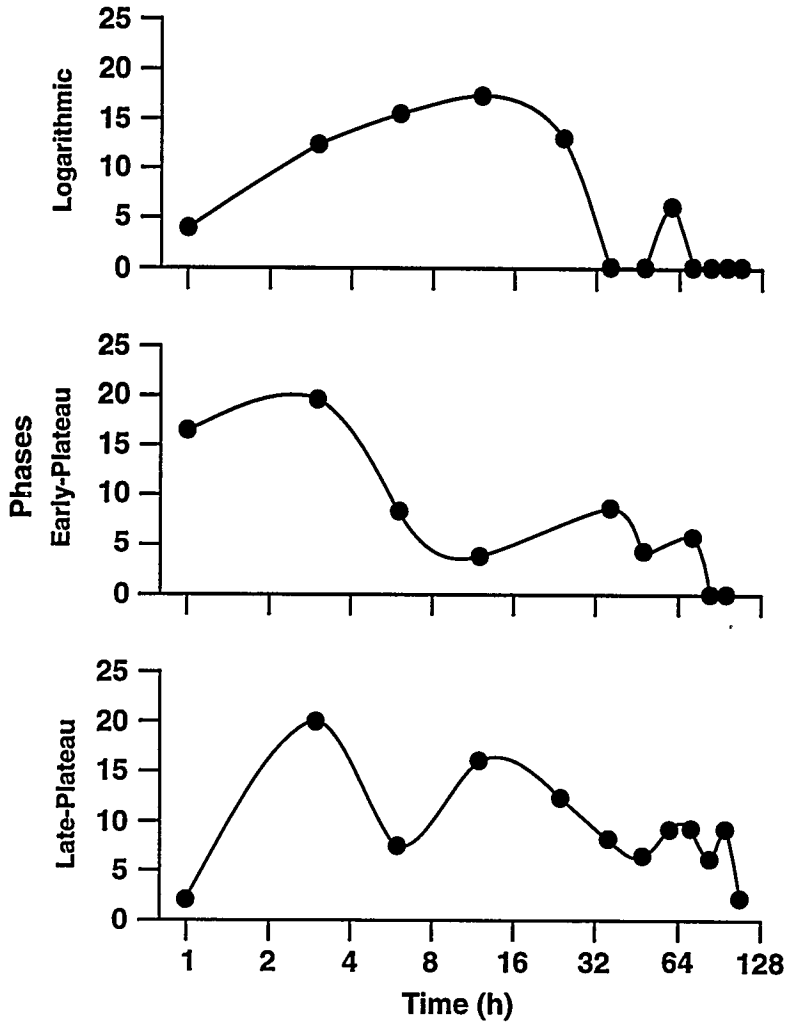

Figure 1. Percentage of p53-positive cells after 4 Gy X rays have increased p53 staining compared to unirradiated control cells at time of exposure. Data from a single experiment.

In order to compare p53 protein response with cell-cycle events, DNA content was measured at the same time intervals after 0 and 4 Gy X-irradiation. The percentages of cells with G_1/G_0 DNA content differed in the three phases of growth (Fig. 2). In the later phases, unirradiated cell culture contained a higher percentage of cells in G_1 associated with growth inhibition. In logarithmic phase cells, the percentage of G_1 cells fell initially in the exposed group, accompanied by a rise in G_2/M cells due to arrest in G_2 (data not shown). However, the percentage of G_1 cells rose sharply at 12 h, indicating G_1 arrest. The increase in G_1 cells was accompanied by an equally sharp decline in S phase cells (data not shown). At later times, the percentage of G_1 cells continued to rise at a slower rate, presumably due to growth inhibition as demonstrated in control cells. While there was a noticeable increase in G_1 phase cells in irradiated early-plateau phase cells, no such increase was noted in late-plateau phase cells.

From these data, it can be concluded that the magnitude of the p53 response is not dependent on the phase of culture growth. Rather, the p53 response is related to dose (Kastan *et al.*, 1991; Hickman *et al.*, 1994). However, the temporal course of the p53 response does appear to be determined by culture growth phase. Radiation-induced arrest in G_1 also appears to be culture growth-phase dependent. Radiation-induced G_1 arrest is demonstrated in logarithmic phase cells that also

possess a substantially longer period of p53 response than later culture growth phases. Also, the initiation of radiation-induced arrest in G_1 coincides with the peak of the p53 response. The earlier peak of the p53 response in later phases of growth may precede other cell-cycle regulatory events necessary for radiation-induced arrest in G_1. It is noteworthy that p53 protein accumulates even when radiation-induced arrest is not evident. This supports the proposed role of p53 in the enhancement of DNA repair. However, the increased p53 levels in irradiated plateau-phase cells may only represent a failed attempt to alter cell cycling, or may indicate a role for p53 S-phase and G_2-phase regulation after radiation (data not shown). This project supports the concept of a role for the p53 response in each phase of culture growth; however, the capacity for p53-dependent G_1 arrest is culture growth-phase dependent. This work further illustrates the importance of growth phase in experiments involving cell-cycle regulation.

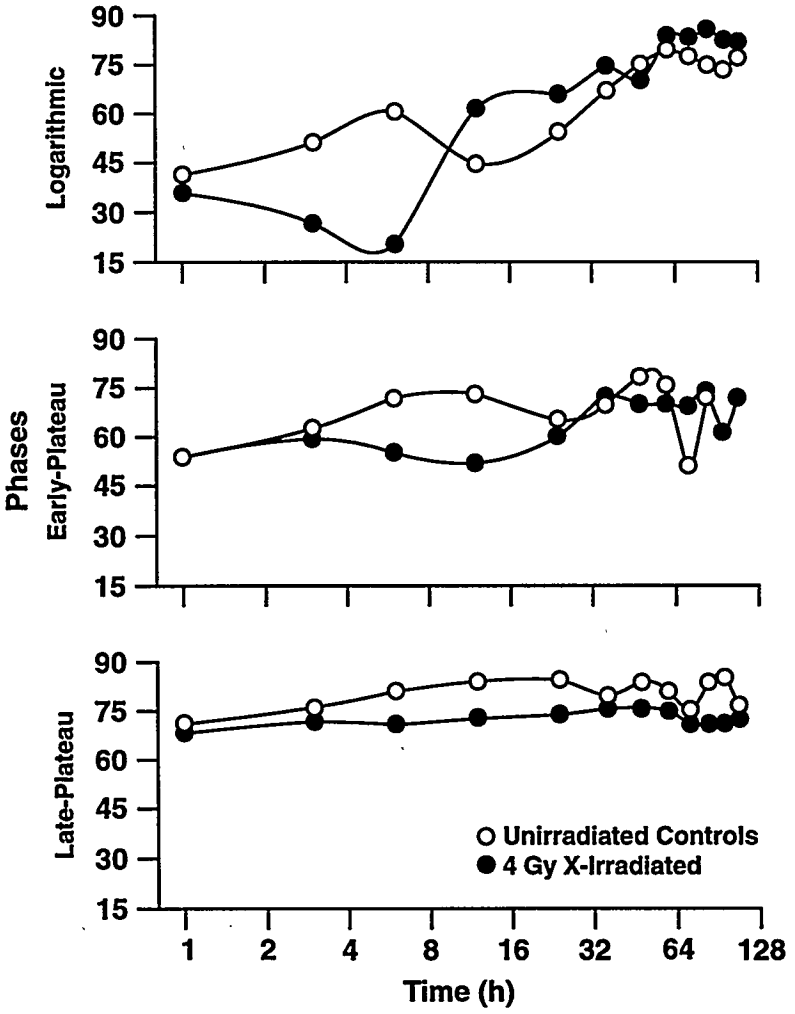

Figure 2. Percentage of cells in G_1 phase of cell cycle. Data from a single experiment.

(Research sponsored by the Office of Health and Environmental Research, U.S. Department of Energy, under Contract No. DE-AC04-76EV01013.)

INDIVIDUAL VARIATION IN p53 AND Cip1 EXPRESSION PROFILES IN NORMAL HUMAN FIBROBLAST STRAINS FOLLOWING EXPOSURE TO HIGH-LET RADIATION

Thomas R. Carpenter, Neil F. Johnson, Frank D. Gilliland**, John F. Lechner, Susan E. Phillips, and William A. Palmisano*

Exposure to α-particles emitted by radon progeny appears to be the second-leading cause of lung cancer mortality (Lubin, J. H. *et al. J. Natl. Cancer Inst. 87*: 817, 1995). However, individual susceptibility to the carcinogenic effects of α-particles remains poorly characterized. Variation in susceptibility to cancer produced by certain classes of DNA-damaging chemicals is suspected to involve differences in metabolic activation (Kouri, R. E. *et al. Cancer Res. 42*: 5030, 1982; Uematsu, F. *et al. Jpn. J. Cancer Res. 82*: 254, 1991) and detoxication (Seidergard, J. *et al. Proc. Natl. Acad. Sci. USA 85*: 7293, 1988). Susceptibility to α-particle-induced cancer may involve variations in capacity or opportunity to repair DNA damage. Heritable diseases involving DNA repair processes including xeroderma pigmentosum (Robbins, II., J. *et al. Ann. Intern. Med. 80*: 221, 1974) and ataxia-telangiectasia (Hecht, F. *et al. Lancet 2*: 1193, 1966) are associated with increased cancer incidence. However, only 0.5–1% of cancers are thought to be due to heritable disease (Easton, D. F. *Br. Med. Bull. 50*: 527, 1994). Subtle variations in DNA repair capacity would more likely explain radon-related lung cancer susceptibility. The p53 tumor suppressor protein accumulates as a cellular response to DNA damage from ionizing radiation and regulates arrest in the G_1 portion of the cell cycle (Kuerbitz, S. J. *et al. Proc. Natl. Acad. Sci. USA 89*: 7491, 1992). Arrest in G_1 is thought to provide additional time for DNA repair prior to replication in S phase (Lu, X. and D. P. Lane. *Cell 75*: 765, 1993). Congenital mutation of one copy of the p53 gene results in increased cancer susceptibility; however, such mutations are relatively rare events (Malkin, D. *et al. Science 250*: 1233, 1990). While upstream regulation of p53 protein stability is poorly understood, variations in the ability to accumulate p53 following DNA damage represent potential variations in lung cancer susceptibility related to radon progeny. Further, transcription of the cell-cycle regulatory gene Cip1 is regulated by p53 and increases following ionizing radiation (Dulić, V. *et al. Cell 76*: 1013, 1992). Cip1 protein binds cyclin/cdk complexes, inhibiting kinase activity required for entry to S phase, and thereby causes arrest in G_1 (Zhang, H. *et al. Genes Dev. 8*: 1750, 1994). Therefore, variations in the expression of Cip1 following α-particle exposure may also be a susceptibility factor in radon-related lung cancers. The purpose of the present investigation was to measure p53 and Cip1 protein induction following α-particle exposure of fibroblast lines from nine individuals to determine if there were significant variations.

As an initial screening, variation in the p53 response was examined in third passage fibroblast cultures obtained from nine neonatal foreskin samples (surgical waste). The resulting fibroblast lines were grown on 1.5 μm Mylar® and were exposed to 0.25 Gy of α-particles from an electroplated ^{238}Pu source. Three populations were identified by flow cytometry as having statistically different mean percentages of p53-positive cells (ANOVA $p < 0.05$). The three groups were labeled as low responders ($n = 3$, $\bar{X} = 1\% \pm 3.4\%$), moderate responders ($n = 5$, $\bar{X} = 11.8\% \pm 4.6\%$), and high responders ($n = 1$, $\bar{X} = 27.3\% \pm 1\%$) (Fig. 1).

Each fibroblast line was then exposed to graded doses of α-particles and harvested 6 h after exposure. Immunostaining for p53 revealed a positive dose-response relationship in each moderate-

*UNM/ITRI Graduate Student

**New Mexico Tumor Registry and Department of Medicine, University of New Mexico, Albuquerque, New Mexico

responder cell line. The high-responder cell line demonstrated a relatively sensitive p53 response that reached maximal at 0.5 Gy, but did not increase with further increases in dose. The low-responder cell lines failed to accumulate protein at doses < 0.5, and one cell line (HFF10) possessed reduced levels of p53 protein at 2 Gy (data not shown).

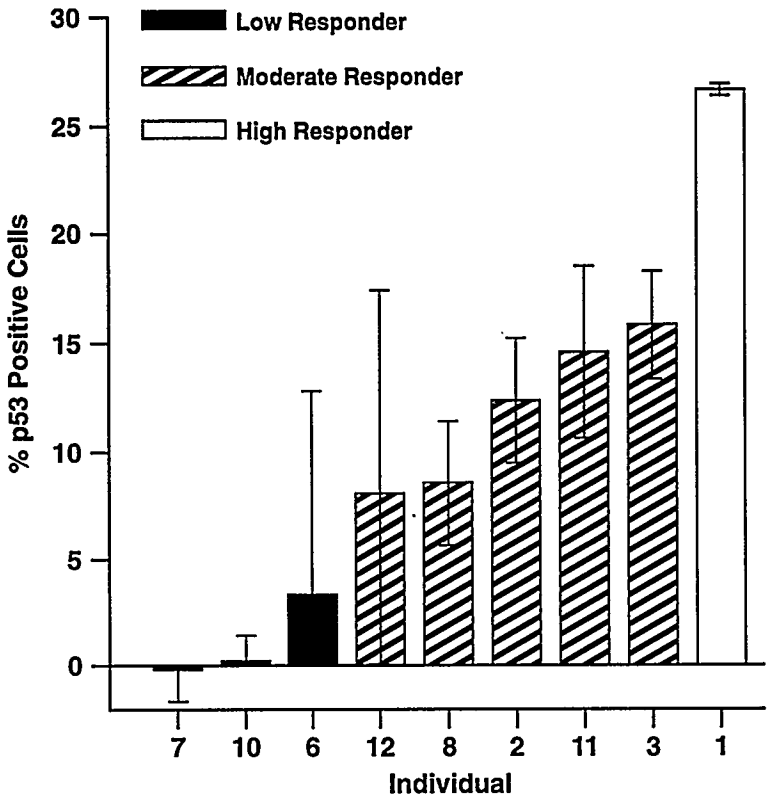

Figure 1. Flow cytometric determination of percent of cells with p53 protein levels above control levels 6 h following 0.25 Gy α-particle irradiation. Error bars represent the standard errors for three experiments.

Cip1 immunostaining of these cell lines revealed that the high responders and the low responders failed to demonstrate a significant increase in Cip1 protein (Fig. 2). Neither high nor low responders exceeded 10% Cip1 positive cells at 2 Gy, while moderate responders averaged 52%. Clonogenic survival following graded doses of α-particles were determined according to the methods of Puck, T. T. and P. I. Marcus (*J. Exp. Med. 103*: 653, 1956). No significant differences in clonogenic survival were observed among the low-, moderate-, or high-responder cell lines (data not shown).

These findings indicate that some differences exist among the cell lines in the p53-regulated response to α-particle-induced DNA damage. The p53 protein response at 0.25 Gy indicates three significantly different levels of response exist. The groups were designated as low, moderate, and high responders based upon p53 protein levels. The differences in p53 protein response among the cell lines are less distinct across a broader range of doses. However, the low responders did tend to have less sensitive responses than the moderate responders; specifically, a greater dose is required to cause a detectable accumulation of p53 protein. The insensitive p53 response of the low-responder group could indicate an inability to respond to low doses of α-particles or less DNA damage by low doses of α-particles. Because residential radon exposures occur at low concentrations, variations in the cellular response to low doses of α-particles may indicate important differences in the risk of lung cancer. The high responder appears to reach maximal response at lower doses than moderate

responders, which do not appear to reach a response plateau at 2 Gy. This cell line may be a sensitive responder or may indicate a greater level of DNA damage by low doses of α-particles.

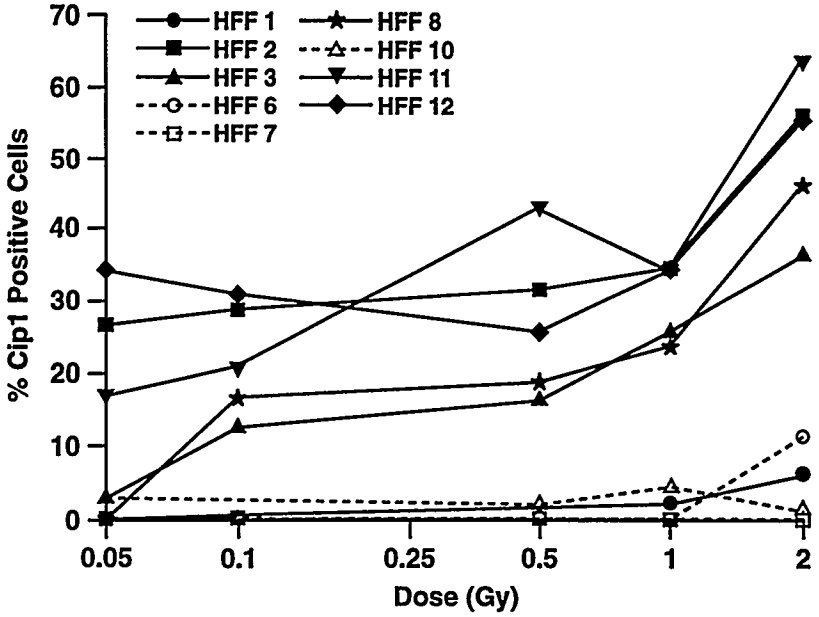

Figure 2. Flow cytometric measurement of percent of HFF cells with Cip1 protein levels above control levels 6 h following α-particle irradiation. Open symbols indicate low responders (○, □, △), closed symbols indicate moderate (■, ▲, ★, ▼, ♦) or high (●) responders. Data points reflect pooled samples from six separate exposures.

The expression of Cip1 protein indicates the differences in response are biologically relevant. Moderate responders demonstrate a dose-dependent increase in Cip1 staining following α-particle exposures. The low responders all failed to accumulate detectable levels of Cip1 protein at doses < 1–2 Gy. However, each cell line did accumulate some p53 protein at lower doses, indicating additional regulatory mechanisms must act to prevent the expression of Cip1 protein in these individuals. Failure to detect Cip1 expression among these individuals could be due to either a lack of Cip1 protein or the presence of a conformation not detected by the polyclonal Cip1 antibody. Lack of Cip1 protein may allow continued progression of G_1 phase cells to S phase, decreasing opportunity for repair. However, this lack of Cip1 expression is not reflected in decreased clonal survival. No significant differences in clonal survival are evident among the cell lines. The lack of difference in cell survival may indicate the p53 response is not a determinant of cell survival under these circumstances. Rather, diminished p53 response may determine the extent of sub-lethal damage that remains unrepaired, as suggested by the increased incidence of radiation-induced cancer in p53 nullizygous mice (Lee, J. M. *et al. Oncogene 9*: 3731, 1994). Decreased opportunity for repair due to diminished p53 and Cip1 response without reductions in survival may indicate a substantial risk factor for radon-induced lung cancer. However, further characterization of the types of p53 response to α-particles including mutational incidence is required before conclusions regarding lung cancer risk can be made.

(Research sponsored by the Office of Health and Environmental Research, U.S. Department of Energy, under Contract No. DE-AC04-76EV01013.)

A METHOD FOR DOUBLE-LABELING SPUTUM CELLS FOR p53 AND CYTOKERATIN

Robin E. Neft, Lauren A. Tierney, Steven A. Belinsky, Frank D. Gilliland**, Richard E. Crowell***, and John F. Lechner*

Molecular and immunological techniques may enhance the usefulness of sputum cytology as a screening tool for lung cancer. These techniques may also be useful in detecting and following the early progression of disease from metaplasia to dysplasia, carcinoma *in situ*, and finally to invasive carcinoma. Longitudinal information on the evolution of these malignant changes in the respiratory epithelium can be gained by prospective study of populations at high risk for lung cancer.

In this investigation, the tumor suppressor gene p53 was initially selected as a potential marker for detection of lung cancer and preneoplastic disease. The nuclear overexpression, which results from a point mutation, leads to stabilization of the protein. This stabilized form of p53 can then be detected by immunohistochemistry (Iggo, R. *et al. Lancet 335*: 675, 1990). Further, p53 is the most frequent gene alteration in human epithelial cancers including lung cancer with up to 50% of non-small cell lung cancers and over 90% of small cell lung cancers having evidence of gene dysfunction (Chiba, I. *et al. Oncogene 5*: 1603, 1992). It is important to be able to identify which cells in a sputum sample are of epithelial origin. Cytokeratin staining of sputum samples identifies oral-pharyngeal cells and airway epithelial cells. Carcinomas, whether of primary or metastatic origin, can also be identified using broad specificity cytokeratin antibodies (Moll, R. *et al. Cell 31*: 11, 1982). The purpose of this study was to determine if sputum cells from people with or at risk of developing lung cancer could be double-labeled with antibodies to p53 and cytokeratins to facilitate the identification of neoplastic and preneoplastic cells.

Samples used to validate this procedure consisted of induced or spontaneously expectorated sputum obtained from individuals with diagnosis of lung cancer. Material was also collected from individuals whose smoking history (pack years) placed them at risk for lung cancer. Cytopathologic and histopathologic diagnoses (where applicable) were available on all specimens. SV40 large T-antigen immortalized human bronchial epithelial cells (BEAS-2B), which overexpress a stabilized form of p53 protein (Reddel, R. R. *et al. Cancer Res. 48*: 1904, 1988), were used as positive controls for dilution experiments with p53 and cytokeratin antibodies to optimize the staining procedure.

A 4–6 mL sample of sputum was rinsed twice with Dulbecco's phosphate buffered saline (DPBS) containing 0.1% BRIJ nonionic detergent (Sigma, St. Louis, MO) for 5 min followed by a 30 min wash on a laboratory shaker. All subsequent volumes were 1 mL, and all washes were conducted on a shaker. Cells were centrifuged, and the pellet was transferred to a 1.5 mL microcentrifuge tube. Antigen retrieval was accomplished by adding 1 mL of boiling citrate buffer (Citra Buffer, Biogenix, San Ramon, CA) to the tube which was then placed in a heating block at 100°C for 7 min. Samples were subsequently rinsed in deionized water followed by DPBS and were blocked for 30 min by adding 1 mL of DPBS that contained 5% normal horse serum and 0.2% bovine serum albumin (BSA) (Sigma). A human-specific monoclonal antibody to the p53 protein (DO-7, DAKO, Carpinteria, CA) was added at a 1:100 dilution in DPBS containing 0.2% BSA and placed on a shaker overnight at

*UNM/ITRI Graduate Student

**New Mexico Tumor Registry and Department of Medicine, University of New Mexico, Albuquerque, New Mexico

***Pulmonary Department, University of New Mexico, and Veterans Administration Medical Center, Albuquerque, New Mexico

4°C. A horse anti-mouse biotinylated secondary antibody (Vector, Burlingame, CA) was applied at a 1:200 dilution and incubated for 30 min. The cells were then washed twice for 5 min in 100 mM Tris-HCl (pH 8.2), and an alkaline phosphatase-conjugated streptavidin (Vector Elite Kit, Vector) was applied as per the manufacturers instructions. Subsequent washes were performed in 100 mM Tris-HCl (pH 8.2). The alkaline phosphate substrate Vector Red (Vector) was added with levamisol as recommended by the manufacturer and incubated on a shaker for 15 min at room temperature. Following staining for p53, the cells were washed twice in DPBS/BRIJ, then incubated with a anti-pancytokeratin monoclonal antibody cocktail (Sigma, clones C-11, PCK-26, CY-90, Ks-1A3, M20, A53-B/A2) at a 1:400 dilution for 1 h at 37°C. The monoclonal anti-pan cytokeratin antibody cocktail used in this study is broadly reactive to epitopes present in normal and neoplastic human epithelial cells. Following incubation with the primary antibody, the cells were washed in DPBS/BRIJ, incubated in a 1:32 dilution of fluorescein (FITC)-conjugated sheep anti-mouse IgG for 30 min at 37°C, and rinsed. Smears were made from the cell suspensions using Vectashield fluorochrome mounting media (Vector), protected from light, and stored at 4°C. FITC and Vector Red conjugate-immunolabeled cells were visualized by epifluorescence using a FITC excitation filter system (high-performance "IB" filter cube) and an Olympus BH-2 fluorescence microscope. The highly fluorescent Vector Red product was visualized as a bright red fluorescent precipitate. Use of fluorescence with the Vector Red substrate provides amplification over conventional light microscopy.

Double-labeling of positive control BEAS-2B cells was observed under fluorescent and white light. BEAS-2Bs contained bright red nuclei and green cytoplasm under fluorescent light and reddish-brown nuclei under white light. Sputum epithelial cells were also double-labeled for p53 and cytokeratin. The bright green cytoplasm and red nucleus, which are easily discernible, facilitate a rapid identification of p53-positive epithelial cells in sputum. In addition, the Vector Red substrate can be easily seen with white light. Neoplastic and dysplastic cells showing evidence of neoplasia or atypia (nuclear/cytoplasmic ratio, nuclear molding and irregular nuclear membrane) were identified. To date, in two cases that have been scored, there was concordance between p53-positive exfoliated cells in sputum and paraffin-embedded sections of surgically resected tumor from the same individual. The paraffin sections of tumor were positive for p53 expression, and the corresponding sputum contained epithelial cells with bright red nuclei.

Performing this procedure in suspension prevents the inadvertent transfer of cells from one specimen to another as occurs during routine slide processing (floaters) and the loss of cells diagnostic for neoplasia from slides. Further, in sparsely cellular samples, a number of samples from a patient can be combined. In addition, wash techniques to eliminate background and processing techniques can be performed using small volumes, antibody can be saved, and wash steps are more thorough. In suspension, most of the exposed surface area of the cells come in contact with antibody. Airway epithelial cells frequently dislodge as tissue fragments and are present in sputum as rafts of cells, several layers thick. Suspension labeling facilitates permeabilization of cells and provides access to antigenic sites by antibody.

This work is significant because double-labeling of cells in sputum with p53 and cytokeratin antibodies facilitates rapid screening of p53 positive neoplastic and preneoplastic lung cells by brightfield and fluorescence microscopy. This technique quickly confirmed the epithelial and histopathologic and/or morphologic nature of the cells by immunofluorescence. Ultimately, this procedure may be useful in the development of other molecular markers that define the progression to malignancy and may be beneficial as a screening technique for individuals at risk for developing lung cancer.

(Research sponsored by the Office of Health and Environmental Research, U.S. Department of Energy, under Contract No. DE-AC04-76EV01013.)

INVERSE RELATIONSHIP OF TUMORS AND MONONUCLEAR CELL LEUKEMIA INFILTRATION IN THE LUNGS OF F344 RATS

David L. Lundgren, William C. Griffith, and Fletcher F. Hahn

In 1970 the F344 rat, along with the $B6C3F_1$ mouse, were selected as the standard rodents for the National Cancer Institute Carcinogenic Bioassay Program for studies of potentially carcinogenic chemicals. The F344 rat has also been used in a variety of other carcinogenesis studies, including numerous studies at ITRI. A major concern to be considered in evaluating carcinogenic bioassay studies using the F344 rat is the relatively high background incidence of mononuclear cell leukemia (MCL) (also referred to as large granular lymphocytic leukemia, Fischer rat leukemia, or monocytic leukemia). Incidences of MCL ranging from 10 to 72% in male F344 rats to 6 to 31% in female F344 rats have been reported (Goodman, D. G. *et al. Toxicol. Pharmacol. 48*: 237, 1979; *Pathology of the Fischer Rat* [G. A. Boorman *et al.* eds.], Academic Press, San Diego, 1990; Chandra, M. and C. F. Frith. *Cancer Lett. 62*: 49, 1992).

Negative correlations in the incidences of MCL infiltration of the liver and hepatocellular foci and liver tumors have been reported in F344 rats used in 2 y cancer bioassay feeding studies with various chemical compounds (Haseman, J. K. *Fundam. Appl. Toxicol. 3*: 1, 1983; Lijinsky, W. *et al. Carcinogenesis 4*: 1189, 1983; Young, S. S. and C. L. Gries. *Fundam. Appl. Toxicol. 4*: 632, 1984; Haseman, J. K. *Risk Anal. 5*: 161, 1985; Harada, T. *et al. Vet. Pathol. 27*: 110, 1990). Haseman (1983) raised the question as to how bioassay data should be interpreted because the presence of MCL apparently lowers the incidence of liver lesions. One suggestion was that rats with MCL be censored when data from studies of the effects of ingested compounds on altered hepatocellular foci are evaluated (Harada *et al.*, 1990).

The purpose of this study was to determine if there was a correlation between the presence of MCL infiltration in the lungs and a lower incidence of primary and metastatic lung tumors in F344 rats from studies conducted at ITRI. The hypothesis was, that if MCL correlated with a lower incidence of hepatocellular foci and liver tumors in the F344 rat, there would also be a similar correlation of the incidence of lung tumors.

Male and female F344/Crl rats (3571) reared at this Institute (F344/Crl-ITRI) and used in several life-span radiation carcinogenesis studies (Table 1) were evaluated to determine if MCL infiltration of the lung correlated with a decreased incidence of lung tumors. The extent of MCL in the rats in these studies ranged from just the beginning proliferation of leukemic cells in the spleen to severe infiltration of other organs, primarily the liver and lung. For this evaluation, only rats with early to severe MCL infiltration of the lung were considered. First, the dose-response relationships of the crude incidence of lung tumors in rats with and without MCL infiltration of the lung were compared using single exponential functions fitted to the data. Because this comparison does not take into account when the MCL infiltration occurred in relation to the lung tumors, a second method using a case-control analysis was used. Using this method, the proportion of rats with MCL was compared between rats with lung tumors to rats without lung tumors matched by sex, age at death, and radiation dose to the lung. Both primary lung tumors (432 rats with tumors) and tumors that had metastasized from elsewhere in the rats to the lung (175 rats with metastatic tumors) were evaluated. The incidences of rats with MCL infiltration of the lung in rats with and without lung tumors were compared using Fisher's exact test.

Table 1

Case-Control Analyses of Lung Tumors in Young Adult Male and Female F344/Crl-ITRI Rats Exposed by Inhalation to Radioactive Aerosols and Control Rats with or Without Mononuclear Cell Leukemia (MCL) Infiltration of the Lung

Type of Exposure and Study[a]	Total Number of Rats per Study	Rats with Primary Benign or Malignant Lung Tumors and Matching Controls[b]			Rats with Metastatic Tumors in Lungs and Matching Controls		
		MCL+ Rats per Number with Tumors (%)	MCL+ Rats per Number without Tumors (%)	Statistical Difference (p)[c]	MCL+ Rats per Number with Tumors (%)	MCL+ Rats per Number without Tumors (%)	Statistical Difference (p)[c]
Controls[d]	845	5/18 (28)	9/18 (50)	0.15	2/51 (4)	15/51 (29)	0.00046
$^{144}CeO_2$:							
Single	180	1/21 (5)	12/21 (57)	0.00025	1/11 (9)	6/11 (54)	0.032
Repeated	152	0/11 (0)	3/11 (27)	0.11	1/7 (14)	3/7 (43)	0.28
$^{239}PuO_2$:							
Single	408	10/55 (18)	25/55 (45)	0.0019	1/17 (6)	7/17 (41)	0.016
Repeated	297	20/67 (30)	30/67 (45)	0.054	5/16 (31)	5/16 (31)	1.0
Once	763	37/146 (25)	48/146 (33)	0.099	1/15 (7)	6/15 (40)	0.040
$^{244}Cm_2O_3$	926	9/114 (8)	20/114 (18)	0.023	3/58 (5)	11/58 (19)	0.021
All Combined	3571	82/432 (19)	147/432 (34)	<0.0001	14/175 (8)	53/175 (30)	<0.0001

[a]Sources of data: Single and repeated $^{144}CeO_2$ exposure (Lundgren *et al.*, 1992); single and repeated $^{239}PuO_2$ exposure (Lundgren *et al. Radiat. Res. 142*: 39, 1995); untreated rats exposed once to $^{239}PuO_2$ (1980-81 Annual Report, p. 178; Lundgren, D. L. *et al. Hum. Exp. Toxicol. 9*: 295, 1990; Lundgren, D. L. *et al. Health Phys. 60*: 353, 1991); exposed once to $^{244}Cm_2O_3$ (1991–92 Annual Report, p. 123).

[b]Matched by sex, age at death, and lifetime radiation dose to lungs (see test for details).

[c]Fisher's exact test to determine if there were significant differences in the incidences of infiltration of the lung with MCL in rats with and without lung tumors.

[d]The control rats were combined from those in all of the studies cited above and were either unexposed, sham exposed once or repeatedly, or exposed once or repeatedly to stable particulate aerosols.

The crude incidences of MCL in the groups of F344/Crl-ITRI rats in the studies cited in Table 1 ranged from 7.9 to 49% and were not related to α- or β-particle doses to the lungs. This was in contrast with the findings that whole-body exposure of 2-mo-old F344 rats to graded single doses of X rays up to 2.4 Gy decreased the incidence of MCL later in life from about 50% in the unexposed rats to about 5% in those receiving 2.4 Gy (Hellman, S. *et al. Cancer Res. 42*: 433, 1982). These differences may be due to different radiation dose patterns, i.e., whole-body vs. primarily thoracic exposure. A comparison of functions fitted to the crude incidences of lung tumors in rats with and without infiltration of the lung with MCL at death from the study of the effects of a single inhalation exposure to $^{144}CeO_2$ (Lundgren, D. L. *et al. Radiat. Res. 132*: 325, 1992) is illustrated in Figure 1. Based on 95% confidence intervals of the curve parameters, the curves were significantly different indicating that the incidence of primary lung tumors was different in rats with and without MCL. Similar comparisons of the dose-response relationships in the other studies cited in Table 1 indicated similar, though not as pronounced, trends, i.e., a lower incidence of lung tumors in rats with MCL infiltration of the lung relative to those without infiltration of the lung.

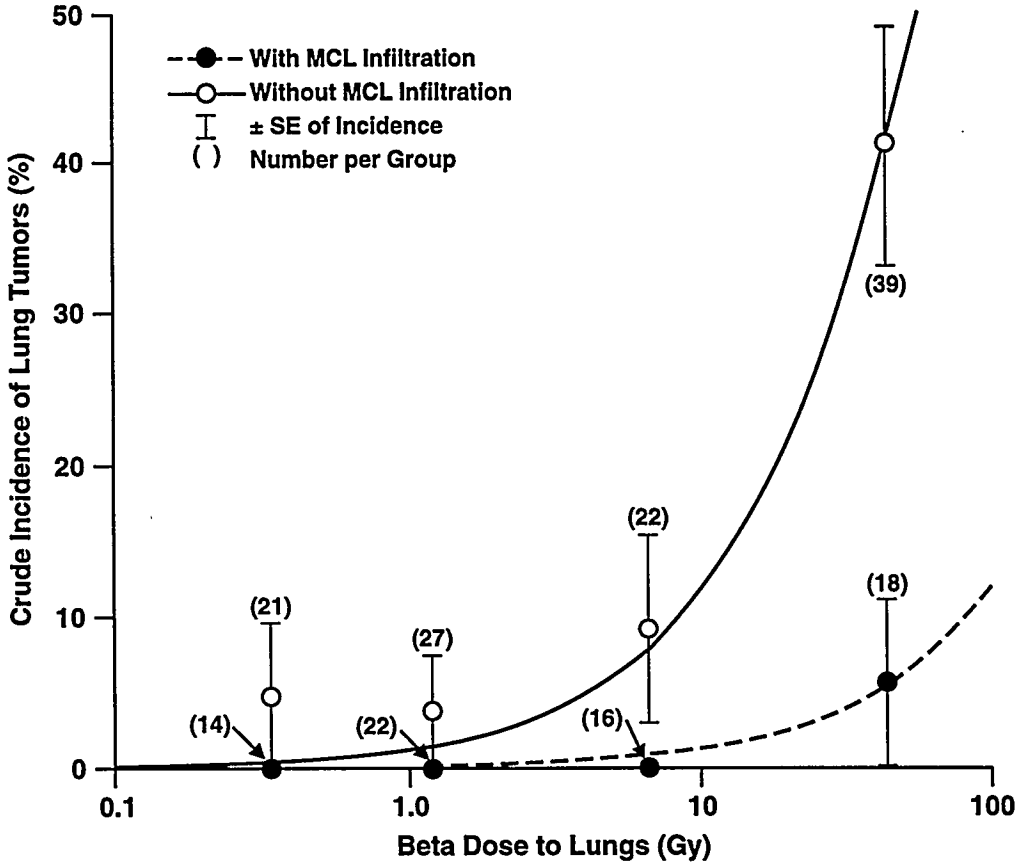

Figure 1. Lung tumor dose-response relationships in F344/Crl-ITRI rats (Lundgren, D. L. *et al.*, 1992) that died with or without mononuclear cell leukemia (MCL) infiltration of the lung after a single inhalation exposure to aerosols of $^{144}CeO_2$. Curves are single exponential Weibull distribution model fits to each data set. The parameter for the curve for the rats with MCL infiltration of the lung was $100(1.0–e^{-0.0013D})$ and for the rats without MCL infiltration of the lung $100(1.0–e^{-0.012D})$, where D is radiation dose in Gy.

As summarized in Table 1, the incidence of MCL infiltration of the lung was significantly less ($p \leq 0.05$) in five of the seven groups of F344/Crl-ITRI rats with primary lung tumors and less in four of the seven groups with metastatic lung tumors. Although the differences were not always statistically significant, there were lower incidences of primary and metastatic lung tumors in rats with MCL infiltration of the lung in all but one group of the 14 compared. When all data sets were combined, the differences were significant at $p < 0.0001$ for both primary and metastatic lung tumors. Rats with MCL infiltration of the lung had about half as many primary lung tumors (19%) as did the matched control rats without MCL in the lung (34%). An even greater difference was seen in the occurrence of metastatic lung tumors in rats with MCL infiltration of the lungs (8%) compared with rats that did not have MCL infiltration of the lungs (30%). Differences in the survival times of rats with and without MCL infiltration of the lung did not explain for the results reported here because the rats were matched by age. The survival and radiation doses to the lungs between rats with primary or metastatic lung tumors and the case-control matched rats also were not significantly different (Student's *t* test $p > 0.05$). There were no consistent differences between sexes nor tumor types.

Possible mechanisms for the inverse relationship of MCL and lung tumors are: (1) production of a substance by MCL that acts in a manner similar to angiostatin, an angiogenesis inhibitor, which mediates the suppression of metastases of Lewis lung carcinomas (O'Reilly, M. S. *et al. Cell 79*: 315, 1994), (2) suppression of the development of lung tumors by natural killer cell activity associated with the MCL cell population (Ward, J. M. and G. W. Reynolds. *Am. J. Pathol. 111*: 1, 1983), (3) mechanism(s) yet to be recognized, and (4) conversely, the presence of a paraneoplastic syndrome associated with lung tumors could suppress the incidence of MCL. However, no such syndromes have been described in rats.

The findings present a rather dichotomous situation in that primary lung tumors in the F344/Crl-ITRI rats induced by α-particle radiation are typically slowly developing lesions whose precursors may be present as early as 180 d (9 mo of age) after exposure to inhaled $^{239}PuO_2$ (Herbert, R. A. *et al. Radiat. Res. 134*: 29, 1993). In contrast, MCL is a rapidly progressing lesion once the leukemia cells begin proliferating in the spleen, and begins to occur at about 18 to 20 mo of age (*Pathology of the Fischer Rat*, 1990; Harada *et al.*, 1990). Therefore, how leukemia, which occurs late in the life of the F344 rat, can affect the incidence of lung tumors, whose development is initiated much earlier, is unclear. This could suggest the alternate explanation that lung tumors could suppress the development of leukemia, thus creating the observed inverse relationship of MCL infiltration of the lung and lung tumors.

Gaining an understanding of the mechanisms involved in the negative correlations noted should enhance our understanding of the mechanisms involved in the development of lung cancer. The data presented also indicate that infiltration of the lung by MCL should be taken into consideration when evaluating the dose-response relationships of inhaled carcinogens in the F344 rat.

(Research sponsored by the Office of Health and Environment Research, U.S. Department of Energy, under Contract No. DE-AC04-76EV01013.)

CYCLIN D EXPRESSION IN PLUTONIUM-INDUCED LUNG TUMORS IN F344 RATS

*Fletcher F. Hahn and Gregory Kelly**

The genetic mechanisms responsible for α-radiation-induced lung cancer in rats following inhalation of ^{239}Pu is an ongoing area of research in our laboratory. Previous studies have examined the status of the p53 gene by immunohistochemistry. Only two tumors (2/26 squamous cell carcinomas) exhibited detectable levels of p53 products. Both were the result of mutations in codons 280 and 283 (Kelly, G. *et al. Radiat. Res. 142*: 263, 1995). More recent studies of X-ray-induced lung tumors in rats showed a similar lack of involvement of p53.

We hypothesized that if p53 was not involved in the development of lung tumors induced in the rat by ^{239}Pu, then other genes regulating the cell cycle may be involved, such as the cyclin D_1 gene. The purpose of this study was to determine whether the cyclin D_1 gene is altered in the lung tumors of rats that inhaled $^{239}PuO_2$.

Animal exposures, necropsies, and tissue preparations have been described (Herbert, R. A. *et al. Radiat. Res. 134*: 29, 1993). Briefly, 360 F344/N female rats were exposed at 13 wk of age to a respirable aerosol of $^{239}PuO_2$ resulting in about 3.7 kBq initial lung burden. In addition, 140 control animals were similarly exposed to a sham aerosol of diluent. At sacrifice, gross lesions were fixed in paraformaldehyde and processed for histologic evaluation. The right lung lobe was snap-frozen in liquid N_2 and stored at –70°C. Random sections from the left lobe were embedded in paraffin, sectioned at 4 μm, and examined with a light microscope.

Four-micrometer thick sections of 39 primary lung tumors were deparaffinized, rehydrated, and rinsed twice in 0.5% BRIJ® 35 solution (Sigma Chemical Co., St. Louis, MO). The slides were digested in pepsin and cryptic cyclin D_1 protein epitopes unmasked by microwaving the slides in CITRA® antigen retrieval buffer (Biogenex, Inc., San Ramon, CA). Endogenous peroxidase activity was blocked with 3.0% H_2O_2 in PBS. Immunoreactivity for cyclin D_1 was detected by preincubation in 5% normal horse serum, 1% BSA, in 1X automation buffer followed by application of primary antibody or normal horse serum (negative controls) at a 1:75 dilution in 1X automation buffer containing 1% BSA. The primary antibody used in these experiments was a mouse anti-human cyclin D_1 monoclonal (cyclin D_1 [17-13G], Santa Cruz Biotechnology, Inc., Santa Cruz, CA). Bound primary antibody was detected with a Vectastain® avidin-biotin peroxidase complex kit (Vector Laboratories, Inc., Burlingame, CA) using a goat anti-horse IgG secondary antibody at a 1:200 dilution in 1X automation buffer containing 1% BSA and 5% normal rat serum. Negative controls consisted of an identical dilution of specific isotype (IgG_1) antibody applied to serial tissue sections as described above. Normal lung tissue adjacent to lung tumors was used as an internal negative control on tissue sections. Slides were counterstained with Mayer's hematoxylin.

DNA from each sample of lung tumor or normal lung tissue was digested with either *Taq* I, *Hind* III, or *EcoR* I restriction endonuclease at 37°C. The digested DNA fragments were size fractionated by electrophoresis through a 1% agarose gel. The DNA was transferred to a Nytran filter by capillary action and cross-linked to the filter by ultraviolet illumination. Filters were prehybridized in 6X saline sodium citrate (SSC)/10X Denhardt's solution/0.5% sodium dodecyl sulfate (SDS)/50 μg/mL ssDNA mixed with approximately 10^6 counts per minute of ^{32}P-labeled probe at 65°C for 14 h. A mouse cyclin D_1 cDNA clone (from Dr. C. J. Sherr, Howard Hughes Medical Institute, St. Jude Children's

*SouthWest Scientific Resources, Inc., Albuquerque, New Mexico

Research Hospital, Memphis, TN) was used as a probe on these Southern blots. The filters were then washed in 6X SSC/0.1% SDS twice at room temperature, followed by more stringent washes in 1X SSC/0.5% SDS at 65°C and two times in 0.1X SSC/0.5% SDS at 65°C. Finally, the filters were placed on Kodak-AR radiograph film with intensifying screens.

Thirty-nine rat lung tumors, including 25 squamous cell carcinomas, 11 adenocarcinomas, and 3 adenosquamous carcinomas, were examined for elevated levels of the cyclin D_1 protein by immunohistochemistry. Samples of normal lung from unexposed rats were used as negative controls. Seventy-nine percent of the tumors examined (31/39) expressed elevated levels of cyclin D_1, while the normal rat lung was negative for cyclin D_1 expression. When segregated by diagnosis, 76% of the squamous cell carcinomas (19/25), 82% of the adenocarcinomas (9/11), and all of the adenosquamous carcinomas (3/3) expressed elevated levels of the cyclin D_1 protein (Table 1). On average, when cyclin D_1 was overexpressed, its expression was generally moderate to intense; however, two of the tumors demonstrated very intense staining. The antibody staining for cyclin D_1 was nuclear with patchy immunoreactivity of groups of cells throughout the neoplasm.

Table 1

Cyclin D Expression in Pu-Induced Rat Lung Tumors

Tumor Diagnosis	Total	Positive Samples	Percent Positive
Squamous cell carcinoma	25	19	76%
Adenocarcinoma	11	9	82%
Adenosquamous carcinoma	3	3	100%
Total	39	31	79%

No detectable polymorphism, amplification, or deletion within the rat cyclin D_1 gene was observed by Southern blot analysis of 19 ^{239}Pu-induced lung tumors. Tumors were selected for Southern blots based on the availability of sufficient DNA for the analysis. Each tumor sample along with samples of normal rat DNA displayed identical cyclin D_1-specific fragment sizes and similar intensities after digestion with *EcoR* I, *Taq* I, or *Hind* III.

Recent reports indicate that the *ras* oncogene is an upstream regulator of cyclin D_1 expression (Filmus, J. *et al. Oncogene 9*: 3627, 1994). Previous studies in our laboratory have shown that 46% of plutonium-induced rat lung tumors have an activated Ki-*ras* oncogene (Stegelmeier, B. L. *et. al. Mol. Carcinog. 4*: 43, 1991). Twenty-one plutonium-induced rat lung tumors with cyclin D_1 overexpression had been examined for Ki-*ras* activation. Cyclin D_1 expression and *ras* activation are compared in Table 2. The high frequency of cyclin D_1 expression and the frequent activation of Ki-*ras* suggest an interactive correlation. Sixty-two percent (13/21) of the sample set exhibited both elevated levels of cyclin D_1 and activated Ki-*ras*. Interestingly, almost 24% of the tumors expressing elevated levels of cyclin D_1 had a wild-type Ki-*ras*, suggesting that Ki-*ras* may not be the only mediator of cyclin D_1 expression.

Table 2

Cyclin D Expression and Ki-*ras* Mutations
in Pu-Induced Rat Lung Tumors

	Mutant Ki-*ras*	Normal Ki-*ras*
Elevated cyclin D_1 expression	13[a]	5
Normal cyclin D_1 expression	2	1

[a]Number of tumors.

In conclusion, we have found that α-radiation-induced rat lung tumors have a high incidence (31 of 39) of cyclin D_1 overexpression. These data are consistent with the hypothesis that overexpression of the cyclin D_1 gene abrogates the normal inhibitory role of the retinoblastoma (Rb) protein in cell-cycle progression. Elimination of the Rb-induced cell-cycle stop by overexpression of cyclin D_1 would have a similar effect on the cell cycle as the lack of a functional p53. Cells lacking a DNA damage-induced cell-cycle pause would accumulate mutations in the genome at an accelerated rate. These data suggest that elevated cyclin D_1 expression may be important in the genesis of plutonium-induced lung tumors in the rat.

(Research sponsored by the Office of Health and Environmental Research, U.S. Department of Energy, under Contract No. DE-AC04-76EV01013.)

EXPRESSION OF CYCLIN D_1 DURING ENDOTOXIN-INDUCED ALVEOLAR TYPE II CELL HYPERPLASIA IN RAT LUNG AND THE DETECTION OF APOPTOTIC CELLS DURING THE REMODELING PROCESS

Johannes Tesfaigzi, Marcy B. Wood, and Neil F. Johnson

Our studies have shown that endotoxin intratracheally instilled into the rat lung induces proliferation of alveolar type II cells (Tesfaigzi, J. *et al. Proc. Am. Assoc. Cancer Res. 36:* 130, 1995). In that study, the alveolar type II cell hyperplasia occurred 2 d after instillation of endotoxin and persisted for a further 2 d. After the hyperplasia, the lung remodeled and returned to a normal state within 24–48 h (Tesfaigzi, J. *et al.*, unpublished observation). Understanding the mechanisms involved in the remodeling process of this transient hyperplasia may be useful to identify molecular changes that are altered in neoplasia. The purpose of the present study was to corroborate induction of epithelial cell hyperplasia by endotoxin and to delineate mechanisms involved in tissue remodeling after endotoxin-induced alveolar type II cell hyperplasia.

Male Fischer 344/N rats, 8–10 wk of age (Taconic Laboratories, Germantown, NY) received a single intratracheal instillation of 1 mg endotoxin (lipopolysaccharide from *Escherichia coli* 0111:B4, Sigma Chemicals Co., St. Louis, MO) in pyrogen-free saline. One day after instillation, three endotoxin-instilled rats were injected with 5-bromo-2-deoxyuridine (BrdU) (Sigma) at 50 μg/g body weight in saline and sacrificed 2 h later as described to label cells undergoing DNA synthesis (Johnson, N. F. *et al. Toxicol. Appl. Pharmacol. 103*: 143, 1990). All other animals received injections of BrdU 2 d after instillation because previous studies had shown that BrdU incorporation is maximum at this time point (Tesfaigzi *et al.*, 1995). These rats were then sacrificed 2 h after BrdU injection on days 2–6. Lung tissues were prepared for analysis by immunohistochemistry and electron microscopy as described (Harkema, J. R. and J. A. Hotchkiss. *Am. J. Pathol. 141*: 307, 1992). To differentiate between epithelial cells and inflammatory cells in the lung, tissue sections from each animal were immunostained with BrdU antibody followed by a monoclonal antibody to cytokeratin. Tissue sections were also doubled stained with antibodies to cyclin D_1 and cytokeratin.

Cyclin D_1 was expressed only during the G_1 phase of the cell cycle. Nuclei that stained for cyclin D_1 indicated cells that were cycling and, therefore, cells that were proliferating. At 1 d post instillation, a number of epithelial cells in both hyperplastic and nonhyperplastic areas were staining positively for cyclin D_1. At 3 d post instillation, hyperplastic cells continued to stain for cyclin D_1 indicating that epithelial cells were still proliferating. At days 4–6, however, essentially no immunostaining of epithelial cells for cyclin D_1 was observed, indicating that hyperplasia was no longer a feature of the lung tissue. Histological sections of lungs from rats after 5 and 6 d post instillation were comparable to the lungs of control rats. This demonstrated that the lung had remodeled. These findings agree with previous studies that also showed that endotoxin-induced hyperplasia develops by day 2, continues through day 4, and regresses by day 5 (Tesfaigzi *et al.*, 1995).

Double immunostaining of tissue sections for BrdU and cytokeratin confirmed the findings from the cyclin D_1 slides. Increased numbers BrdU-labeled epithelial cells were present as early as 1 d after endotoxin instillation, indicating that cells were synthesizing DNA and preparing to divide. The number of BrdU-labeled epithelial cells continued to increase through the second day after instillation and persisted through day 4. At day 3, some BrdU-positive epithelial cells were detected in the alveolar spaces indicating that some hyperplastic cells were sloughing off. At days 5 and 6 post instillation, BrdU-labeled cells with flattened nuclei were observed, indicating that some hyperplastic type II cells may have differentiated into type I cells.

When analyzed by electron microscopy, lung tissue sections from rats 4 d after endotoxin instillation showed the presence of alveolar type II and fibroblast cells with condensed chromatin in the nuclei. Because chromatin condensation is one characteristic of cells undergoing programmed cell death (Martin, S. J. *et al. Trends Biochem. Sci. 19*: 26, 1994), apoptosis may be one mechanism that reduces the number of cells during the remodeling after hyperplasia.

In conclusion, immunostaining with cyclin D1 and cytokeratin shows that endotoxin induced epithelial cell proliferation and resulted in hyperplasia in the lung which persisted through 4 d post-instillation. This hyperplasia regressed within 24–48 h. The detection of some newly formed epithelial cells in alveolar airspace and BrdU- and cytokeratin-positive cells with flattened nuclei suggests that during the remodeling process epithelial cells may slough off and partly differentiate into type I cells. Differentiation of alveolar type II cells into alveolar type I cells has been reported (Evans, M. J. *et al. Exp. Mol. Pathol.* 22: 142, 1975) for rats exposed to NO_2. Finally, apoptosis of hyperplastic alveolar type II cells plays a role in reducing the numbers of epithelial cells during the remodeling of the lung. Further studies will investigate the possibility that mechanisms inducing the apoptotic program in endotoxin-induced hyperplasias are disrupted in the $^{239}PuO_2$-induced hyperplastic lung lesions and thereby may contribute to the development of neoplasms.

(Research sponsored by the Office of Health and Environmental Research, U.S. Department of Energy, under Contract No. DE-AC04-76EV01013.)

INCREASED EXPRESSION OF Bcl-2 DURING MUCOUS CELL METAPLASIA INDUCED BY ENDOTOXIN AND OZONE

Johannes Tesfaigzi, Lana M. Ray, Jon A. Hotchkiss**, and Jack R. Harkema***

Apoptosis or programmed cell death is accompanied by characteristic morphological changes that distinguish apoptosis from other forms of cell death. These changes include DNA fragmentation, chromatin condensation, cell shrinkage, cell surface pseudopodia, and finally the cellular collapse into membrane-enclosed apoptotic bodies (Martin, S. J. *et al. Trends in Biochem. Sci. 19*: 26, 1994) which are rapidly engulfed by macrophages or neighboring cells. Although the morphological features of apoptotic cells are well studied, the biochemical events that control apoptosis are not understood (Steller, H. *Science 267*: 1445, 1995). Programmed cell death is triggered by a variety of pathways that are initiated by different stimuli including noxious agents, DNA damage, the activation of TNF receptors, or the withdrawal of growth factors (Thompson, C. B. *Science 267*: 1456, 1995). The central process of programmed cell death involves a cascade of biochemical events that begins with the initiation of a family of cysteine proteases, including the interleukin-1-β-converting enzyme, CPP-32, and Apopain (Nicholson, D. W. *et al. Nature 376*: 37, 1995). The ratio of Bax, a death-inducer gene, to Bcl-2, an apoptosis suppressor gene, determines whether or not the main apoptotic pathway is blocked (Steller, 1995). Apoptosis is suppressed if the ratio of Bcl-2/Bax is > 1, and cells undergo apoptosis if the ratio is < 1. The overexpression of Bcl-2 has been shown to block the apoptotic program triggered by a variety of agents. Therefore, Bcl-2 must be involved in blocking the central pathway of the cell death program.

Mucous cell metaplasia can be induced in the tracheobronchial airways of rats exposed to endotoxin, a lipopolysaccharide-protein molecule found in the outer walls of gram-negative bacteria and in nasal transitional epithelium of rats by repeated exposure to ambient levels of ozone (Harkema, J. R. and J. A. Hotchkiss. *Toxicol. Lett. 68*: 251, 1993). A single intratracheal instillation of endotoxin also induces transient mucous cell metaplasia in rat bronchial epithelia (Tesfaigzi, J. *et al.*, unpublished observation). The purpose of the present study was to investigate whether a regulator of the apoptotic process (Bcl-2) is involved in the remodeling of the bronchial epithelium after endotoxin instillation and whether similar processes can be observed in the ozone-induced mucous cell metaplasia in rat nasal epithelia.

Male F344/N rats, 8–9 wk of age (Taconic Laboratories, Germantown, NY), received a single intratracheal instillation of 1 mg endotoxin (lipopolysaccharide from *Escherichia coli* 0111:B4, Sigma Chemicals Co., St. Louis, MO) in pyrogen-free saline. Two days after instillation, each rat was injected with 5-bromo-2-deoxyuridine (BrdU) at 50 μg/g body weight in saline to label cells undergoing DNA synthesis. Every 24 h, 1, 2, 3, 4, 5, and 6 d after endotoxin instillation, six rats were sacrificed by intraperitoneal injection with Nembutal (Abbott Laboratories, North Chicago, IL) for up to 6 d. Tissue sections (5 μm thick) were prepared from the left lung lobes for immunohistochemical staining as described earlier (1993–94 *Annual Report*, p. 134). For studies of mucous cell metaplasia after exposure to ozone, female F344/N rats (Taconic Laboratories, Germantown, NY) were exposed to 0.8 ppm ozone, 6 h/d for 1 and 3 mo. Transversely sectioned 5 μm tissues samples were prepared from these rats as described by Johnson, N. F. *et al.* (*Toxicol. Appl. Pharmacol. 103*: 143, 1990).

---

*Department of Energy/Associated Western Universities Teacher Research Associates Program (TRAC) Participant

**Department of Pathology, Michigan State University, East Lansing, Michigan

To verify the immunoreaction of Bcl-2, antibodies raised to three different epitopes of the Bcl-2 protein were used. Two of these antibodies were purchased from Santa Cruz Biotechnology, Inc., Santa Cruz, CA, and PharMingen, San Diego, CA. The third Bcl-2 antibody was obtained from Dr. J. C. Reed, La Jolla Research Foundation, San Diego, CA. The antibody to BrdU was purchased from Beckton Dickinson, San Jose, CA. The antigen retrieval method was optimized for each antibody used. Lead buffer was used for the Bcl-2 antibody from Santa Cruz, and a 1:10 citra buffer was used for the Bcl-2 antibodies from PharMingen and from Dr. J. C. Reed's laboratory. The immunoreactions were detected using standard immunohistochemical procedures and counterstained with hematoxylin.

In rats sacrificed 3 d post-instillation, about 12% of cells in the epithelium of the main bronchus stained intensively for Bcl-2. Only one or two epithelial cells of the same region immunostained in rats sacrificed 4 d after instillation, and no immunostaining was observed in rats sacrificed after 5 and 6 d. To verify the specificity of the immunoreaction, two additional antibodies to Bcl-2 raised to different antigenic epitopes were used. These antibodies also stained a similar number of mucous cells with a similar labeling intensity. A peptide control solution was available for only one Bcl-2 antibody. Preincubation of this antibody with the peptide resulted in a significant decrease in the immunoreaction. These experiments suggested that the observed immunoreaction was specific for the Bcl-2 protein. These tissue sections were further stained with alcian blue to determine how many acidic glycoprotein-producing mucous cells were Bcl-2 positive. These slides showed that the immunostaining for Bcl-2 was limited to a few mucous cells in the bronchial epithelium, while adjacent mucous cells showed no staining for the Bcl-2 protein.

The antibody to BrdU labeled a few cells in the bronchial epithelium, suggesting that new cells were formed after endotoxin instillation. To determine the correlation between the newly formed and Bcl-2 overexpressing mucous cells, the number of labeled cells in the main bronchus of two rats, sacrificed 3 d post-instillation was quantified. Bcl-2 and BrdU labeled cells on serial tissue sections were counted in two regions of the bronchial epithelium. On average, the ratio of cells immunostained for Bcl-2 and BrdU per 100 bronchial epithelial cells was 2:1 (Fig. 1). The number and location of BrdU staining cells did not correlate with the number and location of cells immunostained for Bcl-2. Therefore, it is not likely that newly formed mucous cells overexpress Bcl-2 due to endotoxin instillation.

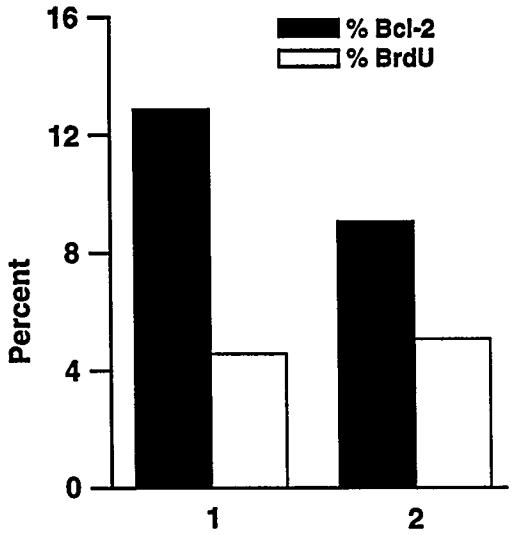

Figure 1. The number of bronchial epithelial cells expressing Bcl-2 and BrdU. The bars represent the percent of cells that showed immunostaining for Bcl-2 and BrdU on serial tissue sections. The mean of two regions on the main bronchial epithelium is shown for two rats.

Examination of the rat nasal epithelia for the expression of Bcl-2 before and after exposure to ozone produced results similar to those observed in the endotoxin-exposed bronchial epithelia. In nasal epithelia of control rats, no Bcl-2 was detected. However, when the numbers of Bcl-2 labeled cells per 100 epithelial cells were analyzed at six regions of the nasal turbinates of rats exposed to 1 mo of ozone, on average 50% of the epithelial cells immunostained for Bcl-2 with varying levels of intensity. Although sustained mucous cell metaplasia was observed in the epithelia of the nasal turbinates after exposure to ozone for 3 mo in the six regions analyzed, only 19% of the epithelial cells contained Bcl-2. This observation suggested that, similar to the endotoxin-induced mucous cell metaplasia, a time-dependent regulation of Bcl-2 synthesis occurred in rats exposed to ozone.

In conclusion, this study showed that high levels of Bcl-2 were detected in some mucous cells at specific time points during mucous cell metaplasia, and this expression was reduced at later time points or was absent after remodeling of this epithelium. Because the cells staining for BrdU did not correlate with the cells expressing Bcl-2, further studies are needed to elucidate how certain mucous cells are designated to differentially express Bcl-2. These mechanisms may be critical to understand the selective deletion of cells that are no longer required to form the remodeled epithelium and more generally during the development in a multicellular organism. The disruption of these mechanisms may be one factor involved in the initial selection of preneoplastic cells.

(Research sponsored by the Office of Health and Environmental Research, U.S. Department of Energy, under Contract No. DE-AC04-76EV01013.)

TRANSFECTION OF NORMAL HUMAN BRONCHIAL EPITHELIAL CELLS WITH THE *bcl-2* ONCOGENE

Christopher H. Kennedy, Karla D. Kenyon, Johannes Tesfaigzi, and John F. Lechner*

In vitro studies examining the transformation of virus-immortalized human bronchial epithelial (HBE) cells after exposure to chemical and physical carcinogens have contributed to our understanding of the mechanisms that underlie the development of lung cancer. Virus-immortalized HBE cells have been used because of both the limited life span of normal human bronchial epithelial (NHBE) cells in culture (approximately 30–35 population doublings) and their resistance to *in vitro* malignant transformation. For example, human papillomavirus (HPV)-immortalized HBE cells have been used to study the genetic changes that occur after exposure to α-particles *in vitro* (Hei, T. K. *et al. Carcinogenesis 15*: 431, 1994). Although this model may prove to be useful for studying the 18% or less of bronchogenic carcinomas found to contain HPV sequences (Ostrow, R. S. *et al. Cancer 59*: 433, 1987; Béjui-Thivolet, F. *et al. Hum. Pathol. 21*: 114, 1990), it is not an appropriate model for studying the majority of lung epithelial malignancies in which HPV DNA is not detected. This view is supported by the fact that HPV-immortalized cell lines commonly exhibit aneuploidy (Willey, J. C. *et al. Cancer Res. 51*: 5373, 1991).

This study was developed to determine whether the life span of NHBE cells can be extended by overexpresson of the *bcl-2* oncogene. Overexpression of *bcl-2* has been shown to enhance cellular viability by inhibiting programmed cell death (Hockenbery, D. M. *et al. Nature 348*: 334, 1990) and is associated with certain lung carcinomas (Ikegaki, N. *et al. Cancer Res. 54*: 6, 1994; Pezzella, F. *et al. N. Engl. J. Med. 329*: 690, 1993). The goal of this study was to isolate clonal HBE cells that overexpress *bcl-2*, exhibit a normal karyotype, and undergo an increased number of population doublings relative to NHBE cells.

Prior to transfection of NHBE cells with a plasmid containing the human *bcl-2* cDNA sequence (pEBS-bcl-2), the transfection conditions for LipofectAMINE™ (Gibco BRL, Rockville, MD) and plasmid DNA were optimized with a mammalian reporter vector designed to express β-galactosidase, pCMVβ (Clonetech, Palo Alto, CA). The NHBE cells were plated on 60 mm Petri dishes, grown to 40–50% confluence in bronchial epithelial growth medium (BEGM, Clonetics, San Diego, CA) and treated with pre-incubated mixtures containing 2–3 μg pCMVβ and 0–48 μL LipofectAMINE™. After a 6 h incubation, the transfection media was replaced with BEGM. Approximately 48 h after transfection, the cells were fixed with 2% formaldehyde/0.05% glutaraldehyde, stained overnight with X-gal (Promega, Madison, WI) at 37°C, and visualized by light microscopy.

Because hygromycin is to be used for the selection of cells transfected with the pEBS-bcl-2 plasmid, an assay was performed to determine the lowest dose of this antibiotic necessary to kill 100% of nontransfected NHBE cells (LD_{100}). The NHBE cells were plated on 60 mm Petri dishes, grown to 70% confluence, and treated with a range of doses (25–350 μg/mL BEGM) of hygromycin (Boehringer Mannheim, Indianapolis, IN). After 15 d of hygromycin treatment, the cells were fixed with 10% neutral-buffered formalin and stained with crystal violet.

The pEBS-bcl-2 plasmid, a gift from Dr. Vishva Dixit at the University of Michigan Medical School, was used to transform competent *E. coli* cells. Ampicillin-resistant colonies were grown on agar overnight at 37°C. Transformants were selected and grown in 1 L of Luria broth containing 100 μg/mL ampicillin. Milligram quantities of the pEBS-bcl-2 plasmid DNA were then purified using

---

*Department of Energy/Associated Western Universities Summer Student Research Participant

the Plasmid Mega Prep kit (Qiagen, Chatsworth, CA). Ten μg of purified pEBS-bcl-2 plasmid DNA was digested with *Xba*I restriction endonuclease to excise the *bcl*-2 insert. The 1.9 kb insert was separated from the 11 kb plasmid by agarose gel electrophoresis. To prepare a vector control, the band representing the pEBS7 vector was cut out of the gel and electroeluted into a dialysis bag. This linear vector was then recircularized with T4 DNA ligase and cloned as described above.

A pilot transfection was performed with 7×10^5 NHBE cells using pre-incubated mixtures containing both 24 and 32 μL LipofectAMINE™ with 3 μg pEBS-bcl-2 DNA. After a 6 h incubation, the cells were washed once with HEPES-buffered saline, and the transfection medium was replaced with BEGM. Approximately 72 h after transfection, the cells were dissociated with trypsin, and two samples (2.5×10^4 cells/sample) were removed from each suspension and cytospun onto glass slides in preparation for immunohistochemical analysis with a polyclonal antibody specific for the bcl-2 protein. The remaining cells were replated and treated for 10 d with hygromycin (50 μg/mL BEGM) to select for transfectants.

Transfection conditions were optimized using the pCMVβ vector (Table 1). Although a ratio of 32 μL LipofectAMINE™ to 3 μg plasmid DNA did not result in the highest efficiency (3.3%), higher ratios resulted in significant cytotoxicity.

Table 1

NHBE Transfection Efficiency with pCMVβ

LipofectAMINE™ (μL)	pCMVβ (μg)	Transfection Efficiency (%)[a]
0	2	0
4	2	0.16
8	2	0.45
16	2	0.62
32	2	0[b]
24	3	0.32
32	3	3.3
48	3	13.7[c]

[a]The number of stained (blue) and unstained cells was scored in 10 random fields for each dish. The value shown is the total number of stained cells divided by the total number of cells times 100.
[b]Only two cells were observed in 10 random fields due to the cytotoxicity of the LipofectAMINE™; therefore, the transfection efficiency was designated as zero.
[c]Although a high transfection efficiency was determined, very few cells were present on the dish due to the cytotoxicity of the LipofectAMINE™.

The hygromycin cytotoxicity assay was performed using nontransfected NHBE cells. After 15 d of treatment, the LD_{100} value was determined to be 50 μg hygromycin/mL BEGM.

The identity of the purified pEBS7 vector was verified by *Xba*I digestion followed by agarose gel electrophoresis. It was determined that the purified pEBS7 plasmid DNA does not contain the *bcl*-2 insert (1.9 kB) and is the correct size (11 kb) by comparison with digested pEBS-bcl-2 plasmid DNA.

Immunohistochemical analysis of NHBE cells transfected with the *bcl*-2 oncogene suggested that these cells transiently expressed the bcl-2 protein, although no cells survived the hygromycin selection.

This results of this study suggest that: (1) NHBE cells can be transiently transfected with the pCMVβ vector; and (2) the antibiotic hygromycin kills nontransfected NHBE cells and therefore can be used to select for hygromycin-resistant transfected cells. A large-scale transfection (5×10^6 cells) will be performed using the results obtained from this study. If stable transfectants are isolated and these cells exhibit an extended number of population doublings relative to NHBE cells, the transfected clones will be irradiated with ^{238}Pu α-particles *in vitro* and used as a model to elucidate the genetic events that characterize radiation-induced malignant transformation of NHBE cells.

(Research sponsored by the Office of Health and Environmental Research, U.S. Department of Energy, under Contract No. DE-AC04-76EV01013.)

METHYLATION OF THE ESTROGEN RECEPTOR CpG ISLAND DISTINGUISHES SPONTANEOUS AND PLUTONIUM-INDUCED TUMORS FROM NITROSAMINE-INDUCED LUNG TUMORS

Steven A. Belinsky, Stephen B. Baylin, and Jean-Pierre J. Issa**

CpG islands located in the promoter region of genes constitute one mechanism for regulating transcription. These islands are normally free of methylation, regardless of the expression state of the gene. Hypermethylation of CpG islands, the addition of a methyl group to the internal cytosine within CpG dinucleotides, can cause silencing of a gene. Hypermethylation has been detected as an early event at specific chromosome loci during the development of colon cancer (Makos, M. *et al. Proc. Natl. Acad. Sci. [USA] 89*: 1929, 1992) and represents one mechanism used by neoplastic cells to inactivate tumor suppressor genes. Recent studies have demonstrated this mechanism in inactivation of the VHL tumor suppressor gene in 19% of sporadic renal tumors (Herman, J. G. *et al. Proc. Natl. Acad. Sci. [USA] 91*: 9700, 1994) and the $p16^{INK4a}$ tumor suppressor gene in 30% of non-small cell lung cancers (Merlo, A. *et al. Nature Med. 1*: 686, 1995). A recent report indicates that the estrogen receptor gene could also be inactivated through methylation (Ottaviano, Y. L. *et al. Cancer Res. 54*: 2552, 1994). In addition, estrogen receptor CpG island methylation arises as a direct function of age in normal colonic mucosa and is present in virtually all colonic tumors. In cultured colon cancer cells, methylation-associated loss of expression of the estrogen receptor gene results in deregulated growth, suggesting a role for the estrogen receptor in colon cancer development (Issa, J-P. *et al. Nature Genetics 7*: 535, 1994). These results provide further evidence that gene silencing through methylation could be a predominant epigenetic mechanism underlying the development of many different types of cancer. The purpose of the current investigation was to determine whether estrogen receptor CpG island methylation is involved in the development of lung cancer.

Estrogen receptor CpG island methylation was examined in lung tumors induced by 4-methylnitrosamino-1-(3-pyridyl)-1-butanone (NNK) in A/J mice and F344/N rats as described previously (Belinsky, S. A. *et al. Cancer Res. 52*: 3164, 1992; Belinsky, S. A. *et al. Cancer Res. 50*: 3772, 1990). Methylation was also examined in lung tumors from sham A/J mice and tumors induced in the F344/N rat by X-rays or plutonium as described (Belinsky, S. A. *et al. Radiat. Res.*, in press; Stegelmeier, B. *et al. Mol. Carcinog. 4*: 43, 1991). The estrogen receptor gene has a typical CpG island that begins in its promoter and extends into the first exon. This island contains several methylation-sensitive restriction enzyme sites, including a NotI endonuclease site. Restriction enzyme digestion followed by Southern blotting and probing with a fragment of the first exon of the estrogen receptor gene were used to study the methylation state of this gene (Issa *et al.*, 1994). The effect of estrogen receptor gene methylation on expression was examined by reverse transcriptase polymerase chain reaction of cDNAs generated from RNA isolated from NNK-induced tumors and cell lines derived from X-ray-induced tumors.

The frequency for methylation of the estrogen receptor CpG island in rodent lung tumors is summarized in Figure 1. Five of six spontaneous A/J mouse tumors and 13/16 plutonium-induced rat lung tumors had significant methylation of the estrogen receptor CpG island. In contrast, only 3/16 NNK-induced rat lung tumors and 2/9 NNK-induced mouse lung tumors exhibited such methylation. The prevalence of estrogen receptor methylation in X-ray-induced tumors was intermediate, 9 of 21, to that observed in plutonium and NNK-induced tumors. Levels of estrogen receptor gene expression correlated with the methylation status of the tumor or cell line (data not shown). The present results suggest that in rodent lung carcinogenesis, spontaneous and radiation-induced tumors may evolve along

*Johns Hopkins University, Baltimore, Maryland

different molecular pathways than NNK-induced tumors and that CpG island methylation of the estrogen receptor gene could be a marker for environmental exposure to radiation. Studies are in progress to examine estrogen receptor methylation in human non-small-cell lung cancers from cigarette smokers and uranium miners.

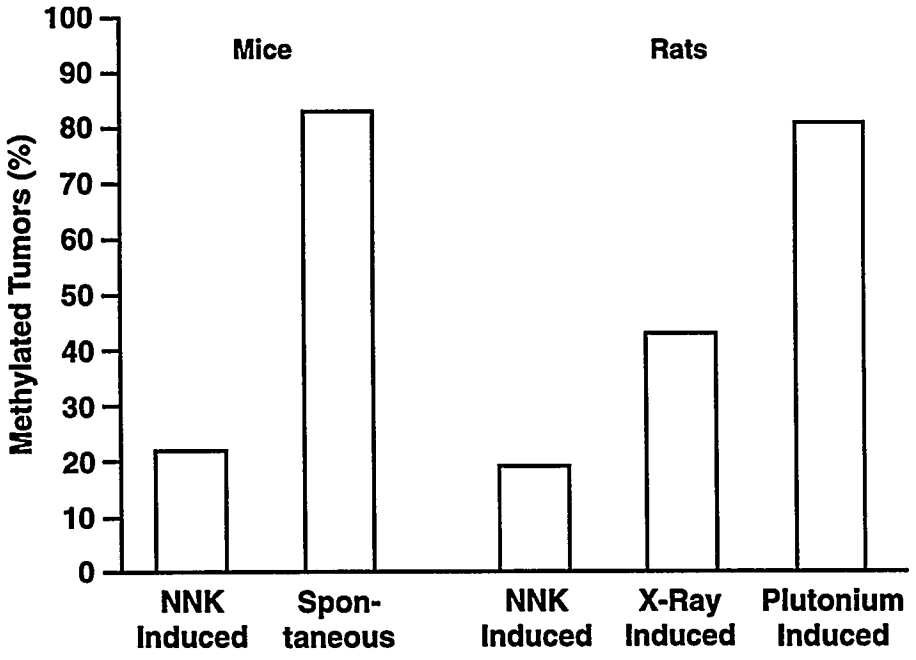

Figure 1. Estrogen receptor methylation in rodent lung tumors.

(Research at ITRI sponsored in part by NIH SPORE Contract No. 1-P50-CA58184, through Johns Hopkins University, and by the U.S. Department of Energy, under Contract No. DE-AC04-76EV01013.)

EXPRESSION OF THE $p16^{INK4a}$ TUMOR SUPPRESSOR GENE IN RODENT LUNG TUMORS

Deborah S. Swafford, Johannes Tesfaigzi, and Steven A. Belinsky*

Aberrations on the short arm of chromosome 9 are among the earliest genetic changes in human cancer. $p16^{INK4a}$ is a candidate tumor suppressor gene that lies within human 9p21, a chromosome region associated with frequent loss of heterozygosity in human lung tumors (Kamb, A. *et al. Science 264*: 436, 1995). The $p16^{INK4a}$ protein functions as an inhibitor of cyclin D_1-dependent kinases that phosphorylate the retinoblastoma (*Rb*) tumor suppressor gene product enabling cell-cycle progression. Thus, overexpression of cyclin D_1, mutation of cyclin-dependent kinase genes, or loss of $p16^{INK4a}$ function, can all result in functional inactivation of *Rb*. Inactivation of *Rb* by mutation or deletion can result in an increase in $p16^{INK4a}$ transcription, suggesting that an increased $p16^{INK4a}$ expression in a tumor cell signals dysfunction of the pathway (Shapiro, G. I. *et al. Cancer Res. 55[3]*: 505, 1995). The $p16^{INK4a}$ gene, unlike some tumor suppressor genes, is rarely inactivated by mutation. Instead, the expression of this gene is suppressed in some human cancers by hypermethylation of the CpG island within the first exon or by homozygous deletion (Merlo, A. *et al. Nature Med. 1[7]*: 686, 1995). Chromosome losses have been observed at 9p21 syntenic loci in tumors of the mouse and rat (Wiseman, R. *et al. Proc. Natl. Acad. Sci. 91*: 3759, 1994; Testa, J. R. *et al. Cytogenet. Cell Genet. 60*: 247, 1992), two species often used as animal models for pulmonary carcinogenesis. Expression of $p16^{INK4a}$ is lost in some mouse tumor cell lines, often due to homozygous deletion (Quelle, D. *et al. Oncogene 11*: 635, 1995). These observations indicate that $p16^{INK4a}$ dysfunction may play a role in the development of neoplasia in rodents as well as humans. The purpose of the current investigation was to define the extent to which $p16^{INK4a}$ dysfunction contributes to the development of rodent lung tumors and to determine the mechanism of inactivation of the gene.

The expression of the $p16^{INK4a}$ gene in rodent tissues was analyzed by reverse transcriptase polymerase chain reaction (RT-PCR). Because the required sequence information for the rat $p16^{INK4a}$ gene was not known, a fragment of the $p16^{INK4a}$ cDNA from an F344/N rat lung tumor was obtained by RT-PCR using primers based on the published mouse sequence (Quelle *et al.*, 1995). The fragment was inserted into the TA cloning vector™ (Stratagene, La Jolla, CA), and four clones of the fragment were sequenced by the dideoxy chain termination method. A comparison of the cloned fragment to the published sequence of mouse $p16^{INK4a}$ is shown in Figure 1. The overall homology between the mouse and rat sequences within this fragment is 83%, and the conserved sequences that define the INK protein family are present. This sequence information will facilitate future studies focused on investigating $p16^{INK4a}$ expression in rat tumors and cell lines.

Messenger RNAs were isolated from 15 A/J mouse lung tumors induced by the tobacco-specific nitrosamine 4-(methylnitrosamino)-1-(3-pyridyl)-1-butanone (NNK), and from four cell lines established from NNK-induced tumors. Reverse transcription produced cDNAs that were used as templates for PCR amplification of fragments of p16, cyclin D_1, and a constitutively expressed housekeeping gene, glyceraldehyde-phosphate dehydrogenase (GAPDH). The relative amounts of $p16^{INK4a}$ and cyclin D_1 PCR products compared to the GAPDH products provided an index of expression levels. Results of this analysis, shown in Figure 2, indicate that $p16^{INK4a}$ expression was retained, but varied 3-fold, among tumors as compared to normal lung tissue. In contrast, the tumor cell lines did not appear to express the transcript.

---

*UNM/ITRI Graduate Student

```
ATGGAGTCCGCTGCAGACAGACTAGCCAGGGCAGCGGCTGG-C-GTGAGC
|||||||||||||||||||||||| |||||||| ||  | || | ||| ||
ATGGAGTCCGCTGCAGACAGACTGGCCAGGGCGGCC-CAGGGCCGTGTGC

ACGAGGT-CGG-CACTGCTGGAAGCCGGGGCTTCACCAAACGCCCCGAAC
| || || ||| |||||||||||||||||||| ||| || ||||||||||||
ATGACGTGCGGGCACTGCTGGAAGCCGGGGTTTCGCCCAACGCCCCGAAC

ACTTTCGGTCGTACCCCGATACAGGTGATGATGATGGGCAACG-TGAAAT
  |||||||||||||||||||| |||||||||||||||||||||| | |  |
TCTTTCGGTCGTACCCCGATTCAGGTGATGATGATGGGCAACGGTCACGT

-GCGGAGCTCTCCTCGTCTC--CTATG-TGCGAGATTCGAACTGCGAGGA
 ||  |||||| || | |||  ||| | ||| ||||||||||||||||||
AGC--AGCTCTTCT-G-CTCAACTACGGTGC-AGATTCGAACTGCGAGGA

CCCCACCACCCTCTCCCGACCGGTCG-ACGACCG-AGCGCGGGAGGGCTT
|||||| ||| |||||||| ||||| | ||||| | |||||||||| |||||
CCCCACTACCTTCTCCCGCCCGGT-GCACGAC-GCAGCGCGGGAAGGCTT

CCTAGACACTCTGGTAGTACTG-CACCAGG-CAGGGGCGCGGCTGGATGT
||| |||||| |||||| || | | ||| || |||||||| ||||||||||||
CCTGGACACGCTGGTGGTGC-GTCACG-GGTCAGGGGCTCGGCTGGATGT

GCGCGATGCCT
|||||||||||
GCGCGATGCCT
```

Figure 1. The sequence of the cloned fragment of rat $p16^{INK4a}$ (top) is shown compared to published sequence of the analogous region of cDNA from the mouse (bottom). The highlighted regions indicate conserved sequences within the INK gene family.

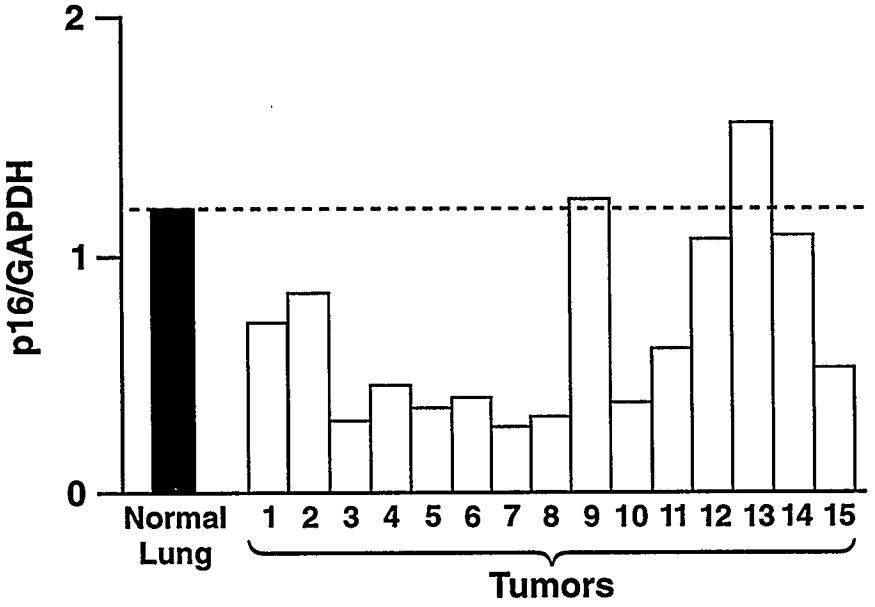

Figure 2. The relative abundance of RT-PCR products of $p16^{INK4a}$ and GAPDH in NNK-induced mouse lung tumor samples. The dotted line represents the relative abundance of the two products in normal lung tissue.

$p16^{INK4a}$ expression may be lost or varied due to factors including mutation, dysfunction of the *Rb* pathway, loss of one or both alleles, or methylation of the 5′ region of the gene. Experiments were designed to address these potential mechanisms. Single-strand conformational polymorphism analysis of the amplification products did not reveal any mutations in a 300 base-pair sequence extending from the beginning of the coding region to the middle of the second exon (data not shown). To address potential dysfunction of the *Rb* pathway, both *Rb* and cyclin D_1 were examined. Cyclin D_1 PCR products were present in all tumor samples at the same level as control tissue; additionally, cyclin D_1 protein levels in tumor tissues, assessed by Western blot, were not different from control lung. Western blot analysis also detected the presence of the Rb protein in each of seven tumor samples analyzed. Although allelic loss is difficult to detect in inbred mouse strains, DNA microsatellite analysis (data not shown) revealed the absence of a marker within the 9p21 syntenic region in the four tumor cell lines, suggesting that both alleles of the gene may be deleted, an observation consistent with complete lack of expression. This result has been confirmed by Southern blot using a 200 base-pair probe covering the first exon of the gene. In the primary tumors, Southern blot confirmed the presence of at least one $p16^{INK4a}$ allele. Preliminary analysis of methylation at specific sites within the region of the probe did not indicate a detectable level of gene methylation.

There is no evidence to suggest a loss of function of the $p16^{INK4a}$ tumor suppressor gene in these primary murine lung tumors by mutation, deletion, or methylation. The present studies did not determine whether the lower levels of $p16^{INK4a}$ transcript in some tumors represent loss of one allele, as suggested by a previous microsatellite analysis of similar lung tumors in hybrid mice (Herzog, C. R. *et al. Cancer Res. 54*: 4007 1994). *Rb* gene deletion or cyclin D_1 overexpression do not appear to be mechanisms of *Rb* suppression in these tumors; however, dysfunction elsewhere in the pathway requires further evaluation. The consistent lack of $p16^{INK4a}$ expression in tumor cell lines may indicate that loss of $p16^{INK4a}$, whether it occurs during tumor development or during establishment of the cell line, significantly enhances survival in culture. Further experiments are underway to determine the mechanism of diminished expression of $p16^{INK4a}$ in mouse lung tumors. Together, these data will help define the role of the $p16^{INK4a}$/*Rb* pathway in NNK-induced rodent lung tumors and cell lines.

(Research sponsored by the Office of Health and Environmental Research, U.S. Department of Energy, under Contract No. DE-AC04-76EV01013.)

EXPRESSION OF A TGF-β REGULATED CYCLIN-DEPENDENT KINASE INHIBITOR IN NORMAL AND IMMORTALIZED AIRWAY EPITHELIAL CELLS

Lauren A. Tierney, Catherine Bloomfield**, Neil F. Johnson, and John F. Lechner*

Tumors arising from epithelial cells, including lung cancers are frequently resistant to factors that regulate growth and differentiation in normal cells (Harris, C. C. *et al. Growth Factors and Their Receptors: Genetic Control and Rational Application*, Alan R. Liss Inc., 1989). One such factor is transforming growth factor-β (TGF-β). Escape from the growth-inhibitory effects of TGF-β is thought to be a key step in the transformation of airway epithelial cells (Mausi, T. *et al. Proc. Natl. Acad. Sci. USA 83*: 2438, 1986). This observation is supported by the fact that most lung cancer cell lines are not growth inhibited by TGF-β or serum, which contains TGF-β. In fact, most lung cancer cell lines require serum for growth (Lechner, J. F. *et al. Cancer Res. 43*: 5915, 1983). In contrast, normal human bronchial epithelial (NHBE) cells are exquisitely sensitive to growth-inhibitory and differentiating effects of TGF-β. When plated at low density, in the presence of picoMolar (pM) concentrations of TGF-β, NHBE cells terminally differentiate and ultimately die (Yang, K. *et al. Am. J. Pathol. 137*: 833, 1990). The recent identification of a novel cyclin-dependent kinase inhibitor, $p15^{INK4B}$, which is regulated by TGF-β, suggests a mechanism by which TGF-β mediates growth arrest in NHBE cells. $p15^{INK4B}$ was first identified in human keratinocytes, which in the presence of TGF-β, showed a 30-fold induction of $p15^{INK4B}$ at the transcript level (Hannon, G. J. *et al. Nature 371*: 257, 1994). $p15^{INK4B}$ is thought to act by binding to the cyclin-dependent kinase/cyclin D1 (CDK4 or 6/cyclin D1) complex, thus preventing the phosphorylation of the retinoblastoma gene product (pRb) and subsequent G1/S checkpoint arrest (reviewed in Hopkin, K. J. *NIH Res. 6*: 40, 1994). The purpose of this study was two-fold: (1) to determine if $p15^{INK4B}$ is induced by TGF-β in NHBE cells or immortalized bronchial epithelial (R.1) cells and if that induction corresponds to a G1/S cell-cycle arrest; (2) to determine the temporal relationship between $p15^{INK4B}$ induction, cell-cycle arrest, and the phosphorylation state of the pRB because it is thought that $p15^{INK4B}$ acts indirectly by preventing phosphorylation of the RB gene product. In this study, expression of $p15^{INK4B}$ was examined in NHBE cells and R.1 cells (Ke, Y. *et al. Differentiation 38*: 60, 1988) at different time intervals following TGF-β treatment. The expression of this kinase inhibitor and its relationship to the cell cycle and the pRb phosphorylation state were examined in cells that were both sensitive (NHBE) and resistant (R.1) to the effects of TGF-β.

Keratinocytes, NHBE cells, and R.1 cells were plated on chamber slides, grown to 70% confluence, and treated with 10 pM TGF-β for 0, 4, 8, or 24 h. Slides were fixed in methanol and immunostained with an affinity-purified rabbit polyclonal anti-$p15^{INK4B}$ antibody (K-18, Santa Cruz Biotechnologies, Santa Cruz, CA) which was pre-titered by using TGF-β-treated keratinocytes as a positive control. A rhodamine-conjugated secondary antibody was used to detect the immunoreacted anti-$p15^{INK4B}$ antibody. Cells were visualized using a mercury lamp and epifluorescence microscopy.

Immunostaining for flow-cytometric detection of $p15^{INK4B}$ was performed in suspension essentially as described above except that a FITC-conjugated streptavidin complex (Vector) was used. Cell suspensions were also stained for DNA with 25 μg of propidium iodide (PI) following treatment with 100 μg RNase. Samples were analyzed on a FACStar flow cytometer (Becton Dickenson Immunocytometry Systems, San Jose, CA). The cells were separated into G0/G1 and G2/M populations based on the PI fluorescence and forward scatter. Relative levels of $p15^{INK4B}$ were

---

*UNM/ITRI Graduate Student

**NASA/Lovelace-Anderson Endowment Fund Summer Student Research Participant

determined by comparing histograms of the unexposed (time 0) and exposed NHBE and R.1 cells and applying a cumulative subtraction method.

The pRB phosphorylation state was analyzed by SDS-PAGE and immunoblotting (Ludlow, J. W. *et al. Cell 56*: 57, 1989). Phosphorylation state of the pRb protein was determined by examining for mobility shifts in two 105 kd bands representing the fast migrating, under-phosphorylated form and the slower migrating, phosphorylated form as previously described (Mittnact, S. and R. Weinberg. *Cell 65*: 381, 1991).

$p15^{INK4B}$ expression as detected by immunocytochemistry and flow-cytometry (Fig. 1) was induced in NHBE cells after TGF-β treatment. Maximal induction in two separate experiments occurred at 8 h post TGF-β treatment, and $p15^{INK4B}$ expression returned to control levels by 24 h post-treatment (Fig. 1A). Cytologically, cells lacking p15INK4B expression at 24 h showed characteristic features of squamous differentiation. These results suggest that $p15^{INK4B}$ is essential for growth arrest in G1, but that other downstream events are involved in initiation of the terminally differentiated phenotype. As expected, induction of the protein paralleled both the accumulation of cells in G1 phase at 8 h (Fig. 1B) and the appearance of the predominately under-phosphorylated form of the pRb, indicating that induction of $p15^{INK4B}$ and pRb phosphorylation are coupled events and suggesting that $p15^{INK4B}$ prevents pRb phosphorylation in NHBE cells. The TGF-β-resistant R.1 cells (BEAS-2B) showed no evidence of $p15^{INK4B}$ up-regulation following TGF-β treatment, nor did these cells accumulate in the G1 phase of the cell cycle. Consistent with other viral oncoprotein immortalized cells, the inactivated pRb protein was primarily in the under-phosphorylated state in R.1 cells (Ludlow, *et al.*, 1989).

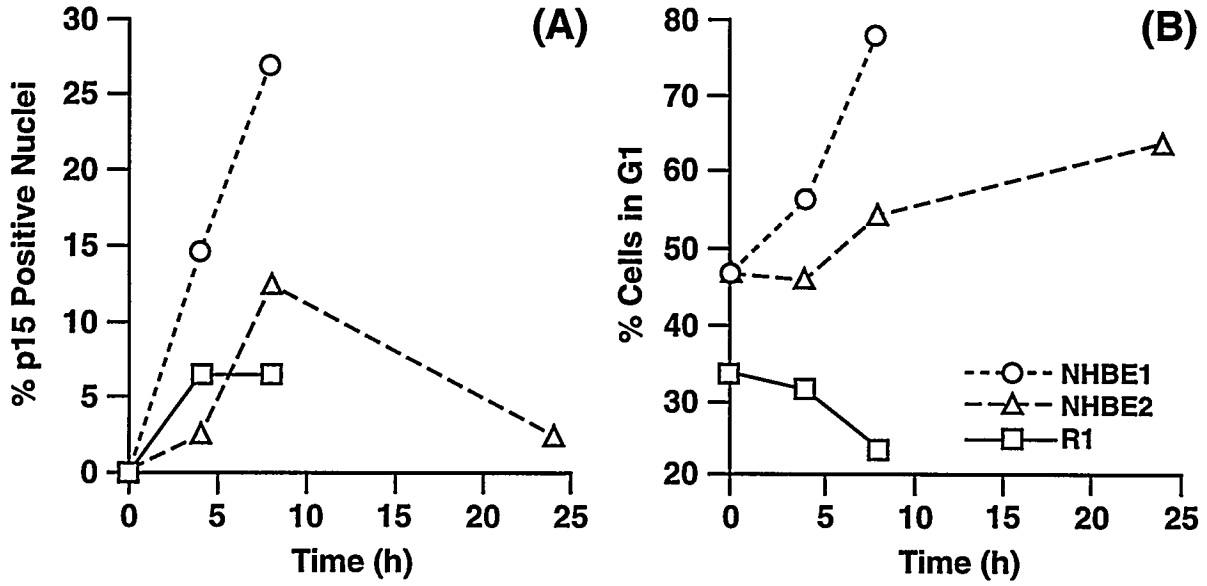

Figure 1. (A) Induction of the $p15^{INK4B}$ protein in two clones of NHBE cells following treatment with 10 pM TGF-β. $P15^{INK4B}$ was not induced in immortalized BEAS-2B subclone (R.1). (B) Percent of cells arrested in G1 following treatment with 10 pM TGF-β. Growth of BEAS-2B subclones (R.1) did not arrest in response to TGF-β.

These results suggest that the cyclin-dependent kinase inhibitor, $p15^{INK4B}$, is involved in airway epithelial cell differentiation and that loss or reduction of expression plays a role in the resistance of transformed or neoplastic cells to the growth-inhibitory effects of TGF-β. Consequently, the loss of $p15^{INK4B}$ function may represent a step toward epithelial cell transformation and the subsequent

formation of epithelial cancers. These findings are supported by the fact that $p15^{INK4B}$ and the related protein, $p16^{INK4A}$ at chromosome location 9p21 are frequently lost in lung cancer (Washimi, O. *et al. Cancer Res. 55*: 514, 1995). Mechanistic studies including transfection of cells lacking $p15^{INK4B}$ expression with the wild-type $p15^{INK4B}$ gene may provide evidence that $p15^{INK4B}$ is a functional growth suppressor gene in airway epithelial cells.

(Research sponsored by the Office of Health and Environmental Research, U. S. Department of Energy, under Contract No. DE-AC04-76EV01013.)

ALTERED EXPRESSION OF THE IQGAP1 GENE IN HUMAN LUNG CANCER CELL LINES

Charles E. Mitchell, William A. Palmisano, John F. Lechner, Andre Bernards, and Lawrence Weissbach**

IQGAP1 is a GTPase activation protein that accelerates GTP hydrolysis by normal p21 *ras* proteins. Therefore, IQGAP1 could act as an upstream affecter of p21 *ras* activity by converting excess amounts of active GTP-21 *ras* to inactive GDP-21 *ras*. IQGAP1 displays extensive sequence similarity to the catalytic domain of all previously reported *ras* GAPs, including the tumor suppressor gene protein neurofibromatosis type 1 (NF1) (Weissbach, L. *et al. J. Biol. Chem. 269*: 20517, 1994). It has been shown that abnormal NF1 protein cannot negatively regulate the activity of *ras* proteins in neuroblast cells. This observation supports the hypothesis that NF1 is a tumor suppressor gene whose product acts upstream of *ras*. IQGAP1 is primarily expressed in lung, where it may play a role similar to NF1 in regulating the activity of H-*ras* or K-*ras* proteins.

We have previously investigated loss of heterozygosity (LOH) in a panel of human primary lung cancer tissues using IQGAP1 as a probe (1993–94 Annual Report, p. 126). LOH was found in 20–25% of samples analyzed. Several studies show that other genetic alterations such as point mutations, frame-shift mutations, small deletions, and alteration in gene expression may be responsible for the initiation and/or progression of cancer (Lee, W.-H. *et al. Science 235*: 1394, 1987). The purpose of the present investigation was to determine whether alterations in the expression of the IQGAP1 gene were present in human lung cancer cell lines.

SW900, Calu-1, Calu-3, Calu-6, A549, A427 (human lung cancer cell lines), and SW480 (human liver cancer cell line) were obtained from ATCC (Rockville, Maryland), while 3-90t, 54-t, 76-t, 114-87-t, and 253-t (human lung cancer cell lines) were obtained from Dr. Jill Siegfried (University of Pittsburgh, Pittsburgh, PA). Normal human bronchial epithelial cells were obtained from Clonetics (San Diego, CA). Each cell line was grown to 70% confluency, harvested, and subjected to total cellular RNA isolation using Tri Reagent (Molecular Research Center, Inc., Cincinnati, OH) according to the manufacturer's recommendations. Twenty μg of RNA from each cell line was size fractionated on a denaturing formaldehyde agarose (1.0%) gel and transferred onto Zetaprobe GT membrane (Bio-Rad Laboratories, Inc., Hercules, CA) by capillary action. The IQGAP1 cDNA probe was radiolabeled with [a-^{32}P]dCTP using randomly primed synthesis. The IQGAP1 cDNA probe was hybridized overnight at 65°C in 7.0% SDS/0.25 M Na_2HPO_4, pH 7.2. The membrane was washed twice at room temperature for 30 min each time in 5.0% SDS/20 mM Na_2HPO_4 and once at 65°C for 1 h in 1.0% SDS/20 mM Na_2HPO_4 before exposure to X-ray film at –70°C. Following autoradiography, the membrane was stripped and rehybridized with a glyceraldehyde-3-phosphate dehydrogenase (GAPDH) radiolabeled cDNA probe as a control for gel loading and transfer.

The blots showed that the IQGAP1 transcript was approximately 7.5–8.0 kilobases in size (Fig. 1A). Four of the 12 cell lines (253-t, 76-t, SW900, and A427) showed reduced or complete loss of IQGAP1 expression. Normal and lung cancer cell line RNA expressed similar levels of GAPDH (Fig. 1B). Southern analysis of these same cell lines showed no structional alterations at the DNA level (data not shown).

The IQGAP1 gene is expressed at high levels in normal lung (Weissbach *et al.*, 1994). A loss of expression could play a major role in the initiation and/or progression of lung cancer. In the

*Massachusetts General Hospital, Boston, Massachusetts

present study, one third of the cell lines investigated exhibited altered expression of IQGAP1, and our previous report documented that 20–25% of tumors have LOH of the IQGAP1 gene as detected by Southern analysis. Thus, a change in expression and/or structural alteration of IQGAP gene is a frequent event in human lung cancer.

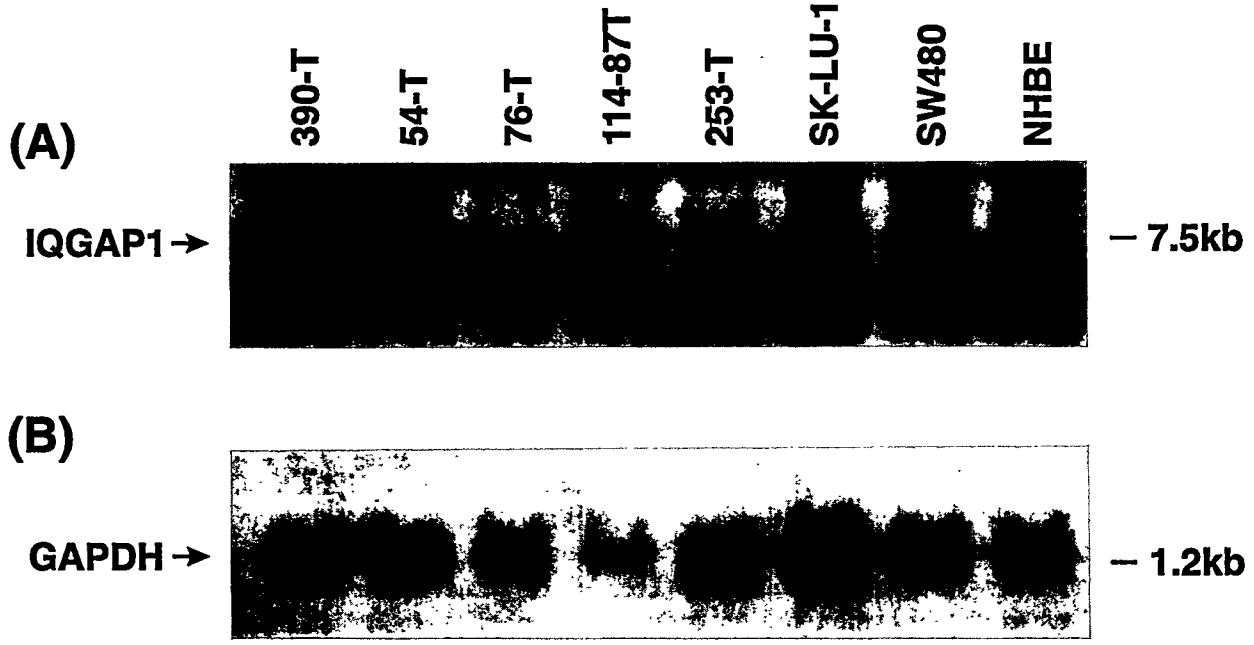

Figure 1. (A) Representative Northern analysis of IQGAP1 expression in normal and human lung cancer cell lines. Each lane was loaded with 20 μg of total RNA from each cell line. All cell lines except 253t and 76t express a 7.5-kB mRNA of IQGAP1. (B) A glyceraldehyde-3-phosphate dehydrogenase (GAPDH) cDNA was used as a control for RNA integrity.

IQGAP1 functions as other GAPs by controlling the activity of *ras*. Although *ras* is ubiquitously expressed in cells, the expression of IQGAP1 may be the predominant regulator of *ras* activity in the lung due to its unique tissue specificity. Dysfunctions in GAPs are associated with higher levels of *ras* proteins in the active *ras* state and with higher levels of cell proliferation. The H-*ras* protein has been shown to be overexpressed in many human lung tumors, and it remains to be determined if this overexpression is related to alterations in the IQGAP1 gene. Future studies will focus on defining this possible relationship. Additional studies will also focus on determining the mechanisms responsible for the reduced expression of IQGAP1. These investigations will contribute to an understanding of the role(s) the IQGAP1 gene plays in the initiation and /or progression of lung cancer.

(Research sponsored by the Office of Health and Environmental Research, U.S. Department of Energy, under Contract No. DE-AC04-76EV01013.)

CHARACTERIZATION OF CLONED CELLS FROM AN IMMORTALIZED FETAL PULMONARY TYPE II CELL LINE

Rogene F. Henderson, James J. Waide, and John F. Lechner

A cultured cell line that maintained expression of pulmonary type II cell markers of differentiation would be advantageous to generate a large number of homogenous cells in which to study the biochemical functions of type II cells. Type II epithelial cells are the source of pulmonary surfactant and a cell of origin for pulmonary adenomas. Last year our laboratory reported the induction of expression of two phenotypic markers of pulmonary type II cells (alkaline phosphatase activity and surfactant lipid synthesis) in cultured fetal rat lung epithelial (FRLE) cells, a spontaneously immortalized cell line of fetal rat lung type II cell origin (1993–94 Annual Report, p. 68). Subsequently, the induction of the ability to synthesize surfactant lipid became difficult to repeat. We hypothesized that the cell line was heterogenous and some cells were more like type II cells than others. The purpose of this study was to test this hypothesis and to obtain a cultured cell line with type II cell phenotypic markers by cloning several FRLE cells and characterizing them for phenotypic markers of type II cells (alkaline phosphatase activity and presence of surfactant lipids).

FRLE cells (Passage-87) were cultured in RPMI Medium 1640/10% fetal bovine serum (FBS) containing 100 units penicillin and 0.1 mg streptomycin/mL in tissue culture dishes. The cells were incubated in a 37°C incubator with 5% CO_2. At confluency, the cells were harvested by trypsinization and diluted to a final concentration of 0.67 cells/200 µL of media containing 10% FBS. Each well of a 96-well Corning tissue culture plate received 200 µL cell suspension. After 7–10 days of culture, wells with cells were harvested and transferred to 24-well Corning tissue culture plates. Finally, cells were transferred to 60 mm dishes to obtain sufficient numbers for phospholipid and alkaline phosphatase assays.

Cell lines were treated with 2 mM butyrate for induction of alkaline phosphatase as reported earlier (1993–94 Annual Report, p. 68). Alkaline phosphatase activity was assayed by standard clinical chemistry techniques. The surfactant phospholipids (disaturated phospholipids) were assayed by first separating the disaturated phospholipids from the other phospholipids by cryochromatography (Henderson, R. F. and M. H. Clayton. *Anal. Biochem. 70*: 440, 1976) and quantitation of the disaturated phospholipids by phosphorus analysis (Rouser, M. T. *et al. Lipids 1*: 85, 1966).

The results are shown in Figure 1. Thirty cloned cell lines were analyzed for induced alkaline phosphatase activity (on x-axis) and for percent of phospholipids that were disaturated (i.e., surfactant). Two clones had both high percentage disaturated phospholipids and high inducibility of alkaline phosphatase activity. These clones will be investigated further for their usefulness in studying the biochemical functions of type II cells.

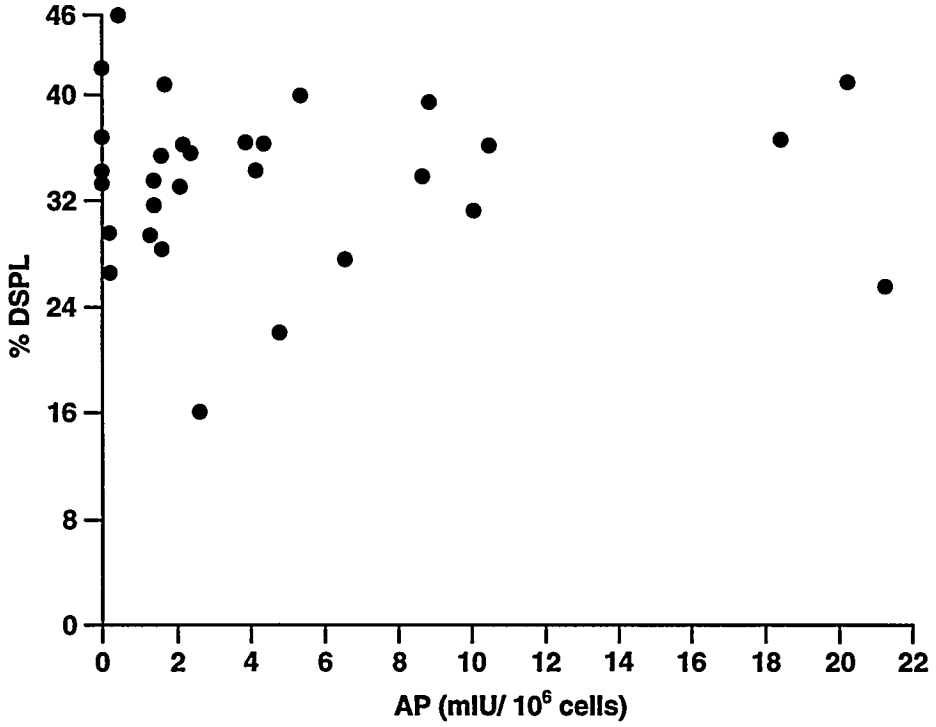

Figure 1. Correlation of induced alkaline phosphatase activity and disaturated phospholipid content in cloned FRLE cells. AP is alkaline phosphatase activity; DPSL is disaturated phospholipid; mIU is milli International Units.

(Research sponsored by the Office of Health and Environmental Research, U.S. Department of Energy, under Contract No. DE-AC04-76EV01013.)

VI. NONCARCINOGENIC RESPONSES TO INHALED TOXICANTS

SUBCHRONIC INHALATION OF CARBON TETRACHLORIDE ALTERS THE TISSUE RETENTION OF ACUTELY INHALED PLUTONIUM-239 NITRATE IN F344 RATS AND SYRIAN GOLDEN HAMSTERS

Janet M. Benson, Edward B. Barr, David L. Lundgren, and Kristen J. Nikula

Carbon tetrachloride (CCl_4) has been used extensively in the nuclear weapons industry, so it is likely that nuclear plant workers have been exposed to both CCl_4 and plutonium compounds. Future exposures may occur during "cleanup" operations at weapons productions sites such as the Hanford, Washington, and Rocky Flats, Colorado, facilities.

The purpose of this pilot study was to determine whether subchronic inhalation of CCl_4 by CDF (F344)/CrlBR rats and Syrian golden hamsters, at concentrations expected to produce some histological changes in liver, alters the hepatic retention and toxic effects of inhaled ^{239}Pu nitrate. The rationale underlying the use of the rats and hamsters as well as the experimental design has been previously described (1993–94 Annual Report, p. 146). Groups of male and female CDF (F344)/CrlBR rats and hamsters (Charles River Laboratories, Raleigh, NC) were exposed in whole-body inhalation chambers to air (controls), 5, 20, or 100 ppm CCl_4 6 h/d, 5 d/wk, for 16 wk. Subgroups of rats were also exposed once, nose-only, to aerosols of ^{239}Pu nitrate after 4 wk of exposure to air or CCl_4. The remaining animals were exposed once, nose-only, to an aerosol of ^{85}Sr-fused aluminosilicate particles (^{85}Sr-FAPs) to evaluate the effects of CCl_4 inhalation on particle clearance from the lung. All animals were then exposed for an additional 12 wk to CCl_4. Animals exposed to ^{239}Pu were sacrificed at intervals ranging from 4 h–13 wk post ^{239}Pu exposure for quantitation of ^{239}Pu in lung, liver, kidney, and femur and for histopathological evaluation of these tissues. ^{85}Sr activity was determined by whole-body counting throughout a 13 wk period following the ^{85}Sr-FAP exposure.

Body weight gain in male and female rats was significantly depressed only in animals inhaling 100 ppm CCl_4. Weight gain was depressed in male and female hamsters in a CCl_4 concentration-dependent manner (1993–94 Annual Report, p. 146). The depression in weight gain was not affected by co-exposure to ^{239}Pu.

Preliminary histopathological evaluations of hamster livers revealed no lesions in control animals and only minimal, variable lesions in hamsters exposed to 5 ppm CCl_4. Livers from all hamsters exposed to 20 ppm CCl_4 had degenerative hepatocellular lesions. All livers of hamsters exposed to 100 ppm had degenerative and necrotizing lesions and evidence of regeneration in the presence of ongoing injury. Histopathological changes in rat livers have not been evaluated to date.

The clearance patterns of ^{239}Pu from the lungs of rats and hamsters were different, but were unaffected by CCl_4 inhalation. The clearance pattern for ^{239}Pu from lungs of male and female rats was best described using a two-component, negative exponential equation. About 82–88% of the initial ^{239}Pu lung burden cleared with a half-time of 14–19 d. The remaining ^{239}Pu was retained in the lung over the time period evaluated. Clearance of ^{239}Pu from lungs of hamsters was best modeled using a single-component, negative exponential equation. The half-time for clearance of ^{239}Pu from hamster lungs was 35–50 d. Inhalation of 20 and 100 ppm CCl_4 by hamsters decreased ^{239}Pu uptake by liver (Fig. 1A, B). Uptake was slightly decreased in male hamsters exposed to 5 ppm CCl_4, but was unaffected in females exposed to 5 ppm CCl_4. Uptake of ^{239}Pu by liver and subsequent clearance were unaffected in rats inhaling 5 and 20 ppm CCl_4. Although uptake of ^{239}Pu was unaffected in rats inhaling 100 ppm CCl_4, clearance of the ^{239}Pu was impaired (Fig. 2A, B).

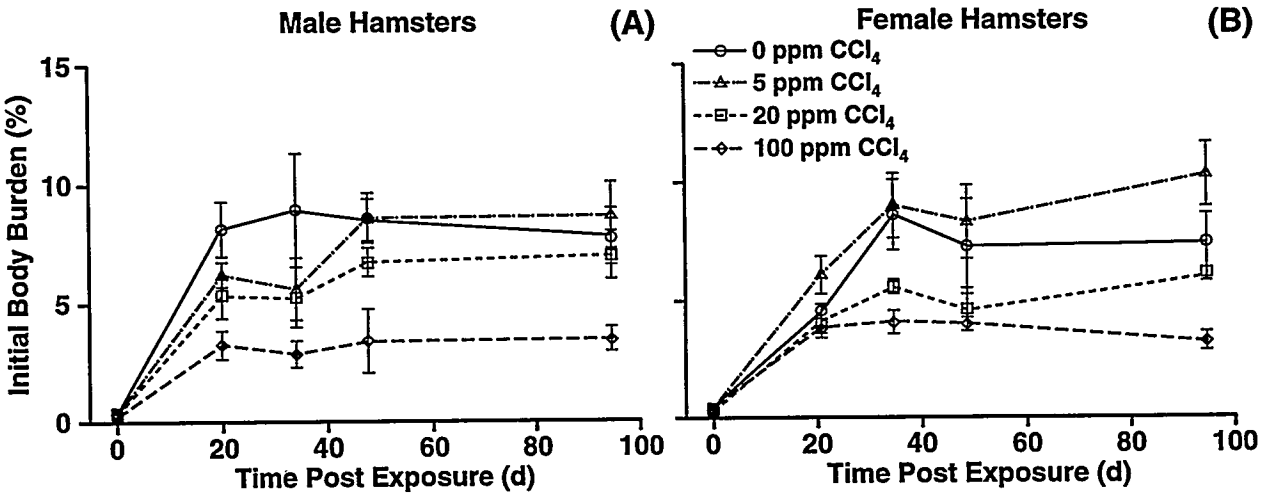

Figure 1. Uptake and retention of ^{239}Pu by male (A) and female (B) hamster liver. Results represent the mean percent initial lung burden ± SEM of six values.

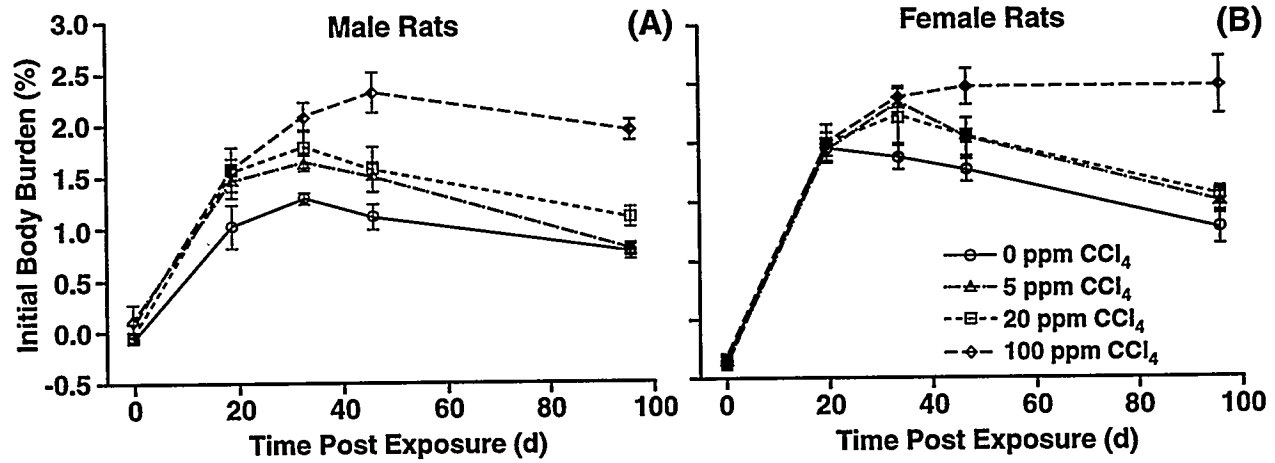

Figure 2. Uptake and retention of ^{239}Pu by male (A) and female (B) rat liver. Results represent the mean percent initial lung burden ± SEM of six values.

Data on the distribution of ^{239}Pu in lung, liver, kidney, and skeleton of female rats and hamsters are summarized in Table 1. Similar results were obtained in male rats and hamsters. A slightly greater percentage of the ^{239}Pu initial body burden (IBB) was retained in the hamsters (33% of the IBB) compared to rats (26%) 96 d after the ^{239}Pu exposure. The tissue distribution among control hamsters and rats also differed, with a greater percentage of the ^{239}Pu IBB present in lungs, livers, and kidneys and a lesser percentage of ^{239}Pu IBB in the skeleton of the hamsters compared to the rats. Inhalation of 20 or 100 ppm CCl_4 increased the retention of ^{239}Pu in liver, kidneys, and skeleton in male rats (data not shown). These effects were less pronounced in female rats (Table 1). Inhalation of 100 ppm CCl_4 decreased the retention of ^{239}Pu in livers of male and female hamsters. Inhalation of 20 or 100 ppm CCl_4 had no effect on liver retention of ^{239}Pu, but increased the retention of ^{239}Pu in the skeletons of male and female hamsters.

Table 1

Influence of CCl_4 Inhalation on the Tissue Distribution of ^{239}PuO in Female Rats and Hamsters

CCl_4 Concentration (ppm)	Percent ^{239}Pu Initial Body Burden (mean ± SEM) at 96 Days Post Exposure				
	Lung	Liver	Kidney	Skeleton	Total
Rats					
0	14.4 ± 1.2	1.26 ± 0.13	0.08 ± 0.002	10.7 ± 0.78	26
5	13.2 ± 1.2	1.35 ± 0.07	0.07 ± 0.004	9.68 ± 0.32	24
20	13.8 ± 0.8	1.52 ± 0.07	0.09 ± 0.005	10.6 ± 0.42	25
100	13.3 ± 1.0	2.44 ± 0.24	0.18 ± 0.010	11.6 ± 0.80	28
Hamsters					
0	21.9 ± 2.4	7.19 ± 1.2	0.13 ± 0.01	3.70 ± 0.64	33
5	27.0 ± 3.9	9.92 ± 1.3	0.25 ± 0.06	4.07 ± 0.48	41
20	21.4 ± 4.1	5.73 ± 0.22	0.17 ± 0.02	9.47 ± 1.9	37
100	28.0 ± 2.7	3.25 ± 0.39	0.11 ± 0.02	9.39 ± 1.3	41

Inhalation of 20 and 100 ppm CCl_4 by hamsters reduces uptake of ^{239}Pu solubilized from lung, shunting the ^{239}Pu to the skeleton. In rats, inhalation of 100 ppm CCl_4 appears to enhance the retention of ^{239}Pu by liver, but has no effect on the distribution of ^{239}Pu to other tissues, including the skeleton. The results of this pilot study suggest that inhalation of concentrations of CCl_4 that are hepatotoxic can alter the whole-body retention and tissue distribution of acutely inhaled, moderately soluble ^{239}Pu. However, inhalation of nontoxic concentrations of CCl_4 (5 ppm in hamster, 5 and 20 ppm in rat) has little effect on the whole-body retention or tissue distribution of inhaled moderately soluble $^{239}Pu(NO_3)_4$, and thereby may not enhance the radiation dose of moderately soluble ^{239}Pu in these animals.

(Research sponsored by the Assistant Secretary for Defense Programs, U.S. Department of Energy, under Contract No. DE-AC04-76EV01013.)

BERYLLIUM-INDUCED IMMUNE RESPONSE IN C3H MICE

Janet M. Benson, David E. Bice, Kristen J. Nikula,
Sara M. Clarke, Sally M. Thurlow*, and Duane E. Hilmas**

Studies conducted at ITRI over the past several years have investigated whether Beagle dogs, monkeys, and mice are suitable models for human chronic beryllium-induced lung disease (CBD). Recent studies have focused on the histopathological and immunopathological changes occurring in A/J and C3H/HeJ mice acutely exposed by inhalation to Be metal (1991–92 Annual Report, p. 171). Lung lesions in both strains of mice included focal lymphocyte aggregates comprised primarily of B lymphocytes and lesser amounts of T-helper lymphocytes and microgranulomas consisting chiefly of macrophages and T-helper lymphocytes. The distribution of proliferating cells within the microgranulomas was similar to the distribution of T-helper cells. These results strongly suggested that A/J and C3H/HeJ mice respond to inhaled Be metal in a fashion similar to humans in terms of pulmonary lesions and the apparent *in situ* proliferation of T-helper cells.

The purpose of this study was to further characterize the pulmonary histopathological responses of the C3H/HeJ mouse to inhaled Be metal as a function of Be lung burden and to determine whether the changes observed in lung are immune-mediated or nonspecific responses to Be. Endpoints evaluated included: (1) histopathological changes in lung as a function of Be lung burden, (2) immunohistochemical identification of lymphocyte populations present in the lung lesions, (3) abilities of lung lymphocytes to proliferate in response to $BeSO_4$ challenge *in vitro*, (4) the presence of a delayed-type hypersensitivity response to a footpad injection of $BeSO_4$, and (5) the presence of Be-specific IgG antibodies in serum.

Groups of 80 female C3H/HeJ mice, 8 ± 1 wk of age, were sham exposed "nose only" to filtered air or were exposed to Be metal aerosols to achieve target lung burdens of 10, 20, and 40 μg Be. Groups of eight mice per exposure level were sacrificed 7 d after the exposure for quantitation of Be initial lung burdens. Additional groups of 14–16 mice were sacrificed 60, 120, and 240 d after the exposure for endpoint evaluation. Subgroups of mice were challenged 48 h before sacrifice by intradermal injection of $BeSO_4$ in the right hind footpad to evaluate Be-induced, delayed-type hypersensitivity. Footpad thicknesses were measured using an engineering gauge 24 and 48 h later. The left hind footpad injected with saline was used as a control.

All mice were sacrificed using an overdose of pentobarbital. Blood for IgG measurement was obtained by cardiac puncture. Methods for measuring Be-specific IgG have been described (Clark, S. M. *J. Immunol. Methods 137*: 65). Lungs to be evaluated for Be were acid digested, and Be concentrations were determined by flame atomic absorption spectroscopy. The left lungs of animals sacrificed for evaluation of histopathology (6–8 mice/exposure groups/time period) were perfused with Tissue Tek and frozen in liquid nitrogen, or perfused with periodate-lysine-paraformaldehyde and embedded in paraffin prior to sectioning for immunohistochemical staining. Lung-associated lymph nodes and spleens were also frozen for histological evaluation. Right lungs were fixed in 10% neutral-buffered formalin, sectioned at 5 μm, and stained with hematoxylin and eosin. Popliteal lymph nodes were examined and weighed as a secondary indicator of the presence of a delayed hypersensitivity response in challenged footpads.

*DynCorp of Colorado, Inc., Golden, Colorado

Separate groups of mice (9/exposure group/time period) were sacrificed for isolation of lung lymphocytes for the lymphocyte proliferation assays. Lungs were perfused through the heart to remove blood and minced in a small volume of RPMI culture medium. The minced lungs were passed through a tissue sieve, and the cell suspensions were washed three times in incomplete culture medium. The cell suspensions from individual mice were incubated overnight at 37°C. The unattached cells, enriched in lymphocytes, were harvested the next day, washed, and counted. Cells from three mice per exposure group were pooled, and 150,000 cells per well were seeded into 96-well culture plates. Triplicate wells per sample were treated with medium (control cells), phytohemagglutinin (10 μg/well; positive control mitogen), or 0.1, 0.25, or 0.5 μM $BeSO_4$. Cells were incubated for 72 h, spiked with ^3H-labeled thymidine, and harvested 24 h later. ^3H activity in control and challenged samples was measured by liquid scintillation spectroscopy.

Be-inhalation resulted in chronic granulomatous pneumonia with multiple discrete interstitial aggregates of lymphocytes. There were perivascular and interstitial infiltrates comprised primarily of lymphocytes, monocytes, and plasma cells. Bronchiole-associated and perivascular lymphocytes were also increased. The severity of the lesions increased with Be lung burden and time after exposure. Immunohistochemical staining of lungs from high-dose mice at 240 d post exposure indicated that the majority of the lymphocytes in the discrete aggregates were B cells.

Mice administered $BeSO_4$ in the right hind footpad did not show typical delayed-type hypersensitivity responses to the challenge. The thickness of the footpad was not significantly increased in Be-exposed mice (Table 1), nor was the challenge associated with reddening of the footpad or enlargement of the associated popliteal lymph nodes (data not shown). Proliferation of lung lymphocytes in response to PHA stimulation was 1.7–4-fold greater than control cell proliferation. No increased proliferation over control levels occurred in lymphocytes incubated with $BeSO_4$ (Table 1). Be-specific IgG was detected at 240 d post exposure in 1/6 mice with a 20 μg Be ILB and in 4/6 mice with a 40 μg Be ILB.

Results of these studies confirm lymphocyte involvement in the pulmonary response to inhaled Be metal. Although both B lymphocytes- and T-helper lymphocytes have been identified as components of the lymphocyte aggregates and microgranulomas in the lung, we have been unable to confirm the presence of type II cell-mediated immune responses in the Be-exposed mice using *in vitro* and *in vivo* assays. The lack of a cell-mediated response is in contrast to findings that lymphocytes obtained from lungs and blood of some Be-exposed (presumably sensitized) humans proliferate *in vitro* in response to Be challenge. On the other hand, the presence of Be-specific IgG antibodies in serum from mice with the higher Be lung burdens suggests that Be has induced a humoral immune response. These results are consistent with recent findings by a co-author (S. M. Clarke) of Be-specific IgG antibodies in workers occupationally exposed to Be.

Table 1

Summary of Results of Immunological Endpoints in Mice Sacrificed 240 Days After Inhaling Be Metal

Beryllium Exposure Group (μg Be/lung)	Lymphocyte Stimulation Index[a] (mean ± SEM; n = 3)				Footpad Thickness[b] (mm) (mean ± SEM; n = 6)		Be-Specific IgG in Serum[c] (no. positive/ no. tested)
	PHA	0.1 μM Be	0.25 μM Be	0.5 μM Be	Control	48 h	
0	4.7 ± 2.6	1.1 ± 0.23	0.62 ± 0.11	0.54 ± 0.14	2.09 ± 0.03	2.10 ± 0.03	0/6
10	1.7 ± 0.04	1.0 ± 0.18	0.70 ± 0.11	1.1 ± 0.30	2.07 ± 0.02	2.12 ± 0.03	0/6
20	4.1 ± 1.8	1.3 ± 0.09	1.1 ± 0.12	1.08 ± 0.22	2.09 ± 0.05	2.22 ± 0.06	1/6
40	ND[d]	ND	ND	ND	2.12 ± 0.02	2.22 ± 0.02	4/6

[a]Calculated as $\frac{^3H \text{ disintegrations per minute in mitogen-stimulated cultures/fraction of lymphocytes in the cell preparation}}{^3H \text{ disintegrations per minute in control cell cultures/fraction of lymphocytes in the cell preparation}}$.

[b]Triplicate measurements were made on each mouse at each time using an engineering gauge.

[c]Each sample was tested in duplicate at eight dilutions (1/30 to 1/3840). Unknowns were compared to the normal control plus two standard deviations of the mean. Responses of unknown samples above this control value were considered positive.

[d]ND = not determined; lung lymphocytes isolated for these mice do not survive well in culture, especially when incubated with additional $BeSO_4$.

(Research sponsored by the Office of Health and Environmental Research, U.S. Department of Energy, under Contract No. DE-AC04-76EV01013.)

ACUTE INHALATION TOXICITY OF CARBONYL SULFIDE

Janet M. Benson, Fletcher F. Hahn, Edward B. Barr,
Johnnye L. Lewis, Alfred W. Nutt, and Alan R. Dahl*

Carbonyl sulfide (COS), a colorless gas, is a side product of industrial procedures such as coal hydrogenation and gasification. It is structurally related to and is a metabolite of carbon disulfide. COS is metabolized in the body by carbonic anhydrase to hydrogen sulfide (H_2S), which is thought to be responsible for COS toxicity (Chengalis, C. P. P. and R. A. Neal. *Toxicol. Appl. Pharmacol. 55:* 198, 1980). No threshold limit value for COS has been established.

The purpose of this study was to: (1) determine the median lethal concentration (LC_{50}) of COS; (2) determine target organs for COS toxicity; and (3) compare the effects of acutely inhaled COS with those of H_2S.

Initially, a range-finding study was conducted to estimate the LC_{50} for COS. Groups of three male and three female F344/Hsd rats (Harlen Sprague-Dawley, Indianapolis, IN; approximately 12 wk old) were exposed nose-only for 4 h to 250–1000 ppm COS to establish approximate lethality. During the exposures, COS gas (Aldrich Chemical Co., 96% pure) was metered from a lecture bottle and diluted as necessary to achieve the desired exposure concentrations. The concentration of COS in the inhalation chamber was monitored continuously throughout each exposure using a Miran Model 1A infrared spectrophotometer calibrated each exposure day using COS. Groups of seven male and female F344/Hsd rats were then exposed to 0, 500, 590, and 700 ppm COS for 4 h to determine the LC_{50}. During the exposures, rats were observed for behavioral changes. Heart rate, body temperature, and activity levels were monitored by computer in subsets of two males and two females using biotelemetric transmitters implanted 1 wk prior to exposure. An additional nine males and nine females were included in the LC_{50} studies and sacrificed after 1–4 h of exposure for measurement of the percentages of oxy- and carboxyhemoglobin in arterial blood. Rats dying during or within 24 h of exposure were counted as "dead" for calculations of the LC_{50}. All rats dying during or following COS exposure were subjected to a complete necropsy, and all tissues were fixed in 10% neutral buffered formalin for subsequent evaluation of histopathological changes. Surviving rats were observed for 14 d for clinical signs of toxicity and then sacrificed, necropsied, and tissues fixed in formalin for evaluation of histopathological changes.

All animals exposed to > 700 ppm COS died; no animals exposed to < 500 ppm died. The median lethal concentration was estimated at 590 ppm. The time to death was inversely proportional to the COS exposure concentration. Animals exposed to 1000, 700, and 500 ppm died in 2–3 h, 3–4 h, and from 4 h to within 24 h after exposure, respectively. During the exposures, the rats exhibited excitation followed by depression. Heart rates dropped steadily during the exposures, and temperature dropped from 37–35°C. The percentage of oxyhemoglobin in control animals averaged approximately 8%. Oxyhemoglobin percentages increased to as much as 24% in rats exposed for 4 h to 700 ppm COS, suggesting that COS inhibits respiration via cytochrome aa_3. Carboxyhemoglobin levels were unaffected by COS exposure.

A third group of studies was conducted to determine the nature and persistence of toxic effects of acute exposure to sublethal concentrations of COS. Groups of 34 male and female rats were exposed to 0, 450, 500, and 550 ppm COS for 4 h and held for up to 14 d post exposure for evaluation of clinical signs of toxicity. Subgroups of five males and five females were sacrificed 1,

*Westinghouse Savannah River Company, Aiken, South Carolina

2, 4, 7, and 14 d after the exposure by exsanguination while under pentobarbital anesthesia. Blood was taken for evaluation of hematology and serum chemistry. Right lungs were lavaged for determination of protein content and total and differential cell counts. Left lungs and remaining tissues were fixed in 10% neutral buffered formalin for histopathological evaluation. In addition, some brains were frozen in liquid nitrogen, or fixed in glutaraldehyde or Karnovsky's fixative for more detailed electron microscope evaluations of COS effects. Formalin-fixed tissues were trimmed and sectioned at 5 μm. Sections were stained using hematoxylin and eosin.

Some rats surviving exposure to 500 and 550 ppm COS exhibited mild to severe behavioral changes including barrel rotations, "wet dog" shakes, ataxia, head tilt, body tilt, and Straub tail. The ataxia was associated with the right hind quarter of the rats. Partial to complete recovery from these symptoms was achieved during the 14-d observation period. No behavioral changes were observed among rats exposed to 450 ppm COS.

The major target organ for COS toxicity was the brain. Vacuolation of myelin sheaths in the cerebellar peduncles, corpus callosum, or pyramidal tracts was the major lesion in all rats exposed to 1000 or 750 ppm. Focal necrosis of the cerebellar cortex and focal necrosis/gliosis of the cerebellar peduncles were the primary lesions in rats exposed to 500 and 590 ppm COS and surviving 3 to 14 d. There was generally good correlation between the presence of brain lesions and observation of behavioral changes in rats sacrificed after exposure to 500–590 ppm COS. No brain lesions were present in rats sacrificed 14 d after exposure to 450 ppm COS.

Hematological parameters such as red and white blood cell counts and white blood cell differential counts were not affected by exposure to sublethal concentrations of COS. Total numbers of nucleated cells recovered from lung by bronchoalveolar lavage and differential cell counts were also not affected by acute exposure to sublethal concentrations of COS. The latter results were consistent with the lack of histopathological changes occurring in the lungs.

Results of these studies indicate COS (with an LC_{50} of 590 ppm) is slightly less acutely toxic than H_2S (LC_{50} of 440 ppm). Increases in blood oxyhemoglobin content in rats exposed to COS suggest that COS, like H_2S inhibits respiration via cytochrome aa_3. Both COS and H_2S appear to target the brain; however, lesions associated with COS inhalation focus on the white matter of cerebellum and are not consistent with anoxia. Inhalation of H_2S produces both cerebellar and cerebral lesions that are consistent with anoxia. In conclusion, the toxic effects associated with acute COS inhalation may not be totally due to its conversion to H_2S within the body.

(Research sponsored by the Westinghouse Savannah River Company with the U.S. Department of Energy, under Contract No. DE-AC04-76EV01013.)

DYSFUNCTION OF PULMONARY IMMUNITY IN ATOPIC ASTHMA: POSSIBLE ROLE OF T HELPER CELLS

*David E. Bice and Mark R. Schuyler**

Atopic asthma is characterized by the production of allergen-specific IgE and IgG_4 antibody and airway hyperreactivity caused by interactions between the immune system and inhaled allergens. Recent studies suggest that the production of IgE and IgG_4 antibody important in atopic disease requires help from Th2 lymphocytes, while Th1 lymphocytes support the production of immune responses that would not cause asthma (Nusslein, H. G. and H. L. Spiegelberg. *J. Clin. Lab. Anal. 4*: 414, 1990; Ishizaka, A. *et al. Clin. Exp. Immunol. 79*: 392, 1990). The evaluation of cells from the lungs of asthmatics indicated that they have elevated Th2 immune responses (Robinson, D. *et al. J. Allergy Clin. Immunol. 92*: 313, 1993). However, no study has compared the immune responses that develop in asthmatics and normals (people without asthma) after their lungs are exposed to a neoantigen. The purpose of this study was to determine if Th2 immunity would be produced to a neoantigen, keyhole limpet hemocyanin (KLH), deposited in the lungs of asthmatics, while Th1 immunity would be produced to KLH deposited in the lungs of nonasthmatics.

Nine atopic asthmatics and nine nonatopic controls were used in this study. All subjects were nonsmokers, < 40 y of age, with normal chest films. None was exposed to chronic medications, immunotherapy, or corticosteroid therapy for at least 6 mo prior to enrollment in this study. The mean age ± SEM for the asthmatics was 23.9 y of age while the normals were 24.3 ± 2.2 y of age. The male:female ratio was 3:6 for both normals and asthmatics. Normals had negative skin tests to 11 common aeroallergens and normal spirometry. Atopic asthmatics had at least two positive immediate skin tests with a mean of 7.7 positive skin tests (range = 5–11). None of the asthmatics had experienced symptomatic asthma within 4 wk prior to this study. Asthmatics airway reactivity to methacholine was determined as previously described (Chi, H. *et al. J. Allergy Clin. Immunol. 64*: 592, 1975), and all demonstrated either an increase of FEV_1 of at least 20% after inhalation of 200 μg albuterol or were reactive with a ≥ 20% decrease in FEV_1 after inhalation of < 25 mg/mL methacholine.

Each subject was immunized by instillation of 500 μg KLH (Vandenbark, A. A. *et al. Cell. Immunol. 60*: 240, 1981) in 1 mL into the superior lingula division of the lung using a fiberoptic bronchoscope. The right lingula of each subject served as an unexposed control. For fiberoptic bronchoscopy, subjects were premedicated with 1 mg atropine, lidocaine was used for local anesthesia, and midozolam (up to 2.5 mg i.v.) was administered as needed. Oxygen was supplemented and pulse oximetry monitored.

Blood and lung lavage samples from the left and right lingula lobes were used to evaluate the immune responses that developed. The levels of anti-KLH IgG_1, IgG_2, IgG_3, IgG_4, IgA_1, IgA_2, and IgM in serum and the production of anti-KLH antibody by blood lymphocytes were evaluated using blood samples taken multiple times through 25 d after instillation of KLH. We also evaluated the level of anti-KLH antibody in bronchoalveolar lavage fluid from both the control and immunized lung lobes at 11 d after immunization.

Anti-KLH antibody was found in serum from all subjects. There was no difference between atopics and normals in the levels or kinetics of anti-KLH IgG_1, IgG_2, IgG_3, IgA_1, IgA_2, and IgM.

*Veterans Administration Medical Center, and Department of Medicine, University of New Mexico, Albuquerque, New Mexico

Data are shown for IgG_1 (Fig. 1). However, atopics produced significantly more ($p < 0.05$) anti-KLH IgG_4 than normal controls (Fig. 2). Specific anti-KLH antibody was produced by blood cells from most subjects at d 8–12 after immunization, although there were no differences between asthmatics and normals. Anti-KLH IgA_1 and IgA_2 antibody was detected in bronchoalveolar lavage fluid from the immunized lung lobes of both groups of subjects with no difference between atopics and normals.

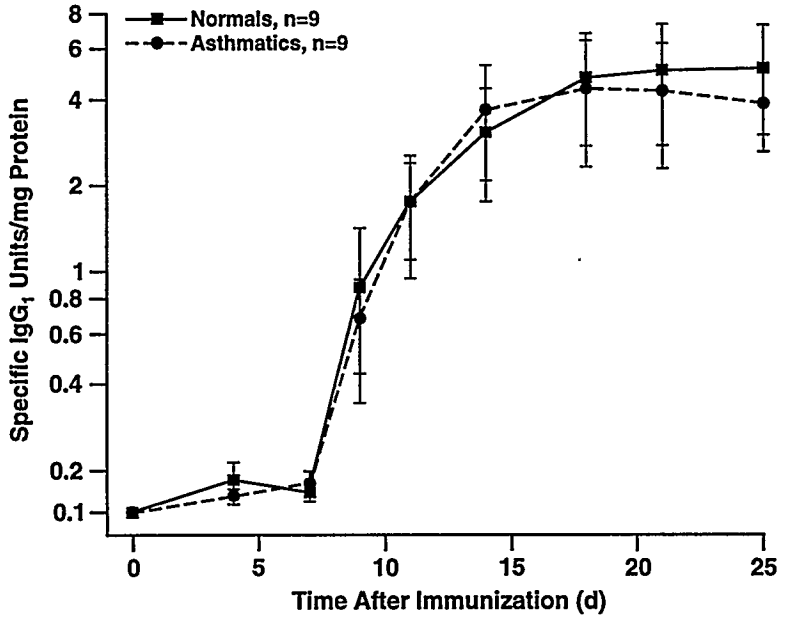

Figure 1. No significant differences were observed in the levels of anti-keyhole limpet hemocyanin (KLH) IgG_1 antibody (mean ± SE) in serum from normals (■) and from asthmatics (●).

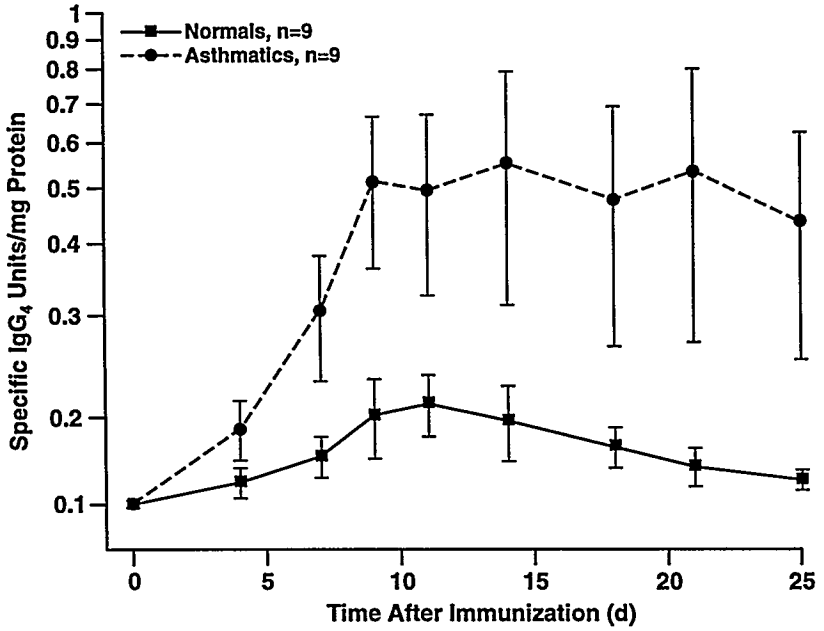

Figure 2. Significantly more anti-keyhole limpet hemocyanin (KLH) IgG_4 antibody (mean ± SE) was present in serum from asthmatics (●) than in serum from normals (■).

Because the production of IgG_4 requires Th2 immune help, the higher level of anti-KLH IgG_4 in the serum of asthmatics suggests that a Th2 immune response was produced to a neoantigen deposited in their lungs. One possible explanation for this result is that asthmatics are more susceptible genetically for the development of Th2 immune responses in their lungs. However, other risk factors such as the inhalation of pollutants and allergens especially at a young age may also be important in the induction of Th2 immunity and asthma (Ehrlich, R. *et al. Am. Rev. Respir. Dis. 145*: 594, 1992; Castleman, W. L. *et al. Am. J. Pathol. 137*: 821, 1990). A major concern is that the establishment of Th2 immune responses in the lungs of children could result in a permanent asthmatic status.

(Research sponsored by the Office of Health and Environmental Research, U.S. Department of Energy, under Contract No. DE-AC04-76EV01013.)

NONSPECIFIC AIRWAY REACTIVITY IN A MOUSE MODEL OF ASTHMA

D. David S. Collie, Julie A. Wilder**, and David E. Bice*

Animal models are indispensable for studies requiring an intact immune system, especially for studying the pathogenic mechanisms in atopic diseases, regulation of IgE production, and related biologic effects. Mice are particularly suitable and have been used extensively for such studies because their immune system is well characterized. Further, large numbers of mutants or inbred strains of mice are available that express deficiencies of individual immunologic processes, inflammatory cells, or mediator systems (Martin, T. R. *et al. J. Appl. Physiol. 64*: 2318, 1988). By comparing reactions in such mice with appropriate control animals, the unique roles of individual cells or mediators may be characterized more precisely in the pathogenesis of atopic respiratory diseases including asthma. However, given that asthma in humans is characterized by the presence of airway hyperresponsiveness to specific and nonspecific stimuli, it is important that animal models of this disease exhibit similar physiologic abnormalities. In the past, the size of the mouse has limited its versatility in this regard. However, recent studies (Martin *et al.*, 1988; DiCosmo, B. F. *et al. J. Clin. Invest. 94*: 2028, 1994; Brusselle, G. *et al. Am. J. Respir. Cell Mol. Biol. 12*: 254, 1995) indicate the feasibility of measuring pulmonary responses in living mice, thus facilitating the physiologic evaluation of putative mouse models of human asthma that have been well characterized at the immunologic and pathologic levels.

The purpose of this study was to assess nonspecific airway reactivity (NS-AHR) in a putative mouse model of human asthma. The model uses a heterozygous transgenic mouse that has had its germline DNA altered so that 20–30% of its T cells express a T-cell receptor (TCR) specific for an epitope of ovalbumin (OVA) (Murphy, K. A. *et al. Science 250*: 1720, 1990). Previous studies using transgenic mice from the University of New Mexico transgenic colony demonstrated that mice exposed to two to four OVA aerosol challenges (1 mg/m^3) develop peribronchial and perivascular inflammation with eosinophils in the infiltrates, antibodies to OVA, and elevated levels of total IgE. These features are consistent with those seen in human asthma. The particular immunologic advantage that this model holds lies in the ability to follow antigen-specific T cell traffic during evolution of an anti-OVA pulmonary immune response. Further, the high percentage of responding T cells should significantly improve the sensitivity of assays to detect antigen-specific cytokine responses during the development and manipulation of pulmonary inflammatory processes.

The development of nonspecific airway reactivity was assessed in six OVA-TCR+ Balb/c transgenic mice exposed to three aerosols of OVA administered at 14-d intervals. Responses were assessed 48–72 h following the last aerosolization and were compared to the responses of seven nonexposed Balb/c control mice. Pulmonary physiology was assessed using a specially fabricated volume displacement plethysmograph. Mice were anesthetized and mechanically ventilated via a surgically placed tracheal cannula. Pleural surface pressure was equilibrated to body surface pressure by surgically opening each side of the chest. Signals from respective transducers were amplified as appropriate, and data were acquired and analyzed by custom-designed computer software to yield values for total pulmonary resistance (R_L). NS-AHR was assessed by exposing mice to half-$\log_{10}$ increasing doses of methacholine [MCh; acetyl-(-methylcholine chloride)] (Sigma, St. Louis, MO) administered intravenously via a catheter inserted in the tail vein. R_L was assessed following each injection and the peak response recorded. Adequate time was allowed to facilitate the return of R_L to within 10% of the baseline values. A maximum dose of 3700 μg/mL MCh was used. Responsiveness was quantified by interpolation or extrapolation from each animal's dose-response curve to estimate the dose required to increase the R_L to 200% of the preinfusion value ($PC_{200}R_L$).

---

*Postdoctoral Fellow

**UNM/ITRI Pulmonary Epidemiology and Toxicology Training Program Participant

The response to infusion of saline and 14 μg/mL methacholine resulted in a significantly greater increase in R_L for the transgenic mice than for the controls (Mann-Whitney U test; $p < 0.05$) (Fig. 1). At higher methacholine dose rates, a trend toward increased responsiveness for the transgenics was apparent, but the variance within groups precluded statistical significance. $PC_{200}R_L$ values were significantly lower for the transgenic group than for the controls (Fig. 2) (Mann-Whitney U test; $p < 0.05$). Baseline measurements of R_L did not differ between the groups.

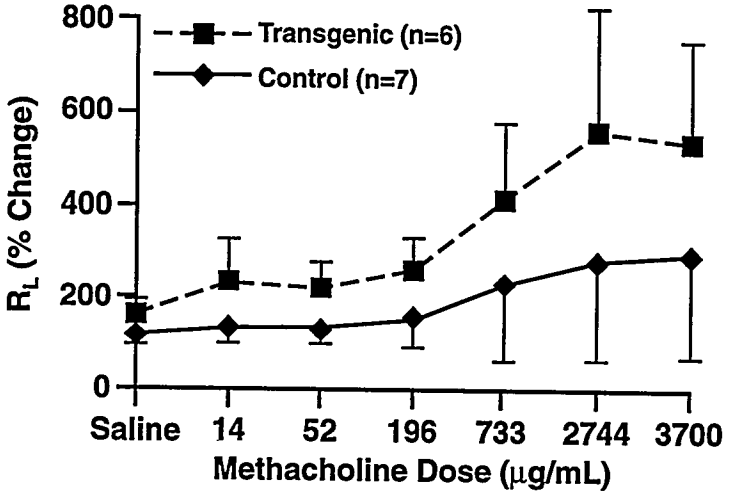

Figure 1. Methacholine dose-response curves for control and transgenic mice. Error bars represent S.E. of the mean.

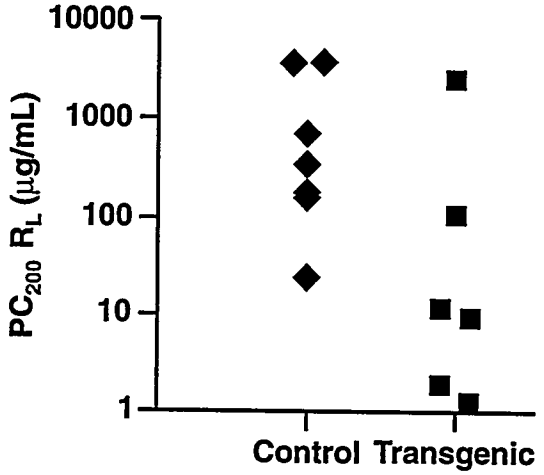

Figure 2. Airway reactivity of control and transgenic mice expressed in terms of $PC_{200}R_L$ values.

Our preliminary conclusion is that repeated aerosol exposure of OVA to OVA-TCR ± mice results in the development of airway hyperreactivity. This finding supports the relevance of this model for future evaluation of factors affecting the development and expression of human asthma.

Future work will provide details of the morphometry of the methacholine-induced bronchoconstriction and will further seek to determine the relationship between cigarette smoke exposure and the development of NS-AHR in the transgenic mouse model.

(Research sponsored by the Office of Health and Environmental Research, U.S. Department of Energy, under Contract No. DE-AC04-76EV01013.)

VII. THE APPLICATION OF MATHEMATICAL MODELING TO RISK ESTIMATES

COMPARISON OF BONE CANCER RISKS IN BEAGLE DOGS FOR INHALED PLUTONIUM-238 DIOXIDE, INHALED STRONTIUM-90 CHLORIDE, AND INJECTED STRONTIUM-90

*William C. Griffith, Bruce A. Muggenburg, Fletcher F. Hahn, Raymond A. Guilmette, Bruce B. Boecker, and Ray D. Lloyd**

There is a continuing need to understand dose-response relationships for ionizing radiation in order to protect the health of the public and nuclear workers from undue exposures. However, relatively few human populations have been exposed to doses of radiation high enough to cause observable, long-term health effects from which to derive dose-response relationships. This is particularly true for internally deposited radionuclides, although much effort has been devoted to epidemiological studies of the few types of exposures available, including lung cancers in uranium miners from the inhalation of the radioactive decay products of Ra, liver cancers in patients injected with Thorotrast X-ray contrast medium containing Th, bone cancers in radium dial painters who ingested Ra, and bone cancers in patients who received therapeutic doses of Ra. These four types of exposures to internally deposited radionuclides provide a basis for understanding the health effects of many other radionuclides for which a potential for exposure exists. However, potential exposures to internally deposited radionuclides may differ in many modifying factors, such as route of exposure, population differences, and physical, chemical, and elemental forms of radionuclides. The only means available to study many of these modifying factors has been in laboratory animals, and to then extrapolate the results to humans.

Many animal studies have been performed that mimic potential exposures of people in order to understand how these modifying factors affect radiation dose-response relationships. Insights into modifying factors can be best understood by investigators combining studies for analyses. Joint analyses can be formulated for radionuclides that have lung, bone, or liver as their target organ.

The purpose of this report is to discuss how joint analyses of results from lifetime studies of health risks in dogs with internally deposited radionuclides can help fill gaps in human data in this important area. An example of such an analysis is given using bone cancer risk.

To illustrate the possibilities for combining studies, an analysis has been made of the effect of linear energy transfer and route of exposure based upon studies of bone tumor induction in Beagle dogs with inhaled $^{238}PuO_2$ (Muggenburg, B. A. *et al. Radiat. Res.*, in press) and inhaled $^{90}SrCl_2$ done at the ITRI (Gillett, N. A. *et al. Int. J. Radiat. Biol. 61*: 821, 1992), and from injected ^{90}Sr done at the University of Utah (Lloyd, R. D. *et al. Health Phys. 30*: 183, 1976). The exposed dogs living at least 1 y after exposure are shown in Table 1 classified as to how long each dog lived after exposure, the cumulative radiation dose to the skeleton each dog received by death, and whether the dog developed a bone tumor. The radiation doses are absorbed doses averaged over the total skeletal mass. Both ^{238}Pu and ^{90}Sr are retained in the dog skeleton with very long biological half-lives, and because of their long physical half-lives, continue to irradiate the skeleton throughout the lifetime of the dog. The study of inhaled $^{238}PuO_2$ included 144 dogs with doses from 0.06–8.7 Gy; 93 dogs developed bone tumors with doses from 0.2–6 Gy, and there were seven dogs with doses below 0.2 Gy (median 0.1 Gy). The study of inhaled $^{90}SrCl_2$ included 59 dogs with doses from 5–200 Gy; 30 developed bone cancers with doses from 26–200 Gy, and there were 14 dogs with doses below 26 Gy (median 6 Gy). The study of injected ^{90}Sr included 85 dogs with doses from 0.7–160 Gy; 19

*Radiobiology Division, University of Utah School of Medicine, Salt Lake City, Utah

developed bone cancer with doses from 18–160 Gy, and there were 40 dogs with doses below 18 Gy (median 4 Gy).

Table 1

Number of Dogs with Bone Tumors and Number of Dogs at 3-y Intervals after Exposure for Ranges of Average Bone Doses Calculated to Time of Death. The dogs had to live at least 1 y after exposure.

	Longevity After Exposure (y)					
Dose Range	1–2	3–5	6–8	9–11	12–14	15–17
Inhaled $^{238}PuO_2$						
0.03–0.1 Gy	–	–	0/1	–	0/1	0/1
0.1–0.3 Gy	–	0/2	0/1	1/3	1/6	0/1
0.3–1 Gy	–	0/2	5/9	10/14	0/10	0/1
1–3 Gy	0/3	33/36	13/15	7/10	–	–
3–10 Gy	1/2	18/24	1/1	–	–	–
Inhaled $^{90}SrCl_2$						
3–10 Gy	–	–	0/2	0/2	0/3	0/2
10–30 Gy	–	–	1/1	0/2	0/4	–
30–100 Gy	2/3	3/3	4/6	0/2	0/5	0/1
100–30 Gy	6/8	9/10	4/4	1/2	–	–
Injected ^{90}Sr						
0.3–1 Gy	–	–	0/2	0/2	0/2	–
1–3 Gy	–	0/2	0/1	0/1	0/4	0/3
3–10 Gy	–	–	0/4	0/6	0/9	0/2
10–30 Gy	–	–	0/2	1/2	0/4	–
30–100 Gy	3/4	4/7	5/9	0/4	2/6	0/1
100–300 Gy	1/1	2/6	1/1	–	–	–

The bone cancers were analyzed with a proportional hazards model to estimate the relative risk. This type of analysis describes how the age-specific tumor rates are altered by radiation dose. The change with radiation dose is described by a relative risk function. The function for the relative risk used in this study was $1 + \alpha d + \beta d^{\gamma}$ (d is the time-dependent average skeletal dose in Gy; α, β, and γ are estimated by maximum likelihood methods) for each radionuclide, and differences between radionuclides were tested using likelihood ratios.

There were no significant differences in bone cancer incidence between the two routes of exposure of inhalation and injection of ^{90}Sr (Fig. 1). There was a large difference between ^{90}Sr and ^{238}Pu, and because the estimated exponent, γ, was different for the two radionuclides (4.2 for ^{90}Sr and 2.0 for ^{238}Pu), the relative difference between them decreased with increasing dose. The relative differences

in Figure 1 should not be confused with the quality factor for α-emitters used in radiation protection, because the doses in Figure 1 are based upon average skeletal dose and not the endosteal cell dose used in radiation protection. The endosteal cell dose is about a factor of 20 higher for ^{238}Pu and a factor of 2 higher for ^{90}Sr. This would narrow the difference between the curves by about a factor of 10, so that the quality factor of 20 used for radiation protection to describe the difference in response between α and β emitters would be adequate. The linear term, αd, was not significant for any of the studies, indicating an effective threshold for bone tumors. If a linear dose response exists, it must be small for ^{90}Sr because of the relatively large number of dogs at lower doses. This analysis would estimate the linear coefficient for ^{90}Sr, α, as 0.21 per Gy with a 95% confidence interval of –0.50 to 0.90. This suggests that it would require about 15 Gy from ^{90}Sr for even a doubling of the low spontaneous risk of bone cancer.

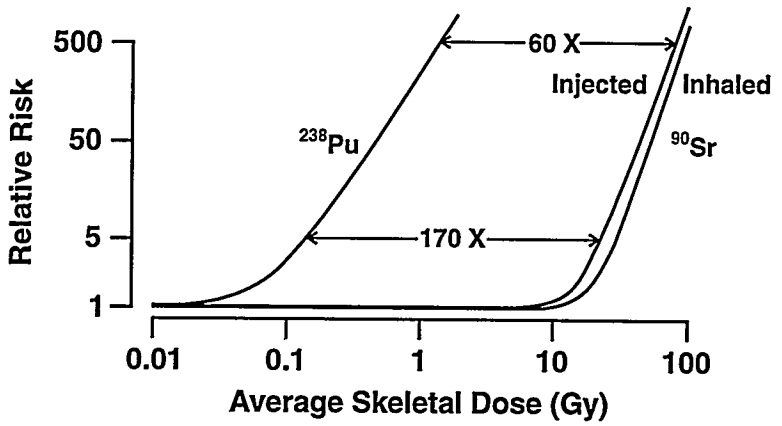

Figure 1. Estimates of the relative risk in a proportional hazards model for bone cancer in dogs that inhaled $^{238}PuO_2$, dogs that inhaled $^{90}SrCl_2$, and in dogs injected with ^{90}Sr. The increase in average skeletal dose for a relative risk of 5 and 500 between inhaled $^{238}PuO_2$ and injected ^{90}Sr is shown.

Three conclusions can be drawn from this example. A constant relative biological effectiveness factor cannot be derived for the differences in the induction of bone cancers between β-emitters and α-emitters deposited in the skeleton; the route of exposure for ^{90}Sr in a soluble form does not alter the dose-response relationship for bone tumors; and there is an apparent threshold dose for the induction of bone tumors. The presence of a threshold suggests that many radiation protection guidelines may be conservative for bone cancer because few workers are exposed to doses anywhere near the thresholds found in this example. This example demonstrates the advantages of comparisons of studies between laboratories for understanding dose response relationships.

(Research sponsored by the Office of Health and Environmental Research, U.S. Department of Energy, under Contract No. DE-AC04-76EV01013.)

LIFETIME TUMOR RISK COEFFICIENTS FOR BEAGLE DOGS THAT INHALED CERIUM-144 CHLORIDE

Bruce B. Boecker, Fletcher F. Hahn, William C. Griffith, and Bruce A. Muggenburg

Reported here is one of the life-span radionuclide toxicology studies being conducted at ITRI in Beagle dogs. These studies are examining the life-span health risks of inhaled β-, γ- and α-emitting radionuclides to expand available knowledge on these risks especially for the many cases for which human data are not available. The outcomes of these studies are providing important information on dosimetry and dose-response relationships for these inhaled radionuclides and the relative importance of a broad range of dose- and effect-modifying factors. A number of these studies are currently coming to completion. Much of the ITRI effort is being directed to final reviews of the dosimetric, clinical, and pathologic results and writing summary manuscripts.

The purpose of this report is to present the life-span tumorigenesis data in dogs exposed by inhalation to the β-emitting radionuclide ^{144}Ce as $^{144}CeCl_3$ in a CsCl vector aerosol. Particular emphasis is directed to the resulting risk coefficient data for tumors in various target organs.

Fifty-five dogs inhaled a $^{144}CeCl_3$ aerosol and 15 served as controls. The long-term retained burdens (LTRB) in the ^{144}Ce-exposed dogs ranged from 0.10–13 MBq/kg, and the survival times ranged from 21 to 5498 d after the inhalation exposure, which occurred at an age of approximately 13 mo.

Dosimetry information was obtained from dogs that inhaled $^{144}CeCl_3$ and were serially sacrificed in companion dosimetry studies and from dogs that died from 21 to 1826 d after exposure in the life-span study. These results, consisting of whole-body retention, tissue distribution, and excretion data, were used to construct biokinetic models to describe the metabolic patterns and to calculate doses to target organs and tissues. These results have been described in detail (1991–93 ITRI Biennial Report on Long-Term Dose-Response Studies of Inhaled or Injected Radionuclides, p. 39).

When all dogs in the life-span study had died, all dosimetric, clinical, and pathologic materials and data were reviewed to ensure consistency of interpretation and analysis over the past ~ 20 y. The main late-occurring biological effects were tumors in the organs and tissues that received the highest radiation doses: lung, liver, bone, bone marrow, and bone-associated oral and nasal mucosae. The thyroid and kidneys also received relatively high β doses but the observed numbers of tumors in these organs were indistinguishable from background levels. The dosimetric and tumorigenesis data were used to calculate tumor risk coefficients for the various target organs.

Risk coefficients for the development of tumors (malignant and benign) in the lung, liver, bone, bone marrow, and bone-associated oral and nasal mucosae were first calculated on an annual basis (based on time after exposure) by dividing the corrected number of dogs with tumors detected in a given year by the sum of all absorbed doses to that tissue for dogs surviving at the start of that year. In these calculations, the time-to-tumor diagnosis was used instead of the time of death to compensate for several cases in which the interval between diagnosis and death was a year or more. The number of dogs with tumors observed in a particular organ or tissue in a given year was corrected for the occurrence of tumors in the same organ or tissue in 84 control dogs that survived 2 or more years in ITRI studies involving radionuclide forms that behaved as a relatively soluble form in body fluids ($^{90}SrCl_2$, $^{144}CeCl_3$, $^{91}YCl_3$, $^{137}CsCl$, and $^{238}PuO_2$). The first ^{144}Ce-exposed dog that died with a tumor was euthanized at 799 d post exposure with an osteosarcoma. By this time, 14 ^{144}Ce-exposed dogs had died of early occurring, nontumor effects, leaving a population of 41 exposed dogs. Each

annual risk coefficient calculated as described above was multiplied by the fractional survival of this population of 41 dogs at the start of the year being calculated. The corrected annual risk coefficients were then summed to obtain the lifetime tumor coefficients.

The total β-dose coefficients and lifetime tumor risk coefficients for the target organs in this study are given in Table 1. These dose coefficients were normalized to the LTRB of ^{144}Ce in each dog. As shown, the β-dose coefficients range from 9 to 59 Gy per MBq LTRB/kg body mass. Liver had the highest dose coefficient, reflecting the large fraction of ^{144}Ce reaching the systemic circulation that is deposited and tenaciously retained in the liver. Four of the entries involve bone or bone-associated tissues. The assumptions used to calculate these dose coefficients are given in the footnotes to Table 1.

Table 1

Lifetime Tumor Risk Coefficients for Beagle Dogs that Inhaled $^{144}CeCl_3$

Organ or Tissue	Total β-Dose Coefficient (Gy/(MBq LTRB/kg)[a]	Number of Dogs with Tumors				Lifetime Risk Coefficient (Tumors/10^4 Gy)
		^{144}Ce-Exposed (41)[b]		Controls (84)[b]		
		Malignant	Benign	Malignant	Benign	
Liver	59	9	4	1	3	98
Bone-Associated Nasal Mucosa	30[c]	5	0	0	0	79
Lung	24	3	1	6	0	41
Bone	18[d]	1	0	0	0	12
Bone-Associated Oral Mucosa	18[d]	3	0	0	0	58
Bone Marrow	9[e]	2	1	0	0	81

[a]Long-term retained burden per kg body mass.
[b]Total number of dogs.
[c]Based on observed concentrations in the nasal turbinates and a fractional energy absorption of 0.42 (Cuddihy, R. G. *et al. Health Phys. 30*: 53, 1976).
[d]Based on an average absorbed dose to bone and a fractional energy absorption of 0.79 (Cuddihy *et al.*, 1976).
[e]Estimated to be 0.5 of the bone dose coefficient (Beddoe, A. H. and F. W. Spiers. *Radiat. Res. 80*: 423, 1979).

The tumor risk coefficient for the liver was the highest of the six calculated values, reflecting the 13 tumors that were found there. All three of the bone-associated tumor types (bone marrow, oral mucosa, and nasal mucosa) had similar risk coefficients in the range of 58 to 81 tumors per 10^4 Gy, whereas the value for bone itself was only 12 tumors per 10^4 Gy. These results indicate that the risks of tumors in bone-associated tissues were considerably higher than for bone. These observations presumably reflect the initial deposition of ^{144}Ce on bone surfaces and the effectiveness with which bone-associated tissues are irradiated by the β radiations from ^{144}Ce and its short-lived progeny, ^{144}Pr.

Although these dogs were exposed to $^{144}CeCl_3$ by inhalation, the risk coefficient for lung tumors was less than those calculated for either the liver or the bone-associated tissues.

Radiation doses and effects in tissues adjacent to bone, specifically those of epithelial or marrow origin, should be considered when determining risks from internally deposited, bone-seeking radionuclides such as ^{144}Ce. The property of ^{144}Ce depositing on and remaining associated with bone surfaces for long times may be an important factor in determining the β-radiation dose to bone marrow and epithelium adjacent to bone. These results demonstrate the importance of studies in laboratory animals to determine important dose and dose-response information for health protection practices for which direct human data are not available.

(Research sponsored by the Office of Health and Environmental Research, U.S. Department of Energy, under Contract No. DE-AC04-76EV01013.)

RESPONSE-SURFACE MODELS FOR DETERMINISTIC EFFECTS OF LOCALIZED IRRADIATION OF THE SKIN BY DISCRETE β/γ-EMITTING SOURCES

B. R. Scott

Individuals who work at nuclear reactor facilities can be at risk for deterministic effects in the skin from exposure to discrete β- and γ-emitting (βγE) sources (e.g., βγE hot particles) on the skin or clothing. Deterministic effects are non-cancer effects that have a threshold and increase in severity as dose increases (e.g., ulcer in skin). Hot βγE particles are ^{60}Co- or nuclear fuel-derived particles with diameters > 10 μm and < 3 mm and contain at least 3.7 kBq (0.1 μCi) of radioactivity (Scott, B. R. and J. W. Hopewell. *Proceedings of the 10th International Congress of Radiation Research*, Vol. 1, P15-5, 1995). For such βγE sources on the skin, it is the beta component of the dose that is most important (*Limits for Exposure to "Hot Particles" on the Skin*, NCRP Report 106, National Council on Radiation Protection and Measurements, Bethesda, MD, 1989). To develop exposure limitation systems that adequately control exposure of workers to discrete βγE sources, models are needed for evaluating the risk of deterministic effects of localized β irradiation of the skin. The purpose of this study was to develop dose-rate and irradiated-area dependent, response-surface models for evaluating risks of significant deterministic effects of localized irradiation of the skin by discrete βγE sources and to use modeling results to recommend approaches to limiting occupational exposure to such sources.

In the present study, published data for effects of localized β irradiation of pig skin (similar in radiosensitivity to human skin) were used to assess likely effects of localized irradiation of the skin of humans (Hopewell, J. W. *Radiat. Prot. Dosim. 39*: 11, 1991). In Hopewell's work, plaque sources that contained ^{90}Sr/^{90}Y (β_{max} = 2.28 MeV) or ^{170}Tm (β_{max} = 0.97 MeV) were used to deliver localized beta radiation doses to the flank skin of female large white pigs, 12–14 wk old. Plaque diameters ranged from 0.1–19 mm for ^{170}Tm sources; for the ^{90}Sr/^{90}Y sources, diameters ranged from 2–40 mm. Central axis dose rates and doses were reported by Hopewell for a depth of 16 μm, based on measurements with a tissue-equivalent extrapolation ionization chamber (collecting electrode effective area of 1.1 mm^2). Effective dose percentiles for 10% and 50% (i.e, ED_{10} and ED_{50}) reported by Hopewell for moist desquamation were used in the present study in developing a response-surface model that depends on dose rate and irradiated area. Corresponding effective dose percentiles for acute ulceration (which did not depend on dose rate) were used to obtain a response-surface model for the risk of acute ulceration.

The VARSKIN MOD2 dosimetry code (*VARSKIN MOD2 and SADDE MOD2: Computer Codes for Assessing Skin Dose from Skin Contamination*, U.S. Nuclear Regulatory Commission Report NUREG/CR-5873, PNL-7913, 1992) was used to assess the spatial distribution of the beta radiation dose. Model uncertainty was evaluated by Monte Carlo calculations (Crystal Ball Version 3.0, Decisioneering, Denver, CO, 1993).

Weibull-type, response-surface models were developed for evaluating the risk (and associated thresholds) of early deterministic effects (moist desquamation, acute ulceration) of localized β irradiation of skin. The covariates used include the irradiated area, A(70), at a depth of 70 μm (nominal depth of basal layer); the central axis dose, D(16), at a depth of 16 μm averaged over 1.1 mm^2; and for moist desquamation, the corresponding dose rate DR(16). Details on the associated mathematics are provided elsewhere (Scott and Hopewell, 1995).

Figure 1 shows a surface for the threshold absorbed dose, T(16), for moist desquamation, based on a response-surface model. Covariates are the irradiated area, A(70) in cm^2, and the dose rate, DR(16) in Gy/min. Values of A(70) in Figure 1 span three regimes: (1) the *hot-particle regime*

corresponds to $0 < A(70) \leq 4$ cm^2; (2) the *small-field regime* corresponds to 4 cm^2 $< A(70) \leq 20$ cm^2; and (3) the *large-field regime* corresponds to values of $A(70) > 20$ cm^2. For the hot-particle regime, acute deep ulceration is the major deterministic effect of concern.

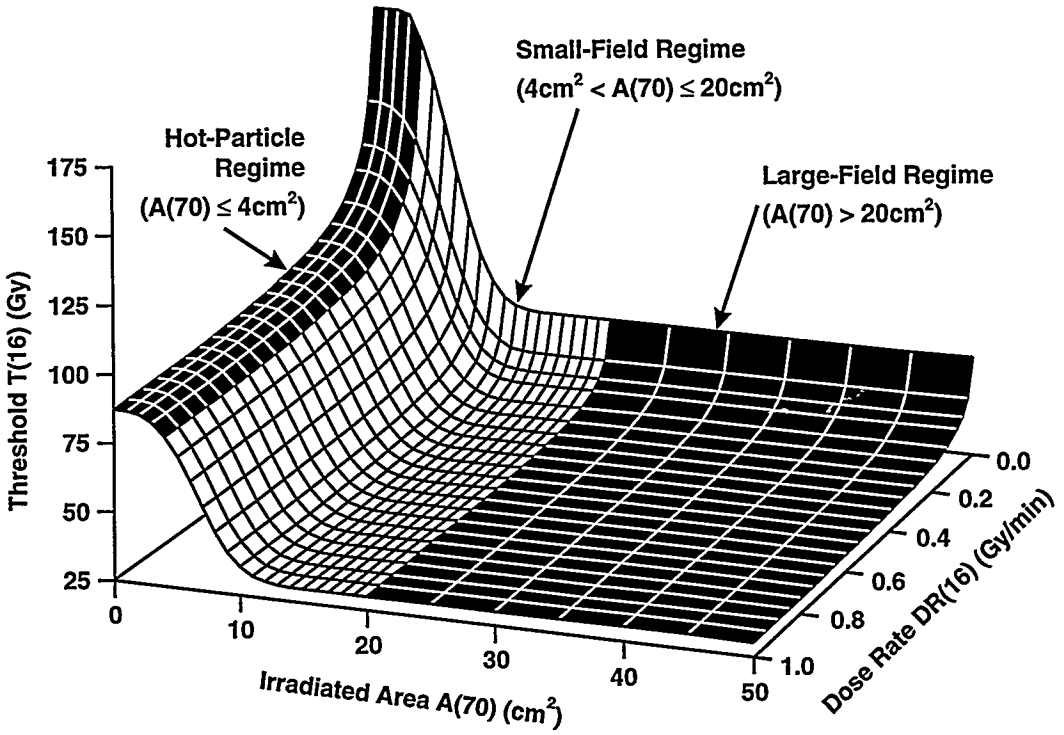

Figure 1. Response-surface for the beta radiation threshold (in Gy) for moist desquamation in skin as a function of irradiated area, A(70) in cm^2, and the absorbed dose rate, DR(16) in Gy. For β radiation, equivalent doses and equivalent dose rates will be identical to the indicated absorbed doses and dose rates, respectively.

Figure 2 shows a response surface reflecting the risk of acute ulceration as a function of A(70) and dose D(16) for exposure of the skin of humans to βγE hot particles. Of special interest for radiation protection considerations is how the acute ulceration risk changes as the local dose D(16) and irradiated area change, for the hot-particle regime. Results in Figure 2 indicate that risk decreases progressively as the irradiated area decreases. Also for radiation protection consideration, it would be useful to have an estimate of the threshold dose (evaluated at 70 μm depth) for acute ulceration evaluated at the irradiated-area boundary between the hot-particle and small-field regimes. The boundary of A(70) = 4 cm^2 corresponds to the approximate area irradiated by 3 mm diameter ^{90}Sr/^{90}Y plaques. Recall that a βγE hot particle, as defined, has a diameter < 3 mm in any direction. Based on experimental results published by Hopewell, J. W. (1991) for acute ulceration induced by 2 or 4 mm diameter ^{90}Sr/^{90}Y plaques and on use of a Weibull response-surface model, the threshold dose for acute ulceration when A(70) = 4 cm^2 was estimated by the Monte Carlo method to have a lower 5 percentile of 1 Gy. The dose was averaged over 1 cm^2 at a depth of 70 μm.

The 1-Gy, 5-percentile value can be compared to the present annual equivalent dose limits for deterministic effects recommended by the International Commission on Radiation Protection (ICRP) for localized irradiation of the skin. The ICRP Publication 60 (*Annals of the ICRP 21*, No. 1–3, 1991) recommended an annual limit of 500 mSv (corresponding to 0.5 Gy β radiation) evaluated at a depth of 70 μm and averaged over 1 cm^2, regardless of the area irradiated. Results from the present study indicate that a 500 mSv equivalent dose limit (evaluated at a depth of 70 μm and averaged over

1 cm^2) is protective against deterministic effects of βγE hot particles (so far as preventing acute ulceration). Here, the highly plausible assumption is made that the particle irradiates the skin for only a short time before being detected by monitoring. A 500 mSv equivalent dose limit could therefore be applied to βγE hot particles on the skin. For the small- and large-field regimes, limits developed for general radioactive contamination of relative large areas of the skin could apply.

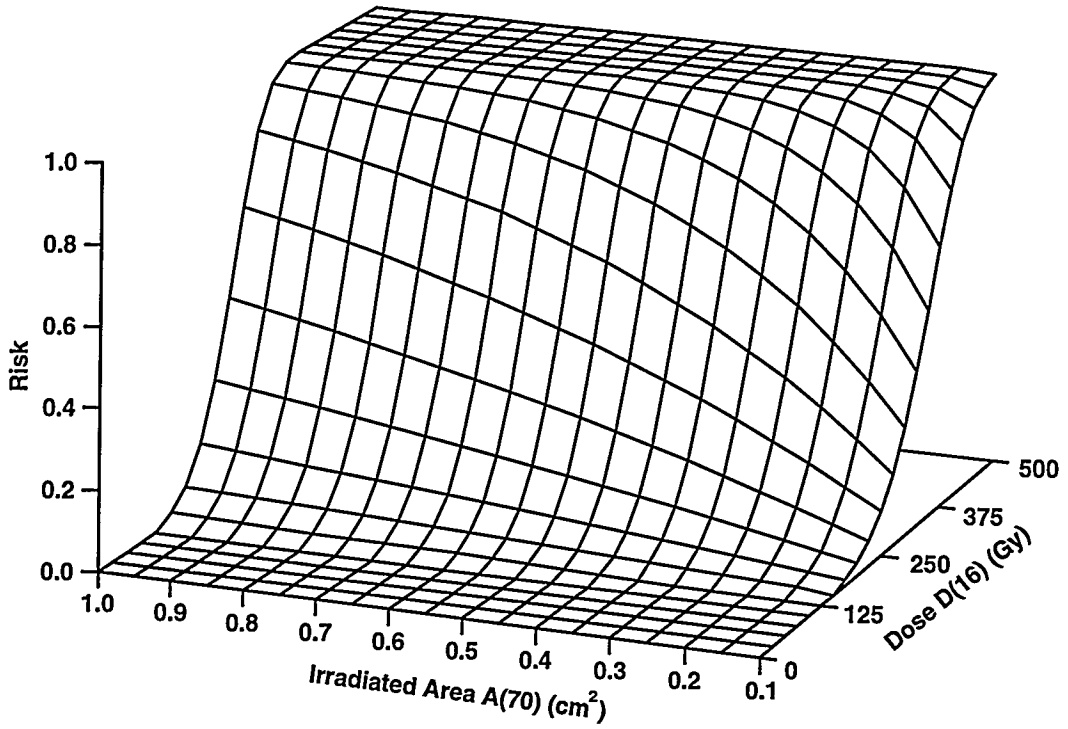

Figure 2. Risk surface for acute ulceration as a function of the irradiated area, A(70) in cm^2, and absorbed dose, D(16) in Gy. Corresponding equivalent doses will be identical to D(16).

A more sophisticated exposure limitation scheme could also be introduced which would apply not only to the skin but also to the respiratory tract, gastrointestinal tract, eye, and ear. The approach is based on use of the irradiated-volume (mass) weighting factor, $W_V = V^n$, which accounts for the decrease in the risk of a given deterministic effect that occurs when the irradiated tissue volume (mass) is reduced (Scott, B. R. *Health Phys. 69(6)*, December 1995, in press); n is called the volume parameter; and the fractional volume (mass) V represents the ratio, M_{irr}/M_{ref}, where M_{irr} is the irradiated tissue mass, and M_{ref} is a larger reference tissue mass that contains M_{irr}. When the irradiated mass is reduced from M_{ref} to M_{irr}, more dose is needed for the same level of risk as for irradiating M_{ref}. Thus, for a fixed level of risk, the required equivalent dose H_{irr} to M_{irr} is greater than the required equivalent dose H_{ref} to M_{ref}. Multiplying H_{irr} by W_V yields the smaller corresponding dose to M_{ref} for the same risk. With this approach, limits can be set based on the weighted equivalent dose $W_V H_{irr}$. If $H_{ref,lim}$ is the tissue-specific equivalent dose limit for tissue masses $\leq M_{ref}$, then a generic limiting scheme for controlling deterministic effects of localized irradiation of M_{irr} by a hot particle (or any discrete βγE source) is

$$W_V H_{irr} < H_{ref,lim}.$$

With this limiting scheme, the weighted equivalent dose $W_V H_{irr}$ to M_{irr} is constrained to remain below the equivalent dose limit $H_{ref,lim}$. In some cases, M_{ref} may represent the mass of an entire organ or organ component (e.g., lens of the eye). The volume-weighting factor approach can also be used for stochastic effects (cancer) provided the volume parameter n is set to one (Scott, 1995).

The significance of the research results is as follows: (1) response-surface models are now available for evaluating the risk of specific deterministic effects of localized irradiation of the skin; (2) modeling results have been used to recommend approaches to limiting occupational exposure of workers to β radiation from $\beta\gamma$E sources on the skin or on clothing; and (3) the generic irradiated-volume, weighting-factor approach to limiting exposure can be applied to other organs including the eye, the ear, and organs of the respiratory or gastrointestinal tract and can be used for both deterministic and stochastic effects.

(Research sponsored by the Assistant Secretary for Defense Programs, U.S. Department of Energy, under Contract No. DE-AC04-76EV01013.)

VIII. APPENDICES

APPENDIX A

STATUS OF LONGEVITY AND SACRIFICE EXPERIMENTS IN BEAGLE DOGS

Each annual report of the Inhalation Toxicology Research Institute from 1967 (LF-38) through 1987–1988 (LMF-121) included an appendix containing detailed tabular information on all dogs in the life-span studies of inhaled radionuclides and many sacrifice series associated with these studies. In LMF-121, similar kinds of summary tables were also included for dogs in long-term and life-span studies of injected actinides that were conducted at the University of Utah. All dogs remaining alive in the Utah studies were transferred to ITRI on September 15, 1987, where they were maintained and studied for the remainder of their life spans. Responsibility for managing the completion of the Utah life-span studies has been assigned to ITRI. A small team of investigators at the University of Utah and investigators at ITRI are working together to complete the observations and summaries.

Along with other changes made in the regular ITRI Annual Report beginning with Report LMF-126, *Inhalation Toxicology Research Institute Annual Report, 1988–1989*, it was decided that the growing body of detailed information on these studies in dogs would no longer be included. Instead, separate periodic reports are being prepared that contain specific updated information on all ITRI and University of Utah long-term and life-span studies in Beagle dogs. The first three of these reports, entitled *Annual Report on Long-Term Dose-Response Studies of Inhaled or Injected Radionuclides*, were published as Report LMF-128 for 1988–1989, as Report LMF-130 for 1989–1990, and as Report LMF-135 for 1990–1991. These reports described the studies, updated experimental design charts, survival plots, pathology summaries and detailed tabular information on all dogs in a manner consistent with past practices. The most recent report, ITRI-139, was published as the *Biennial Report on Long-Term Dose-Response Studies of Inhaled or Injected Radionuclides*, 1991–1993.

Recognizing that these data are of interest to a limited number of individuals, these reports are provided without charge to individuals requesting them. To obtain these reports, please send a request to:

Director
Inhalation Toxicology Research Institute
P. O. Box 5890
Albuquerque, NM 87185-5890

LOVELACE BIOMEDICAL AND ENVIRONMENTAL RESEARCH INSTITUTE
Directors and Officers

R. O. McClellan, DVM, Chairman
D. J. Ottensmeyer, MD, Vice Chairman
J. L. Mauderly, DVM, President
C. H. Hobbs, DVM, Vice President
B. B. Boecker, PhD, Asst. Secretary/Treasurer (non-director)
J. F. Lechner, PhD, Asst. Secretary/Treasurer (non-director)
J. A. Lopez, BSChE, Asst. Secretary/Treasurer (non-director)

J. P. Bundrant
N. Corzine
J. Doull, MD
B. D. Goldstein, MD
W. A. Gross, PhD
D. E. Kilgore, MD
J. Lovelace Johnson
D. P. Pasternak, MD
M. W. Twiest, MD
A. C. Upton, MD

INHALATION TOXICOLOGY RESEARCH INSTITUTE
J. L. Mauderly, DVM, Director
C. H. Hobbs, DVM, Associate Director
B. B. Boecker, PhD, Assistant Director for Research
J. F. Lechner, PhD, Assistant Director for Research
J. A. Lopez, BSChE, Assistant Director for Administration

Scientific Groups

- Aerosol Science
  H. C. Yeh, PhD
- Chemistry and Biochemical Toxicology
  W. E. Bechtold, PhD
- Molecular and Cellular Toxicology
  N. F. Johnson, PhD
- Pathology
  F. F. Hahn, DVM, PhD
- Pathophysiology
  J. M. Benson, PhD

Office of the Director

- Special Assistant to Director
  R. K. Jones, MD
- Executive Assistant
  M. B. Morgan
- Internal Auditor
  E. C. Bankey, MBA
- Education Coordinator
  D. E. Bice, PhD

Scientific Programs

- Aerosols
  Y. S. Cheng, PhD
- Applied Toxicology
  C. H. Hobbs, DVM
- Cancer Mechanisms
  J. F. Lechner, PhD
- Chemical Toxicology
  A. R. Dahl, PhD
- Pathogenesis
  J. F. Lechner, PhD
- Radiation Toxicology
  R. A. Guilmette, PhD

Research Support Sections and Units

- Analytical Chemistry
  W. E. Bechtold, PhD
- Animal Care
  D. G. Burt, DVM
- Biomathematics
  B. B. Boecker, PhD
- Chronic Studies
  J. M. Benson, PhD
- Clinic
  B. A. Muggenburg, DVM, PhD
- Clinical Pathology
  F. F. Hahn, DVM, PhD
- Exposure
  E. B. Barr, MSEE
- Histopathology
  F. F. Hahn, DVM, PhD
- Necropsy
  J. Hogan, BA

Administrative Support Sections and Units

- Computer
  J. H. Diel, PhD
- Engineering, Construction and Environmental Restoration
  A. C. Grace, III, MS
- Facility Operations and Maintenance
  W. F. Beierman, BSEE
- Financial Management
  K. M. Aragon, MBA
- Environment, Safety and Health
  S. R. Rohrer, MBA, PhD
- Human Resources
  B. K. Solari, BA
- Library
  S. E. Spurlock, MLS, MIS
- Procurement
  D. L. Webb (Acting)
- Property Management
  D. L. Webb
- Quality Assurance
  D. L. Harris, MS
- Technical Communications
  P. L. Bradley, MA

LOVELACE BIOMEDICAL AND ENVIRONMENTAL RESEARCH INSTITUTE
INHALATION TOXICOLOGY RESEARCH INSTITUTE
ORGANIZATIONAL STRUCTURE

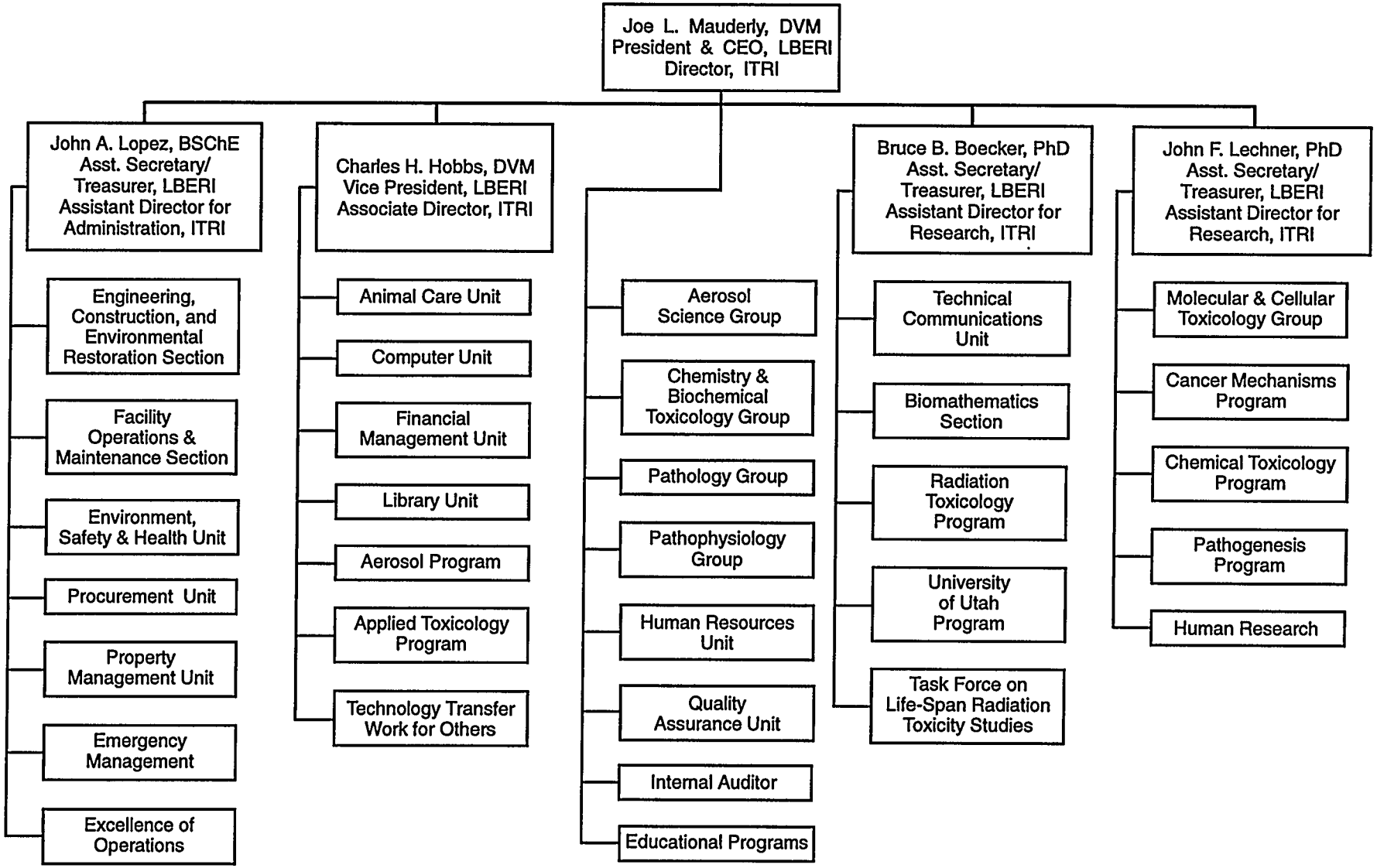

STAFF OF THE INHALATION TOXICOLOGY RESEARCH INSTITUTE

DIRECTORATE

Joe L. Mauderly, DVM, Director
Charles H. Hobbs, DVM, Associate Director
Bruce B. Boecker, PhD, Assistant Director for Research
John F. Lechner, PhD, Assistant Director for Research
John A. Lopez, BSChE, Assistant Director for Administration

ADMINISTRATIVE SUPPORT

E. C. Bankey, MBA	Internal Auditor
L. L. Burton	Executive Secretary
M. G. Campos	Clerical Specialist
R. K. Jones, MD*	Special Assistant to the Director
M. B. Morgan	Executive Assistant to Director

AEROSOL SCIENCE GROUP

H. C. Yeh, PhD	Supervisor/Aerosol Scientist
Y. S. Cheng, PhD	Aerosol Scientist
B. Fan, PhD	Postdoctoral Fellow
G. A. Feather, BS	Research Technologist
A. F. Fencl, BS	Sr. Research Technologist
T. D. Holmes, BS	Sr. Research Technologist
M. D. Hoover, PhD	Aerosol Scientist
M. Marcinkovich	Research Technologist
G. J. Newton, BS	Aerosol Scientist
S. M. Smith, BS	Graduate Student
Y. Wang, BS*	Graduate Student
D. Yazzie	Research Technologist

Exposure Section

E. B. Barr, MSEE	Supervisor/Aerosol Scientist
R. D. Brodbeck	Technical Specialist
R. K. White, BS	Technical Specialist

BIOMATHEMATICS SECTION

B. B. Boecker, PhD	Assistant Director for Research
W. C. Griffith, Jr., PhD	Biomathematician
B. R. Scott, PhD	Biophysicist

CHEMISTRY AND BIOCHEMICAL TOXICOLOGY GROUP

W. E. Bechtold, PhD	Supervisor/Chemist
T. A. Ahlert, BS	Sr. Research Technologist
M. L. Allen	Research Technologist
A. R. Dahl, PhD	Toxicologist
R. F. Henderson, PhD	Toxicologist
M. J. Meyer, BS*	Graduate Student
K. D. Rohrbacher, BS*	Laboratory Assistant
G. G. Scott, MS	Sr. Research Technologist
J. A. Stephens	Sr. Research Technologist
M. R. Strunk, BA	Sr. Research Technologist
J. R. Thornton-Manning, PhD	Toxicologist
J. J. Waide, MS	Sr. Research Technologist

Analytical Chemistry Section

W. E. Bechtold, PhD	Supervisor/Chemist
K. R. Ahlert	Technical Specialist
L. I. Archuleta	Laboratory Technician
S. N. Lucas	Laboratory Technician
A. M. Maestas	Laboratory Technician
P. R. Romero-Stagg	Laboratory Technician
D. M. Sugino	Laboratory Technician

*Part-time employee

MOLECULAR AND CELLULAR TOXICOLOGY GROUP

N. F. Johnson, PhD	Supervisor/Exptl. Pathologist
S. A. Belinsky, PhD	Molecular Biologist
D. M. Gurule*	Laboratory Assistant
H. J. Harms, BS	Research Technologist
S. S. Hayes, BS	Research Technologist
R. J. Jaramillo, BS	Sr. Research Technologist
S. E. Jones, DVM	Exptl. Pathol. Program Graduate Student
C. H. Kennedy, PhD	Molecular Toxicologist
D. M. Klinge, BS	Sr. Research Technologist
J. L. Lane, BS	Research Technologist
T. A. Liberati, DVM	Postdoctoral Fellow
S. K. Middleton, BS	Research Technologist
C. E. Mitchell, PhD	Molecular Biologist
M. M. Murphy, BS	Research Technologist
R. E. Neft, PhD	Cell Biologist
W. A. Palmisano, PhD	Molecular Biologist
S. E. Phillips, BS	Research Technologist
D. S. Swafford, BS	Graduate Student
J. Tesfaigzi, PhD	Molecular Biologist
L. A. Tierney, DVM	Graduate Student
L. M. Watrin, BS	Research Technologist

PATHOLOGY GROUP

F. F. Hahn, DVM, PhD	Supervisor/Exptl. Pathologist
K. Avila, BS	Research Technologist
D. E. Bice, PhD	Immunologist
D. D. S. Collie, BVM&S, PhD	Postdoctoral Fellow
P. Y. Cossey, BS	Sr. Research Technologist
K. M. Garcia, BA	Sr. Research Technologist
D. A. Kracko, BS	Sr. Research Technologist
J. L. Lewis, PhD*	Toxicologist
K. J. Nikula, DVM, PhD	Experimental Pathologist
K. H. Pyon, PhD	Postdoctoral Fellow
D. A. Rodgers, PhD*	UNM Postdoctoral Fellow
K. A. Schafer, DVM	Exptl. Pathol. Program Graduate Student
J. A. Wilder, PhD	UNM Postdoctoral Fellow
M. B. Wood, BS	Administrative Assistant

Clinical Pathology Section

F. F. Hahn, DVM, PhD	Supervisor/Exptl. Pathologist
C. H. Pertab	Research Technologist

Histopathology Section

F. F. Hahn, DVM, PhD	Supervisor/Exptl. Pathologist
S. C. Barnett	Research Technologist
Y. N. Knighton	Laboratory Technician

Necropsy Section

J. Hogan, BA	Supervisor/Chief Res. Technologist
J. L. DuBoise	Laboratory Technician
B. Pacheco	Laboratory Technician
R. B. Garlick	Laboratory Technician

PATHOPHYSIOLOGY GROUP

J. M. Benson, PhD	Supervisor/Toxicologist
L. F. Blair	Sr. Research Technologist
D. C. Esparza, BS	Sr. Research Technologist
G. L. Finch, PhD	Toxicologist
K. G. Gillett, BS	Sr. Research Technologist
R. A. Guilmette, PhD	Radiobiologist
A. M. Holmes	Research Technologist
D. L. Lundgren, PhD	Radiobiologist
E. J. Salas	Research Technologist
M. B. Snipes, PhD	Radiobiologist
B. M. Tibbetts, BA	Research Technologist
K. L. Williamson	Research Technologist

Chronic Studies Section

J. M. Benson, PhD	Supervisor/Toxicologist
C. A. Dison	Sr. Research Technologist

Clinical Section

B. A. Muggenburg, DVM, PhD	Supervisor/Physiologist
M. A. Berry, DVM*	Clinical Veterinarian
M. A. Billau, AS	Research Technologist

*Part-time employee

ANIMAL CARE UNIT

D. G. Burt, DVM	Supervisor/Attending Veterinarian
E. Amaro	Animal Caretaker
S. L. Batson, BS	Chief Animal Technologist
D. M. Bolton	Animal Technician
D. T. Cordaro	Sr. Animal Technician
F. E. Delgado	Animal Technician
J. M. Duran	Sr. Animal Technician
F. B. Kleinschnitz	Animal Caretaker
A. D. Murrin	Clerical Specialist
M. V. Nysus*	Animal Caretaker
E. R. Perez*	Animal Caretaker
J. F. Quintana*	Animal Caretaker
C. G. Romero	Animal Technician
S. Walker	Animal Technician
C. C. Ynostroza, AS	Sr. Animal Technician

COMPUTER UNIT

J. H. Diel, PhD	Computer Resources Manager
M. F. Conrad, AS	Research Technologist
R. L. Lucero-Maldonado*	Laboratory Technician
S. C. McLellan	Laboratory Technician
E. Taplin, BBA	Administrative Systems Analyst

ENGINEERING, CONSTRUCTION AND ENVIRONMENTAL RESTORATION SECTION

A. C. Grace, III, MS	Supervising Engineer
J. A. Detmer	Technical Secretary
T. A. Knowlton*	Laboratory Assistant
I. M. Nitz	Clerical Specialist
A. A. Powell*	Laboratory Assistant
G. A. Saiz*	Laboratory Assistant
J. P. Samora, MS	Engineer

FACILITY OPERATIONS AND MAINTENANCE SECTION

W. F. Beierman, BSEE	Supervising Engineer
E. Anzures	Electrical Maintenance Worker
R. T. Cossey, ASEE	Instrum. & Controls Maint. Worker/ Technical Specialist
F. D. Cox	Sr. Research Technologist
A. R. Espalin	General Maintenance Worker
E. M. Gallegos*	Laboratory Assistant
D. D. Griego	Research Assistant
J. R. Mann	HVAC Mechanic & Central Plant Operator
A. F. Monnin	Sr. Research Technologist
T. B. Orwat	Technical Specialist
B. D. Romero	Janitor
A. D. Szydlowski*	Laborer
F. R. Torrez	HVAC Mechanic & Central Plant Operator

FINANCIAL MANAGEMENT UNIT

K. M. Aragon, MBA	Financial Resources Manager
B. A. Lorenzo	Clerical Specialist
A. I. Medrano	Clerical Specialist
P. S. Ohl, BS	Asst. Financial Resources Manager
K. J. Rima*	Clerical Specialist

ENVIRONMENT, SAFETY AND HEALTH UNIT

S. R. Rohrer, MBA, PhD	Environment, Safety and Health Manager
K. L. Abeyta	Research Technologist
L. C. Haling	Executive Secretary
J. R. Lackey	Sr. Research Technologist
M. H. LeForce, MS	Industrial Hygienist
J. M. Mauser, MS	Engineer
C. W. Pohl	Research Technologist
P. S. Puckett*	Laboratory Assistant
W. C. Schleyer, III, MS	Health Physicist
T. T. Simpson, AAS	Research Technologist
T. L. Zimmerman	Research Technologist

*Part-time employee

HUMAN RESOURCES UNIT

B. K. Solari, BA	Human Resources Manager
S. L. Abeita	Clerical Specialist
A. F. Baca	Surveillance Worker
Y. B. Cordova	Clerical Specialist
J. A. Davis, BS	Asst. Human Resources Manager
T. J. Hoskins	Clerical Specialist
J. T. Nunez	Clerical Specialist
P. Padilla	Surveillance Worker
G. J. Quintana	Surveillance Worker
I. J. Salinas	Surveillance Worker

LIBRARY UNIT

S. E. Spurlock, MLS, MIS	Technical Library Resources Manager
C. S. Snidow	Clerical Specialist

PROCUREMENT UNIT

D. L. Webb	Acting Procurement Manager
V. K. Aragon	Clerical Specialist
R. L. Ripple	Clerical Specialist
L. Vigil	Clerical Specialist

PROPERTY MANAGEMENT UNIT

D. L. Webb	Property Manager
C. C. Duran*	Laborer
A. J. Garcia	Clerical Specialist
K. Garcia	Clerical Specialist

QUALITY ASSURANCE UNIT

D. L. Harris, MS	Quality Assurance Manager
M. M. Nelson, BS	Administrative Specialist

TECHNICAL COMMUNICATIONS UNIT

P. L. Bradley, MA	Technical Communications Manager
C. M. Herrera	Clerical Specialist
S. L. Perez	Clerical Specialist
W. L. Piper, BA	Clerical Specialist
S. F. Randock, BA	Clerical Specialist

TASK FORCE ON LIFE-SPAN RADIATION TOXICITY STUDIES**

B. B. Boecker, PhD	Assistant Director for Research
M. G. Campos	Clerical Specialist
M. F. Conrad, AS	Research Technologist
J. H. Diel, PhD	Computer Resources Manager
K. M. Garcia, BA	Sr. Research Technologist
K. G. Gillett, BS	Sr. Research Technologist
W. C. Griffith, Jr., PhD	Biomathematician
R. A. Guilmette, PhD	Radiobiologist
F. F. Hahn, DVM, PhD	Experimental Pathologist
B. A. Muggenburg, DVM, PhD	Physiologist
K. J. Nikula, DVM, PhD	Experimental Pathologist
B. R. Scott, PhD	Biophysicist
M. B. Snipes, PhD	Radiobiologist

*Part-time employee

**Individuals have primary assignment in Scientific Groups or Units on preceding pages.

EDUCATIONAL PARTICIPANTS

Name	School/University	ITRI Group/Unit/Section
Summer Student Research Participants		
Catherine I. Bloomfield	Brown University, RI	Molecular & Cellular Toxicology Group
Kristina Dam	Mount St. Mary's College, CA	Chemistry & Biochemical Toxicology Group
Debbie M. Gurulé	University of New Mexico, NM	Molecular & Cellular Toxicology Group
Karla D. Kenyon	Humboldt State University, CA	Molecular & Cellular Toxicology Group
Martin H. Schmid	Colorado State University, CO	Aerosol Science Group
Department of Energy/Associated Western Universities Teacher Research Associates Program (TRAC) Participants		
Lance A. Belin	Lancaster High School, TX	Biomathematics Section
Andrew J. Engel	Los Alamos Middle School, NM	Pathology Group
James C. Kiss	Rangeview High School, CO	Pathology Group
Lana M. Ray	Grundy County High School, TN	Molecular & Cellular Toxicology Group
Janice L. Rogers	Bernalillo High School, NM	Molecular & Cellular Toxicology Group
Kathy E. Spencer	Los Lunas Middle School, NM	Pathophysiology Group
Minority Student Research Participant		
Debbie M. Gurulé	University of New Mexico, NM	Molecular & Cellular Toxicology Group
Minority High School Student Program Participants		
Carlos Gonzales	Rio Grande High School, NM	Chemistry & Biochemical Toxicology Group
Uyen Tina Tran	Manzano High School, NM	Molecular & Cellular Toxicology Group
Student Research Participants		
Gina Adams	University of New Mexico, NM	Pathophysiology Group
Robert Astur	University of New Mexico, NM	Pathophysiology Group
Faith Barrington	University of New Mexico, NM	Pathophysiology Group
Michelle M. Busch	Sandia Preparatory High School, NM	Molecular & Cellular Toxicology Group
Amy E. Byse	Purdue University, IN	Pathology Group
William M. Fitzpatrick	University of New Mexico, NM	Environment, Safety and Health Unit
David T. Killough	Texas A&M University, TX	Aerosol Science Group
Amy Koerner	University of New Mexico, NM	Pathophysiology Group
Christine A. Ryder	University of New Mexico, NM	Molecular & Cellular Toxicology Group
Michael Weisend	University of New Mexico, NM	Pathophysiology Group

ITRI EDUCATIONAL PARTICIPANTS

Name	School/University	ITRI Group/Unit/Section
Student Employees – 1994		
Rickhard Bjorgum	University of New Mexico	Facility Operations & Maintenance Section
Nicole L. Britnell	University of New Mexico	Animal Care Unit
Richard E. Crocker	University of New Mexico	Animal Care Unit
Christopher C. Duran	University of New Mexico	Property Management Unit
Martha L. Emery	University of New Mexico	Animal Care Unit
Ernest M. Gallegos	University of New Mexico	Facility Operations & Maintenance Section
Richard L. Gonzales	University of New Mexico	Engineering, Construction & Environmental Restoration Section
Jonathan C. Hawkins	University of New Mexico	Facility Operations & Maintenance Section
Thomas A. Knowlton	University of New Mexico	Engineering, Construction & Environmental Restoration Section
Salomon J. Moya	University of New Mexico	Engineering, Construction & Environmental Restoration Section
Monique V. Nysus	University of New Mexico	Animal Care Unit
Elma R. Perez	University of New Mexico	Animal Care Unit
Adam A. Powell	University of New Mexico	Engineering, Construction & Environmental Restoration Section
Paul S. Puckett	University of New Mexico	Environment, Safety & Health Unit
Gregory A. Saiz	University of New Mexico	Engineering, Construction & Environmental Restoration Section
Carrie R. Shumate	Albuquerque – Technical Vocational Institute	Property Management Unit
Shelton L. Sunrise	University of New Mexico	Animal Care Unit
Andrew D. Szydlowski	University of New Mexico	Facility Operations & Maintenance Section

UNM/ITRI Graduate Students	Postdoctoral Fellows	Purdue/ITRI Experimental Pathology Program Graduate Students
Thomas R. Carpenter, DVM	D. David S. Collie, BVM&S, PhD	Susan E. Jones, DVM
Albert W. Hickman, Jr.	Bijian Fan, PhD	Kenneth A. Schafer, DVM
Mark J. Meyer	Teresa A. Liberati, DVM	
Kevin D. Rohrbacher	Luqi Pei, PhD	UNM/ITRI Pulmonary Epidemiology and Toxicology Training Program Participants
Gary G. Scott	Kee H. Pyon, PhD	
Shawna M. Smith		Julie A. Wilder, PhD
Deborah S. Swafford		Darrell A. Rodgers, PhD
Lauren A. Tierney, DVM		
Yansheng Wang		

PROGRAM AND PROJECT TITLES	SPONSOR*	COORDINATOR
BRUCE B. BOECKER, ASSISTANT DIRECTOR		
Radiation Toxicology – R. A. Guilmette, Program Manager		
Effective Dose from Inhaled Nuclear Energy Materials	DOE/OHER	R. A. Guilmette
Dose-Response Relationships for Inhaled Radionuclides	DOE/OHER	B. A. Muggenburg
Radiation Dose and Injury to Critical Cells from Radon	DOE/OHER	N. F. Johnson
Deposition of Radon and Radon Progeny in the Respiratory Tract	DOE/OHER	H. C. Yeh
Toxicity of Injected Radionuclides – ITRI Effort	DOE/OHER	B. B. Boecker
Toxicity of Injected Radionuclides – Utah Effort	DOE/OHER	S. C. Miller
Statistical Analysis of Data from Radiobiologic Animal Studies	DOE/OHER	W. C. Griffith
Improved Exposure Assessment Using ^{210}Pb Measurements for Epidemiologic Studies	DOE/OHER	R. A. Guilmette
Solubility Measurements for Implementing 10 CFR Part 20	NRC	R. A. Guilmette
Internal Dosimetry	DOE/WSRC	R. A. Guilmette
Carcinogenicty of Depleted Uranium	USAMRDC	F. F. Hahn
INSRP/BEES Panel	DOE/BNL	M. D. Hoover
Deposition and Clearance of Locally Delivered Particles in Airways of Dogs and Humans	Genentech	B. A. Muggenburg
p53 Protein Expression as a Dosimeter for Genotoxicity	NIH/NIEHS	N. F. Johnson
CHARLES H. HOBBS, ASSOCIATE DIRECTOR		
Aerosols – Y. S. Cheng, Program Manager		
Biologically Relevant Properties of Energy Related Aerosols	DOE/OHER	Y. S. Cheng
Underground Aerosol Characterization at the WIPP Site	DOE/AL	G. J. Newton
Y-12 Radiological Protection Program	DOE/Y-12	M. D. Hoover
HQ Health Physics Study	DOE/HQ	M. D. Hoover
Inhalation Hazards for Uranium Mill Tailings	DOE/UMTRAP	G. J. Newton
Evaluation of Respirators-II for Asbestos Fibers	NIOSH/CDC	Y. S. Cheng
Experimental Tests on Continuous Air Monitors	DOE/EG&G	M. D. Hoover
Air Sampling Program at SNL Area V	DOE/SNL	G. J. Newton
Dissolution of Metal Tritides in Biological Systems	DOE/SNL	Y. S. Cheng
Russian Topaz-II Study	DOE/SNL	M. D. Hoover
Calibration/Performance Evaluation of Aero-Disperser	AProcI	Y. S. Cheng
Radiochem Analytical Support	DOE/SNL	G. J. Newton
Calibration Hardware Design/Modification of Beryllium Air Monitor	DOE/LLNL	M. D. Hoover
Design Modifications for BLI Biological Materials	DOE/SNL	Y. S. Cheng
Aerosol Characterization Services on Ultraviolet Lidar Systems	DOE/SNL	Y. S. Cheng

PROGRAM AND PROJECT TITLES	SPONSOR*	COORDINATOR
Applied Toxicology – C. H. Hobbs, Program Manager		
Effects of L-Deprenyl on Physiologic Functions	DAHI	B. A. Muggenburg
Treatment of Chronic Prostatic Hypertrophy	IMI	B. A. Muggenburg
Combined Exposure, Plutonium – Cigarette Smoke	DOE/DP	G. L. Finch
Combined Exposure, Plutonium – Beryllium	DOE/DP	G. L. Finch
Combined Exposure, Plutonium – X Ray	DOE/DP	D. L. Lundgren
Combined Exposure, Plutonium – Chemical Carcinogen	DOE/DP	D. L. Lundgren
Combined Exposure, Radiation – Solvents	DOE/DP	J. M. Benson
Effects of Physical/Chemical HMs on Inflammatory and Proliferative Response Induced in the Lung	IPA	R. F. Henderson
Evaluation of Bioavailability of Nickel Compounds	EPRI	J. M. Benson
Effects of Ozone on Airway Mucous Cells	MSU	C. H. Hobbs
Blood Flow and Vascular Resistance in Dogs Given Blood Substitutes or After Blood Volume Changes	TLI	B. A. Muggenburg
Vehicle Effects on FCE-28044 IV Pharmacokinetics and Subcutaneous Dermal Toxicity in Rats	UNM	F. F. Hahn
ER Projects Assessment Council	DOE/LANL	C. H. Hobbs
Two-Year Repeated Inhalation	IPA	J. M. Benson
Evaluation of Dust Monitors	IPA	E. B. Barr
JOHN F. LECHNER, ASSISTANT DIRECTOR		
Cancer Mechanisms – J. F. Lechner, Program Manager		
Links Between Radiation-Induced Lung Cancer in Laboratory Animals and People	DOE/OHER	F. F. Hahn
Pre-Malignant Events in Radiation-Induced Lung Cancer	DOE/OHER	J. Tesfaigzi
Lung Cancer in Uranium Miners – Gene Dysfunction	DOE/OHER	J. F. Lechner
Cellular Models of Radiation-Induced Lung Cancer	DOE/OHER	J. F. Lechner
Molecular Mechanisms of Radiation-Induced Cancer	DOE/OHER	J. F. Lechner
Gene Dysfunction in Chemical Induced Carcinogenicity	DOE/OHER	S. A. Belinsky
Identification of Intrinsic Human Genes that Govern Susceptibility to Rn-Induced Cancer	DOE/OHER	W. A. Palmisano
Detection of Molecular Markers to Lung Cancer in Uranium Miners	JHU	J. F. Lechner
Chemical Toxicology – A. R. Dahl, Program Manager		
Influence of Respiratory Tract Metabolism on Effective Dose	DOE/OHER	J. R. Thornton-Manning
Biological Markers of Human Exposure to Organic Compounds	DOE/OHER	W. E. Bechtold
Mechanisms of Granulomatous Disease from Inhaled Beryllium	DOE/OHER	J. M. Benson

PROGRAM AND PROJECT TITLES	SPONSOR*	COORDINATOR
Study of Biomarkers of Dosimetry from Exposure to 1,3 Butadiene	NCI	W. E. Bechtold
Nitrogen Heterocycles: Metabolic Effect and Toxicity	WSU	J. L. Lewis
Human Sensitivity to Genotoxic Effects of Butadiene	UTMB	W. E. Bechtold
Metabolism of 1,3-Butadiene, Butadiene Monoepoxide and Butadiene Diepoxide by Human and Mouse Liver and Lung Tissue Homogenates	CMA	J. R. Thornton-Manning
Exposure of $B6C3F_1$ Mice to 1,3-Butadiene	CMA	J. R. Thornton-Manning
Fate of Inhaled Vapors in Rats and Dogs	NIH/NIEHS	A. R. Dahl
Carcinogenicity of Inhalants: A Dosimetric Approach	NIH/NIEHS	A. R. Dahl
Disposition of Inhaled Toxicants in the Olfactory System	NIH/NIDCD	J. L. Lewis
Dosimetry of Benzene in Bone Marrow	APetrol	W. E. Bechtold
Toxicity and Toxicokinetics of Inhaled Carbonyl Sulfide	DOE/WSRC	A. R. Dahl
Acrylate Nasal Uptake	Rohm Haas	A. R. Dahl
Carcinogenicity of Butadiene Diepoxide in Mice and Rats	HEI	R. F. Henderson
S-Phenylcysteine in Albumin as a Benzene Biomarker	HEI	W. E. Bechtold
Pathogenesis – J. F. Lechner, Program Manager		
Cellular & Biochemical Mediators of Respiratory Tract Disease	DOE/OHER	J. F. Lechner
Airway Epithelial Injury, Adaptation and Repair	DOE/OHER	J. F. Lechner
Role of Immune Responses in Respiratory Diseases	DOE/OHER	D. E. Bice
Evaluation of Pulmonary Immune Responses to Viral Agents	UA	D. E. Bice
Tobacco Smoke Effects on Mucin Production in Rat Airways	UCSF	C. H. Hobbs

* APetrol – American Petroleum Institute
AProcI – Amherst Process Instruments
CMA – Chemical Manufacturers Association
DAHI – Deprenyl Animal Health, Inc.
DOE/AL – Department of Energy Operations Office, Albuquerque
DOE/BNL – Department of Energy, Brookhaven National Laboratory
DOE/DP – Department of Energy, Defense Programs
DOE/EG&G – Department of Energy, Rocky Flats Plant
DOE/HQ – Department of Energy, Headquarters
DOE/LANL – Department of Energy, Los Alamos National Laboratory
DOE/LLNL – Department of Energy, Lawrence Livermore National Laboratory
DOE/OHER – Department of Energy, Office of Health and Environmental Research
DOE/SNL – Department of Energy, Sandia National Laboratories
DOE/UMTRAP – Department of Energy, Uranium Mill Tailings Remediation Action Program
DOE/WSRC – Department of Energy, Westinghouse Savannah River Co.
DOE/Y-12 – Department of Energy, Y-12 Plant
EPRI – Electric Power Research Institute
HEI – Health Effects Institute
IMI – Indigo Medical, Inc.
IPA – Institute of Polyacrylic Absorbents
JHU – Johns Hopkins University
MSU – Michigan State University
NCI – National Cancer Institute
NIDCD – National Institute on Deafness and Communicable Diseases
NIH/NIEHS – National Institutes of Health/National Institute of Environmental Health Sciences
NIOSH/CDC – National Institute of Occupational Safety & Health/Centers for Disease Control
NRC – Nuclear Regulatory Commission
TLI – The Lovelace Institutes
UA – University of Arizona
UCSF – University of California-San Francisco
UNM – University of New Mexico
USAMRDC – US Army Medical and Research Development Command
UTMB – University of Texas Medical Branch at Galveston
WSU – Wayne State University

APPENDIX D

PUBLICATION OF TECHNICAL REPORTS

OCTOBER 1, 1994 – SEPTEMBER 30, 1995

Bechtold, W. E. and J. A. Hotchkiss: *Immunoaffinity Chromatography in the Analysis of Toxic Effects of Complex Chemical Mixtures*, Health Effects Institute Report, Cambridge, MA (in press).

Belinsky, S. A., C. E. Mitchell, K. J. Nikula and D. S. Swafford: *Examination of Target Genes Involved in Induction of Lung Cancer by Carbon Black and Diesel Exhaust*, Health Effects Institute Report, Cambridge, MA (in press).

Harkema, J. R. and J. L. Mauderly: *Consequences of Prolonged Inhalation of Ozone on F344 Rats: Collaborative Studies. Part V: Effects on Pulmonary Function*, Research Report No. 65, Health Effects Institute, Cambridge, MA, 1994.

Harkema, J. R., K. T. Morgan, E. A. Gross, P. T. Catalano and W. C. Griffith: *Consequences of Prolonged Inhalation of Ozone in F344/N Rats: Collaborative Studies. Part VII: Effects on the Nasal Mucociliary Apparatus*, Research Report No. 65, Health Effects Institute, Cambridge, MA, 1994.

Mauderly, J. L., M. B. Snipes, E. B. Barr, S. A. Belinsky, J. A. Bond, A. L. Brooks, I. Y. Chang, Y. S. Cheng, N. A. Gillett, W. C. Griffith, R. F. Henderson, C. E. Mitchell, K. J. Nikula and D. G. Thomassen: *Pulmonary Toxicity of Inhaled Diesel Exhaust and Carbon Black in Chronically Exposed Rats. Part 1: Neoplastic and Nonneoplastic Lung Lesions*, Research Report 68, Health Effects Institute, Cambridge, MA, 1994.

Meyer, L. C., G. J. Newton, A. W. Cronenberg and G. G. Loomis: *La-Oxides as Tracers for PuO_2 to Simulate Contaminated Aerosol Behavior*, EGG-WTD-11161, Idaho National Engineering Laboratory, Idaho Falls, ID, 1994.

Sextro, R. G., A. Bostrum, D. Brenner, D. Chambers, R. Guilmette, P. Hopke, G. M. Mantanoski, M. Reimer, A. Siniscalchi and J. E. Watson: *Recommendations for Radon Research: A Report of the Radon Science Initiative Subcommittee of the Radiation Advisory Committee*, U.S. Environmental Protection Agency, 1995.

APPENDIX E

ITRI PUBLICATIONS IN THE OPEN LITERATURE PUBLISHED, IN PRESS, OR SUBMITTED BETWEEN OCTOBER 1, 1994 – SEPTEMBER 30, 1995

Au, W. W., W. E. Bechtold, E. B. Whorton and M. S. Legator: Chromosome Aberrations and Response to Gamma-Ray Challenge in Lymphocytes of Workers Exposed to 1,3-Butadiene. *Mutat. Res. 334*: 125-130, 1995.

Bartczak, A., S. A. Kline, R. Yu, C. P. Weisel, B. D. Goldstein, G. Witz and W. E. Bechtold: Evaluation of Assays for the Identification and Quantitation of Muconic Acid, a Benzene Metabolite in Human Urine. *J. Toxicol. Environ. Health 42*: 245-258, 1994.

Bechtold, W. E., M. R. Strunk, J. R. Thornton-Manning and R. F. Henderson: Analysis of Butadiene, Butadiene Monoxide, and Butadiene Diepoxide in Blood by Gas Chromatography/Gas Chromatography/Mass Spectroscopy. *Chem. Res. Toxicol. 8(2)*: 182-187, 1995.

Belinsky, S. A., J. F. Lechner and N. F. Johnson: An Improved Method for Isolation of Type II and Clara Cells from Mice. *In Vitro Cell. Dev. Biol. 31*: 361-366, 1995.

Belinsky, S. A., S. K. Middleton, S. M. Picksley, F. F. Hahn and K. J. Nikula: Alterations in the K-ras and p53 Pathways in X-ray-Induced Lung Tumors in the Rat. *Radiat. Res.* (in press).

Belinsky, S. A., K. J. Nikula, S. B. Baylin and J.-P. J. Issa: Increased Cytosine DNA-Methyltransferase Activity is Target Cell Specific and an Early Event in Lung Cancer. *Proc. Nat. Acad. Sci. USA* (in press).

Belinsky, S. A., K. J. Nikula, S. B. Baylin and J.-P. J. Issa: Microassay for Measuring Cytosine DNA-Methyltransferase Activity During Tumor Progression. *Toxicol. Lett.* (in press).

Benson, J. M., I. Y. Chang, Y. S. Cheng, F. F. Hahn, C. H. Kennedy, E. B. Barr, K. R. Maples and M. B. Snipes: Particle Clearance and Histopathology in Lungs of F344/N Rats and B6C3F_1 Mice Inhaling Nickel Oxide or Nickel Sulfate. *Fundam. Appl. Toxicol.* (in press).

Benson, J. M., Y. S. Cheng, A. F. Eidson, F. F. Hahn, R. F. Henderson and J. A. Pickrell: Time Course of Lesion Development in F344/N Rats Subchronically Exposed by Inhalation to Nickel Subsulfide. *Toxicology* (in press).

Bice, D. E.: Immunologic Responses of the Respiratory Tract to Inhaled Materials. In *Concepts in Inhalation Toxicology* (R. O. McClellan and R. F. Henderson, eds.), pp. 413-440, Taylor & Francis, Washington, DC, 1995.

Bice, D. E.: Pulmonary Immunology. In *Immune System Toxicology* (D. A. Lawrence, ed.), Vol. 5, Comprehensive Toxicology Series, Elsevier Scientific Publications/Pergamon Press, New York, NY (in press).

Bice, D. E., A. J. Williams and B. A. Muggenburg: Long-Term Antibody Production in Canine Lung Allografts: Implications in Pulmonary Immunity and Asthma. *Am. Rev. Respir. Dis.* (in press).

Bice, D. E. and B. A. Muggenburg: Pulmonary Immune Memory: Localized Production of Antibody in the Lung After Antigen Challenge. *Immunology* (submitted).

Boecker, B. B.: Comparison of Old and New ICRP Models for Respiratory Tract Dosimetry. *Radiat. Prot. Dosim. 60(4)*: 331-336, 1995.

Boecker, B. B., W. C. Griffith, R. A. Guilmette, F. F. Hahn, B. A. Muggenburg, S. C. Miller, R. D. Lloyd and G. N. Taylor: The Role of Laboratory Animals in Studying the Late-Occurring Effects of Radionuclides Deposited in the Liver and Skeleton. In *Health Effects of Internally Deposited Radionuclides: Emphasis on Radium and Thorium* (G. van Kaick, A. Karaoglou and A. M. Kellerer, eds.), pp. 287-298, World Scientific Publishing, Singapore, 1995.

Boecker, B. B. and W. C. Griffith: Cancer from Internal Emitters. To be published in *Proceedings of the Xth International Congress of Radiation Research*, held in Wurzburg, Germany, August 27–September 1, 1995 (in press).

Butler, C. R., C. B. Radu and J. P. Samora: ITRI Hot Ponds Environmental Restoration Project: Lessons Learned. To be published in the *Proceedings of the ER '95 Meeting*, held in Denver, CO, August 13-18, 1995 (in press).

Carpenter, T. R., R. J. Jaramillo and N. F. Johnson: Cell Cycle Arrests and p53, Mdm2, Gadd45, and Cyclin G Protein Expression Following Alpha-Particle Exposure. *Cancer Res.* (submitted).

Chen, B. T., J. V. Benz, G. L. Finch, J. L. Mauderly, P. J. Sabourin, H. C. Yeh and M. B. Snipes: Effect of Exposure Mode on Amounts of Radiolabeled Cigarette Particles in Lungs and Gastrointestinal Tracts of F344 Rats. *Inhal. Toxicol. 7*: 1095-1108, 1995.

Chen, B. T., H. C. Yeh and N. F. Johnson: Design and Use of a Virtual Impactor and an Electrical Classifier for Generation of Test Fiber Aerosols with Narrow Size Distributions. *J. Aerosol Sci.* (in press).

Chen, B. T., H. C. Yeh and B. J. Fan: Evaluation of the TSI Small-Scale Powder Dispenser. *J. Aerosol Sci.* (in press).

Cheng, K. H., D. L. Swift, Y. S. Cheng, Y. F. Su and H. C. Yeh: Local Mass Transfer Coefficients of the Human Nasal Passage from Measurements of Aerosol Deposition in a Nasal Cast. *Inhal. Toxicol. 6 (Suppl.)*: 393-395, 1994.

Cheng, K. H., Y. S. Cheng, H. C. Yeh and D. L. Swift: Deposition of Ultrafine Aerosols in the Head Airways During Natural Breathing and During Simulated Breath Holding Using Replicate Human Airway Casts. *Aerosol Sci. Technol. 23(3)*: 465-474, 1995.

Cheng, K. H., D. L. Swift, Y. H. Yang, Y. S. Cheng, and H. C. Yeh: Application of Both a Physical Theory and Statistical Procedure in the Analyses of an *In Vivo* Study of Aerosol Deposition. In *Proceedings of the 1995 International Conference on Aerosol Science and Technology*, pp. 231-236, College of Public Health, National Taiwan University, Taipei, Taiwan, 1995.

Cheng, K. H., Y. S. Cheng, H. C. Yeh and D. L. Swift: Calculation of Mass Transfer Coefficients in the Human Oral Passage. *J. Biomech. Eng.* (submitted).

Cheng, K. H., Y. S. Cheng, H. C. Yeh and D. L. Swift: An Experimental Method for Measuring Deposition Efficiency of Inhaled Aerosols in Human Oral Airway. *Am. Ind. Hyg. Assoc. J.* (submitted).

Cheng, K. H., Y. S. Cheng, H. C. Yeh, R. A. Guilmette, S. Q. Simpson, Y-H Yang and D. L. Swift: *In Vivo* Measurements of Nasal Airway Dimensions and Ultrafine Aerosol Deposition in the Human Nasal and Oral Airways. *J. Aerosol Sci.* (submitted).

Cheng, Y. S.: Dissolution and Radiation Dosimetry of Metal Tritides. In *1993 Radiation Protection Workshop Proceedings*, pp. K15-K28, U.S. Department of Energy, 1994.

Cheng, Y. S. and O. R. Moss: Inhalation Exposure Systems. In *Concepts in Inhalation Toxicology* (R. O. McClellan and R. F. Henderson, eds.), pp. 25-66, Taylor & Francis, Washington, DC, 1995.

Cheng, Y. S., W. E. Bechtold, C. C. Yu and I. F. Hung: Incense Smoke: Characterization and Dynamics in Indoor Environments. *Aerosol Sci. Technol. 23*: 271-281, 1995.

Cheng, Y. S., Q. H. Powell, S. M. Smith and N. F. Johnson: Silicon Carbide Whiskers: Characterization and Aerodynamic Behaviors. *Am. Ind. Hyg. Assoc. J. 56*: 970-978, 1995.

Cheng, Y. S.: Denuder Systems and Diffusion Batteries. In *Air Sampling Instruments*, American Conference of Governmental Industrial Hygienists, Cincinnati, OH (in press).

Cheng, Y. S. and B. T. Chen: Aerosol Sampler Calibration. In *Air Sampling Instruments*, American Conference of Governmental Industrial Hygienists, Cincinnati, OH (in press).

Cheng, Y. S., S. M. Smith, H. C. Yeh, D. B. Kim, K. H. Cheng and D. L. Swift: Deposition of Ultrafine Aerosols and Thoron Progeny in Replicas of Nasal Airways of Young Children. *Aerosol Sci. Technol.* (in press).

Cheng, Y. S., T. R. Chen, P. T. Wasiolek and A. Van Engen: Air Quality and Radon Exposure in the Carlsbad Caverns. *Environ. Sci. Technol.* (submitted).

Cheng, Y. S., H. C. Yeh, R. A. Guilmette, S. Q. Simpson, K. H. Cheng and D. L. Swift: Nasal Deposition of Ultrafine Particles in Human Volunteers and Its Relationship to Airway Geometry. *Aerosol Sci. Technol.* (submitted).

Dahl, A. R. and P. Gerde: Uptake and Metabolism of Toxicants in the Respiratory Tract. *Environ. Health Perspect. 102 (Suppl. 11)*: 67-70, 1994.

Dahl, A. R., D. J. Zastrow and J. A. Hotchkiss: Advances in Comparative Nasal Enzymology Between F344 Rats and Humans. *Inhal. Toxicol. 6 (Suppl.)*: 357-360, 1994.

Dahl, A. R.: Metabolic Characteristics of the Respiratory Tract. In *Concepts in Inhalation Toxicology* (R. O. McClellan and R. F. Henderson, eds.), pp. 175-190, Taylor & Francis, Washington, DC, 1995.

Dahl, A. R.: Metabolism of Isoprene *In Vivo*. *Toxicology* (in press).

Dahl, A. R.: Toxicokinetics: Concepts of Dose. In *General Principles/Comprehensive Toxicology* (J. Bond, ed.), Vol. 1, Elsevier Science Ltd./Pergamon (submitted).

Dahl, A. R., L. K. Brookins and P. M. Gerde: An Exposure System for Measuring Nasal and Lung Uptake of Vapors in Rats. *Fundam. Appl. Toxicol.* (submitted).

Dungworth, D. L., F. F. Hahn and K. J. Nikula: Noncarcinogenic Responses of the Respiratory Tract Lung to Inhaled Toxicants. In *Concepts in Inhalation Toxicology* (R. O. McClellan and R. F. Henderson, eds.), pp. 533-546, Taylor & Francis, Washington, DC, 1995.

Dunnick, J. K., M. R. Elwell, A. E. Radovsky, J. M. Benson, F. F. Hahn, K. J. Nikula, E. B. Barr and C. H. Hobbs: Comparative Carcinogenic Effects of Nickel Subsulfide, Nickel Oxide, or Nickel Sulfate Hexahydrate Chronic Exposures in the Lung. *Cancer Res. 55*: 5251-5256, 1995.

Elliget, K. A. and J. F. Lechner: A Protocol for Normal Human Bronchial Epithelial Cell Cultures. In *Protocols in Cell and Tissue Culture* (J. B. Griffiths, A. Doyle and G. Newell, eds.), John Wiley and Sons, Ltd., West Sussex, U.K. (in press).

Fan, B. J., Y. S. Cheng and H. C. Yeh: Evaluation of the Performance of an Annular Diffusion Chamber. To be published in *Proceedings of the Scientific Conference on Obscuration and Aerosol Research*, held in Aberdeen, MD, June 2-5, 1994 (in press).

Fan, B. J., Y. S. Cheng and H. C. Yeh: Entrance Flow Effect on the Gas Collection Efficiency of an Annular Diffusion Denuder. *Aerosol Sci. Technol.* (submitted).

Finch, G. L., P. J. Haley, M. D. Hoover and R. G. Cuddihy: Responses of Rats Lungs Following Inhalation of Beryllium Metal Particles to Achieve Relatively Low Lung Burdens. *Ann. Occup. Hyg. 38 (Suppl. 1)*: 419-424, 1994.

Finch, G. L., K. J. Nikula, B. T. Chen, E. B. Barr, I. Y. Chang and C. H. Hobbs: Effect of Chronic Cigarette Smoke Exposure on Lung Clearance of Tracer Particles Inhaled by Rats. *Fundam. Appl. Toxicol. 24*: 76-85, 1995.

Finch, G. L., M. D. Hoover, F. F. Hahn, K. J. Nikula, S. A. Belinsky, P. J. Haley and W. C. Griffith: Animal Models of Beryllium-Induced Lung Disease. *Environ. Health Perspect.* (in press).

Finch, G. L., C. H. Hobbs, D. L. Lundgren, J. M. Benson, F. F. Hahn, K. J. Nikula, W. C. Griffith, M. D. Hoover, E. B. Barr, S. A. Belinsky, B. B. Boecker and J. L. Mauderly: Worker Risk Issues for Combined Exposures to Radionuclides and Chemicals - An Experimental Toxicology Approach. To be published in the *Proceedings of the ER '95 Meeting*, held in Denver, CO, August 13-18, 1995 (in press).

Finch, G. L., K. J. Nikula, S. A. Belinsky, Barr. E. B., G. D. Stoner and J. F. Lechner: Failure of Cigarette Smoke to Induce or Promote Lung Cancer in the A/J Mouse. *Cancer Lett.* (in press).

Gerde, P., B. A. Muggenburg, M. D. Hoover and R. F. Henderson: Clearance of Particles and Lipophilic Solutes from Central Airways. *Ann. Occup. Hyg. 38 (Suppl. 1)*: 211-214, 1994.

Gerde, P., B. A. Muggenburg, R. F. Henderson and A. R. Dahl: Particle-Associated Hydrocarbons and Lung Cancer; the Correlation Between Cellular Dosimetry and Tumor Distribution. In *NATO ASI Series, Cellular and Molecular Effects of Mineral and Synthetic Dusts and Fibres* (J. M. G. Davis and M. C. Jaurand, eds.), Vol. H 85, pp. 337-346, Springer-Verlag, Heidelberg, Germany, 1994.

Gordon, T. and J. R. Harkema: Cotton Dust Produces an Increase in Intraepithelial Mucosubstances in Rat Airways. *Am. Rev. Respir. Dis. 151*: 1981-1988, 1995.

Griffith, W. C., B. B. Boecker, C. R. Watson and G. C. Gerber: Possible Uses of Animal Databases for Further Statistical Evaluation and Modeling. To be published in the *Proceedings of the Xth International Congress of Radiation Research*, held in Wurzburg, Germany, August 27-September 1, 1995 (in press).

Guilmette, R. A., Y. S. Cheng, H. C. Yeh and D. L. Swift: Deposition of 0.005-12 μm Monodisperse Particles in a Computer-Milled, MRI-Based Nasal Airway Replica. *Inhal. Toxicol. 6 (Suppl.)*: 395-399, 1994.

Guilmette, R. A. and T. J. Gagliano: Construction of a Model of Human Nasal Airways Using *In Vivo* Morphometric Data. *Ann. Occup. Hyg. 38 (Suppl. 1)*: 69-75, 1994.

Hahn, F. F., W. C. Griffith, C. H. Hobbs, B. A. Muggenburg and B. B. Boecker: Biological Effects of ^{91}Y in Relatively Insoluble Particles Inhaled by Beagle Dogs. *Ann. Occup. Hyg. 38 (Suppl. 1)*: 275-280, 1994.

Hahn, F. F.: Carcinogenic Responses of the Lung to Inhaled Toxicants. In *Concepts in Inhalation Toxicology* (R. O. McClellan and R. F. Henderson, eds.), pp. 319-353, Taylor & Francis, Washington, DC, 1995.

Hahn, F. F., B. A. Muggenburg and B. B. Boecker: Hepatic Lesions Induced by Chronic Beta Irradiation from ^{144}Ce in Dogs. In *Health Effects of Internally Deposited Radionuclides: Emphasis on Radium and Thorium*, pp. 337-340, World Scientific Publishing, Singapore, 1995.

Hahn, F. F.: Radiation-Induced Adenosquamous Cell Carcinoma, Lung of Rats. In *ILSI Monograph: Pathology of Laboratory Animals, Respiratory System* (T. C. Jones, ed.), International Life Sciences Institute Press, Washington, DC (in press).

Hahn, F. F.: Radiation-Induced Squamous Cell Carcinoma, Lung of Rats. In *ILSI Monograph: Pathology of Laboratory Animals, Respiratory System* (T. C. Jones, ed.), International Life Sciences Institute Press, Washington, DC (in press).

Hahn, F. F.: Radiation-Induced Adenocarcinoma, Lung of Rats. In *ILSI Monograph: Pathology of Laboratory Animals, Respiratory System* (T. C. Jones, ed.), International Life Sciences Institute Press, Washington, DC (in press).

Hahn, F. F.: Radiation-Induced Sarcoma, Lung of Rats. In *ILSI Monograph: Pathology of Laboratory Animals, Respiratory System* (T. C. Jones, ed.), International Life Sciences Institute Press, Washington, DC (in press).

Hahn, F. F., B. A. Muggenburg and B. B. Boecker: Hepatic Lesions from Internally Deposited $^{144}CeCl_3$. *Toxicol. Pathol.* (in press).

Haley, P. J., K. F. Pavia, D. S. Swafford, D. R. Davila, M. D. Hoover and G. L. Finch: The Comparative Pulmonary Toxicity of Beryllium Metal and Beryllium Oxide in Cynomolgus Monkeys. *Immunopharmacol. Immunotoxicol. 16(4)*: 627-644, 1994.

Harkema, J. R. and J. A. Hotchkiss: Ozone-Induced Proliferative and Metaplastic Lesions in Nasal Transitional and Respiratory Epithelium: Comparative Pathology. *Inhal. Toxicol. 6 (Suppl.)*: 187-204, 1994.

Harkema, J. R., C. M. Wierenga, L. K. Herrera, J. A. Hotchkiss, W. A. Evans, D. G. Burt and C. H. Hobbs: Strain-Related Differences in Ozone-Induced Secretory Metaplasia in the Nasal Epithelium of Rats. *Inhal. Toxicol. 6 (Suppl.)*: 420-422, 1994.

Harkema, J. R. and J. L. Mauderly: Pulmonary Function Alterations in F344 Rats Following Chronic Ozone Inhalation. *J. Air Waste Manage. Assoc.* (in press).

Harkema, J. R., J. L. Mauderly and W. C. Griffith: Pulmonary Function Alterations in F344 Rats Following Chronic Ozone Inhalation. *Inhal. Toxicol.* (in press).

Henderson, R. F. and K. S. Bakshi: Summary of Panel Discussions. *Environ. Health Perspect. 102 (Suppl. 11)*: 125-127, 1994.

Henderson, R. F.: Biological Markers in the Respiratory Tract. In *Concepts in Inhalation Toxicology* (R. O. McClellan and R. F. Henderson, eds.), pp. 441-504, Taylor & Frances, Washington, DC, 1995.

Henderson, R. F., K. E. Driscoll, J. R. Harkema, R. C. Lindenschmidt, I. Y. Chang, K. R. Maples and E. B. Barr: A Comparison of the Inflammatory Response of the Lung to Inhaled versus Instilled Particles in F344 Rats. *Fundam. Appl. Toxicol. 24*: 183-197, 1995.

Henderson, R. F., G. G. Scott and Waide J. J.: Source of Alkaline Phosphatase Activity in Epithelial Lining Fluid of Normal and Injured F344 Rat Lungs. *Toxicol. Appl. Pharmacol. 134*: 170-174, 1995.

Henderson, R. F.: Particulate Air Pollution and Increased Mortality: Biological Plausibility for Causal Relationship. To be published in the *Proceedings of the Air and Waste Management Association Meeting*, held in San Antonio, TX, June 18-23, 1995 (in press).

Henderson, R. F.: Species Differences in Metabolism of 1,3-Butadiene. In *Biological Reactive Intermediates V: Basic Mechanistic Research in Toxicology and Human Risk Assessment* (R. Snyder *et al.*, eds.), Plenum Publishing Corporation, New York, NY (in press).

Henderson, R. F.: Species Differences in Metabolism of Benzene. *Environ. Health Perspect.* (in press).

Henderson, R. F.: Strategies for Use of Biological Markers of Exposure. *Toxicol. Lett.* (in press).

Henderson, R. F., J. R. Thornton-Manning, W. E. Bechtold and A. R. Dahl: Metabolism of 1,3-Butadiene: Species Differences. *Toxicology* (in press).

Hickman, A. W., W. C. Griffith, G. S. Roessler and R. A. Guilmette: Application of a Canine ^{238}Pu Biokinetic/Dosimetry Model to Human Bioassay Data. *Health Phys. 68(3)*: 359-370, 1995.

Hobbs, C. H., J. L. Mauderly and M. B. Snipes: Workshop Overview: The Maximum Tolerated Dose for Inhalation Bioassays: Toxicity vs. Overload. *Fundam. Appl. Toxicol.* (in press).

Hoover, M. D. and G. J. Newton: Calibration and Operation of Continuous Air Monitors for Alpha-Emitting Radionuclides. In *1993 Radiation Protection Workshop Proceedings*, pp. G27-G39, U.S. Department of Energy, 1994.

Hotchkiss, J. A., W. A. Evans, K. R. Maples, B. T. Chen, G. L. Finch and J. R. Harkema: Regional Differences in the Effects of Cigarette Smoke on Stored Microsubstances in Respiratory Epithelium of the F344 Rat Nasal Septum. *Inhal. Toxicol. 6 (Suppl.)*: 440-443, 1994.

Hotchkiss, J. A., L. K. Herrera, J. R. Harkema, J. S. Kimbell, K. T. Morgan and G. E. Hatch: Regional Differences in Ozone-Induced Nasal Epithelial Cell Proliferation in F344 Rats: Comparison with Computational Mass Flux Predictions of Ozone Dosimetry. *Inhal. Toxicol. 6 (Suppl.)*: 390-392, 1994.

Hotchkiss, J. A., W. A. Evans, B. T. Chen, G. L. Finch and J. R. Harkema: Regional Differences in the Effects of Mainstream Cigarette Smoke on Stored Mucosubstances and DNA Synthesis in F344 Rat Nasal Epithelium. *Toxicol. Appl. Pharmacol. 131*: 316-324, 1995.

Hotchkiss, J. A., H. Kim, F. F. Hahn, R. F. Novak and A. R. Dahl: Pyridine Induction of Sprague-Dawley Rat Renal Cytochrome P4502E1: Immunohistochemical Localization and Quantitation. *Toxicol. Lett. 78*: 1-7, 1995.

Johnson, N. F.: An Overview of Animal Models for Assessing Synthetic Vitreous Fibers (SVFs) Safety. *Reg. Toxicol. Pharmacol. 20*: S7-S21, 1994.

Johnson, N. F.: Phagosomal Ph and Glass Fiber Dissolution in Cultured Rat Nasal Epithelial Cells and Alveolar Macrophages: A Preliminary Study. *Environ. Health Perspect. 102 (Suppl. 5)*: 97-102, 1994.

Johnson, N. F.: Radiobiology of Lung Target Cells. *Radiat. Prot. Dosim. 60(4)*: 327-330, 1995.

Johnson, N. F., A. W. Hickman, T. R. Carpenter and G. J. Newton: Biodosimetric Approach for Estimating Alpha-Particle Dose to Respiratory Tract Epithelial Cells. To be published in *Proceedings of the Fifth International Inhalation Symposium "Correlations Between In Vitro and In Vivo Investigations in Inhalation Toxicology,"* held in Hannover, Germany, February 20-24, 1995, International Life Sciences Institutes Press, Washington, DC (in press).

Johnson, N. F. and F. F. Hahn: Mesothelioma Induction Following Intrapleural Inoculation of F344 Rats with Silicon Carbide Whiskers and Continuous Ceramic Filaments. *Toxicol. Lett.* (submitted).

Kelly, G., B. L. Stegelmeier and F. F. Hahn: p53 Alterations in Plutonium-Induced F344 Rat Lung Tumors. *Radiat. Res. 142*: 263-269, 1995.

Kelly, G., W. C. Griffith, B. A. Muggenburg, L. A. Tierney, J. F. Lechner and F. F. Hahn: A Canine Model of Mammary Gland Cancer. *Lab. Invest.* (submitted).

Kelsey, K. T., J. K. Wienecke, J. Ward, W. Bechtold and J. Fajen: Sister Chromatid Exchanges, Glutathione S-Transferase O Deletion and Cytogenic Sensitivity to Diepoxybutane in Lymphocytes from Butadiene Monomer Production Workers. *Mutat. Res.* (in press).

Kennedy, C. H. and J. F. Lechner: *In Vitro* Carcinogenesis of Human Bronchial Epithelial Cells. To be published in *Proceedings of the Fifth International Inhalation Symposium "Correlations Between In Vitro and In Vivo Investigations in Inhalation Toxicology,"* held in Hannover, Germany, February 20-24, 1995, International Life Sciences Institutes Press, Washington, DC (in press).

Lechner, J. F.: Urban Air Carcinogens and Their Effects on Health. *Publications of the National University of Mexico* (in press).

Lewis, J. L., K. J. Nikula and L. A. Sachetti: Induced Xenobiotic-Metabolizing Enzymes Localized to Eosinophilic Globules in Olfactory Epithelium of Toxicant-Exposed F344 Rats. *Inhal. Toxicol. 6 (Suppl.)*: 422-425, 1994.

Lewis, J. L. and A. R. Dahl: Olfactory Mucosa: Composition, Enzymatic Localization, and Metabolism. In *Handbook of Clinical Olfaction and Gustation* (R. L. Doty, ed.), pp. 33-52, Marcel Dekker, New York, 1995.

Lundgren, D. L., P. J. Haley, F. F. Hahn, J. H. Diel, W. C. Griffith and B. R. Scott: Pulmonary Carcinogenicity of Repeated Inhalation Exposure of Rats to Aerosols of $^{239}PuO_2$. *Radiat. Res. 142*: 39-53, 1995.

Malkinson, A. M. and S. A. Belinsky: The Use of Animal Models in Preclinical Studies Relating to Lung Cancer. In *Lung Cancer: Principles and Practice* (A. Turrusi *et al.*, eds.), J. B. Lippencott, Philadelphia, PA (in press).

Mauderly, J. L., E. B. Barr, A. F. Eidson, J. R. Harkema, R. F. Henderson, J. A. Pickrell and R. K. Wolff: Pneumonoconiosis in Rats Exposed Chronically to Oil Shale Dust and Diesel Exhaust, Alone and in Combination. *Ann. Occup. Hyg. 38 (Suppl. 1)*: 403-409, 1994.

Mauderly, J. L.: Assessment of Pulmonary Function and the Effects of Inhaled Toxicants. In *Concepts in Inhalation Toxicology* (R. O. McClellan and R. F. Henderson, eds.), pp. 355-412, Taylor & Francis, Washington, DC, 1995.

Mauderly, J. L.: Current Assessment of the Carcinogenic Hazard of Diesel Exhaust. *Toxicologic and Environmental Chemistry 49*: 167-180, 1995.

Mauderly, J. L.: Current Concepts on Airborne Particles and Health. *Publications of the National University of Mexico* (in press).

Mauderly, J. L.: Lung Overload: The Dilemma and Opportunities for Resolution. *Inhal. Toxicol.* (in press).

Mauderly, J. L.: Usefulness of Animal Models for Predicting Human Responses to Chronic Inhalation of Particles. *Chest* (in press).

Mauderly, J. L., D. A. Banas, W. C. Griffith, F. F. Hahn, R. F. Henderson and R. O. McClellan: Diesel Exhaust is not a Pulmonary Carcinogen in CD-1 Mice Exposed Under Conditions Carcinogenic to F344 Rats. *Fundam. Appl. Toxicol.* (in press).

Melo, D. R., D. L. Lundgren, B. A. Muggenburg and R. A. Guilmette: Prussian Blue Decorporation of ^{137}Cs in Beagles of Different Ages. *Health Phys.* (submitted).

Mitchell, C. E., S. A. Belinsky and J. F. Lechner: Detection and Quantitation of Mutant K-ras Codon 12 Restriction Fragments by Capillary Electrophoresis. *Anal. Biochem. 224*: 148-153, 1995.

Moss, O. R. and Y. S. Cheng: Generation and Characterization of Test Atmospheres: Particles. In *Concepts in Inhalation Toxicology* (R. O. McClellan and R. F. Henderson, eds.), pp. 91-126, Taylor & Francis, Washington, DC, 1995.

Muggenburg, B. A., R. A. Guilmette, W. C. Griffith, F. F. Hahn, N. A. Gillett and B. B. Boecker: The Toxicity of Inhaled Particles of $^{238}PuO_2$ in Dogs. *Ann. Occup. Hyg. 38 (Suppl. 1)*: 269-274, 1994.

Muggenburg, B. A., F. F. Hahn, W. C. Griffith, B. B. Boecker and R. D. Lloyd: The Biological Effects of ^{224}Ra Injected into Dogs. In *Health Effects of Internally Deposited Radionuclides: Emphasis on Radium and Thorium*, pp. 299-306, World Scientific Publishing, Singapore, 1995.

Muggenburg, B. A., R. A. Guilmette, J. A. Mewhinney, N. A. Gillett, J. L. Mauderly, W. C. Griffith, J. H. Diel, B. R. Scott, F. F. Hahn and B. B. Boecker: Toxicity of Inhaled $^{238}PuO_2$ in Beagle Dogs. *Radiat. Res.* (in press).

Newton, G. J., W. E. Bechtold, M. D. Hoover, F. Ghanbari, P. S. Herring and H. N. Jow: A Case Study on Determining Air Monitoring Requirements in a Radioactive Materials Handling Area. In *1993 Radiation Protection Workshop Proceedings*, pp. G14-G26, U.S. Department of Energy, 1994.

Newton, G. J., M. D. Hoover and R. H. Reif: Determination of Aerosol Size Distribution at UMTRA Project Sites. To be published in *Proceedings of the ER '95 Meeting*, held in Denver, CO, August 13-18, 1995 (in press).

Nikula, K. J. and J. L. Lewis: Olfactory Mucosal Lesions in F344 Rats Following Inhalation Exposure to Pyridine at Threshold Limit Value Concentrations. *Fundam. Appl. Toxicol. 23*: 510-517, 1994.

Nikula, K. J., B. A. Muggenburg, I. Y. Chang, W. C. Griffith, F. F. Hahn and B. B. Boecker: Biological Effects of $^{137}CsCl$ Injected in Beagle Dogs. *Radiat. Res. 142*: 347-361, 1995.

Nikula, K. J., R. F. Novak, I. Y. Chang, A. R. Dahl, D. A. Kracko, R. C. Zangar, S. G. Kim and J. L. Lewis: Induction of Nasal Carboxylesterase in F344 Rats Following Inhalation Exposure to Pyridine. *Drug Metab. Dispos. 23(5)*: 529-535, 1995.

Nikula, K. J., M. B. Snipes, E. B. Barr, W. C. Griffith, R. F. Henderson and J. L. Mauderly: Comparative Pulmonary Toxicities and Carcinogenicities of Chronically Inhaled Diesel Exhaust and Carbon Black in F344 Rats. *Fundam. Appl. Toxicol. 25*: 80-94, 1995.

Oberdoerster, G., F. Miller and A. R. Dahl: The Bioavailabity of Inhaled Particle-Borne Organic Compounds. In *Principles and Methods for Assessing Respiratory Tract Injury Caused by Inhaled Substances* (G. Oberdoerster, ed.), International Programme on Chemical Safety, World Health Organization (in press).

Pei, L., J. J. Waide, J. R. Thornton-Manning and R. F. Henderson: Depletion of Glutathione in Lungs and Bone Marrow of $B6C3F_1$ Mice by Inhalation Exposure to Benzene. *Toxicology* (submitted).

Phalen, R. F., H. C. Yeh and S. B. Prasad: Pulmonary Retention of Particles and Fibers: Biokinetics and Effects of Exposure Concentration. In *Concepts in Inhalation Toxicology* (R. O. McClellan and R. F. Henderson, eds.), pp. 129-149, Taylor & Francis, Washington, DC, 1995.

Radu, C. B., B. R. Scott, A. Grace and C. R. Butler: ITRI Hot Ponds Soil Remediation Based on DOE RESRAD Code. To be published in *Proceedings of the ER '95 Meeting*, held in Denver, CO, August 13-18, 1995 (in press).

Rothman, N., R. Haas, R. B. Hayes, S.-N. Yin, J. Weimels, S. Campleman, P. J. E. Compton-Quintana, Y.-Z. Dosemeci, M. Wang, N. Titenko-Holland, K. B. Meyer, G-L Li, L. P. Zhang, W. E. Bechtold, W. Lu, P. Kolancha, L.-J. Xi, W. Blot and M. T. Smith: Benzene Induces Gene-Duplicating Mutations at the Glycophorin A Locus in the Bone Marrow of Exposed Workers. *Proc. Natl. Acad. Sci.* (in press).

Rothman, N., G. L. Li, R. B. Hayes, M. Dosemeci, W. E. Bechtold, G. Marti, Y. Z. Wang, M. Linet, L. J. Xi, W. Lu, M. T. Smith, N. Titenko-Holland, L. P. Zhang, W. Blot and S. N. Yin: Hematotoxicity Among Chinese Workers Heavily Exposed to Benzene. *Am. J. Public Health* (in press).

Sanders, C. L. and D. L. Lundgren: Pulmonary Carcinogenesis in the F344 and Wistar Rat Following Inhalation of $^{239}PuO_2$. *Radiat. Res. 144*: 206-214, 1995.

Schuyler, M., B. Edwards, K. Gott and K. J. Nikula: Experimental Hypersensitivity Pneumonitis: Effect of Thy 1.2+ and CD8+ Cell Depletion. *Am. J. Respir. Crit. Care Med. 151*: 1834-1842, 1995.

Scott, B. R., C. W. Langberg and M. Hauer-Jensen: Models for Estimating the Risk of Ulcers in the Small Intestine After Localized Single or Fractionated Irradiation. *Br. J. Radiol. 68*: 49-57, 1995.

Scott, B. R.: A Generic Model for Estimating the Risk of Deterministic Effects of Partial Organ Irradiation by Hot Particles. *Health Phys.* (in press).

Shivapurkar, N., S. A. Belinsky, D. C. Wolf, Z. Tang and O. Alabaster: Absence of p53 Gene Mutations in Rat Colon Carcinomas Induced by Azoxymethane. *Cancer Res. 96*: 63-70, 1995.

Snipes, M. B.: Pulmonary Retention of Particles and Fibers: Biokinetics and Effect of Exposure Concentrations. In *Concepts in Inhalation Toxicology* (R. O. McClellan and R. F. Henderson, eds.), pp. 225-255, Taylor & Frances, Washington, DC, 1995.

Snipes, M. B., A. L. Barnett, J. R. Harkema, J. A. Hotchkiss, A. H. Rebar and L. J. Reddick: Specific Biological Effects of an Anti-Rat PNM Antiserum Intraperitoneally Injected into F344/N Rats. *Vet. Clin. Pathol. 24(1)*: 1-7, 1995.

Snipes, M. B.: Current Information on Lung Overload in Non-Rodent Mammals: Contrast with Rats. *Inhal. Toxicol.* (in press).

Snipes, M. B., J. R. Harkema, J. A. Hotchkiss and D. E. Bice: Pulmonary Retention and Clearance of Particles in F344 Rats after Depletion of Circulating Polymorphonuclear Leukocytes. *Exp. Lung Res.* (submitted).

Snipes, M. B., J. W. Spoo, B. A. Muggenburg, K. J. Nikula, M. D. Hoover, W. C. Griffith and R. A. Guilmette: Evaluation of the Clearance of Particles Deposited on the Conducting Airways of Beagle Dogs. *J. Aerosol Med.* (submitted).

Stoeber, W. and J. L. Mauderly: Model-Inferred Hypothesis of a Critical Dose for Overload Tumor Induction by Diesel Soot and Carbon Black. *Inhal. Toxicol 6*: 427-458, 1994.

Swafford, D. S., K. J. Nikula, C. E. Mitchell and S. A. Belinsky: Low Frequency of Alteration in p53, K-ras, and mdm2 in Rat Lung Neoplasms Induced by Diesel Exhaust or Carbon Black. *Carcinogenesis 16(5)*: 1215-1221, 1995.

Swift, D. L., Y. S. Cheng, Y. F. Su and H. C. Yeh: Ultrafine Aerosol Deposition in the Human Nasal and Oral Passages. *Ann. Occup. Hyg. 38 (Suppl. 1)*: 77-81, 1994.

Taya, A., J. A. Mewhinney and R. A. Guilmette: Subcellular Distribution of ^{241}Am in Beagle Lungs Following Inhalation of $^{241}Am(NO_3)_3$. *Ann. Occup. Hyg. 38 (Suppl. 1)*: 265-268, 1994.

Tesfaigzi, J., J. Th'ng, J. A. Hotchkiss, J. R. Harkema and P. S. Wright: A Small Proline-Rich Protein, sPRR1, is Up-Regulated Early During Tobacco-Smoke-Induced Squamous Metaplasia. *Am J. Respir. Cell Mol. Biol.* (submitted).

Tesfaigzi, J., N. F. Johnson and J. F. Lechner: Endotoxin Instillation Induces Alveolar Type II Cell Proliferation in the Rat Lung. *Exp. Lung Res.* (submitted).

Thornton-Manning, J. R., A. R. Dahl, W. E. Bechtold, W. C. Griffith and R. F. Henderson: Disposition of Butadiene Monoepoxide and Butadiene Diepoxide in Various Tissues of Rats and Mice Following a Low-Level Inhalation Exposure to 1,3-Butadiene. *Carcinogenesis 16(8)*: 1723-1731, 1995.

Thornton-Manning, J. R., A. R. Dahl, W. E. Bechtold, W. C. Griffith, L. Pei and R. F. Henderson: Gender Differences in the Metabolism of 1,3-Butadiene in Sprague Dawley Rats Following a Low-Level Inhalation Exposure. *Carcinogenesis* (in press).

Thornton-Manning, J. R., A. R. Dahl, W. E. Bechtold and R. F. Henderson: Gender and Species Differences in the Metabolism of 1,3-Butadiene to Butadiene Monoepoxide and Butadiene Diepoxide in Rodents Following Low-Level Inhalation Exposures. *Toxicology* (in press).

Thornton-Manning, J. R. and A. R. Dahl: Nasal Tract, Biochemistry. To be published as a book chapter in *Encyclopedia of Human Biology*, Academic Press, Inc. (in press).

Thornton-Manning, J. R., J. A. Hotchkiss, K. D. Rohrbacher, X. Ding and A. R. Dahl: Nasal Cytochrome P450 2A (CYP2A): Identification, Cellular Localization, and Xenobiotic Metabolic Activity. *Arch. Biochem. Biophys.* (submitted).

Tierney, L. A., F. F. Hahn and J. F. Lechner: p53, erbB2, and K-*ras* Gene Dysfunctions are Rare in Spontaneous and Plutonium-239-Induced Canine Lung Neoplasia. *Radiat. Res.* (in press).

Tokiwa, T., M. M. Lipsky, D. T. Smoot and J. F. Lechner: A Method for Transforming Human Liver Epithelial Cells by Transfection Using a Plasmid Containing SV40 Early Region Gene. *J. Tissue Culture Methods 16*: 57-60, 1994.

Ward, J. B., M. M. Ammenheuser, W. E. Bechtold, E. B. Whorton and M. S. Legator: hprt Mutant Lymphocyte Frequencies in Workers at a 1,3-Butadiene Production Plant. *Environ. Health Perspect. 102(9)*: 79-85, 1994.

Wasiolek, P. T. and Y. S. Cheng: Measurements of the Activity-Weighted Size Distributions of Radon Decay Products Outdoors in Central New Mexico with Parallel and Screen Diffusion Batteries. *Aerosol Sci. Technol. 23(3)*: 401-410, 1995.

Weissman, D. N., D. E. Bice, R. E. Crowell and M. R. Schuyler: Intrapulmonary Antigen Deposition in the Human Lung: Local Responses. *Am. J. Respir. Cell Mol. Biol. 11(5)*: 607-614, 1994.

Wilkins, E., P. Atanasov and B. A. Muggenburg: Integrated Implantable Device for Long-Term Glucose Monitoring. *Biosensors & Bioelectronics 10*: 485-494, 1995.

Yamada, Y., A. Koizumi, S. Fukuda, J. Inaba, Y. S. Cheng and H. C. Yeh: Deposition of Ultrafine Monodisperse Particles in a Human Tracheobronchial Cast. *Ann. Occup. Hyg. 38 (Suppl. 1)*: 91-100, 1994.

Yeh, H. C., B. A. Muggenburg, R. A. Guilmette, M. B. Snipes, R. S. Turner, R. K. Jones and J. P. Smith: Characterization of Aerosols Produced During Total Hip Replacement Surgery in Dogs with ^{51}Cr-Labeled Blood. *J. Aerosol Sci. 26(3)*: 511-518, 1995.

Yeh, H. C., R. S. Turner, R. K. Jones, B. A. Muggenburg, D. L. Lundgren and J. P. Smith: Characterization of Aerosols Produced During Surgical Procedures in Hospitals. *Aerosol Sci. Technol.* 22: 151-161, 1995.

APPENDIX F

PRESENTATIONS BEFORE REGIONAL, NATIONAL, OR INTERNATIONAL SCIENTIFIC MEETINGS AND EDUCATIONAL AND SCIENTIFIC SEMINARS

OCTOBER 1, 1994 – SEPTEMBER 30, 1995

Bechtold, W. E. and K. R. Ahlert: Selective Extraction of ^{239}Pu from Tissues and Feces Using TRU·Spec Resin. 40th Annual Conference on Bioassay, Analytical, and Environmental Radiochemistry, Cincinnati, OH, November 14-18, 1994.

Bechtold, W. E.: S-Phenylcysteine in Albumin as a Benzene Biomarker. Annual Meeting of the Health Effects Institute, Chicago, IL, April 30-May 2, 1995.

Bechtold, W. E. and T. Buckley: Roundtable Discussion, Biological Monitoring for Chemical Carcinogens in the Work Place: Internal Dose Markers. American Industrial Hygiene Conference and Exposition, Kansas City, MO, May 20-26, 1995.

Bechtold, W. E., R. F. Henderson, S. Li and R. B. Hayes: Characterization of Worker Exposures in a Butadiene Production Facility. International Symposium on Evaluation of Butadiene and Isoprene Health Risks, Blaine, WA, June 27-29, 1995.

Belinsky, S. A.: Finding the Needle in the Haystack: Molecular Biology Approaches to Detect Gene Dysfunction. Department of Thoracic Surgery, University of New Mexico, Albuquerque, NM, October 25, 1994.

Belinsky, S. A.: Genetic and Epigenetic Alterations in Lung Cancer. Chemical Industry Institute of Toxicology, Research Triangle Park, NC, December 7, 1994.

Belinsky, S. A.: Genetic and Epigenetic Alterations in Lung Cancer. The Lovelace Institutes, Albuquerque, NM, February 14, 1995.

Belinsky, S. A., S. K. Middleton, K. J. Nikula and F. F. Hahn: Alterations in the p53 Pathway in X-ray-Induced Rat Lung Tumors. 86th Annual Meeting of the American Association of Cancer Research, Toronto, Ontario, Canada, March 18-22, 1995.

Belinsky, S. A.: A Microassay for Measuring Cytosine DNA-Methyltransferase Activity During Tumor Progression. International Congress of Toxicology - VII, Seattle, WA, July 2-6, 1995.

Belinsky, S. A.: Identification of Trisomy 7 in Cultured Bronchial Cells from Individuals at High Risk of Developing Lung Cancer. Specialized Program of Research Excellence (SPORE) Meeting, Rockville, MD, July 16, 1995.

Benson, J. M., E. B. Barr, D. L. Lundgren and K. J. Nikula: Pulmonary Retention and Tissue Distribution of ^{239}Pu Nitrate in F344 Rats and Syrian Hamsters Inhaling Carbon Tetrachloride. Annual Meeting of the Society of Toxicology, Baltimore, MD, March 5-9, 1995.

Bice, D. E.: Asthma: A Dysregulation of Pulmonary Immunity. Annual Meeting of the American Thoracic Society, Seattle, WA, May 22, 1995.

Bice, D. E.: Animal Models of Asthma and Roles of Pulmonary Immunity. 3M Corporation, St. Paul, MN, August 29, 1995.

Boecker, B. B.: Cancer from Internal Emitters. Tenth International Congress of Radiation Research, Wurzburg, Germany, August 27-September 1, 1995.

Burt, D. G., C. H. Hobbs and W. C. Griffith: Substrain Differences in Body Weight and Survival of F344 Rats Housed in Inhalation Chambers. 45th American Association of Laboratory Animal Science (AALAS) Annual Meeting, Pittsburgh, PA, October 16-20, 1994.

Carpenter, T. R. and N. F. Johnson: Characterization of the p53 Response to Alpha Particle Irradiation in the Human Tumor Cell Strain A549. 86th Annual Meeting of the American Association of Cancer Research, Toronto, Ontario, Canada, March 18-22, 1995.

Cheng, K. H., D. L. Swift, Y. S. Cheng, and H. C. Yeh: An Experimental Method for Measuring Deposition Efficiency of Aerosols in the Human Oral Airway. American Industrial Hygiene Conference and Exposition, Kansas City, MO, May 20-26, 1995.

Cheng, Y. S.: Health Effects of Inhaled Toxic Aerosols. Seminar at Mehary Medical College, Nashville, TN, March 17, 1995.

Cheng, Y. S.: Behavior of Aerosol Particles in the Lung. Seminar at the College of Pharmacy, Florida A & M University, Tallahassee, FL, April 6, 1995.

Cheng, Y. S., H. C. Yeh, and R. A. Guilmette: Deposition of Ultrafine Particles in the Human Oral Airway. International Society of Aerosols in Medicine International Congress, Hamilton, Ontario, Canada, May 15-19, 1995.

Cheng, Y. S., M. B. Snipes and H. N. Jow: Radiation Dosimetry of Metal Tritides. Health Physics Society Annual Meeting, Boston, MA, July 23-27, 1995.

Dahl, A. R., L. K. Brookins and P. Gerde: An Instrument for Determining Nasal and Lung Absorption of Gases During Variable Cyclic Breathing. Annual Meeting of the Society of Toxicology, Baltimore, MD, March 5-9, 1995.

Dahl, A. R.: Metabolism of Isoprene *In Vivo*. International Symposium on Evaluation of Butadiene and Isoprene Health Risks, Blaine, WA, June 27-29, 1995.

Dahl, A. R. and P. Gerde: Modeling Target Dose of Organic Compounds to the Lung. Fourth International Society for the Study of Xenobiotics Meeting, Seattle, WA, August 27-31, 1995.

Finch, G. L.: Animal Models of Beryllium-Induced Lung Disease. Conference on Beryllium-Related Diseases, National Institute of Environmental Health Sciences, Research Triangle Park, NC, November 8-10, 1994.

Finch, G. L.: Animal Models of Beryllium-Induced Lung Disease. Beryllium Monitoring Committee, Gaithersburg, MD, February 28-March 1, 1995.

Finch, G. L., K. J. Nikula, E. B. Barr, W. E. Bechtold, B. T. Chen and W. C. Griffith: Lung Tumor Synergism Between $^{239}PuO_2$ and Cigarette Smoke Inhaled by F344 Rats. Annual Meeting of the Society of Toxicology, Baltimore, MD, March 5-9, 1995.

Finch, G. L.: Current Issues in Inhalation Toxicology: Ozone, Cigarette Smoke, and Beryllium. Cleveland Clinic Foundation, Cleveland, OH, March 15, 1995.

Finch, G. L., M. D. Hoover, K. J. Nikula, S. A. Belinsky, P. J. Haley and F. F. Hahn: Comparative Pulmonary Responses to Inhaled Beryllium Metal in Rats Versus Mice. International Congress of Toxicology - VII, Seattle, WA, July 2-6, 1995.

Finch, G. L., C. H. Hobbs, D. L. Lundgren, J. M. Benson, F. F. Hahn, K. J. Nikula, W. C. Griffith, M. D. Hoover, E. B. Barr, S. A. Belinsky, B. B. Boecker and J. L. Mauderly: Worker Risk Issues for Combined Exposures to Radionuclides and Chemicals - An Experimental Toxicology Approach. ER '95, Denver, CO, August 13-18, 1995.

Gerde, P. and A. R. Dahl: Absorption of Organic Toxicants by the Lungs: Modeling Portal-of-Entry Dosimetry. Annual Meeting of the Society of Toxicology, Baltimore, MD, March 5-9, 1995.

Gerde, P. and A. R. Dahl: Inhalation of Organic Carcinogens - Modeling Target Dose to the Lung. International Congress of Toxicology - VII, Seattle, WA, July 2-6, 1995.

Griffith, W. C.: Semiparametric Score Test to Determine if Tumors are Incidental in Rodent Survival-Sacrifice Carcinogenesis Experiments. International Congress of Toxicology - VII, Seattle, WA, July 2-6, 1995.

Griffith, W. C., B. B. Boecker, C. R. Watson and G. B. Gerber: Possibilities to Use Animal Databases for Further Statistical Evaluation and Modeling. Tenth International Congress of Radiation Research, Wurzburg, Germany, August 27-September 1, 1995.

Guilmette, R. A., Y. S. Cheng, H. C. Yeh and D. L. Swift: Deposition of Monodisperse Particles in Computer-Milled MRI-Based Nasal Airway Replica. International Society of Aerosols in Medicine International Congress, Hamilton, Ontario, Canada, May 15-19, 1995.

Guilmette, R. A., Y. S. Cheng and M. B. Snipes: Particle Deposition and Clearance Mechanisms: A Look at Current Issues and Research Directions. International Society of Aerosols in Medicine International Congress, Hamilton, Ontario, Canada, May 15-19, 1995.

Hahn, F. F., B. A. Muggenburg and V. Esch: Prostatic Lesions Induced in Beagle Dogs by Diode Laser Treatment. American College of Veterinary Pathologists/American Society of Veterinary Clinical Pathologists Annual Meeting, Montreal, Canada, October 30-November 4, 1994.

Hahn, F. F.: Radiation-Induced Pulmonary Neoplasia. Research Seminar, School of Veterinary Medicine, Purdue University, South Bend, IN, November 7, 1994.

Hahn, F. F.: Pulmonary Pathology. Histopathology Seminar, School of Veterinary Medicine, Purdue University, South Bend, IN, November 7, 1994.

Hahn, F. F., B. A. Muggenburg and B. B. Boecker: Cerium-144 Chloride Deposited in the Liver of Dogs Causes Tumors Similar to Those Caused by Thorotrast. 43rd Annual Meeting of the Radiation Research Society, San Jose, CA, April 1-6, 1995.

Hahn, F. F. and W. C. Griffith: Cerium-144-Induced Lung Tumors in Two Strains of Mice. Tenth International Congress of Radiation Research, Wurzburg, Germany, August 27-September 1, 1995.

Harkema, J. R., C. J. Bresee and J. A. Hotchkiss: Mucous Cell Metaplasia and Cell Proliferation Induced by a Single Intratracheal Instillation of Endotoxin in Rat Airways. American College of Veterinary Pathologists/American Society of Veterinary Clinical Pathologists Annual Meeting, Montreal, Canada, October 30-November 4, 1994.

Harkema, J. R., C. J. Bresee and J. A. Hotchkiss: Secretory Cell Proliferation Induced by a Single Intratracheal Instillation of Endotoxin in Rat Airways. Annual Meeting of the American Thoracic Society, Seattle, WA, May 21-24, 1995.

Henderson, R. F.: Species Differences in Metabolism of 1,3-Butadiene. The Fifth International Symposium on Biological Reactive Intermediates, Munich, Germany, January 4-8, 1995.

Henderson, R. F., W. E. Bechtold and M. R. Strunk: Analysis of Benzene Metabolites and Glutathione in the Bone Marrow of $B6C3F_1$ Mice. Annual Meeting of the Society of Toxicology, Baltimore, MD, March 5-9, 1995.

Henderson, R. F.: Study of the Potential Carcinogenicity of Butadiene Diepoxide in Mice and Rats. Annual Meeting of the Health Effects Institute, Chicago, IL, April 30-May 2, 1995.

Henderson, R. F.: Diesel and Carbon Black Studies at ITRI. New York University, Tuxedo, NY, May 12, 1995.

Henderson, R. F.: Benzene Metabolism in Various Species. Benzene '95, Rutgers University, New Brunswick, NJ, June 16, 1995.

Henderson, R. F., J. R. Thornton-Manning, W. E. Bechtold and A. R. Dahl: General Discussion of Metabolism Pathways of Butadiene (Phase I and Phase II), Species Differences in Uptake and Metabolism. International Symposium on Evaluation of Butadiene and Isoprene Health Risks, Blaine, WA, June 27-29, 1995.

Henderson, R. F.: Strategies for the Use of Biological Markers. International Congress of Toxicology - VII, Seattle, WA, July 2-6, 1995.

Henderson, R. F.: Level of Benzene Exposure Required to Observe Phenolic Metabolites Above Background. International Congress of Toxicology - VII, Seattle, WA, July 2-6, 1995.

Hobbs, C. H., J. L. Mauderly and M. B. Snipes: Design Considerations for Chronic Inhalation Studies: Relevancy vs. Irrelevancy. Workshop Session: The Maximum Tolerated Dose (MTD) for Inhalation Bioassays: Toxicity vs. Overload. Annual Meeting of the Society of Toxicology, Baltimore, MD, March 5-9, 1995.

Hobbs, C. H.: Toxicology for Chemists. "Introduction to Inhalation Toxicology," American Chemical Society, San Francisco, CA, May 2, 1995.

Hoover, M. D.: Evaluation of the Los Alamos Beryllium Realtime Monitor at the ITRI. Beryllium Monitoring Committee, Gaithersburg, MD, February 28-March 1, 1995.

Hotchkiss, J. A., G. L. Finch, A. R. Dahl, K. J. Nikula and J. L. Lewis: Mainstream Cigarette Smoke Exposure Alters Cytochrome P4502G1 Expression in F344 Rat Olfactory Mucosa. Annual Meeting of the Society of Toxicology, Baltimore, MD, March 5-9, 1995.

Johnson, N. F., D. G. Thomassen, A. W. Hickman, T. R. Carpenter and G. J. Newton: Biodosimetric Approach for Estimating Alpha Particle Dose to Respiratory Tract Epithelial Cells. 5th International Inhalation Symposium "Correlations Between *In Vitro* and *In Vivo* Investigations in Inhalation Toxicology," Hannover, Germany, February 20-24, 1995.

Johnson, N. F., T. R. Carpenter and A. W. Hickman: Alpha Particle-Induced Gene Expression and Cell Cycle Changes in Rodent and Human Cells. 43rd Annual Meeting of the Radiation Research Society, San Jose, CA, April 1-6, 1995.

Kennedy, C. K., N. H. Fukishima, R. E. Neft and J. F. Lechner: Induction of Genomic Instability in Normal Human Bronchial Epithelial (NHBE) Cells by Alpha Particles. 86th Annual Meeting of the American Association of Cancer Research, Toronto, Ontario, Canada, March 18-22, 1995.

Lechner, J. F.: Urban Air Carcinogens and Their Effect on Health. Third Annual Meeting of the University Environment Program (UNAM), "Health and Environment," Mexico City, Mexico, October 19-21, 1994.

Lechner, J. F.: *In Vitro* Models of Human Cells for Carcinogenesis Investigations. Environmental Protection Agency, Research Triangle Park, NC, November 14, 1994.

Lechner, J. F., C. H. Kennedy, R. E. Neft and N. H. Fukishima: Induction of Genomic Instability in Normal Human Bronchial Epithelial (NHBE) Cells by Alpha Particles. Keystone Symposium, Molecular Toxicology, Keystone, CO, January 9-15, 1995.

Lechner, J. F.: Recent Advances in Lung Cancer Biology. Radon Epidemiology Meeting, Baltimore, MD, February 13-14, 1995.

Lechner, J. F.: *In Vitro* Carcinogenesis of Human Bronchial Epithelial Cells. 5th International Inhalation Symposium on Correlations Between *In Vitro* and *In Vivo* Investigations in Inhalation Toxicology, Hannover, Germany, February 20-24, 1995.

Lechner, J. F.: High-LET Radiation-Caused Lung Cancer: Comparative Molecular Phenomena Between Humans and Animals. Department of Toxicology, National Institute of Occupational Health, Oslo, Norway, February 27, 1995.

Lechner, J. F.: Molecular Phenomena of Alpha Radiation-Caused Lung Cancer. 43rd Annual Meeting of the Radiation Research Society, San Jose, CA, April 1-6, 1995.

Lechner, J. F.: Epidemiology of Lung Cancer. Lovelace Health System Cancer Registry Workshop, Albuquerque, NM, April 21, 1995.

Lewis, J. L., A. R. Dahl and D. A. Kracko: Metabolism and Transport of Inhaled Xylene to Olfactory Bulb Glomeruli: Nasal Metabolism as a Component of the Nose-Brain Barrier. Association of Chemoreception Sciences Annual Meeting, Sarasota, FL, April 15-22, 1995.

Lewis, J. L., A. R. Dahl and D. A. Kracko: The Nose-Brain Barrier: Nasal Metabolism Modulates Transport of Inhalants to the Central Nervous System. International Congress of Toxicology - VII, Seattle, WA, July 2-6, 1995.

Mauderly, J. L.: Current Concepts on Airborne Particles and Health. Third Annual Meeting of the University Environment Program (UNAM), "Health and Environment," Mexico City, Mexico, October 19-21, 1994.

Mauderly, J. L.: Inhalation Toxicology of Particulates in the Occupational Setting. American College of Occupational and Environmental Medicine State-of-the-Art Conference, Denver, CO, October 24, 1994.

Mauderly, J. L.: Inhalation Toxicology of Particulate Ambient Air Pollutants. American College of Occupational and Environmental Medicine State-of-the-Art Conference, Denver, CO, October 24, 1994.

Mauderly, J. L.: Morbidity and Mortality from Acute Increases in Urban Particulate: Introduction. Annual Meeting of the Society of Toxicology, Baltimore, MD, March 5-9, 1995.

Mauderly, J. L.: Lung Overload: The Dilemma and Opportunities for Resolution. Conference on Overload, Massachusetts Institute of Technology, Cambridge, MA, March 29-30, 1995.

Mauderly, J. L.: Mechanisms of Diesel-Exhaust-Induced Carcinogenesis: Influence of Particulate Matter. Annual Meeting of the Health Effects Institute, Chicago, IL, April 30-May 2, 1995.

Mauderly, J. L.: Association Between Ambient Urban Particulates and Human Mortality and Morbidity. The Case for Biological Plausibility. International Society for Aerosols in Medicine International Congress, Hamilton, Ontario, Canada, May 15-19, 1995.

Mauderly, J. L.: Regulatory Implications of Health Risks Suggested by Environmental Epidemiology, Occupational Exposures, and Toxicology. Annual Meeting of the American Thoracic Society, Seattle, WA, May 21-24, 1995.

Mauderly, J. L.: Usefulness of Animal Models for Predicting Human Responses to Chronic Inhalation Exposures. Thomas L. Petty Aspen Lung Conference on Environmental Lung Disease: Exposure & Mechanisms, Given Institute of Pathology, Aspen, CO, June 7-10, 1995.

Muggenburg, B. A., R. A. Guilmette, N. A. Gillett, F. F. Hahn, W. C. Griffith and B. B. Boecker: Toxicity of Inhaled ^{238}Pu in Beagle Dogs. Tenth International Congress of Radiation Research, Wurzburg, Germany, August 27-September 1, 1995.

Newton, G. J., M. D. Hoover, C. R. Butler and A. C. Grace: Demolition and Removal of Radioactively Contaminated Concrete, Aerosol Measurements. Health Physics Society Annual Meeting, Boston, MA, July 23-27, 1995.

Newton, G. J., M. D. Hoover and R. H. Reif: Determination of Aerosol Size Distributions at UMTRA. ER '95, Denver, CO, August 13-18, 1995.

Newton, G. J., M. D. Hoover, C. R. Butler and A. C. Grace: Demolition and Removal of Radioactively Contaminated Concrete, Aerosol Measurements. Fine Particles Society, Chicago, IL, August 24, 1995.

Nikula, K. J., G. L. Finch, E. B. Barr, W. E. Bechtold, B. T. Chen, W. C. Griffith, M. D. Hoover and J. L. Mauderly: Cigarette Smoke and $^{239}PuO_2$ Interact Synergistically to Induce Lung Cancer in F344 Rats. American College of Veterinary Pathologists/American Society of Clinical Veterinary Pathologists Annual Meeting, Montreal, Canada, October 30-November 4, 1994.

Nikula, K. J., G. L. Finch, M. D. Hoover and S. A. Belinsky: Comparative Pulmonary Carcinogenicity of Beryllium in A/J and C3H/HeJ Mice. Annual Meeting of the Society of Toxicology, Baltimore, MD, March 5-9, 1995.

Nikula, K. J., G. L. Finch, W. C. Griffith, W. E. Bechtold, E. B. Barr, B. T. Chen, C. H. Hobbs, M. D. Hoover and J. L. Mauderly: Cigarette Smoke and ^{239}Pu Interact Synergistically to Induce Pulmonary Neoplasia in F344 Rats. International Congress of Toxicology - VII, Seattle, WA, July 2-6, 1995.

Scott, B. R.: A Model for Estimating the Risk of Deterministic Effects of Partial-Organ Irradiation. 43rd Annual Meeting of the Radiation Research Society, San Jose, CA, April 1-6, 1995.

Scott, B. R., G. J. Newton and M. D. Hoover: Use of DAC-h Can Greatly Overestimate Intake of Hot PuO_2 Particles During Brief Occupational Exposures. Health Physics Society Annual Meeting, Boston, MA, July 23-27, 1995.

Scott, B. R. and J. W. Hopewell: A Model for Deterministic Effects of Focal Irradiation of the Skin by Beta/Gamma-Emitting Hot Particles. Tenth International Congress of Radiation Research, Wurzburg, Germany, August 27-September 1, 1995.

Snipes, M. B., B. A. Muggenburg, W. C. Griffith and R. A. Guilmette: Clearance Patterns for ^{111}In-Oxide Particles Deposited in Airways of Beagle Dogs. International Society for Aerosols in Medicine International Congress, Hamilton, Ontario, Canada, May 15-19, 1995.

Tesfaigzi, J., J. F. Lechner and N. F. Johnson: Apoptosis During Remodeling of Endotoxin-Induced Type II Cell Hyperplasia in Rat Lung. Keystone Symposium on Apoptosis, Tamarron, CO, March 5-11, 1995.

Tesfaigzi, J., N. F. Johnson and J. F. Lechner: Endotoxin-Induced Transient Type II Cell Proliferation in the Rat Lung. 86th Annual Meeting of the American Association of Cancer Research, Toronto, Ontario, Canada, March 18-22, 1995.

Tierney, L. A., F. F. Hahn, W. C. Griffith, J. F. Lechner and G. Kelly: Alterations of p53 and erbB2 Gene Expression in a Canine Model of Familial Mammary Cancer. American College of Veterinary Pathology/American Society of Veterinary Clinical Pathologists Annual Meeting, Montreal, Canada, October 30-November 4, 1994.

Thornton-Manning, J. R., W. E. Bechtold, A. R. Dahl and R. F. Henderson: Comparison of Tissue Concentrations of Butadiene Epoxides in Sprague-Dawley Rats and $B6C3F_1$ Mice Exposed to Low Levels of 1,3-Butadiene (BD) by Inhalation. Annual Meeting of the Society of Toxicology, Baltimore, MD, March 5-9, 1995.

Thornton-Manning, J. R., W. E. Bechtold, A. R. Dahl and R. F. Henderson: Effect of Multiple Dosing and Gender on the Metabolism of 1,3-Butadiene in Rats and Mice. Chemical Manufacturers Association Butadiene Research Review, Baltimore, MD, May 15-16, 1995.

Thornton-Manning, J. R., A. R. Dahl, W. E. Bechtold and R. F. Henderson: Gender and Species Differences in the Metabolism of 1,3-Butadiene to Butadiene Monoepoxide and Butadiene Diepoxide in Rodents Following Low-Level Inhalation Exposures. International Symposium on Evaluation of Butadiene and Isoprene Health Risks, Blaine, WA, June 27-29, 1995.

Thornton-Manning, J. R., S. T. Chen, K. R. Rohrbacher, P. Gerde and A. R. Dahl: Metabolism of Benzo[a]Pyrene in Canine Bronchial, Olfactory, and Nasal Respiratory Mucosa Explants. International Congress of Toxicology - VII, Seattle, WA, July 2-6, 1995.

Thornton-Manning, J. R., S. T. Chen, K. D. Rohrbacher, P. Gerde and A. R. Dahl: Metabolism of Benzo[a]Pyrene in Canine Bronchial, Olfactory, and Nasal Respiratory Mucosa Explants. Fourth International Society for the Study of Xenobiotics Meeting, Seattle, WA, August 27-31, 1995.

Yeh, H. C., B. A. Muggenburg, R. A. Guilmette, M. B. Snipes, R. S. Turner and R. K. Jones: Characterization of Aerosols Produced During Surgical Procedures. International Society for Aerosols in Medicine International Congress, Hamilton, Ontario, Canada, May 15-19, 1995.

APPENDIX G

SEMINARS PRESENTED BY VISITING SCIENTISTS

OCTOBER 1, 1994 – SEPTEMBER 30, 1995

Dr. Richard B. Richardson, Atomic Energy of Canada, Chalk River Laboratories, Chalk River, Ontario, Canada: *Dosimetry of an Acute Intake of Tritiated Water*, October 26, 1994.

Dr. Robin A. F. Cox, Occupational Physician, Fowlmere, UK: *Epidemiological Studies of Workers Exposed to Carbon Black*, November 4, 1994.

Dr. William Jones Williams, University of Wales College of Medicine, Llandough Hospital, Penarth, UK: *Chronic Beryllium Disease*, November 14, 1994.

Dr. Elaine Ostrander, Fred Hutchison Cancer Center, Seattle, WA: *Genetic Mapping in the Dog*, March 13, 1995.

Dr. Gerhard Brand, Retired Professor, School of Medicine, University of Minnesota, Minneapolis, MN: *Do Implants Cause Cancer?*, March 20, 1995.

Dr. Eric Ansoborlo, CEN, Pierrelatte, France: *Uranium Studies in France and Future Trends*, April 18, 1995.

Dr. Magnus Svartengren, Karolinska Institute, Stockholm, Sweden: *Deposition of Particles in Patients with Obstructive Lung Disease*, May 8, 1995.

Dr. Paul Fritsch, Laboratoire de Radiotoxicologie, Bruyeres-Le-Chatel, France: Biological *Dosimetry Using Micronuclei or Apoptosis Scoring on Thick Tissue Sections*, May 11, 1995.

Dr. Grace M. Kepler, Chemical Industry Institute of Toxicology, Research Triangle Park, NC: *Computerized Nasal Dosimetry Modeling*, June 20, 1995.

Dr. JeanClare Seagrave, The Lovelace Institutes, Albuquerque, NM: *Alkaline Phosphatase, An Enzyme Without a Function?*, July 21, 1995.

Dr. Ken Turteltaub, Lawrence Livermore Laboratory, Livermore, CA: *Accelerator Mass Spectrometry in Biomedical Research: New Technology for High Sensitivity Isotope and Chemical Tracing*, July 25, 1995.

Dr. Carmel Mothersill, Radiation Science Centre, College of Technology, Dublin, Ireland: *Genomic Instability Studies*, July 31, 1995.

Dr. Werner Stoeber, Fraunhofer Institute for Toxicology and Aerosol Science (retired), Hannover, Germany: *Is the Pock Model of Alveolar Retention an Extrapolation Model with Predictive Power?*, August 18, 1995.

Dr. Daniel W. Nebert, University of Cincinnati Medical Center, Cincinnati, OH: *Human Genetic Differences in Cancer and Toxicity Caused by Environmental Chemicals*, September 21, 1995.

APPENDIX H

ADJUNCT SCIENTISTS

AS OF SEPTEMBER 30, 1995

Dr. William W. Carlton
School of Veterinary Medicine
Purdue University
West Lafayette, IN 47907

Dr. David Coultas
New Mexico Tumor Registry and
Department of Medicine
University of New Mexico
Albuquerque, NM 87131

Dr. Richard E. Crowell
Department of Medicine
University of New Mexico
Albuquerque, NM 87131

Dr. Frank D. Gilliland
New Mexico Tumor Registry and
Department of Medicine
University of New Mexico
Albuquerque, NM 87131

Dr. William M. Hadley
Dean, College of Pharmacy
University of New Mexico
Albuquerque, NM 87131

Dr. Jack R. Harkema
Department of Pathology
Michigan State University
East Lansing, MI 48824

Dr. Mary Lipscomb
Chair, Department of Pathology
University of New Mexico
Albuquerque, NM 87131

Dr. C. Richard Lyons
Department of Hematology/Oncology
Cancer Center
University of New Mexico
Albuquerque, NM 87131

Dr. Pope Moseley
Chief, Pulmonary Critical Care Division
Department of Medicine
University of New Mexico
Albuquerque, NM 87131

Dr. Alan H. Rebar
Office of Research Program Development
School of Veterinary Medicine
Purdue University
West Lafayette, IN 47907

Dr. Jonathan M. Samet
School of Hygiene and Public Health
Johns Hopkins University
Baltimore, MD 21205

Dr. Mark Schuyler
Albuquerque VA Medical Center
2100 Ridgecrest S.E.
Albuquerque, NM 87108

Dr. David L. Swift
School of Hygiene and Public Health
Johns Hopkins University
Baltimore, MD 21205

APPENDIX I

EDUCATION ACTIVITIES AT THE INHALATION TOXICOLOGY RESEARCH INSTITUTE

During the last 30 years, ITRI education programs have reached over 900 individuals including precollege, undergraduate, and graduate students; teachers of these students; postdoctoral fellows; and visiting scientists. Our programs are designed to increase science awareness, literacy, and participation in environmental health sciences and to provide training in areas of laboratory expertise.

Precollege Students

Precollege students are introduced to environmental health science through Institute tours, in-class demonstrations, science fair judging, and research opportunities.

In 1991, we started the Minority Research Program which involves high school students from underrepresented populations. Participants from this program who choose to enroll at the University of New Mexico (UNM) may be invited to continue their research experience part-time during the academic year and full-time during the summer. This program provides an excellent opportunity for students interested in science to gain intensive research experience. We have had eight participants in the program since 1991, and three participants this summer. One participant, Debbie Gurulé, is a sophomore at the University of New Mexico and has participated in the program since June 1994.

Teacher Programs

Teachers need background and experience in environmental health science to provide their students with relevant and accurate information. Our teacher programs consist of workshops and research opportunities. During FY-1995, ITRI sponsored five teacher workshops reaching 70 teachers.

Teachers interested in intensive research opportunities can participate in our summer research programs. Middle and high school teachers participate in 8 weeks of laboratory research. One program, the Summer Teacher Enrichment Program (STEP), is specifically for New Mexico teachers. A second program, the Teacher Research Associates Program (TRAC), is for teachers throughout the United States. Participants in these programs are involved in all steps of a scientific study, including the design and conduct of experiments, collection and analysis of data, and oral and written presentation of results. Seminars and presentations explore additional scientific or career-related topics. This experience gives teachers background for developing curriculum and incorporating environmental health science into their classroom instruction. Six teachers participated in these programs during FY-1995. Since 1984, 61 teachers have spent summers at ITRI.

Undergraduate Students

Undergraduate students majoring in science or mathematics with an interest in pursuing graduate school are eligible to spend 10 weeks during the summer participating in research. Students initiate and complete a scientific investigation under the direction of an ITRI staff member. Seminars and presentations focus on scientific and career-related topics. The summer culminates in a research symposium where participants present their summer work to the Institute. Five students participated in this program during 1995.

A second educational program for undergraduate students provides work opportunities for engineering students. Eight students worked in various areas of engineering at ITRI during the summer of FY-1995.

Although these programs target undergraduate students, graduate students occasionally participate as well. Since 1967, 692 undergraduate and graduate students have been involved in these educational opportunities.

Graduate Students

The ITRI/UNM Graduate Program provides the opportunity for students to obtain a PhD degree. Course work is completed at UNM, and the research portion of the doctoral degree is carried out at ITRI, with a scientist serving as the research advisor. During FY-1995, the program was expanded to include students seeking degrees outside of the field of toxicology. Also during FY-1995, the program graduated its first student, Dr. Tom Carpenter. Two more students are expected to complete their degrees during FY-1996. Industry continues to support this program. Lilly Laboratories contributed funds which support attendance of students at scientific meetings. Funds from Dupont Central Research and Development provide stipend support.

Graduate students attending other universities can also perform research necessary for their graduate degrees at ITRI. All course work for the advanced degree is completed at the university before the student starts research at ITRI. The advanced degree is awarded by the participating university upon completion of all degree requirements. These graduate programs take advantage of the complementary academic resources available at universities and the research resources available at ITRI. For example, we have joint graduate programs in pathology and medicine with the School of Veterinary Medicine at Purdue University. Graduate veterinary students complete the research portion of a PhD degree at ITRI as part of their residency program in pathology or internal medicine. Since 1966, 62 graduate students have conducted all or part of their research at ITRI.

Postgraduate Training

Research appointments are available to recent doctoral graduates to continue their research training. One program, funded by the National Institutes of Health, is the Pulmonary Epidemiology and Toxicology Training Program which is conducted jointly with UNM. Participants choose to specialize in either epidemiology or toxicology and receive cross-training in the other discipline. There are currently three fellows in this program.

The second program provides research opportunities at ITRI for students in life science, chemistry, veterinary medicine, or engineering. This program develops research capabilities in inhalation toxicology and one or more areas of basic pulmonary biology. During FY-1995, four fellows participated in this program.

University Faculty and Industrial Scientists

Opportunities are available for scientists from universities or industry to visit the Institute or collaborate on research at ITRI. The length of these visits ranges from a few days to obtain information or learn techniques, to a year to conduct research. During FY-1995, participants included scientists from UNM, Albuquerque Veterans Medical Center, Purdue University, Johns Hopkins University, Michigan State University, New York University, and the Chemical Industry Institute of Toxicology.

APPENDIX J

AUTHOR INDEX

*U.S. GOVERNMENT PRINTING OFFICE: 1996-775-000/45017